CARDIOLOGY JOURNAL

Impact Factor: 1.669

July 2020, Vol. 27, No. 4, pp. 329–448

www.cardiologyjournal.org

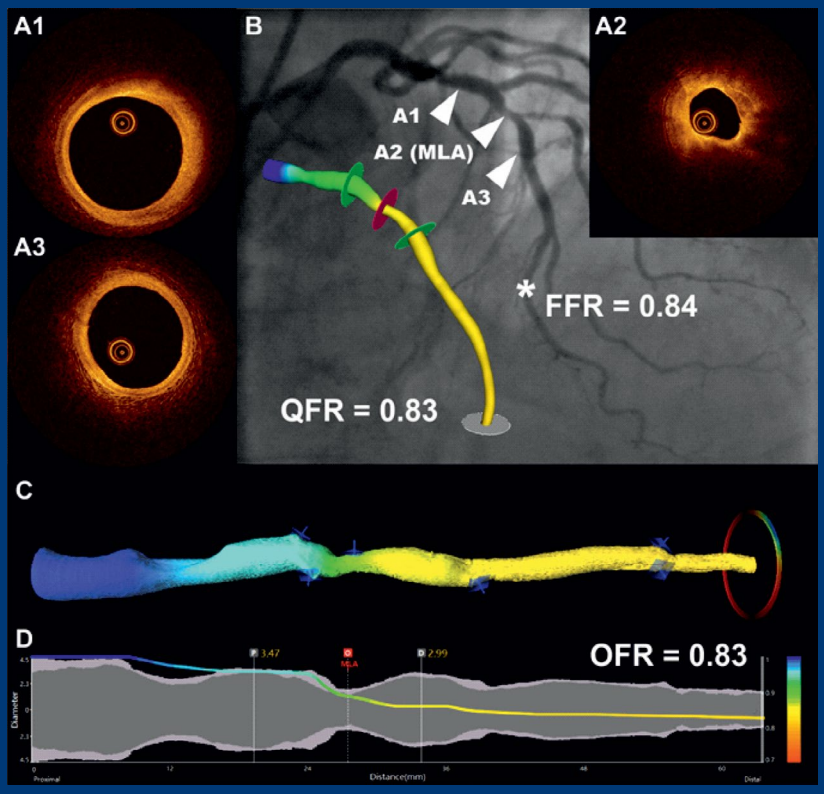

Juan Luis Gutiérrez-Chico et al., see figure legend on page 353

ISSN 1897–5593

VIA MEDICA

CARDIOLOGY JOURNAL

www.cardiologyjournal.org

CARDIOLOGY JOURNAL

www.cardiologyjournal.org

"Cardiology Journal", a bimonthly publication, is an official journal of the Working Groups on Cardiac Rehabilitation and Exercise Physiology, Congenital and Valvular Heart Disease, Echocardiography, Experimental Cardiology, Heart Diseases in Women, Heart Failure, Heart Rhythm, Invasive Cardiology, Noninvasive Electrocardiology and Telemedicine, Pediatric Cardiology and Resuscitation and Intensive Care of the Polish Cardiac Society.

Cardiology Journal (ISSN 1897-5593) is published 6 times a year by VM Media sp. z o.o. VM Group sp.k.

Subscription rates: Paper subscription, 6 issues incl. package and postage institutional — 270 euro. The above prices are inclusive of regular postage costs. Payment should be made to: VM Media sp. z o.o. VM Group sp.k., Grupa Via Medica, Bank BGŻ Paribas SA account number: 15 1600 1303 0004 1007 1035 9021; SWIFT: PPABPLPK. Single issues, subsriptions orders and requests for sample copies should be send to e-mail: prenumerata@viamedica.pl. Electronic orders option available at: https://journals.viamedica.pl/cardiology_journal.

Editorial address: VM Media sp. z o.o. VM Group sp.k., ul. Swietokrzyska 73, 80–180 Gdansk, tel: (+48 58) 320 94 94, fax: (+48 58) 320 94 60, www.cardiologyjournal.org, e-mail: cj@viamedica.pl

Journal has an international indexation in CrossRef, EBSCO, EMBASE, FMJ, Google Scholar, Science Citation Index Expanded, Index Copernicus (156.39 points), MEDLINE, Scopus, SJR, Ulrich's Periodicals Directory, Web of Science CC and WorldCat database, Ministry of Science and Higher Education score (40 points). Current Impact Factor of "Cardiology Journal" (2019) is 1.669.

Advertising: For details on media opportunities within this journal please contact the advertising sales department ul. Swietokrzyska 73, 80–180 Gdansk, tel: (+48 58) 320 94 94, e-mail: viamedica@viamedica.pl
The Editors take no responsibility for the published advertisements.

Editorial policies and author guidelines are published on journal website: www.cardiologyjournal.org

Legal note: https://journals.viamedica.pl/cardiology_journal/about/legalNote

19-0181.004.001

CARDIOLOGY JOURNAL

www.cardiologyjournal.org

July 2020, Vol. 27, No. 4

Table of Contents

VIA MEDICA

EDITORIAL

Cardiology Journal
2020, Vol. 27, No. 4, 329–335
DOI: 10.5603/CJ.2020.0108

ISSN 1897–5593

The legacy of ISCHEMIA

Umberto Ianni[1], Francesco Radico[1], Fabrizio Ricci[2, 3], Matteo Perfetti[4], Federico Archilletti[1], Giulia Renda[1, 3], Nicola Maddestra[4], Sabina Gallina[1], Marco Zimarino[1, 4]

[1]Institute of Cardiology, "G. d'Annunzio" University, Chieti, Italy
[2]Department of Clinical Sciences, Lund University, Clinical Research Center, Malmö, Sweden
[3]Department of Neuroscience, Imaging and Clinical Sciences, "G. d'Annunzio" University, Chieti, Italy
[4]Interventional Cath Lab, ASL 2 Abruzzo, Chieti, Italy

Main findings of the ISCHEMIA trial

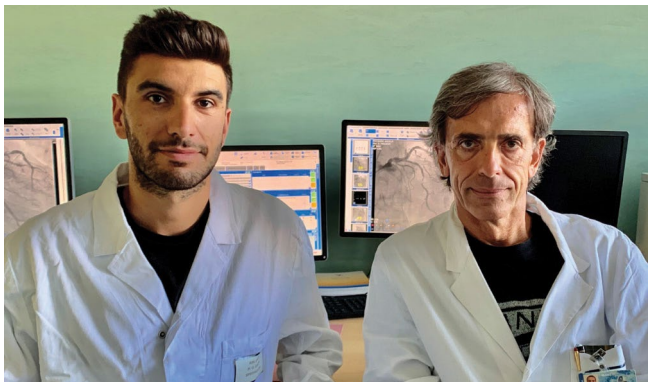

Umberto Ianni, MD and Marco Zimarino, MD, PhD

The long-awaited results of the ISCHEMIA (International Study of Comparative Health Effectiveness with Medical and Invasive Approaches) trial were recently made available in the 'New England Journal of Medicine' [1, 2]. Two main manuscripts detailed on a composite endpoint of death from cardiovascular causes, myocardial infarction (MI), hospitalization for unstable angina, heart failure, or resuscitated cardiac arrest [1] and on quality of life assessment [2]. Overall, the ISCHEMIA trial encompassing 5179 randomized patients with chronic coronary syndromes (CCS), documented that the risk of the primary composite endpoint is similar for an initial invasive strategy with coronary angiography and revascularization, either by percutaneous coronary intervention (PCI) or by coronary artery bypass grafting (CABG) and an initial conservative strategy with optimal medical therapy (OMT) (Fig. 1A) [1]. An initial invasive strategy clearly produced a greater improvement in angina-related health status (Fig. 2) [2]. As for the occurrence of adverse events, when compared with an initial conservative approach, the invasive strategy was associated with an early increased risk, seemingly derived from periprocedural events, that waned and even inverted in the long term, showing a trend towards a protective effect [1].

Such results were in line with previous findings in patients with CCS from COURAGE (Clinical Outcomes Utilizing Revascularization and Aggressive Drug Evaluation) [3] and ORBITA (Objective Randomized Blinded Investigation with optimal medical Therapy of Angioplasty in stable angina) [4] trials. However, the idea that sicker patients, with more disease or more ischemia, would do better with revascularization has not been questioned, as the high-risk population — patients with unprotected left main disease, impaired systolic function, heart failure, recent acute coronary syndromes and/or Canadian Cardiovascular Society class III or IV angina of recent onset — were quite reasonably excluded from the trial.

Amendments and limitations of eligibility criteria

The initial plan was to conduct an international, multi-center randomized trial in 8000 CCS patients, comparing early invasive management followed by routine revascularization with OMT and revascularization only in case of persistent symptoms or MI [5].

Address for correspondence: Marco Zimarino, MD, PhD, Institute of Cardiology, "G. d'Annunzio" University, c/o Ospedale SS. Annunziata, Via dei Vestini, 66013 Chieti, Italy, tel: +39-0871-41512, fax: +39-0871-402817, e-mail: mzimarino@unich.it

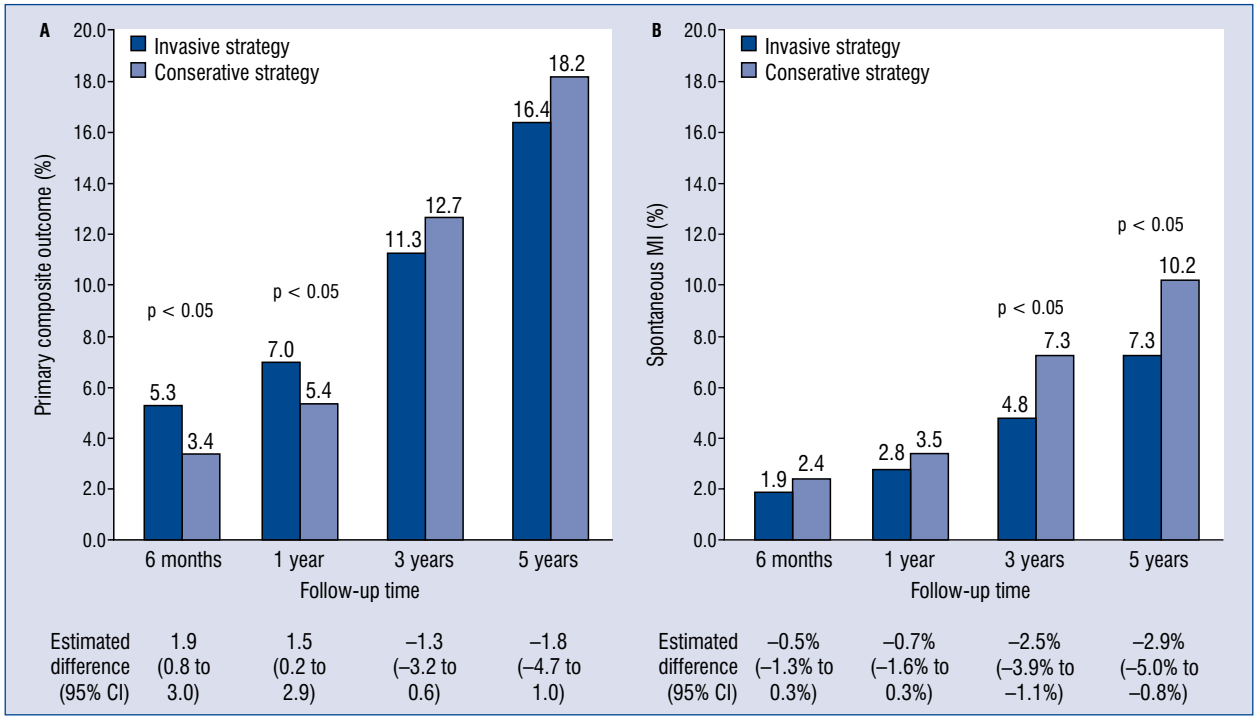

Figure 1. Clinical endpoints differences between treatment groups across a 5-year follow-up and relative estimated difference (95% confidence interval [CI]); **A.** Primary composite outcome; **B.** Spontaneous myocardial infarction (MI).

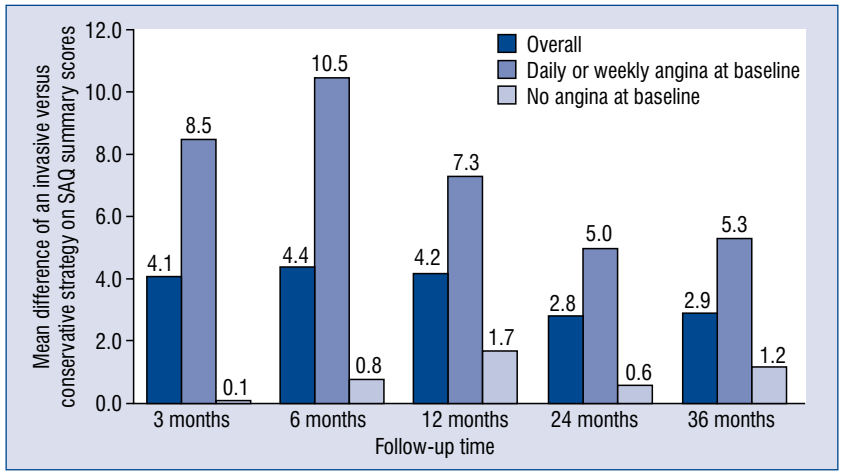

Figure 2. Effect of the invasive strategy on symptoms, estimated as the mean difference of invasive versus conservative strategy on Seattle Angina Questionnaire (SAQ) summary scores, according to baseline angina burden during 36 month follow-up.

This trial design was elegant and designed originally with hard primary endpoints, which would have offered a definitive answer. Randomization to conservative or invasive strategies was carried out after coronary computed tomographic angiographic (CCTA), before coronary angiography, thus preventing physicians from a withdrawing-bias in patients with lesions suitable for immediate stenting. The trial was started in July 2012, but investigators soon realized that the recruitment was slow and event rates lower than anticipated. Consequently, several substantial changes were applied to both the design and the primary endpoint to complete the trial.

The definition of the ischemic burden was central to the primary hypothesis, that extent and severity of ischemia are related to adverse outcomes in CCS, as documented in the COURAGE trial nuclear substudy [6], where patients with ischemia reduction had a lower risk of death or MI, mainly if baseline ischemia was moderate-to-severe (≥ 10% myocardium). The laudable intention that moved the ISCHEMIA investigators to enroll only patients with moderate-to-severe ischemia, having rigorous documentation by stress imaging assessment as single-photon emission computed tomography or stress-echocardiography or stress-cardiac magnetic resonance, was later aborted forcefully. In order to expedite recruitment, patients with a lesser amount of ischemia (≥ 5% myocardium) or with documentation of ischemia on the sole electrocardiogram-exercise test — a diagnostic modality with a much lower diagnostic sensibility — were deemed eligible, reaching the minimal threshold for the predefined power but tarnishing the original ambitious aim. Arguably, the severity of ischemia cannot be measured without imaging, and the lack of standardized grading and inconsistency in reporting of the extent and severity of ischemia across different stress imaging modalities raise major concerns on the accuracy of ischemic burden quantification and patient selection [7, 8]. Furthermore, according to the main study protocol, almost one-third of randomized patients with estimated glomerular filtration rate (eGFR) < 60 mL/min with a "high likelihood" of significant left main disease based on the results of the stress test did not undergo CCTA due to the risk of contrast-induced nephropathy. In this case, trial eligibility relied on the physician determination, carrying a subjective component in the diagnostic pathway and ultimately introducing another potential source of selection bias.

There is also a major concern about the over-interpretation of the ISCHEMIA trial design in clinical practice, where a problematic reading may result in extrapolating beyond the data provided in the study [9]. This is the case when advocating CCTA as the first-line strategy in all patients with chest pain, regardless of the pre-test likelihood of coronary artery disease (CAD) and demonstration of ischemia. In the ISCHEMIA trial, CCTA was primarily aimed at ruling out the presence of significant unprotected left main disease — but surprisingly not a proximal three-vessel disease — and to confirm the presence of obstructive CAD in patients with at least moderate ischemia. Claiming that CCTA should be performed at a population level where the prevalence of the left main disease is predictably low has the potential of exposing a significant number of patients to ionizing radiation and nephrotoxic contrast agents, when alternative and more cost-effective options are available [10, 11].

Finally, about 14% of patients enrolled failed to meet eligibility criteria for ischemia at a later core laboratory evaluation, but they were part of the study population anyway; this cohort showed a trend towards an increased benefit from the conservative strategy, further flawing the main findings of the study.

Changing the primary endpoint: A contingency plan

The ISCHEMIA trial was conducted in accordance with the most rigorous clinical trial standards, and investigators should be commended for preparing a contingency plan in case of lower than expected event rates for the original primary endpoint of cardiovascular death or MI. This prespecified back-up strategy was vital in avoiding a common pitfall of other trials, namely lower-than-projected power because of lower than anticipated event rates. It led to the 5-component endpoint, including cardiovascular death, MI, hospitalization for unstable angina, resuscitated cardiac arrest, or heart failure, as per the original grant proposal awarded by National Heart, Lung, and Blood Institute (NHLBI) in 2011 [8].

Accordingly, projections in 2015, using updated assumptions for the randomization rate and demonstrating an enrollment rate lagging behind timelines and lower than expected adverse events, suggested that the intended goals needed better calibration in favor of a more reasonable and pragmatic target. The sample size was therefore lowered by nearly 35% and the mean follow-up duration by 25% (from 4 to 3.2 years). However, activation of the contingency plan had a price to pay. Indeed, by dropping the prespecified power threshold below 90%, investigators were facing two alternatives: either reporting an underpowered trial with a negative prespecified primary outcome, or a potentially false-positive trial with "re-engineered" alternative outcomes [12].

For the multinational ISCHEMIA trial, conducted at 320 sites in 37 countries, investigators obtained 108 million USD from NHLBI, based on the recognition that trial results would have allowed saving of > 500 million USD/year from the reduction of unnecessary revascularization, clearly exceeding the public fund earmarked [12].

The publication of the trial spurred controversy among the scientific community [13].

As claimed by Antman and Braunwald [14], the most obvious conclusion is that the two strategies seem to have similar efficacy. At the same time, the patients in the invasive-strategy group reported substantially fewer angina symptoms than those in the conservative approach. However, the magnitude of this benefit depended on angina frequency at baseline, with 35% of cases being asymptomatic. Possible reasons for such similar findings are the low-risk of the study population and the potential effect of practice patterns that may have excluded more symptomatic patients. In the main trial, the incidence of the primary outcome was sensitive to the definition of MI, with a substantial prevalence of periprocedural MIs in the early follow-up favoring a conservative strategy and higher incidence of spontaneous MIs in a later course, when the invasive approach showed a protective effect. Investigators adjudicated MI employing a primary or secondary definition, the latter using references from the assay manufacturer's package insert and including contingencies to allow diagnosing MI despite whether they had various elements of the medical record missing. For spontaneous MI, investigators adopted the third universal definition of MI (types 1, 2, 4b, 4c), while for procedural MI (types 4a, 5) creatine kinase myocardial band (CK-MB) was the preferred biomarker and higher thresholds were used: (i) post-PCI, a rise in CK-MB > 5-fold the upper limit of normal (ULN) or a rise in troponin > 35-fold the ULN post-PCI; (ii) post-CABG, a rise in CK-MB > 10-fold the ULN or a rise in troponin > 70-fold the ULN post-PCI. Investigators adopted such thresholds with the aim of compensating for the reduced prognostic relevance of periprocedural as compared to spontaneous MI [15]. A similar controversy recently animated the presentation of the 5-year outcomes of the EXCEL (Evaluation of XIENCE versus Coronary Artery Bypass Surgery for Effectiveness of Left Main Revascularization) trial [16]. Finally, the adoption of a definition of periprocedural MI for both PCI and CABG based on CK rise > 10-fold the ULN or > 5-fold the ULN with new Q-waves, angiographic vessel occlusion, or loss of myocardium on imaging was strongly associated with increased 3-year mortality even after controlling for potential confounders [17].

In the ISCHEMIA trial, the invasive strategy was associated with a trend towards a reduced incidence of death from cardiovascular causes or MI (16.5% vs. 14.9%), as was the primary definition of the study, and a significant absolute risk reduction of 2.9% of spontaneous MI at 5 years (Fig. 1B) [1]. Antman and Braunwald [14] hypothesized as well that ISCHEMIA might have ended before a substantial difference in favor of the invasive strategy had emerged. As therapeutic benefits tend to wane at longer follow-up in aging populations, authors herein, respectfully disagree that prolonging of the study would have unveiled such a difference; nevertheless, by considering a calculated event rate of 3.3 per 100 person-years in the invasive group and of 3.8 per 100 person-years, with a type I error of 5% ($\alpha = 0.05$) and a statistical power of 80%, the study population should have been followed-up for 6.5 years overall. Alternatively, the same difference in the hard-end points would have been detected with a population of about 8000 patients per group, obviously requiring a far larger resource allocation for the trial.

Group comparisons were performed according to the intention-to-treat principle that counts crossovers within originally assigned groups, regardless of the treatment actually received. However, no adjustment for non-adherence to the randomized treatment strategy, such as censoring at the time of crossover, was considered as deemed susceptible to bias as per the study protocol. After randomization, 16% of patients in the invasive arm did not receive any revascularization, while 21% of patients in the conservative-strategy group underwent revascularization, therefore resulting in a bidirectional crossover likely driving potential underestimation of the actual long-term benefit of the invasive approach. However, the prespecified aim of the study was to test the initial management strategy, and, in this view, the intensity of crossover was acceptable despite an invasive approach, which was later pursued in more than one-fourth of the study population. Nevertheless, the intense crossover rate observed in ISCHEMIA, along with slow enrollment, would suggest that keeping an ischemic patient away from revascularization for quite a while can be somewhat tricky in the absence of a sham group as in ORBITA [4].

Special subgroups

Chronic kidney disease

Patients with advanced chronic kidney disease (CKD) have been systematically excluded or only marginally included in most trials on cardiovascular disease, thus preventing a confident estimation of treatment benefits [18]. Patients with advance CKD, defined as an eGFR < 30 mL/min/1.73 m^2 of

the body surface area or on dialysis, and moderate or severe myocardial ischemia were investigated in the ISCHEMIA-CKD (Management of Coronary Disease in Patients with Advanced Kidney Disease) trial [19]. In contrast with the main trial, the use of CCTA angiography was not recommended as a screening test because of the potential risk of acute kidney injury. Therefore, no core-laboratory was used for validation. After a median of 2.2-year follow-up, the primary endpoint — a composite of death and non-fatal MI — was similar in the two groups. The invasive arm experienced a higher incidence of non-procedural stroke and new dialysis initiation. Overall, ISCHEMIA findings have been confirmed even in the CKD population, pending a few considerations. Firstly, the exclusion of patients with reduced ejection fraction and/or refractory angina could have prevented the potential benefits of revascularization. Secondly, the selection of frail and comorbid patients with compromised status could be itself a proxy for futility, where mortality was high (27% at 3 years) in both subgroups, and coronary angiography not performed in 15% of the patients allocated in the invasive arm. Thirdly, selection criteria poorly identified ischemic patients amenable to revascularization, as in the invasive strategy group only 50% of patients underwent revascularization, and the absence of obstructive CAD was documented in one-quarter of the cohort. Beyond confirming the poor outcome of patients with CKD, ISCHEMIA-CKD results highlighted the modest positive predictive value of stress testing for the detection of obstructive epicardial CAD, while suggesting a high prevalence and prognostic significance of coronary microvascular disease in CKD patients with CCS [20].

Ischemia with no obstructive coronary artery disease

Almost 20% of screened patients were excluded from the ISCHEMIA trial for the absence of clear imaging evidence of obstructive coronary disease by CCTA. If they were complaining of ischemic symptoms, they merged into the aligned CIAO-ISCHEMIA (Changes in Ischemia and Angina over One year among ISCHEMIA) trial. Although not yet available in a full-length manuscript, these data were recently presented at the American College of Cardiology 2020 Scientific Session [21], enquire an interesting target population, with a high prevalence of women (66% in CIAO-ISCHEMIA compared with 26% in ISCHEMIA with obstructive CAD, $p < 0.001$). Despite controversial data, such patients now seem to portend a heterogeneous but in general benign prognosis, similar to that of the general population, with the presence of "some" coronary atherosclerosis being the main outcome determinant [22]. However, CIAO-ISCHEMIA was designed to test changes in ischemia and angina symptoms in the population of ischemia and no obstructive coronary artery disease (INOCA) and is not powered to test hard cardiovascular events. At 1 year, in patients in CIAO-ISCHEMIA, stress echocardiograms became normal in about half of patients, and in 45% of cases, they were the same as at baseline or worse. Angina symptoms improved in 42% and worsened in 14% of patients, and the number of medications to control angina on average remained the same. Interestingly, the change in stress test findings and the change in symptoms over 1 year were not related. These findings seem to reject the hypothesis that the extent of myocardial ischemia is responsible for angina in INOCA patients, suggesting that unmeasured determinants would contribute to patient symptoms, possibly including sensory, emotional, autonomic, motor, cognitive and other sex-related components. Again, the association among angina, coronary atherosclerosis and myocardial ischemia has confirmed to be exceedingly elusive.

The extent of revascularization in multivessel coronary artery disease

Since the benefit of revascularization is directly proportional to the extent of ischemia and of the atherothrombotic burden provoking it, then the management of patients with multivessel CAD should be prioritized. In this cohort, there is extensive evidence that complete revascularization confers a more considerable clinical benefit [23], mostly when performed with state-of-the-art techniques, namely second or third generation drug-eluting stent (DES) and extensive use of arterial conduits for CABG [24]. However, while complete revascularization has outlined a relevant advantage in the setting of an acute coronary syndrome, such benefit has not yet been proven in CCS. The ISCHEMIA trial would have been a milestone in this view. A comprehensive definition of the adequacy of myocardial revascularization should take into account the size of the vessel, the severity of the lesion, the ischemic burden caused by the lesion, and the viability of the depending myocardial territory [25]. The quality of the design in the ISCHEMIA trial is also evidenced by the availability of two separate flow-charts, to guide the invasive strategy in both imaging and non-imaging subgroups. The use of fractional flow reserve was strongly recommended [26, 27], and most of the revascu-

larization procedures were performed according to best practice evidence, with > 90% last-generation DES for PCI and internal mammary arteries for CABG [1]. The benefit of the invasive approach, albeit still not significant, was proportional to the extent of CAD. Unfortunately, details regarding the adequacy and methods of revascularization are yet not available, and the scientific community yearningly awaits such data for further argumentations. As an example, it would be interesting to know the prevalence of bifurcations and chronic total occlusions on the total amount of PCI performed in both conservative and invasive strategy groups [28], as lesion complexity seems to affect periprocedural and long-term outcomes [29, 30], and to have a relevant implication on the subsequent dual antiplatelet therapy [31, 32] as well. Similarly, the complexity of the revascularization treatment might have affected the outcome [33].

In this view, the dataset deriving from the ISCHEMIA trial would be extremely valuable to explore the impact of lesion complexity and the optimal duration of antiplatelet therapy on the outcome.

Conclusions

The ISCHEMIA trial highlighted many challenges that cardiologists experience during their daily practice in the diagnosis and management of CCS, and it also delivered reassurance that for patients with at least moderate ischemia and acceptable symptoms who meet the trial criteria, invasive management may be reasonably deferred during optimal titration of OMT. While an extended follow-up of the ISCHEMIA trial would be highly informative and as new cardiac imaging techniques for fully-quantitative assessment of myocardial perfusion appear on the horizon, further prospective research should investigate whether longitudinal changes in adverse coronary plaque characteristics and whether ischemic burden associated with more intensive treatment would reduce the risk of ischemic events.

While guidelines continue to suggest that revascularization should be offered at an earlier stage to patients with the highest ischemia burden [34], the question of whether ischemia truly matters and how revascularization affects outcomes remains unsolved [35].

The view herein, holds that the legacy of the ISCHEMIA trial is two-fold: firstly, reiterating the crucial value of randomized controlled trials, which must be done before hypotheses become false certainties; secondly, recalling the "courage" to follow a pathway, once it has been designed, without hesitation, regardless the expected effects.

Conflict of interest: None declared

References

1. Maron D, Hochman J, Reynolds H, et al. Initial invasive or conservative strategy for stable coronary disease. N Engl J Med. 2020; 382(15): 1395–1407, doi: 10.1056/nejmoa1915922.
2. Spertus J, Jones P, Maron D, et al. Health-Status Outcomes with Invasive or Conservative Care in Coronary Disease. N Engl J Med. 2020; 382(15): 1408–1419, doi: 10.1056/nejmoa1916370.
3. Boden WE, O'Rourke RA, Teo KK, et al. COURAGE Trial Research Group. Optimal medical therapy with or without PCI for stable coronary disease. N Engl J Med. 2007; 356(15): 1503–1516, doi: 10.1056/NEJMoa070829, indexed in Pubmed: 17387127.
4. Al-Lamee R, Thompson D, Dehbi HM, et al. ORBITA investigators. Percutaneous coronary intervention in stable angina (ORBITA): a double-blind, randomised controlled trial. Lancet. 2018; 391(10115): 31–40, doi: 10.1016/S0140-6736(17)32714-9, indexed in Pubmed: 29103656.
5. Maron DJ, Hochman JS, O'Brien SM, et al. ISCHEMIA Trial Research Group. International Study of Comparative Health Effectiveness with Medical and Invasive Approaches (ISCHEMIA) trial: Rationale and design. Am Heart J. 2018; 201: 124–135, doi: 10.1016/j.ahj.2018.04.011, indexed in Pubmed: 29778671.
6. Shaw LJ, Berman DS, Maron DJ, et al. COURAGE Investigators. Optimal medical therapy with or without percutaneous coronary intervention to reduce ischemic burden: results from the Clinical Outcomes Utilizing Revascularization and Aggressive Drug Evaluation (COURAGE) trial nuclear substudy. Circulation. 2008; 117(10): 1283–1291, doi: 10.1161/CIRCULATIONAHA.107.743963, indexed in Pubmed: 18268144.
7. Shaw LJ, Berman DS, Picard MH, et al. Comparative definitions for moderate-severe ischemia in stress nuclear, echocardiography, and magnetic resonance imaging. JACC Cardiovasc Imaging. 2014; 7(6): 593–604, doi: 10.1016/j.jcmg.2013.10.021, indexed in Pubmed: 24925328.
8. Maron D, Harrington R, Hochman J. Planning and Conducting the ISCHEMIA Trial. Circulation. 2018; 138(14): 1384–1386, doi: 10.1161/circulationaha.118.036904.
9. Shaw L, Nagel E, Salerno M, et al. Cardiac Imaging in the Post ISCHEMIA Trial Era - A Multi Society Viewpoint. JACC: Cardiovasc Imaging. 2020.
10. Jang JJ, Bhapkar M, Coles A, et al. PROMISE Investigators. Predictive model for high-risk coronary artery disease. Circ Cardiovasc Imaging. 2019; 12(2): e007940, doi: 10.1161/CIRCIMAGING.118.007940, indexed in Pubmed: 30712364.
11. Ge Y, Pandya A, Steel K, et al. Cost-Effectiveness analysis of stress cardiovascular magnetic resonance imaging for stable chest pain syndromes. JACC Cardiovasc Imaging. 2020; 13(7): 1505–1517, doi: 10.1016/j.jcmg.2020.02.029, indexed in Pubmed: 32417337.
12. Murthy VL, Eagle KA. ISCHEMIA: A Search for clarity and why we may not find it. Am Heart J. 2018; 203: 82–84, doi: 10.1016/j.ahj.2018.03.031, indexed in Pubmed: 30048826.
13. Cortés C, Johnson TW, Silber S, et al. ISCHEMIA trial: The long-awaited evidence to confirm our prejudices. Cardiol J. 2020; 27(4): 336–341, doi: 10.5603/CJ.2020.0109.

14. Antman EM, Braunwald E. Managing stable ischemic heart disease. N Engl J Med. 2020; 382(15): 1468–1470, doi: 10.1056/NEJMe2000239, indexed in Pubmed: 32227752.
15. Koskinas KC, Ndrepepa G, Räber L, et al. Prognostic impact of periprocedural myocardial infarction in patients undergoing elective percutaneous coronary interventions. Circ Cardiovasc Interv. 2018; 11(12): e006752, doi: 10.1161/CIRCINTERVENTIONS.118.006752, indexed in Pubmed: 30545257.
16. Stone G, Kappetein A, Sabik J, et al. Five-year outcomes after PCI or CABG for left main coronary disease. N Engl J Med. 2019; 381(19): 1820–1830, doi: 10.1056/nejmoa1909406.
17. Ben-Yehuda O, Chen S, Redfors B, et al. Impact of large periprocedural myocardial infarction on mortality after percutaneous coronary intervention and coronary artery bypass grafting for left main disease: an analysis from the EXCEL trial. Eur Heart J. 2019; 40(24): 1930–1941, doi: 10.1093/eurheartj/ehz113, indexed in Pubmed: 30919909.
18. Zannad F, Rossignol P. Cardiovascular outcome trials in patients with advanced kidney disease: time for action. Circulation. 2017; 135(19): 1769–1771, doi: 10.1161/CIRCULATIONAHA.117.027338, indexed in Pubmed: 28483826.
19. Bangalore S, Maron DJ, O'Brien SM, et al. ISCHEMIA-CKD Research Group. Management of coronary disease in patients with advanced kidney disease. N Engl J Med. 2020; 382(17): 1608–1618, doi: 10.1056/NEJMoa1915925, indexed in Pubmed: 32227756.
20. Bajaj NS, Singh A, Zhou W, et al. Coronary microvascular dysfunction, left ventricular remodeling, and clinical outcomes in patients with chronic kidney impairment. Circulation. 2020; 141(1): 21–33, doi: 10.1161/CIRCULATIONAHA.119.043916, indexed in Pubmed: 31779467.
21. Reynolds HR. Natural history of symptoms and stress echo findings in patients with moderate or severe ischemia and no obstructive CAD (INOCA): the NHLBI-funded CIAO ancillary study to the ISCHEMIA trial. ACC 2020, March 30, 2020.
22. Radico F, Zimarino M, Fulgenzi F, et al. Determinants of long-term clinical outcomes in patients with angina but without obstructive coronary artery disease: a systematic review and meta-analysis. Eur Heart J. 2018; 39(23): 2135–2146, doi: 10.1093/eurheartj/ehy185, indexed in Pubmed: 29688324.
23. Garcia S, Sandoval Y, Roukoz H, et al. Outcomes after complete versus incomplete revascularization of patients with multivessel coronary artery disease: a meta-analysis of 89,883 patients enrolled in randomized clinical trials and observational studies. J Am Coll Cardiol. 2013; 62(16): 1421–1431, doi: 10.1016/j.jacc.2013.05.033, indexed in Pubmed: 23747787.
24. Zimarino M, Ricci F, Romanello M, et al. Complete myocardial revascularization confers a larger clinical benefit when performed with state-of-the-art techniques in high-risk patients with multivessel coronary artery disease: A meta-analysis of randomized and observational studies. Catheter Cardiovasc Interv. 2016; 87(1): 3–12, doi: 10.1002/ccd.25923, indexed in Pubmed: 25846673.
25. Zimarino M, Curzen N, Cicchitti V, et al. The adequacy of myocardial revascularization in patients with multivessel coronary artery disease. Int J Cardiol. 2013; 168(3): 1748–1757, doi: 10.1016/j.ijcard.2013.05.004, indexed in Pubmed: 23742927.
26. Lee HS, Lee JM, Nam CW, et al. Consensus document for invasive coronary physiologic assessment in Asia-Pacific countries. Cardiol J. 2019; 26(3): 215–225, doi: 10.5603/CJ.a2019.0054, indexed in Pubmed: 31225632.
27. Gutiérrez-Chico JL, Chen Y, Yu W, et al. Diagnostic accuracy and reproducibility of optical flow ratio for functional evaluation of coronary stenosis in a prospective series. Cardiol J. 2020; 27(4): 350–361, doi: 10.5603/CJ.a2020.0071, indexed in Pubmed: 32436590.
28. Gutiérrez-Chico JL, Louvard Y. DECISION-CTO: A „negative" clinical trial? Really? Cardiol J. 2017; 24(3): 231–233, doi: 10.5603/CJ.a2017.0049, indexed in Pubmed: 28417448.
29. Zimarino M, Briguori C, Amat-Santos IJ, et al. Mid-term outcomes after percutaneous interventions in coronary bifurcations. Int J Cardiol. 2019; 283: 78–83, doi: 10.1016/j.ijcard.2018.11.139, indexed in Pubmed: 30528620.
30. Werner GS, Martin-Yuste V, Hildick-Smith D, et al. EUROCTO trial investigators. A randomized multicentre trial to compare revascularization with optimal medical therapy for the treatment of chronic total coronary occlusions. Eur Heart J. 2018; 39(26): 2484–2493, doi: 10.1093/eurheartj/ehy220, indexed in Pubmed: 29722796.
31. Giustino G, Chieffo A, Palmerini T, et al. Efficacy and Safety of Dual Antiplatelet Therapy After Complex PCI. J Am Coll Cardiol. 2016; 68(17): 1851–1864, doi: 10.1016/j.jacc.2016.07.760, indexed in Pubmed: 27595509.
32. Zimarino M, Renda G, De Caterina R. Optimal duration of antiplatelet therapy in recipients of coronary drug-eluting stents. Drugs. 2005; 65(6): 725–732, doi: 10.2165/00003495-200565060-00001, indexed in Pubmed: 15819586.
33. Zimarino M, Corcos T, Favereau X, et al. Rotational coronary atherectomy with adjunctive balloon angioplasty for the treatment of ostial lesions. Cathet Cardiovasc Diagn. 1994; 33(1): 22–27, doi: 10.1002/ccd.1810330106, indexed in Pubmed: 8001097.
34. Neumann FJ, Sousa-Uva M, Ahlsson A, et al. 2018 ESC/EACTS Guidelines on myocardial revascularization. Eur Heart J. 2019; 40(2): 87–165.
35. Al-Lamee R, Jacobs AK. The ISCHEMIA Trial: Was it Worth the Wait? Circulation. 2020 [Epub ahead of print], doi: 10.1161/CIRCULATIONAHA.120.045007, indexed in Pubmed: 32316761.

VIA MEDICA

EDITORIAL

Cardiology Journal
2020, Vol. 27, No. 4, 336–341
DOI: 10.5603/CJ.2020.0109

ISSN 1897–5593

ISCHEMIA trial: The long-awaited evidence to confirm our prejudices

Carlos Cortés[1]*, Thomas W. Johnson[2]*, Sigmund Silber[3]*, Piotr P. Buszman[4], Tudor C. Poerner[5], Francesco Lavarra[6], Borja Ibáñez[7, 8, 9], Yongcheol Kim[10], Karl Mischke[11], Miłosz Jaguszewski[12], Juan Luis Gutiérrez-Chico[13]

[1]San Pedro Hospital, Logroño, Spain
[2]Department of Cardiology, Bristol Heart Institute, Bristol, United Kingdom
[3]Cardiology Practice and Cath Labs, München, Germany
[4]Cardiology Department, Andrzej Frycz-Modrzewski Krakow University, American Heart of Poland, Bielsko-Biala, Poland
[5]Marienhospital, Aachen, Germany
[6]Jilin Heart Hospital, Changchun, China
[7]Centro Nacional de Investigaciones Cardiovasculares (CNIC), Madrid, Spain
[8]IIS-Fundación Jiménez Díaz, Madrid, Spain
[9]CIBERCV, Madrid, Spain
[10]Yonsei University College of Medicine and Yongin Severance Hospital, Yongin, Republic of Korea
[11]Leopoldina Hospital, Schweinfurt, Germany
[12]First Department of Cardiology, Medical University of Gdansk, Poland
[13]Cardio Care Heart Center, Marbella, Spain

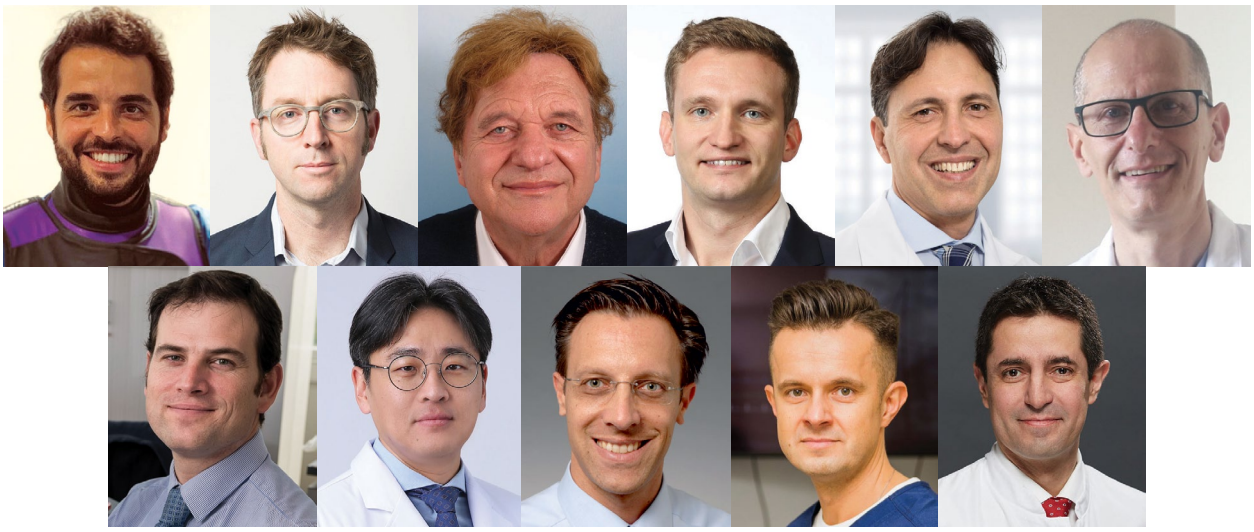

Address for correspondence: Prof. Juan Luis Gutiérrez-Chico, MD, PhD, FESC, FACC, Cardio Care Heart Center, Ventura del Mar 11, 29660 – Marbella, Spain, tel: +34 615 319370, e-mail: juanluis.gutierrezchico@ictra.es

**These authors have equally contributed.*

Introduction

In April 2020 the results of the ISCHEMIA trial were finally fully published [1]. Few trials have triggered such a level of controversy and dispute among cardiologists and cardiac surgeons since its oral presentation at American Heart Association Congress 2019. Some colleagues have heralded the study as the terminator of elective percutaneous coronary intervention (PCI) in patients with chronic coronary syndrome (CCS), while others have speculated about the negligible role left for functional testing, which could be relegated to practical irrelevance after the trial consecrated coronary computed tomography angiography (CCTA) as the gate-keeper of diagnostic workflow, a trend already consolidated in the latest iteration of the guidelines of the European Society of Cardiology [2]. The prompt reaction came as no surprise from all challenged sectors: interventional cardiologists offered their own interpretation of the results, of course diametrically opposed to the one endorsed by their conservative nemesis. Likewise, non-invasive cardiologists articulated the defence of functional tests, advocating their clinical and logistic advantages to counterbalance the threat of the unrelenting CCTA. Symposia and social media have provided a platform for passionate discussions about the future of cardiology after ISCHEMIA, but the bloodiest combats are by far those related to the indications of PCI in patients with CCS.

Why is this happening? Niccolò Machiavelli advised the young Lorenzo de' Medici to be merciless in punishing the rebellion of his rivals, but always respecting their properties, because "*Men sooner forget the death of their father than the loss of their patrimony*" (Il principe) [3]. ISCHEMIA is directly threatening the patrimony (i.e., the modus vivendi, the areas of expertise, the source of prestige) of many heart specialists, who now feel compelled to defend it at any cost. Add to this, the classical rivalry between conservative and interventional cardiologists, fed with envy and resentment regarding the uneven distribution of resources, the mean attitude of the clinical gatekeeper, the arrogant demeanour of interventional colleagues in the discussion of a patient's therapy, etc. (multiple arguments brandished worldwide, even in the most balanced cardiovascular institutes, for years) and the explosive cocktail will be served. **For those resentful of interventional cardiologists and heart surgeons, the least excuse to bash their rivals will always be welcomed; whilst for passionate interventional cardiologists, no study is ever going to dissuade them from stenting. Each one's prejudices will ever prevail, regardless of the evidence.** Let us now make a balanced, scientific, neutral and critical review of the facts from ISCHEMIA, so we can glimpse the truth and better understand the optimal therapeutic options for patients with CCS. As authors a common disclosure is interventional cardiology, but we all share an aspiration for patient-focused care, delivered by a comprehensive team approach, as evidenced by our respective career paths.

Summary of the trial

The ISCHEMIA trial randomized 5179 patients with moderate or severe ischemia on functional testing to an initial invasive (coronary angiography and eventual revascularization) vs. an initial conservative strategy (optimal medical therapy alone): n = 2588 and 2591, respectively. Myocardial ischemia was proven in 75.5% with stress imaging methods (49.6% nuclear, 20.9% echo, 5.0% cardiac magnetic resonance) and in 24.5% with an exercise tolerance test. Following confirmation of ischemia, CCTA was performed to rule out left main (LM) stenosis or non-obstructive coronary artery disease (CAD) [4, 5]. After a median follow-up of 3.2 years, there was no significant difference in the primary endpoint, a composite of cardiac death, non-fatal myocardial infarction (MI) and hospitalization for unstable angina, heart failure or resuscitated cardiac arrest [1]. **Contrary to many other trials, the need for revascularization was left out of the primary outcome**, as the trial tested the initial strategy, rather than clinical benefit of revascularization itself. Within the conservative arm, 26% of patients eventually underwent coronary angiography ("cross-over"), 21% revascularization and 15% were revascularized before the occurrence of an event. Furthermore, 26% of the revascularizations in the invasive arm were surgically performed. These results were interpreted as no clear advantage of an early invasive strategy for the reduction of major clinical endpoints in patients with CCS. Nonetheless, the invasive arm reported significantly better quality of life (QoL) than the conservative arm, particularly in patients who were symptomatic at the time of randomization, results not replicated in asymptomatic patients [6].

…and the winner is…

Clinical trials risk being interpreted in the same way as a soccer match: one arm wins or the match results in a tie. This is a risky oversimplification

of such a precious collection of data, disregarding lots of meaningful information extending beyond a mere p-value [7]. However, it is unavoidable, as cardiologists do not usually have the time or the capacity to "deep dive" into every scientific report, particularly on topics far from their areas of expertise. Therefore, a simple 'soccer-style' report is likely to provide a take-home-message. Thousands of examples can be found concerning the ISCHEMIA trial on social media: invasive strategy won, invasive strategy lost, etc. For those who bet for one strategy, ISCHEMIA has calculated their error likelihood: those arguing against the invasive strategy have a 24.5% probability of being wrong, while those arguing against the conservative strategy have a 0.1% probability of being wrong (results of the Bayesian analysis) [1].

Although the authors conclude that there is no significant difference between the strategies, the data deserve careful attention.

1. The conclusion cannot be applied to important groups of patients excluded from the trial:
   - CCS and LM stenosis;
   - CCS with no proof of myocardial ischemia;
   - CCS with very severe ischemia (e.g. fall in blood pressure, very limited functional capacity) were not likely enrolled by sites;
   - CCS with an unacceptable degree of angina;
   - CCS and left ventricular ejection fraction < 35%;
   - CCS and heart failure New York Heart Association (NYHA) III/IV;
   - CCS and valvular disease.
2. Periprocedural MI had a heavy weight on the final results, however no data have been presented so far differentiating periprocedural MI between PCI and coronary bypass surgery.
3. The study was burdened with slow recruitment and a lower-than-expected incidence of events. When this happens, the suspicion of possible selection bias always overshadows the results. In fact, the initial sample size calculated that 8000 patients would be required to reach the primary endpoint, but had to be reduced to the final 5179 due to difficulties with enrolment.
4. Furthermore, a number of critical variables were unevenly distributed between the groups, in favour of less risk within the conservative arm. The invasive arm had numerically more heart failure (4.3% vs. 3.6%, p = 0.207), stroke (3.2% vs. 2.6%, p = 0.219), cerebrovascular disease (7.8% vs. 6.8%, p = 0.194), peripheral artery disease (4.5% vs. 3.4%, p = 0.049) and were more symptomatic (daily or weekly angina at randomization 21.7% vs. 18.9%, p = 0.049). Of note, the difference in the last two variables was statistically significant. Although this may happen by chance, even after perfect randomization, this observation raises suspicion of selection/allocation bias and has a potential impact on the outcome, disadvantaging the invasive arm.
5. The most powerful argument is however the evolution of the event-curves. For the primary outcome it seems clear that **the initial invasive strategy pays a higher price early, mainly at the expense of a higher incidence of periprocedural MI, but then the invasive management confers an advantage for the event-free survivors over those treated with a conservative strategy**. The slope of the curve flattens in the invasive arm compared with the conservative arm, and the curves intersect at approximately 2 years of follow-up. With continued divergence to **the 4th year of follow-up when the differences in the primary outcome become statistically significant: 13.3% vs. 15.5% in the invasive and conservative arms, respectively**. However, the final report is non-significant. How is this possible? From a statistical point of view there are just two possibilities: 1) either the trends in the curves change after the 4th year or 2) the sample size gets considerably reduced, thus becoming underpowered to prove statistical significance. Looking at the chart, the curves seem to run parallel, but the number at risk reduces from 1463 at 4 years to just 564 at 5 years (a reduction by almost two thirds). This cannot be justified by the number of events. Therefore, the second option (reduction of the sample size) seems the most plausible explanation for the final lack of statistical significance. Keep in mind that the primary endpoint is reported as Cox regression, that takes into account the whole-time range, and the median follow-up is 3.2 years (the study was initially planned for 4 years). Therefore, the primary endpoint in ISCHEMIA reports just a Kaplan-Meier estimate, instead of a truncated follow-up, even for all patients. Actually, in the appendix the hazard rates of all endpoints continue diverging in favour of the invasive strategy [1]. **This confirms that more patients need follow-up for a longer time to report a statistically sig-**

nificant difference in favour of the invasive strategy. The authors calculated the Bayesian likelihood to reach this statistically significant difference, maybe to justify the publication at this point, but still the interventional community will be looking forward to the results following additional follow-up.

The same phenomenon is observed with other hard composite endpoints (cardiovascular death + non-fatal MI; non-fatal MI alone): initially a higher incidence in the invasive arm (due to more peri-procedural MI), followed by a flatter slope than the conservative arm; intersection of the curves at 2 years and statistically significant difference at 4 years. To be precise, non-fatal MI shows the same trend, but it does not reach statistical significance as a separate variable. However, **the incidence of non-procedural MI is significantly higher in the conservative arm** (information available in the supplements). This is in line with results of preceding trials on the topic [8].

In summary, it can be argued whether there is a winner, but it is obvious that an invasive strategy is effective.

Concern in the departments of dermatology worldwide

Those who have strongly advocated for the curtailment of interventional labs for patients with CCS in the post-ISCHEMIA era, must also **keep in mind the superior QoL of the initial invasive strategy in symptomatic patients [6].** Many interventions and medical therapies aim to improve QoL, rather than to reduce major cardiovascular endpoints. This might seem a modest goal, but, for example, the revascularization of chronic total occlusions is justified by the clear improvement in QoL [9], while the benefit in hard endpoints is debatable [7, 10]. Actually, some medical specialties, like dermatology, are almost fully dedicated to the relief of symptoms and the improvement of QoL. Should they worry about the results of ISCHEMIA? Following the rationale of some PCI-haters, the closure of cathlabs post-ISCHEMIA, as a consequence of an unclear reduction in major cardiovascular events, should be mirrored by the restriction of activity of dermatologists to their oncological interventions and the treatment of pemphigus. After an informal survey, dermatologists do not seem concerned at all, maybe because they have not forgotten that their **duty as physicians is also relieving symptoms and improving the quality of life of their patients.**

Back to anatomy in times of physiology

The scenario depicted by some colleagues for CAD after the ISCHEMIA trial elicits some concerns about the role left for physiology. ISCHEMIA used CCTA as gate-keeper, to rule out LM stenosis or non-obstructive CAD. If it is accepted that neither the management strategy nor the level of ischemia in functional tests make any difference on the outcome, then the role left for functional tests would be negligible. Consequently, we would rely on a purely anatomical assessment, an approach whose limitations have been extensively documented previously [11, 12]. ISCHEMIA attempted to incorporate intracoronary physiology into the decision tree within the invasive arm, however, the methodology and realities of investigation were far removed from the evidence-base and current guideline recommendations [13]. This might partially explain the differences in outcome between the ISCHEMIA trial and other physiology-guided trials in patients with CCS [14]. The interventionists' willingness to 'react' to the angiographic anatomy in the light of non-invasive ischemia testing could often result in a suboptimal or even inappropriate interventional approach, at odds with the findings achieved through physiology-guidance, which undoubtedly remains the invasive gold standard to optimize clinical outcomes [14]. Conversely, apparently mild angiographic lesions may have functional significance [15]. These cases may have been denied revascularization in this trial based on the results of computed tomography and angiography [15]. This is a clear step backward. We are still learning about the limitations of anatomy to guide the decision-making in CCS. Stenosis is only one factor contributing to the functional relevance of the lesion and many other epicardial and microcirculatory factors must be considered [16]. The beauty of physiology is integrating all these factors to give the operator meaningful directions to take the best therapeutic decision. Interventional cardiology is constantly evolving and must continue progressing in the direction of physiology-guidance. This is in line with the growing interest in research funding programs for precision medicine. The era of personalized medicine and precision-PCI must not be derailed by a return to an 'out-dated' anatomical assessment and a uniform "prêt-à-porter" strategy. Patients as individuals should be granted individual answers to their medical problems. Interventional cardiology must continue moving toward personalized medicine and away from a "one-size-fits-all"

strategy. The debate is indeed quite old. The COURAGE trial already challenged the role of PCI for CCS [17] in 2007. However, the FAME trials definitively proved the benefit of PCI in CCS, if performed under physiology guidance [12, 14]. In the ISCHEMIA trial, 20.3% of interventions were physiology-guided, and although exceeding the average global usage in routine clinical practice [18], this falls below current recommendations [13, 19].

Attention to the subgroup analysis

A careful analysis of the subgroups is also very educational [20]. Let us remember that subgroup analyses do not necessarily require a statistically significant value. They rather intend to detect trends in order to better understand the results or to generate hypotheses that can be properly tested in future studies. Firstly, subgroup analysis suggests that the degree of ischemia does play a role. The more ischemia, the greater the advantage of an invasive strategy. This trend is consistently observed in the results stratified by degree of baseline ischemia, number of diseased vessels and involvement of the proximal left anterior descending artery. This observation eases the interpretation of the results from a pathophysiological point of view. The study actually ruled out LM disease, the lesion with greatest ischemic burden and most myocardium at jeopardy, because it was deemed unethical to deny revascularization to those patients.

However, it is puzzling to observe that patients with new-onset or worsening angina over the preceding 3 months benefit less from an invasive strategy than the subgroup with a stable profile. This observation highlights the difficulty in obtaining an accurate assessment of symptoms. A patients' perception of their own disease is extremely variable, combined with significant variability in a physicians' interpretation of symptoms, thus challenging the reproducibility of results. All medical schools worldwide emphasise the importance of clinical anamnesis, because otherwise students and future doctors would tend to rely on diagnostic tests instead of talking to the patient, who must always remain the main focus. The anamnesis is critical to humanise medicine, to preserve its most intimate essence, but it is too inaccurate in building solid scientific evidence.

Conclusions

In line with Socratic dialog, knowledge is advanced by a questioning approach: 1) Why did the investigators plan a covariate-adjusted Cox analysis? A randomized trial of that size would not need to adjust for any covariate. Which covariates were then introduced for the adjustment? 2) The statistical decision to use non-parametric tests in a trial with 5179 patients was perhaps not so convincing for all the experts. 3) Why were 111 patients in the invasive arm not revascularized because their anatomy was "not suitable for any kind of revascularisation"? This means 4.3% of the invasive group and 26.4% of the patients not revascularized in that group? Is this representative of current state-of-the-art? Etcetera. We would never finish. While we wait for further data of the curve separation to confirm our interpretation we should agree that the ISCHEMIA trial has given a clear signal of the beneficial effect of an early invasive strategy in patients with CCS: significant improvement in QoL and reduction of non-procedural MI, together with a trend to the reduction of cardiovascular mortality. However, the invasive management pays a price in terms of peri-procedural MIs, thus the comparison starts at a disadvantage. At 2 years the curves cross-over and at 4 years the difference is statistically significant in favour of an invasive strategy. However, the Cox analysis does not reach statistical significance because the number at risk is dramatically reduced (by two-thirds) after 4 years. More patients or a longer follow-up would be required to prove the superiority of an invasive strategy.

Conversely, the advantage of an invasive strategy is less than the interventional cardiologists used to think, so an initial conservative approach might be a reasonable alternative in selected patients [21]. Likewise, the benefit of revascularization in asymptomatic patients is unclear and difficult to justify after ISCHEMIA for prognostic reasons. All these questions will require specific answers in the future, always keeping in mind that coronary interventions are moving toward physiology guidance and precision medicine [22], rather than relying on the haziness of symptoms and the misleading nature of anatomy.

Conflict of interest: None declared

References

1. Maron D, Hochman J, Reynolds H, et al. Initial Invasive or Conservative Strategy for Stable Coronary Disease. N Engl J Med. 2020; 382(15): 1395–1407, doi: 10.1056/nejmoa1915922.
2. Knuuti J, Wijns W, Saraste A, et al. 2019 ESC Guidelines for the diagnosis and management of chronic coronary syndromes. Eur Heart J. 2020; 41: 407–477, doi: 10.1093/eurheartj/ehz425, indexed in Pubmed: 31504439.

3. Machiavelli, Niccolò, 1469-1527. The prince. Reprinted with revisions 1984. Harmondsworth, Eng.; New York, NY: Penguin Books; 1981. Available at: https://search.library.wisc.edu/catalog/999715970702121.
4. Maron DJ, Hochman JS, O'Brien SM, et al. ISCHEMIA Trial Research Group. International Study of Comparative Health Effectiveness with Medical and Invasive Approaches (ISCHEMIA) trial: Rationale and design. Am Heart J. 2018; 201: 124–135, doi: 10.1016/j.ahj.2018.04.011, indexed in Pubmed: 29778671.
5. Hochman JS, Reynolds HR, Bangalore S, et al. ISCHEMIA Research Group. Baseline Characteristics and Risk Profiles of Participants in the ISCHEMIA Randomized Clinical Trial. JAMA Cardiol. 2019; 4(3): 273–286, doi: 10.1001/jamacardio.2019.0014, indexed in Pubmed: 30810700.
6. Spertus JA, Jones PG, Maron DJ, et al. ISCHEMIA Research Group. Health-Status Outcomes with Invasive or Conservative Care in Coronary Disease. N Engl J Med. 2020; 382(15): 1408–1419, doi: 10.1056/NEJMoa1916370, indexed in Pubmed: 32227753.
7. Gutiérrez-Chico JL, Louvard Y. DECISION-CTO: A "negative" clinical trial? Really? Cardiol J. 2017; 24(3): 231–233, doi: 10.5603/CJ.a2017.0049, indexed in Pubmed: 28417448.
8. Bangalore S, Maron D, Stone G, et al. Routine revascularization versus initial medical therapy for stable ischemic heart disease: a systematic review and meta-analysis of randomized trials. Circulation. 2020, doi: 10.1161/circulationaha.120.048194.
9. Werner GS, Martin-Yuste V, Hildick-Smith D, et al. EUROCTO trial investigators. A randomized multicentre trial to compare revascularization with optimal medical therapy for the treatment of chronic total coronary occlusions. Eur Heart J. 2018; 39(26): 2484–2493, doi: 10.1093/eurheartj/ehy220, indexed in Pubmed: 29722796.
10. Lee SW, Lee PH, Ahn JM, et al. Randomized trial evaluating percutaneous coronary intervention for the treatment of chronic total occlusion. Circulation. 2019; 139(14): 1674–1683, doi: 10.1161/CIRCULATIONAHA.118.031313, indexed in Pubmed: 30813758.
11. Toth GG, Toth B, Johnson NP, et al. Revascularization decisions in patients with stable angina and intermediate lesions: results of the international survey on interventional strategy. Circ Cardiovasc Interv. 2014; 7(6): 751–759, doi: 10.1161/CIRCINTERVENTIONS.114.001608, indexed in Pubmed: 25336468.
12. Tonino PAL, De Bruyne B, Pijls NHJ, et al. FAME Study Investigators. Fractional flow reserve versus angiography for guiding percutaneous coronary intervention. N Engl J Med. 2009; 360(3): 213–224, doi: 10.1056/NEJMoa0807611, indexed in Pubmed: 19144937.
13. Neumann F-J, Sousa-Uva M, Ahlsson A, et al. 2018 ESC/EACTS Guidelines on myocardial revascularization. Eur Heart J. 2019; 40: 87–165, doi: 10.1093/eurheartj/ehy394, indexed in Pubmed: 30165437.
14. De Bruyne B, Pijls NHJ, Kalesan B, et al. FAME 2 Trial Investigators. Fractional flow reserve-guided PCI versus medical therapy in stable coronary disease. N Engl J Med. 2012; 367(11): 991–1001, doi: 10.1056/NEJMoa1205361, indexed in Pubmed: 22924638.
15. Jaguszewski M, Zabalza Cerdeiriña M, Alushi B, et al. How should I treat recurrent chest pain and systolic dysfunction after chemotherapy with anthracyclines? EuroIntervention. 2017; 12(13): 1674–1677, doi: 10.4244/EIJV12I13A274, indexed in Pubmed: 28106002.
16. Gutiérrez-Chico JL, Zhao S, Chatzizisis YS. Vorticity: At the crossroads of coronary biomechanics and physiology. Atherosclerosis. 2018; 273: 115–116, doi: 10.1016/j.atherosclerosis.2018.04.001, indexed in Pubmed: 29665968.
17. Boden WE, O'Rourke RA, Teo KK, et al. Optimal medical therapy with or without PCI for stable coronary disease. N Engl J Med. 2007; 356: 1503–1516, doi: 10.1056/NEJMoa070829, indexed in Pubmed: 17387127.
18. Härle T, Zeymer U, Hochadel M, et al. Real-world use of fractional flow reserve in Germany: results of the prospective ALKK coronary angiography and PCI registry. Clin Res Cardiol. 2017; 106(2): 140–150, doi: 10.1007/s00392-016-1034-5, indexed in Pubmed: 27599974.
19. Lee HS, Lee JM, Nam CW, et al. Consensus document for invasive coronary physiologic assessment in Asia-Pacific countries. Cardiol J. 2019; 26(3): 215–225, doi: 10.5603/CJ.a2019.0054, indexed in Pubmed: 31225632.
20. Sleight P. Debate: Subgroup analyses in clinical trials: fun to look at — but don't believe them! Curr Control Trials Cardiovasc Med. 2000; 1(1): 25–27.
21. Figulla HR, Lauten A, Maier LS, et al. Percutaneous Coronary Intervention in Stable Coronary Heart Disease — Is Less More? Dtsch Arztebl Int. 2020; 117(9): 137–144, doi: 10.3238/arztebl.2020.0137, indexed in Pubmed: 32234189.
22. Gutiérrez-Chico JL, Chen Y, Yu W, et al. Diagnostic accuracy and reproducibility of optical flow ratio for functional evaluation of coronary stenosis in a prospective series. Cardiol J. 2020; 27(4): 350–361, doi: 10.5603/CJ.a2020.0071, indexed in Pubmed: 32436590.

VIA MEDICA

EDITORIAL

Cardiology Journal
2020, Vol. 27, No. 4, 342–344
DOI: 10.5603/CJ.2020.0110

ISSN 1897–5593

ISCHEMIA trial: Back to the future or forward to the past?

Ana Pardo Sanz[1], Pedro Marcos Alberca[2], José Luis Zamorano[1]

[1]University Hospital Ramón y Cajal, Madrid, Spain
[2]University Hospital San Carlos, Madrid, Spain



The ISCHEMIA (International Study of Comparative Health Effectiveness with Medical and Invasive Approaches) trial [1] is a publicly funded clinical trial with a complex design, elaboration, communication, and interpretation of the results. There were 5179 patients randomized worldwide in the study. The results of the ISCHEMIA trial showed that patients with significant stable coronary artery disease (CAD) that underwent invasive procedures, such as percutaneous coronary intervention or coronary artery bypass graft surgery plus optimal medical treatment fared no better than patients who received only optimal medical therapy. The initial invasive strategy was associated with a reduction in angina and improved quality of life, only in symptomatic patients.

The main finding was that, among stable patients who had evidence of moderate to severe ischemia on stress testing, an initial invasive strategy, when compared with an initial conservative strategy, was not associated with a reduction in the primary outcome of cardiovascular death, myocardial infarction (MI), hospitalization for unstable angina, hospitalization for heart failure, or resuscitated cardiac arrest over a median follow-up of 3.3 years. The primary composite endpoint occurred in only 15.5% of patients in the conservative arm and 13.8% of patients in the invasive arm ($p = 0.34$); an observed event rate which was lower than predicted. Similar results were also observed for the pre-specified secondary endpoints of cardiovascular death or MI, and across the pre-specified sub-group analyses.

For inclusion into the study, documentation of at least moderate ischemia on stress testing was required. Ischemia severity was based on a core-laboratory interpretation. The chosen stress tests were markedly variable: 50% nuclear myocardial perfusion imaging via single-photon emission computed tomography or positron emission tomography; 25% exercise treadmill testing (without imaging), 20% stress echocardiogram and 5% stress cardiac magnetic resonance imaging. However, the stress core laboratories did not confirm whether the degree of ischemia was enough to qualify for the trial in 13.8% of patients who finally underwent randomization. Patients who were determined by the core laboratory to have moderate ischemia on a non-imaging exercise-stress test did not meet ischemia eligibility, yet some such patients underwent randomization. Non-imaging exercise test criteria were developed to approximate severe ischemia, taking into account the potentially higher false positive rate.

Address for correspondence: Prof. José Luis Zamorano Gómez, University Hospital Ramón y Cajal, Madrid, Spain, e-mail: zamorano@secardiologia.es

In addition to an evaluation of ischemia, most patients underwent computed tomography angiography (CTA) in order to exclude the presence of left main stenosis (≥ 50% stenosis), as well as to exclude patients who had less than 50% stenosis in all arteries, in whom the presence of significant ischemia is less common, and events are generally lower [2]. A total of 1266 patients did not undergo core-laboratory-interpreted CTA for the trial and did not have an available previous CTA within 1 year before the trial for core-laboratory interpretation, and 923 patients had a CTA core-laboratory interpretation in which the number of diseased vessels could not be evaluated. When trial images could be interpreted for this variable, the number of diseased vessels on CTA was based on a 50% stenosis threshold. Data on CAD severity based on 50% stenosis excluded 4 patients with no diseased vessels. Stenosis of the proximal left anterior descending coronary artery was reported when the proximal left anterior descendant segment could be evaluated on CTA. For patients enrolled using a non-imaging exercise stress test, anatomic eligibility confirmation was required and CTA eligibility criteria were more stringent for them, requiring ≥ 70% stenosis in the proximal or mid left anterior descending, proximal or mid right coronary artery, or proximal left circumflex (or circumflex equivalent).

The ISCHEMIA study highlights coronary anatomical assessment with cardiac CTA as an excellent tool to diagnose and evaluate the severity of coronary atherosclerosis. The assessment of the severity of a stenosis is facilitated using the CAD-RADS classification. In the ISCHEMIA study, a cardiac CTA scan was recommended, but was not required on randomization, which was based on the presence of moderate or severe ischemia in functional tests, as previously stated. Besides, cardiac CTA by itself did or did not indicate coronary revascularization, which relied on quantitative invasive coronary angiography. An optimal quality cardiac CTA was attained in more than 50% of patients, of which near 99% disclosed at least one major coronary artery with ≥ 50% of luminal stenosis. In this regard, the SCOT-HEART study [3] showed that a conservative strategy in the treatment of stable angina based on cardiac CTA results compared with a conservative strategy guided by positive functional tests reduces coronary disease mortality and the incidence of MI. This benefit, observed after 5 years of follow-up, was associated with a 60% increase in the prescription of antiplatelet therapy and high potency statins. Undoubtedly, the effect on plaque regression demonstrated with ambitious pharmacological therapy underlies the nexus that connects these observations.

The results of ISCHEMIA trial should be interpreted with caution and it may not be applicable to all patients. A selection bias cannot be excluded, and patients with very severe ischemia on the stress test might be less likely to be considered for study participation. Many patients with left main disease were also excluded with coronary CTA, and so the results are not applicable to them.

The question, at this point is: What is the role of functional testing and coronary computed tomography for patients with stable angina? Should all patients with stable symptoms be treated in a conservative manner, and reserve an invasive approach only if medical therapy alone fails? In light of results obtained, it might be wondered whether it was necessary for the patients with an evaluation for ischemia, if medical therapy would be used to treat nearly all stable patients who do not have left main disease. However, testing for ischemia will continue to have an important role in clinical cardiology. Sometimes, in routine clinical practice, it is unclear if patient symptoms represent angina or not, and an ischemic evaluation can be useful in these scenarios. Similarly, older patients or with long-standing diabetes frequently have silent ischemia, and functional studies could be required to identify the optimal diagnostic and therapeutic algorithm for them.

One of the strengths of the study is the usefulness of the CTA as a first line test to evaluate patients with stable symptoms and suspected CAD. This trial is another sample of the important role of the CTA as gate keeper of the diagnostic workflow, as reflected in the recent guidelines [4]. In patients who do not have known CAD, coronary CTA has an important role in identifying the need for aggressive medical therapy. CTA is also a key that can allow ruling out underlying high-risk coronary anatomy or left main disease, even though ischemia is present, particularly when symptoms are rare and conservative management is being considered. Indeed, one of the strengths of coronary CTA lies in its ability to identify a wide spectrum of CAD, ranging from mild non-obstructive plaque to extensive multi-vessel disease. Another advantage of using coronary CTA as a front-line test has to do with diagnostic efficiency: the majority of individuals with no history of CAD who are evaluated with coronary CTA will have either no CAD, or non-obstructive CAD, and will not need further testing.

In short, **the most relevant conclusion of this trial cannot be left in the absence of differences between the invasive and conservative treatment** [5]. At this point, one might think if all the available technology is being used for identifying which patients could benefit from each therapy [6, 7]. The answer to this question is given by the coronary CTA and the functional stress test, which can stratify risk and guide the algorithm. Trying to give an answer without them is to go back to the past, and not headed into the future. Going forward to the future is the only way to achieve the best individualized treatment for each patient.

Conflict of interest: None declared

References

1. Maron D, Hochman J, Reynolds H, et al. Initial invasive or conservative strategy for stable coronary disease. N Engl J Med. 2020; 382(15): 1395–1407, doi: 10.1056/nejmoa1915922.
2. Hochman JS, Reynolds HR, Bangalore S, et al. Baseline characteristics and risk profiles of participants in the ISCHEMIA randomized clinical trial. JAMA Cardiol. 2019; 4(3): 273–286, doi: 10.1001/jamacardio.2019.0014, indexed in Pubmed: 30810700.
3. Newby DE, Adamson PD, Berry C, et al. SCOT-HEART Investigators. Coronary CT angiography and 5-year risk of myocardial infarction. N Engl J Med. 2018; 379(10): 924–933, doi: 10.1056/NEJMoa1805971, indexed in Pubmed: 30145934.
4. Knuuti J, Wijns W, Saraste A, et al. 2019 ESC Guidelines for the diagnosis and management of chronic coronary syndromes. Eur Heart J. 2020; 41(3): 407–477, doi: 10.1093/eurheartj/ehz425, indexed in Pubmed: 31504439.
5. Gutiérrez-Chico JL, Louvard Y. DECISION-CTO: A „negative" clinical trial? Really? Cardiol J. 2017; 24(3): 231–233, doi: 10.5603/CJ.a2017.0049, indexed in Pubmed: 28417448.
6. Lee HS, Lee JM, Nam CW, et al. Consensus document for invasive coronary physiologic assessment in Asia-Pacific countries. Cardiol J. 2019; 26(3): 215–225, doi: 10.5603/CJ.a2019.0054, indexed in Pubmed: 31225632.
7. Gutiérrez-Chico JL, Chen Y, Yu W, et al. Diagnostic accuracy and reproducibility of optical flow ratio for functional evaluation of coronary stenosis in a prospective series. Cardiol J. 2020; 27(4): 350–361, doi: 10.5603/CJ.a2020.0071, indexed in Pubmed: 32436590.

VIA MEDICA

EDITORIAL

Cardiology Journal
2020, Vol. 27, No. 4, 345–346
DOI: 10.5603/CJ.2020.0111

ISSN 1897–5593

Morphology and physiology together: Is optical coherence tomography the one-stop-shop of invasive cardiology?

Carlo Di Mario, Pierluigi Demola

Structural Interventional Cardiology, Careggi University Hospital, Florence, Italy

Article p. 350

Prof. Carlo Di Mario

In 1974 Lance Gould demonstrated that maximal coronary flow was progressively reduced by applying external constrictors in animal models [1] and physiology became the gold standard to assess the severity of coronary artery disease. Fractional flow reserve (FFR), measured with invasive intracoronary pressure measurements, proved to obtain the same goal and became the accepted method to study intermediate coronary lesions (European Society of Cardiology Class I and American College/American Heart Association Class IIa, both with Level of Evidence A). The results of the randomized FFR trials supporting this strong recommendation gained more interest in the past few months based on the unexpected findings of the International Study of Comparative Health Effectiveness with Medical and Invasive Approaches (ISCHEMIA) trial [2]. This large study used non-invasive methods to detect ischemia, especially with single-photon emission computed tomography gave equivocal results with no mortality advantage and a significant, albeit small, reduction in spontaneous myocardial infarction (MI) at follow-up. Using invasive measurements to detect functionally significant stenoses (FFR ≤ 0.80) like in The Fractional Flow Reserve versus Angiography for Multivessel Evaluation 2 trial (FAME II trial) patients had an improved outcome with percutaneous coronary intervention (PCI) along with optimal medical therapy [3], with the most striking difference being the need of urgent revascularization (11.1% vs. 1.6%, $p < 0.001$). A meta-analysis including other trials of FFR-guided treatment of non-culprit lesions confirmed a significant improvement also for the classical "hard" endpoints of MI and death [4].

Gould and Kirkeeide were also pioneers in confirming in vivo, that all multiple parameters contained in the Pouseille law affects stenosis severity, and not only in a minimal area. Intracoronary imaging with intravascular ultrasound (IVUS) or optical coherence tomography (OCT) overcomes most of the limitations of angiography, with precise luminal measurements which avoid overlapping, foreshortening, and the other limitations of a lumenogram. Unfortunately, the comparison between minimal luminal area (MLA) with OCT and IVUS proved to be poorly correlated with FFR. Conceptually, defining an intermediate stenosis as critical or not in a binary fashion using a dichotomic cut off of MLA is wrong because it does not consider vessel size and lesion length that affect flow dynamics of a lesion. Paradoxically, the first results using a more sophisticated reconstruction based on a morphologic technique to estimate stenosis severity came from quantitative coronary angiography. Conceptually, this correlation can be much better when the lumen measurements are automatically performed with a technique such as OCT that is inherently three-dimensional and where the sharp contour between lumen, cleared by contrast injection, and wall allows fully automated measurements.

Address for correspondence: Pierluigi Demola, MD, Structural Interventional Cardiology, Careggi University Hospital, Florence, Italy, tel: +39 348 8421631, e-mail: pierluigidemola@gmail.com

Optical coherence tomography can detect with accuracy calcium (arc, length and thickness), dissections, stent malposition and helps interventional cardiologists to select the best stent size and length to achieve post-deployment optimization. Is there a need to start OCT only when it is learned from FFR that a lesion needs treatment or can it be used as a one-stop-shop for obtaining all the information needed to decide what to treat and how to do it?

In this issue of 'Cardiology Journal' Gutiérrez-Chico et al. [5] presents a series of 60 patients (76 vessels) studied with FFR because of the presence of intermediate stenoses also receiving an OCT assessment using an algorithm applying flow dynamics to calculate an analogue functional parameter to FFR called optical flow ratio (OFR). OFR showed the same average values of FFR (0.83 ± ± 0.09) with a clinically relevant disagreement (non-significant FFR ≥ 0.80 with critical < 0.80 OFR or vice versa) in only 4 (5.3%) cases. It sounds like a striking correlation between a pressure based and an imaging based index of stenosis severity and the authors should be complimented in confirming that lower sampling rates with OCT did not modify this agreement, that simpler OCT based indices such as MLA were poor predictors and that OFR had very low intra- and inter-observer variability [6].

The recent comparisons between FFR and the most widely validated non-hyperemic index i.e. iFR and among the many new non-hyperemic indices showed that these correlations are critically dependent on the scattering of data around the cut-point used (0.80 for FFR, 0.90 with iFR) [7]. In this study 44% of FFR measurements were between 0.75 and 0.85 that means the majority of data were not within the brackets of a functionally intermediate lesion. A more stringent comparison with most data close to the cutoff would help in validating the index but the ultimate end-point, as in DEFINE-FLAIR and FFR SWEDEHEART, was a clinical follow-up endpoint [8, 9] that requires a much larger sample population. For this study, it was essential to use the non-hyperemic index iFR as a gold standard, modifying the OFR algorithm to perform the estimation in the presence of a baseline flow, and to also repeat the comparison at the end of the procedure. By doing this, an assessment of individual importance of single lesions in serial stenosis or diffuse disease can facilitate procedural planning and confirm that a normal or the best possible physiology was achieved at the end of the PCI.

Conflict of interest: None declared

References

1. Gould KL, Lipscomb K, Hamilton GW. Physiologic basis for assessing critical coronary stenosis. Instantaneous flow response and regional distribution during coronary hyperemia as measures of coronary flow reserve. Am J Cardiol. 1974; 33(1): 87–94, doi: 10.1016/0002-9149(74)90743-7, indexed in Pubmed: 4808557.
2. Maron DJ, Hochman JS, Reynolds HR, et al. ISCHEMIA Research Group. Initial Invasive or Conservative Strategy for Stable Coronary Disease. N Engl J Med. 2020; 382(15): 1395–1407, doi: 10.1056/NEJMoa1915922, indexed in Pubmed: 32227755.
3. De Bruyne B, Pijls NHJ, Kalesan B, et al. FAME 2 Trial Investigators. Fractional flow reserve-guided PCI versus medical therapy in stable coronary disease. N Engl J Med. 2012; 367(11): 991–1001, doi: 10.1056/NEJMoa1205361, indexed in Pubmed: 22924638.
4. Zimmermann FM, Omerovic E, Fournier S, et al. Fractional flow reserve-guided percutaneous coronary intervention vs. medical therapy for patients with stable coronary lesions: meta-analysis of individual patient data. Eur Heart J. 2019; 40(2): 180–186, doi: 10.1093/eurheartj/ehy812, indexed in Pubmed: 30596995.
5. Gutiérrez-Chico JL, Chen Y, Yu W, et al. Diagnostic accuracy and reproducibility of optical flow ratio for functional evaluation of coronary stenosis in a prospective series. Cardiol J. 2020; 27(4): 350–361, doi: 10.5603/CJ.a2020.0071, indexed in Pubmed: 32436590.
6. Cook CM, Jeremias A, Petraco R, et al. Fractional flow reserve/instantaneous wave-free ratio discordance in angiographically intermediate coronary stenoses: an analysis using doppler-derived coronary flow measurements. JACC Cardiovasc Interv. 2017; 10(24): 2514–2524, doi: 10.1016/j.jcin.2017.09.021, indexed in Pubmed: 29268881.
7. Jeremias A, Davies JE, Maehara A, et al. Blinded physiological assessment of residual ischemia after successful angiographic percutaneous coronary intervention: the DEFINE PCI study. JACC Cardiovasc Interv. 2019; 12(20): 1991–2001, doi: 10.1016/j.jcin.2019.05.054, indexed in Pubmed: 31648761.
8. Davies JE, Sen S, Dehbi HM, et al. Use of the instantaneous wave-free ratio or fractional flow reserve in PCI. N Engl J Med. 2017; 376(19): 1824–1834, doi: 10.1056/NEJMoa1700445, indexed in Pubmed: 28317458.
9. Escaned J, Ryan N, Mejía-Rentería H, et al. Safety of the deferral of coronary revascularization on the basis of instantaneous wave-free ratio and fractional flow reserve measurements in stable coronary artery disease and acute coronary syndromes. JACC Cardiovasc Interv. 2018; 11(15): 1437–1449, doi: 10.1016/j.jcin.2018.05.029, indexed in Pubmed: 30093050.

VIA MEDICA

Cardiology Journal
2020, Vol. 27, No. 4, 347–349
DOI: 10.5603/CJ.a2020.0067

ISSN 1897–5593

EDITORIAL COMMENT

Direct oral anticoagulants in cancer-associated venous thromboembolism: It is high time for a change of therapeutic paradigm

Justyna Domienik-Karłowicz[1], Miłosz Jaguszewski[2], Marcin Kurzyna[3]

[1]Department of Internal Medicine and Cardiology, Medical University of Warsaw, Poland
[2]First Department of Cardiology, Medical University of Gdansk, Poland
[3]Department of Pulmonary Circulation, Thromboembolic Diseases and Cardiology, Center of Postgraduate Medical Education, European Health Center, Otwock, Poland

This paper was guest edited by Prof. Krzysztof J. Filipiak



Giancarlo Agnelli and colleagues have recently revealed results of the CARAVAGGIO study at the American College of Cardiology and World Congress of Cardiology's virtual scientific sessions. The outcomes of this trial, simultaneously published in the *The New England Journal of Medicine* [1], support the inclusion of apixaban as another direct oral anticoagulant (DOAC) for cancer patients with newly diagnosed incidental or symptomatic proximal deep vein thrombosis (DVT) or pulmonary embolism (PE). This study seems to finish the ongoing discussion on the possibility of using DOACs in cancer-associated thrombosis (CAT) and change the paradigm, setting the low-molecular-weight heparin (LMWH) as a drug of choice and gold standard in this indication.

Venous thromboembolism (VTE) is the second-leading cause of mortality in cancer patients receiving chemotherapy [2]. The adjusted occurrence of VTE is a significant predictor of limited survival within the first year for all cancer types (HR 1.6–4.2; $p < 0.01$) [3]. Moreover, the risk of VTE varies depending on the type of cancer, the stage of metastatic disease, and receipt of certain anti-cancer therapies [4]. The highest risks apply to pancreatic cancer, hematological malignancy, lung, gastric, and brain cancer. The CLOT trial, published in 2003, showed superior efficacy of dalteparin compared to vitamin K antagonists in the prevention of recurrence of cancer-associated VTE and similar bleeding rates in both groups [5]. It was the basis for explicit recommendations for initial and long-term CAT treatment with LMWH in the following years. Recently the European Society of Cardiology Guidelines suggested that "edoxaban or rivaroxaban should be considered as an alternative to LMWH, with a word of caution for patients with gastrointestinal cancer due to the increased bleeding risk with DOACs" [6]. The latter was added to underline that the increased risk of bleeding may counterbalance the benefits of anticoagulation therapy in cancer patients. The risk of bleeding in patients treated with DOACs is an essential problem in "mucosal" types of cancer occurring in the gastrointestinal tract and urinary system.

Address for correspondence: Justyna Domienik-Karłowicz, MD, PhD, Department of Internal Medicine and Cardiology, Medical University of Warsaw, ul. Lindleya 5, 02–005 Warszawa, Poland, e-mail: jdomienik@tlen.pl

Received: 23.04.2020 Accepted: 12.05.2020

Last, but not least, is the possibility of unfavorable drug interactions of DOACs with chemotherapy, which may occur during concomitant use.

In the Hokusai VTE Cancer study, oral edoxaban was confirmed to be noninferior to subcutaneous dalteparin concerning the composite outcome of recurrent VTE or major bleeding, but the rate of major bleeding was higher with edoxaban than with dalteparin [7]. Similarly, SELECT-D trial rivaroxaban has shown low VTE recurrence but the results for major bleeding were 4% for dalteparin and 6% for rivaroxaban. Unfortunately, the adequate rates for clinically relevant non-major bleeding were 4% for dalteparin and 13% for rivaroxaban [8]. Notably, both studies did not exclude patients with cerebral metastases nor brain tumors.

The newly published CARAVAGGIO study is a multinational, randomized, open-label, investigator-initiated study to compare efficacy and safety of apixaban and dalteparin in 1170 cancer patients with VTE [1]. Patients with basal-cell or squamous-cell carcinomas of the skin, primary brain tumors, brain metastases, and acute leukemias were excluded, but the study was not exclusive any other types of neoplastic disease. Approximately one-third of patients presented cancer at gastrointestinal sites. 585 patients were assigned to receive apixaban at a dose of 10 mg twice daily for the first week and 5 mg twice daily subsequently and 585 patients were assigned to receive dalteparin at a dose of 200 IU/kg of body weight subcutaneously once daily for the first month and 150 IU/kg of bodyweight subsequently over a period of 5 months.

The primary efficacy end-point was defined as the recurrence of VTE. The principal safety outcome was defined as major bleeding. Finally, 1155 patients were included in further analysis. Patients with PE accounted for 52.8% and 57.7% in the apixaban and dalteparin groups, respectively. Approximately 20% of the cases were individuals with incidental DVT or PE who were diagnosed during diagnostic procedures performed for reasons other than clinical suspicion of VTE. 97% of cases presented active cancer at enrollment.

The primary efficacy end-point occurred in 5.6% patients in the apixaban group (32 patients: 13 recurrent DVTs, 19 recurrent PE, including 4 cases of fatal PE) compared to 7.9% (46 patients: 15 recurrent DVT, 32 recurrent PE, including 3 cases of fatal PE) in the dalteparin group ($p < 0.001$ for noninferiority; $p = 0.09$ for superiority in favor of apixaban).

Major bleeding occurred in 3.8% (22) of patients in the apixaban group and 4% (23) of patients in the dalteparin group. Moreover, major gastrointestinal bleeding occurred in 1.9% (11) of patients in the apixaban group and 1.7% (10) patients in the dalteparin group. There were 2 fatal bleeding episodes in the dalteparin group compared to 0 in the apixaban group. Moreover, the rates of clinically relevant non-major bleeding were not significantly higher with apixaban group versus dalteparin (9% and 6%). The incidence of death was similar in both groups — 23.4% in the apixaban versus 26.4% in the dalteparin group. Most deaths were related to cancer — 85.2% and 88.2%, respectively.

The key finding of this study was that oral apixaban is non-inferior to subcutaneous dalteparin for the treatment of VTE in cancer patients up to 6 months after diagnosis. Contradictorily to previous studies involving other DOACs, the occurrence of major bleedings, either general or gastrointestinal, were similar in apixaban and dalteparin groups. The clinical benefit of treatment prolonged for more than 6 months should be assessed in additional studies.

Cancer patients need to have access to a convenient and safe drug. The treatment regimen for VTE with apixaban and rivaroxaban allows for administering oral medications from the first day of therapy, which is exceptionally convenient in cases of DVT and low-risk incidental PE. However, it also requires a physician to make the right decision regarding the choice of DOAC or LMWH based on the type of cancer, comorbidities, bleeding risk, concomitant chemotherapy, and patient preference. The satisfactory safety profile of apixaban showed in the CARAVAGGIO trial, makes this choice easier. However, this work is not yet complete. More extensive research is still needed to allow this heterogeneous group of patients to be treated in a more individualized way, ensuring a satisfactory balance between antithrombotic efficacy and bleeding risk.

Conflict of interest: None declared

References

1. Agnelli G, Becattini C, Meyer G, et al. Caravaggio Investigators. Apixaban for the treatment of venous thromboembolism associated with cancer. N Engl J Med. 2020; 382(17): 1599–1607, doi: 10.1056/NEJMoa1915103, indexed in Pubmed: 32223112.
2. Kuderer NM, Ortel TL, Francis CW. Impact of venous thromboembolism and anticoagulation on cancer and cancer survival. J Clin Oncol. 2009; 27(29): 4902–4911, doi: 10.1200/JCO.2009.22.4584, indexed in Pubmed: 19738120.
3. Chew HK, Wun T, Harvey D, et al. Incidence of venous thromboembolism and its effect on survival among patients with common cancers. Arch Intern Med. 2006; 166(4): 458–464, doi: 10.1001/archinte.166.4.458, indexed in Pubmed: 16505267.
4. Horsted F, West J, Grainge MJ. Risk of venous thromboembolism in patients with cancer: a systematic review and meta-

analysis. PLoS Med. 2012; 9(7): e1001275, doi: 10.1371/journal.pmed.1001275, indexed in Pubmed: 22859911.

5. Lee AYY, Levine MN, Baker RI, et al. Low-molecular-weight heparin versus a coumarin for the prevention of recurrent venous thromboembolism in patients with cancer. N Engl J Med. 2003; 349(2): 146–153, doi: 10.1056/NEJMoa025313, indexed in Pubmed: 12853587.
6. Konstantinides SV, Meyer G, Becattini C, et al. 2019 ESC Guidelines for the diagnosis and management of acute pulmonary embolism developed in collaboration with the European Respiratory Society (ERS). Eur Heart J. 2020; 41(4): 543–603, indexed in Pubmed: 31504429.
7. Raskob GE, van Es N, Verhamme P, et al. Edoxaban for the treatment of cancer-associated venous thromboembolism. N Engl J Med. 2018; 378(7): 615–624, doi: 10.1056/NEJMoa1711948, indexed in Pubmed: 29231094.
8. Young AM, Marshall A, Thirlwall J, et al. Comparison of an oral factor xa inhibitor with low molecular weight heparin in patients with cancer with venous thromboembolism: results of a randomized trial (SELECT-D). J Clin Oncol. 2018; 36(20): 2017–2023, doi: 10.1200/JCO.2018.78.8034, indexed in Pubmed: 29746227.

VIA MEDICA

ORIGINAL ARTICLE

Cardiology Journal
2020, Vol. 27, No. 4, 350–361
DOI: 10.5603/CJ.a2020.0071

ISSN 1897–5593

Diagnostic accuracy and reproducibility of optical flow ratio for functional evaluation of coronary stenosis in a prospective series

Juan Luis Gutiérrez-Chico[1]*, Yundai Chen[2]*, Wei Yu[3]*, Daixin Ding[3], Jiayue Huang[3], Peng Huang[3], Jing Jing[2], Miao Chu[1, 3], Peng Wu[3], Feng Tian[2], Bo Xu[4], Shengxian Tu[3]

[1]Department of Interventional Cardiology, Campo de Gibraltar Health Trust, Algeciras, Spain
[2]Department of Cardiology, PLA General Hospital, Beijing, China
[3]Biomedical Instrument Institute, School of Biomedical Engineering, Shanghai Jiao Tong University, Shanghai, China
[4]Fu Wai Hospital, National Center for Cardiovascular Diseases, Chinese Academy of Medical Sciences, Beijing, China

Abstract

Background: *Evaluating prospectively the feasibility, accuracy and reproducibility of optical flow ratio (OFR), a novel method of computational physiology based on optical coherence tomography (OCT).*

Methods and results: *Sixty consecutive patients (76 vessels) underwent prospectively OCT, angiography-based quantitative flow ratio (QFR) and fractional flow ratio (FFR). OFR was computed offline in a central core-lab by analysts blinded to FFR. OFR was feasible in 98.7% of the lesions and showed excellent agreement with FFR (ICCa = 0.83, r = 0.83, slope = 0.80, intercept = 0.17, kappa = 0.84). The area under curve to predict an FFR ≤ 0.80 was 0.95, higher than for QFR (0.91, p = 0.115) and for minimal lumen area (0.64, p < 0.001). Diagnostic accuracy, sensitivity, specificity, positive predictive value, negative predictive value, positive likelihood ratio and negative likelihood ratio were 93%, 92%, 93%, 88%, 96%, 13.8, 0.1, respectively. Median time to obtain OFR was 1.07 (IQR: 0.98–1.16) min, with excellent intraobserver and interobserver reproducibility (0.97 and 0.95, respectively). Pullback speed had negligible impact on OFR, provided the same coronary segment were imaged (ICCa = 0.90, kappa = 0.697).*

Conclusions: *The prospective computation of OFR is feasible and reproducible in a real-world series, resulting in excellent agreement with FFR, superior to other image-based methods.* (Cardiol J 2020; 27, 4: 350–361)

Key words: optical flow ratio, optical coherence tomography, fractional flow reserve, coronary heart disease

Editorial p. 345

Introduction

The utility and safety of physiology-guided percutaneous coronary intervention (PCI) has been proved in several large randomized trials and in different clinical scenarios, consistently translating into better clinical outcomes than merely angiography-guided PCI [1–3]. Notwithstanding this compelling evidence, the penetrance of physiology in clinical routine is still low [4]. Data from a National German registry reported that fractional flow reserve (FFR) was used in only 3.2% of patients undergoing coronary angiography [5]. The

Address for correspondence: Shengxian Tu, PhD, FACC, FESC, Room 123, Med-X Research Institute, Shanghai Jiao Tong University, No. 1954, Hua Shan Road, Shanghai 200030, China, tel: +86 21 62932631, fax: +86 21 62932156, e-mail: sxtu@sjtu.edu.cn

Received: 15.05.2020 Accepted: 16.05.2020

**The first three authors equally contributed.*

reasons for this evidence-reality mismatch rely on the need for an additional wire, often with limited steerability and navigability, the eventual infusion of adenosine prolonging the procedure and producing discomfort to the patient, or on restrictions in the reimbursement [6]. Most health systems indeed reimburse only one adjuvant tool for PCI, either FFR or an invasive imaging tool in the best of cases, but not both. Thus, some operators give priority to imaging if they anticipate a likely PCI, because imaging can be more useful to assess the PCI result or to guide optimisation.

Among all invasive imaging modalities, optical coherence tomography (OCT) has the highest resolution and enables an accurate assessment of expansion and apposition of the stent [7–9], thus arising as a paramount tool for PCI optimisation [10]. Nonetheless, its ability to assess the functional significance of a stenosis is negligible hitherto [11]. An OCT-based morphofunctional method enabling both accurate estimation of coronary physiology and high resolution imaging for PCI optimisation within a single catheter [12] could spare time and weariness to the interventional team, discomfort to the patient, whilst being instrumental to overcome the reimbursement restraints that are preventing physiology and imaging to expand up to the boundaries where current evidence recommends their use [6, 13].

A novel OCT-based morphofunctional computational method dubbed optical flow ratio (OFR) has been recently developed, combining an estimation of physiology with high resolution imaging in the same OCT pullback [14–16]. OFR showed optimal agreement with FFR in post-hoc retrospective analysis [15, 16]. Furthermore, OFR might improve the accuracy of angiography-based morphofunctional computational methods [16–18] by overcoming the intrinsic limitations of angiography, namely overlapping vessels, foreshortening and calcium interfering with an accurate edge detection of the vessel lumen, because OCT renders the most accurate lumen reconstruction currently available.

We aimed to assess the feasibility and accuracy of OFR in a prospective cohort of consecutive unselected patients, compared with other morphofunctional approaches.

Methods

Study design

This was a prospective and multicenter study to evaluate the feasibility, diagnostic accuracy and reproducibility of OFR analysis in a real-world cohort of consecutive unselected patients, taking FFR as reference standard. Secondary objectives of the study were the comparison of the diagnostic accuracy of OFR (an OCT-based computational method) vs. quantitative flow ratio (QFR, an angiography-based computational method) and the potential impact of OCT pullback speed on the diagnostic accuracy of OFR. Finally, the diagnostic accuracy of computational methods was compared vs. the approach of estimating severity by means of a minimal lumen area (MLA) cutoff.

The study was performed at two centers: Campo de Gibraltar Health Trust, Algeciras (Spain) and Chinese PLA General Hospital, Beijing (China), complying with the principles of good clinical practice and with the Declaration of Helsinki for investigation in human beings. The study protocol was approved by the institutional review boards of these two hospitals. All patients provided written informed consent.

Study population

Patients with coronary artery disease and a clinical indication for FFR measurement (40% to 90% diameter stenosis by visual estimation, without evidence of ischemia by non-invasive tests) were included into the study in the two participating centers between November 2018 and April 2019, with varying enrolment periods in each center depending on the corresponding initiation dates. Exclusion criteria comprised aorta-ostial lesion, prior coronary artery bypass grafting, contraindication for intravenous adenosine, hemodynamic or electrical instability, moderate or severe valvular heart disease, acute coronary syndrome < 72 h depending on the target vessel and the presence of a chronic total occlusion in any other coronary vessel.

Invasive coronary angiography

Coronary angiography was performed through femoral, radial or ulnar approaches, with a ≥ 6 F catheter. After administration of intracoronary nitroglycerine, two angiographic projections of the target vessel at least 25° apart were acquired at ≥ 25 frames/s by a flat panel system, including the whole coronary artery from ostium to distal vessel, minimising vessel overlap and foreshortening, to warrant the highest quality in QFR analysis.

OCT acquisition

An OCT Dragonfly™ catheter (Abbott, St. Paul, Minnesota, USA) was advanced at least 15 mm distally to the stenosis. Then a pullback

was acquired with an OPTIS™ Fourier-domain OCT system at a rotation speed of 180 Hz and a pullback speed of 36 mm/s with non-occlusive technique [19], including the whole vessel up to the guiding catheter. The minimal amount of contrast required to ensure optimal quality was calculated by means of a validated formula [20]. The cases from one center were similarly acquired with a F-1 system and a T-1 catheter (Forssmann Medical Co. Ltd., Nanjing, China), both with analogous technical characteristics to the abovementioned system except for a rotation speed of 100 Hz and a pullback speed of 18 mm/s.

Lesions imaged with the Dragonfly™ catheter (Abbott, St. Paul, Minnesota, USA) underwent a second pullback at 18 mm/s following the same protocol, unless clinically contraindicated due to excessive amount of contrast or instability of the patient. In case of sequential lesions or diffuse coronary heart disease, two consecutive OCT pullbacks could be acquired to cover the whole stenotic segment.

FFR measurement

An Aeris pressure wire (Abbott, St. Paul, Minnesota, USA) was used for FFR measurement. Distal pressure was equalised with the aortic pressure at the tip of the guiding catheter, filled with saline, before advancing the wire distally to the lesion. Hyperemia was induced by means of a continuous intravenous infusion of 140 μg/kg/min adenosine and FFR was then recorded as the minimal distal coronary pressure to aortic pressure ratio (Pd/Pa) value in maximal stable hyperemia. The pressure transducer was then pulled back again to the tip of the guiding catheter: a pressure drift of ± 3 mmHg was considered acceptable. If the pressure drift exceeded this margin, the FFR recording was repeated. For sequential lesions, the FFR at the most distal position was used for comparison with OFR.

OFR and QFR analysis

Optical coherence tomography recordings were centrally analysed in a core-lab setting (CardHemo, Med-X Research Institute, Shanghai Jiao Tong University, China). OFR analysis was performed in all OCT pullbacks unless the OCT catheter were occlusive, thus precluding an optimal visualization of the vessel distally to the stenosis. However, OFR was excluded for comparison vs. FFR if any of the following was present: 1) Vessel spasm or injury during OCT acquisition; 2) Myocardial bridge in the angiography; 3) OCT pullback not covering the entire lesion; 4) Intracoronary thrombus.

Optical flow ratio analysis and QFR analysis were separately performed by two independent analysts in a blinded fashion, using the OctPlus software (version 1.0) and the AngioPlus system, respectively (both from Pulse Medical Imaging Technology, Shanghai, China), following a methodology previously described [14, 15, 21, 22]. Briefly, for OFR computation, lumen contours were automatically delineated in the OCT pullback to render a tubular three-dimensional (3D) reconstruction of the lumen. The ostia of side branches were automatically detected and outlined to calculate the corresponding cross-sectional areas [23]. Manual edition was allowed in case of misleading contour detection. The reference lumen area at the distal part of the bifurcation was then derived according to the principles of fractal geometry [24]. Finally, the reference lumen area was multiplied by a fixed flow velocity of 0.35 m/s to obtain the hypothetic volumetric flow used as boundary condition for the OFR algorithm [15, 16], thus enabling the computation of OFR (i.e., the estimated FFR value) along the reconstructed vessel [14, 15]. For sequential stenosis requiring two different pullbacks, both pullbacks were combined using a fiduciary landmark. Considering OFR1 as the OFR calculated in the proximal pullback at the fiduciary landmark, and considering OFR2 as the OFR in the distal pullback after excluding the vessel proximal to the fiduciary landmark, the combined OFR was calculated as OFR1 + OFR2 – 1.0.

For QFR analysis, the lumen contour of the coronary vessel was automatically detected in two angiographic projections for 3D angiographic reconstruction. Manual correction was allowed in case of suboptimal image quality, following a standard operational procedure [18, 21]. The contrast flow model was used for the computations, calculating the coronary flow as the product of reference lumen area and contrast velocity estimated by Thrombolysis in Myocardial Infarction (TIMI) frame count [18]. The resulting coronary flow was used as boundary condition for the QFR algorithm to compute the estimated FFR value along the reconstructed vessel [18, 21, 22].

Figure 1 shows an example of OFR and QFR analysis. OFR and QFR were compared head-to-head vs. FFR, taking the respective values obtained at the same position where FFR was recorded.

Optical flow ratio analysis was repeated by the first OFR analyst 1 month later and by a second

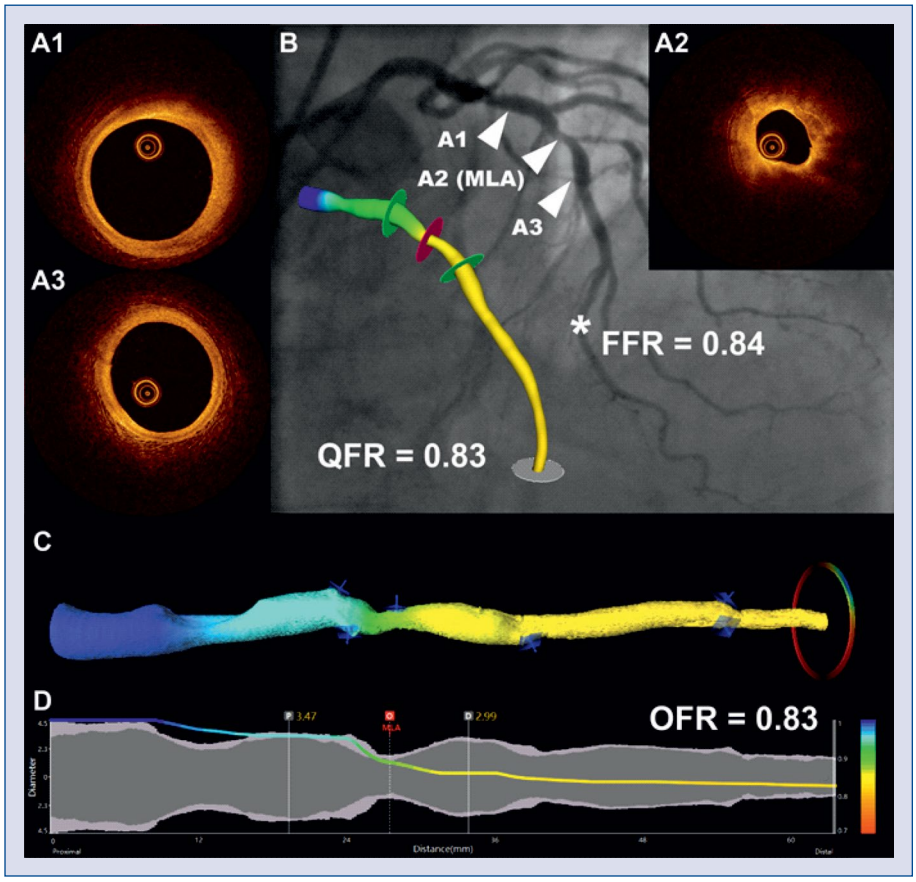

Figure 1. Computation of optical flow ratio (OFR) and quantitative flow ratio (QFR) in an intermediate stenosis in the left anterior descending artery. Cross-sections **A1–A3** correspond to the angiography positions showed in panel **B** (arrow heads), with **A2** as minimal lumen area (MLA). Fractional flow reserve (FFR) measured at a distal position (**B**,*) was 0.84. The computed QFR (**B**) and optical flow ratio (OFR) (**C**) along the vessel are color-coded and superimposed on a three-dimensional reconstruction, both with a value of 0.83 at the marked point (*).The software renders a virtual pressure pullback within the coronary artery (**D**) for optimal co-registration between pressure-drop and anatomy.

analyst, following the same operational procedure and blinded to each other's results and to previously calculated OFR. The analysis time for OFR was recorded, starting from the moment in which OCT images were uploaded into the computation software and ending when the OFR value was finally obtained.

Statistical analysis

Descriptive statistics of continuous variables were reported as mean ± standard deviation (SD) or as median (quartiles) as appropriate, while those of categorical variables were presented as counts (percentages). Continuous variables were compared with unpaired t-test or Mann-Whitney U test, as appropriate, whilst categorical variables were compared with Fisher's exact test. Correlation was evaluated using Pearson's correlation coefficient and linear regression analysis, taking FFR as standard reference. Constant bias was evaluated as the deviation of the intercept from 0, whilst proportional bias was evaluated as the deviation of the slope from 1 in the linear regression. Agreement of the different continuous parameters in the study was reported as intraclass correlation coefficient for the absolute value (ICCa) and by means of Bland-Altman plots. The agreement between OFR, QFR and FFR as dichotomous variables (significant ≤ 0.80, non-significant > 0.80) was reported as kappa coefficient. Diagnostic accuracy, sensitivity (Se), specificity (Sp), positive and negative predictive values (+PV, –PV), positive and negative likelihood ratios (+LR, –LR) were reported. The diagnostic performance was assessed by the area under the curve (AUC) in the receiver-operating characteristic (ROC) curve. An optimal cutoff value of the MLA in OCT to detect a hemodynamically significant FFR was calculated

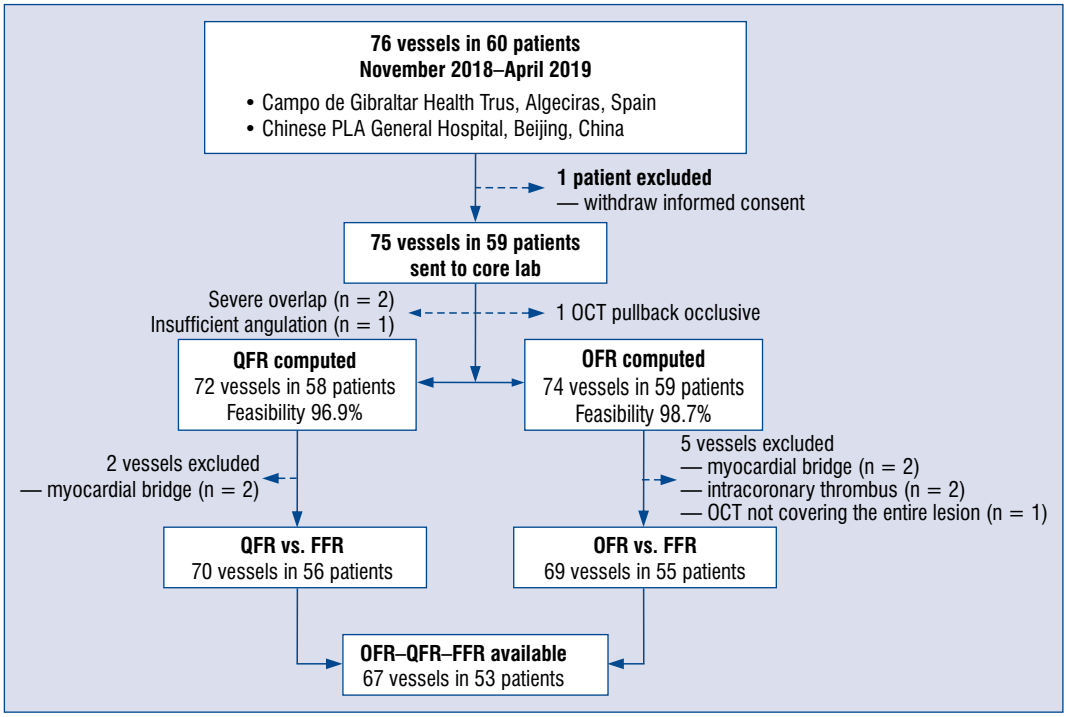

Figure 2. Study flow chart; FFR — fractional flow reserve; OCT — optical coherence tomography; OFR — optical flow ratio; QFR — quantitative flow ratio.

with the Youden index in the series and the corresponding AUC calculated. AUC of the different diagnostic methods were compared with the Delong method using MedCalc 14.12 (MedCalc Software, Ostend, Belgium). For all other statistics the IBM SPSS 24.0 software package (SPSS Inc., Chicago, Illinois) was employed.

Sample size was calculated by Liao's method for studies of agreement [25], assuming an AUC of 0.93, as previously reported [15], and an α error 0.05. Under these premises, $n \geq (\log [1\text{-}0.93] / \log [1\text{-}0.05])$, resulting in a minimal sample size of 52 patients for a reliable estimation of the AUC. Accounting for a 10% of cases unsuitable for analysis, the sample size increased to 58 patients.

Results

Baseline clinical and lesion characteristics

Sixty patients (76 vessels) were prospectively enrolled into the study, but 1 patient withdrew informed consent before FFR acquisition. OCT was occlusive in 1 vessel, but OFR could be computed in the remaining 74 vessels (feasibility 98.7%). Five vessels were however excluded by the corelab for comparison vs. FFR due to myocardial bridge (n = 2), intracoronary thrombus (n = 2) or incomplete OCT imaging of the lesion (n = 1) (Fig. 2), resulting in 55 patients (69 vessels) for paired comparison vs. FFR. OCT was acquired at different pullback speeds in 27 vessels, as previously described. QFR computation was successful in 72 out of 75 vessels (feasibility 96.0%). Unsuccessful QFR computations were due to severe overlap at the interrogated vessel (n = 2) or insufficient difference in angulation between the angiographic projections (n = 1). Two vessels were discarded in the corelab due to myocardial bridge, resulting in 56 patients and 70 vessels for paired comparison QFR vs. FFR.

Baseline characteristics are presented in Tables 1 and 2. Most of the cases corresponded to stable coronary heart disease (72.9%, comprising stable angina, silent ischemia or a prognostic indication), although there were also acute coronary syndromes older than 72 h and provoked by morphologically stable plaques (Table 1). The left anterior descending (LAD) artery was the most commonly interrogated vessel (52.0%), followed by the right coronary artery (RCA) (30.7%). A significant proportion of lesions corresponded to bifurcations (54.7%) or sequential stenosis (46.7%).

The average FFR value was 0.83 ± 0.09. In 26 (34.7%) lesions FFR was ≤ 0.80 and 33 (44.0%)

Table 1. Baseline clinical characteristics (patients, n = 59).

Age [years]	63.4 ± 10.1
Women	9 (15.3%)
Body mass index [kg/m^2]	28.1 [25.4, 30.6]
Diabetes mellitus	23 (39.0%)
Hypertension	40 (67.8%)
Hyperlipidemia	31 (52.5%)
Current smoker	17 (28.8%)
Family history of CAD	6 (10.2%)
Previous PCI	40 (67.8%)
Previous CABG	2 (3.4%)
Previous MI	28 (47.5%)
Clinical presentation:	
Silent ischemia/prognostic indication	32 (54.2%)
Stable angina	11 (18.6%)
Unstable angina	12 (20.3%)
NSTEMI	4 (6.8%)
Patients with FFR measurement in > 1 vessel	15 (25.4%)

Data are presented as mean ± standard deviation, median (Q1–Q2), or number (%), as appropriate; CAD — coronary artery disease; CABG — coronary artery bypass surgery; NSTEMI —non-ST-elevation myocardial infarction; MI — myocardial infarction; PCI — percutaneous coronary intervention; FFR — fractional flow reserve

Table 2. Baseline vessel characteristics (lesions, n = 75).

Target vessel:	
Left anterior descending	39 (52.0%)
Diagonal	5 (6.7%)
Left circumflex	4 (5.3%)
Obtuse marginal	2 (2.7%)
Ramus intermedius	2 (2.7%)
Right coronary artery	23 (30.7%)
Bifurcation lesions	41 (54.7%)
Sequential stenosis	35 (46.7%)
Fractional flow reserve (FFR) data:	
FFR	0.83 ± 0.09
FFR ≤ 0.80	26 (34.7%)
0.75 ≤ FFR ≤ 0.85	33 (44.0%)

Data are presented as mean ± standard deviation or number (%), as appropriate.

lesions had a central FFR value between 0.75 and 0.85 (Table 2).

Agreement between OFR and FFR

Optical flow ratio had the same average value as FFR 0.83 ± 0.09. In the linear regression analysis, taking FFR as reference (y), OFR showed good correlation (r = 0.83), with neither proportional (slope = 0.80) nor constant bias (intercept = 0.17) (Fig. 3). Bland-Altman analysis is presented in Figure 3, showing no significant difference between OFR and FFR (mean difference = 0.00, SD of the difference 0.05). The agreement between both methods was excellent (ICCa = 0.83; 95% confidence interval [CI]: 0.74–0.89).

The agreement between OFR and FFR as dichotomous variables was also excellent (kappa = 0.84; 95% CI: 0.71–0.98).

Agreement between QFR and FFR

In linear regression, taking FFR as reference (y), QFR showed good correlation (r = 0.78), although sensibly more deviated from unbiasedness (slope = = 0.61, intercept = 0.33) (Fig. 3). Bland-Altman analysis is presented in Figure 3, showing no significant difference between QFR and FFR (mean difference = 0.00, SD of the difference 0.07). The agreement between both methods was very good (ICCa = 0.75; 95% CI: 0.63–0.84).

The agreement between QFR and FFR as dichotomous variables was excellent (kappa = 0.78; 95% CI: 0.63–0.93).

Diagnostic performance of OFR, QFR and OCT-MLA

The diagnostic accuracy of OFR was 93% (95% CI: 86–99), with 22 true positives, 42 true negatives, 3 false positives and 2 false negatives, corresponding to a sensitivity, specificity, positive predictive value (PPV), negative predictive value (NPV), positive likelihood ratio (+LR) and negative likelihood ratio (–LR) of 92% (95% CI: 73–99), 93% (95% CI: 82–99), 88% (95% CI: 69–98), 96% (95% CI: 85–99), 13.8 (95% CI: 4.6–41.3), and 0.1 (95% CI: 0.0–0.3). This diagnostic performance was slightly better than that of QFR: diagnostic accuracy, sensitivity, specificity, PPV, NPV, +LR, and –LR of 90% (95% CI: 83–97), 91% (95% CI: 72–99), 89% (95% CI: 77–97), 81% (95% CI: 61–93), 96% (95% CI: 85–99), 8.6 (95% CI: 3.7–19.8), and 0.1 (95% CI: 0.0–0.4), respectively (Table 3).

The AUC of OFR was 0.95, tendentially higher than that of QFR (0.91, p = 0.115) and significantly higher than that of OCT-derived MLA (0.64, p < 0.001), taking for the latter the best cut-off value found in the ROC analysis of the series (1.63 mm^2) (Fig. 4).

In the subgroup analysis (Fig. 5), the diagnostic accuracy of OFR was independent of the coronary vessel (LAD 92%; 95% CI: 83–100,

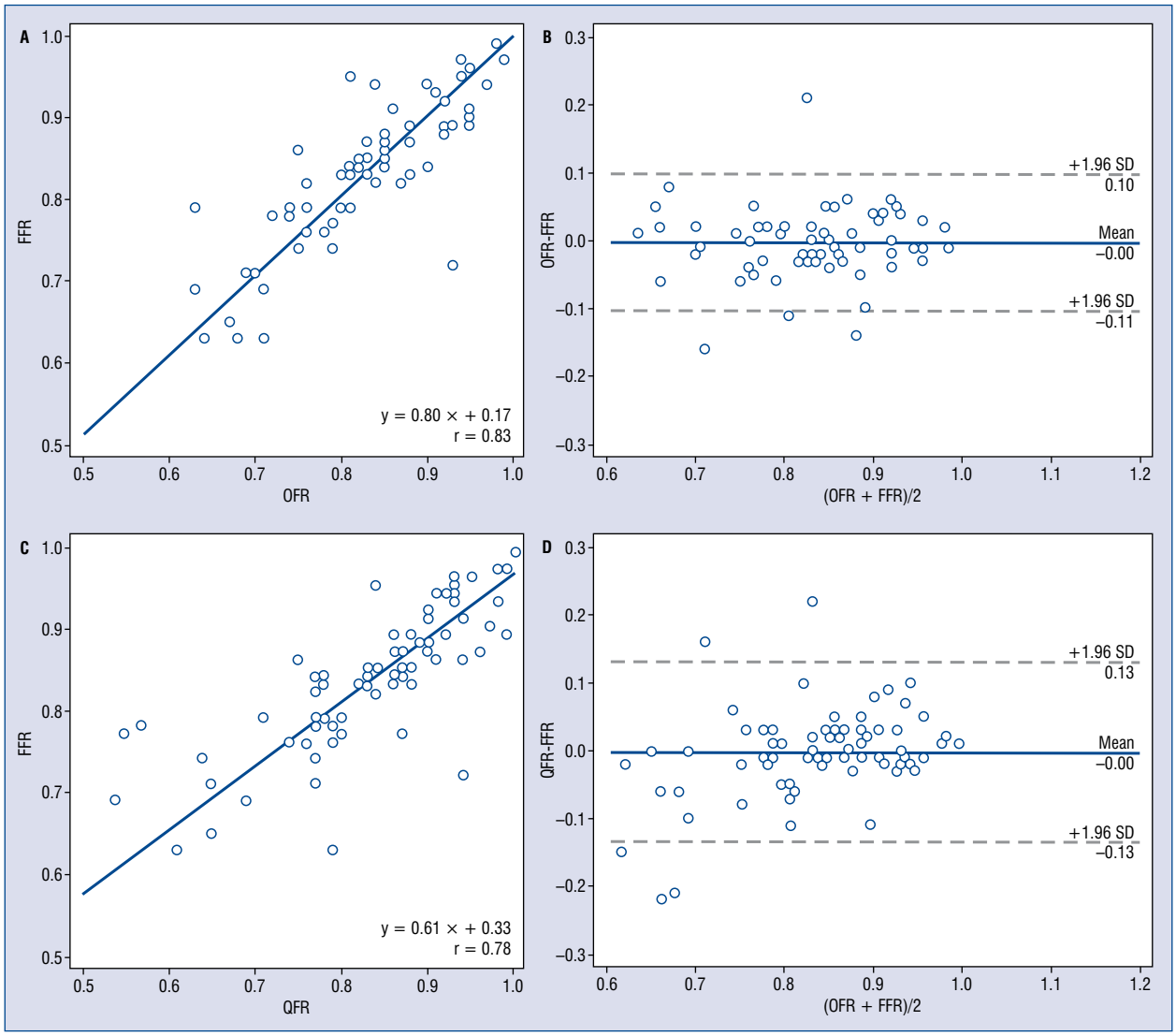

Figure 3. Correlation and agreement between fractional flow reserve (FFR) and optical flow ratio (OFR). Agreement between OFR and FFR: lineal regression (**A**) and Bland-Altman plot (**B**). Agreement between QFR and FFR: lineal regression (**C**) and Bland-Altman plot (**D**); SD — standard deviation.

Table 3. Diagnostic performance of optical flow ratio, quantitative flow ratio (QFR) and optical coherence tomography (OCT)-derived minimum lumen area (MLA) to identify fractional flow reserve ≤ 0.80.

	OFR ≤ 0.80	QFR ≤ 0.80	MLA ≤ 1.63 mm^2
Accuracy	93 (86–99)	90 (83–97)	68 (57–79)
Sensitivity	92 (73–99)	91 (72–99)	54 (33–74)
Specificity	93 (82–99)	89 (77–97)	76 (61–87)
PPV	88 (69–98)	81 (61–93)	54 (33–74)
NPV	96 (85–99)	96 (85–99)	76 (61–87)
+LR	13.8 (4.6–41.3)	8.6 (3.7–19.8)	2.2 (1.2–4.2)
–LR	0.1 (0.0–0.3)	0.1 (0.0–0.4)	0.6 (0.4–1.0)

Data for +LR and –LR presented as ratio (95% CI) or for the rest of parameters as % (95% CI); CI — confidence interval; NPV — negative predictive value; PPV — positive predictive value; +LR — positive likelihood ratio; –LR — negative likelihood ratio

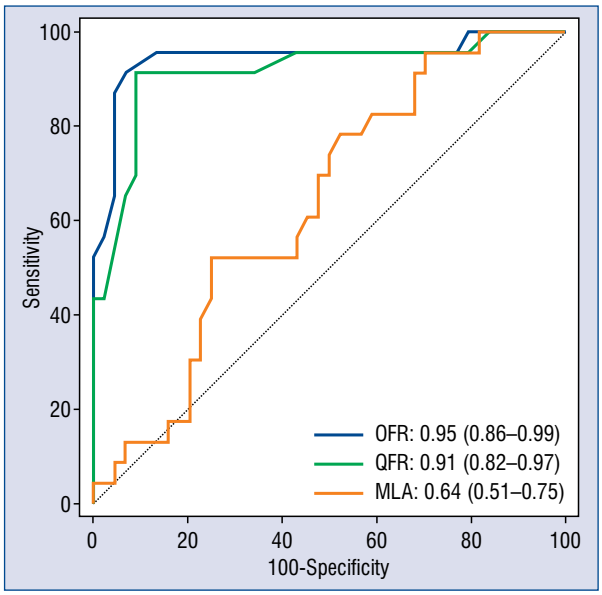

Figure 4. Comparison of receiver-operating curves for optical flow ratio (OFR), quantitative flow ratio (QFR) and optical coherence tomography-derived minimal lumen area (MLA) (cutoff 1.63 mm^2) to identify a flow-limiting coronary stenosis (fractional flow reserve ≤ 0.80). Results presented as area under curves (95% confidence interval).

non-LAD 94%; 95% CI: 85–100, p = 0.866), presence of a bifurcation lesion (bifurcation 92%; 95% CI: 83–100, no bifurcation 94%; 95% CI: 85–100, p = 0.866), sequential stenosis (tandem stenosis 91%; 95% CI: 81–100, single stenosis 94%; 95% CI: 87–100, p = 0.920), history of myocardial infarction (previous myocardial infarction 89%; 95% CI: 79–100, no previous infarction 97%; 95% CI: 91–100, p = 0.445) or the study center (Fig. 5).

Time consumption of OFR computation

The median time required for the computation of OFR once the OCT data were loaded into the software was 1.07 (interquartile range [IQR]: 0.98–1.16) min.

OFR reproducibility

The computation of OFR showed excellent intraobserver and interobserver reproducibility (ICCa = 0.97; 95% CI: 0.95–0.98, ICCa = 0.95; 95% CI: 0.92–0.97, respectively).

Impact of pullback speed

The agreement between OFR of the same vessel acquired at different pullback speed (18 vs. 36 mm/s) was excellent (r = 0.87; 95% CI: 0.73–0.94, ICCa = 0.85; 95% CI: 0.69–0.93, kappa = 0.697) (Fig. 6). The agreement improved if the computation was restricted to the same coronary segment imaged by both pullbacks (r = 0.90; 95% CI: 0.80–0.96, ICCa = 0.90; 95% CI: 0.80–0.95, kappa = 0.697) (Fig. 6).

Discussion

The main findings of this study can be summarised as follows: 1) OFR computation is feasible in a prospective real-world series; 2) OFR has excellent agreement with FFR and high reproducibility; 3) OFR has an excellent diagnostic performance to detect functionally-significant stenosis, tendentially

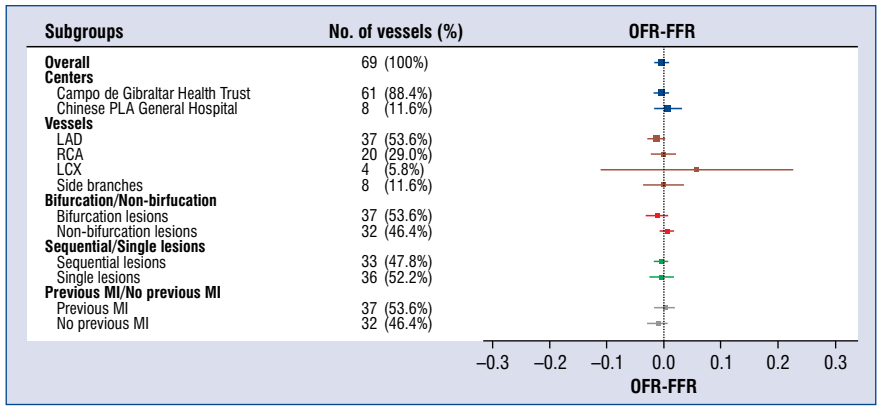

Figure 5. Subgroup analysis, presented as the paired difference optical flow ratio-fractional flow reserve (OFR-FFR). Analysed variables: center, coronary artery, bifurcation vs. non-bifurcation, sequential vs. single lesion, previous myocardial infarction (MI) vs. no previous MI characteristics; LAD — left anterior descending artery; LCX — left circumflex artery; RCA — right coronary artery.

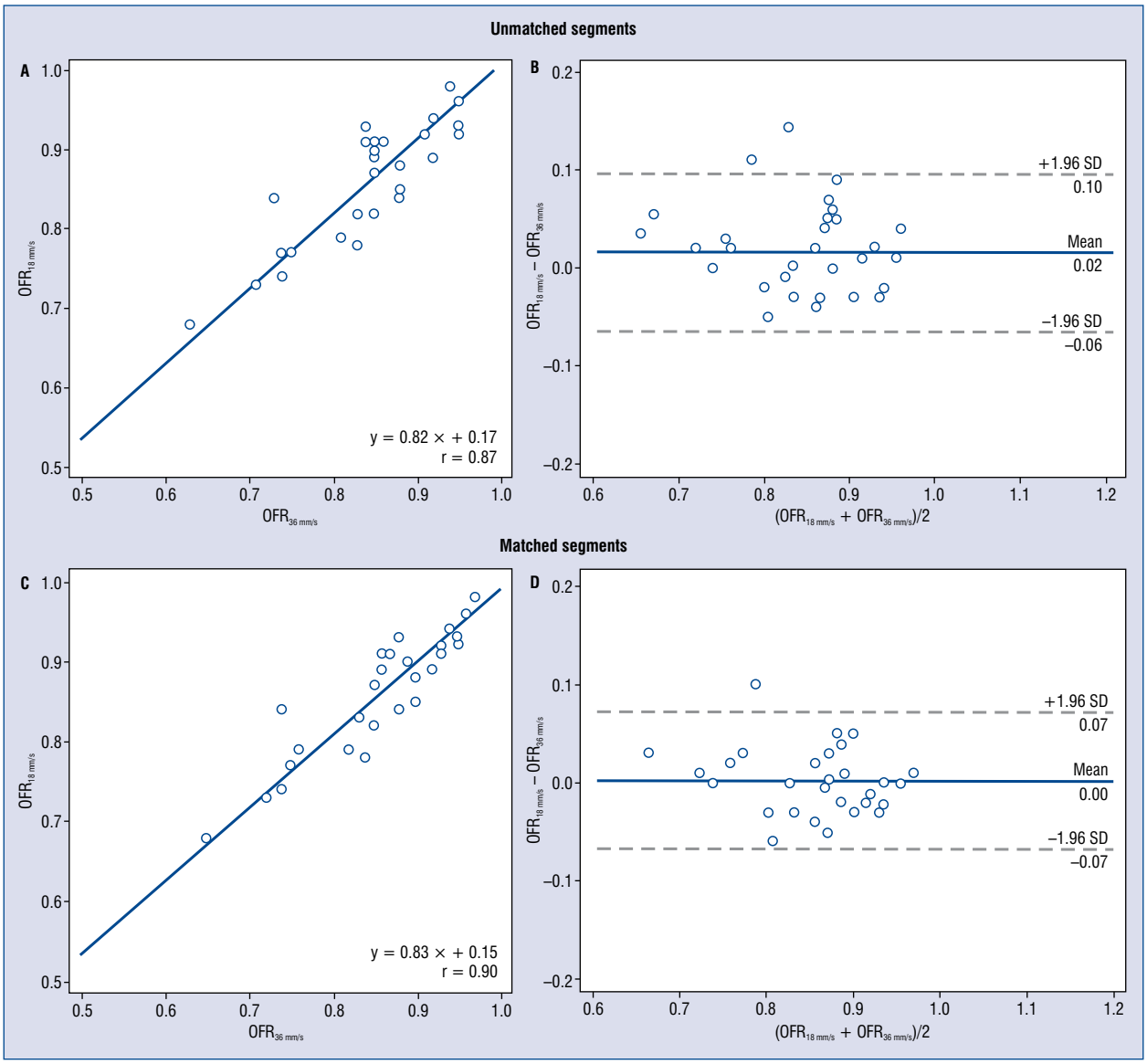

Figure 6. Correlation and agreement between optical flow ratio (OFR) acquired at different pullback speeds. **A.** Correlation and lineal regression of OFR acquired at 36 mm/s (abscises) and OFR acquired at 18 mm/s (ordinates); **B.** Bland-Altman plot for the agreement; Lower panels present the same lineal regression (**C**) and Bland-Altman plot (**D**) after matching the same coronary segment in the optical coherence tomography pullbacks acquired at different pullback speeds.

superior to angiography-based morphofunctional methods and significantly better than using a MLA cut-off; 4) The pullback speed has negligible effect on the computation of OFR, provided the pullbacks are obtained on the same coronary segment.

To the best of our knowledge, this is the first study to prove the feasibility of OFR prospectively in a real-world scenario, confirming the excellent diagnostic performance of previous retrospective reports [15, 16]. Actually, the diagnostic accuracy in this prospective series was even better than in previous post-hoc studies that had reported a diagnostic accuracy of 90–92% [15, 16], increasing to 93% in the current study. This observation can be likely explained by a more careful and dedicated OCT acquisition, specifically aiming to optimise the quality of OFR computation [20]. The consistent accuracy of OFR used on a prospective fashion is of paramount importance to outline the clinical usefulness and the limitations of this novel technology for routine use in the cathlab. As expected, morphofunctional methods outweighed the diagnostic performance of purely morphological methods, like MLA. Measuring MLA to assess

the severity of coronary stenosis was indeed common practice in the past, but this approach is currently discouraged [13]. Relying on the area in just a cross-section is probably too simplistic and disregards many other parameters (lesion length, reference vessel areas, flow, microvascular resistance, amount of subtended myocardium, excentricity of the lesion, etc.) that play a crucial role in determining the functional relevance of a stenosis and can be however integrated in both virtual and wire-based physiology [26]. Remarkably, OFR showed outstanding accuracy in challenging scenarios like bifurcations or sequential lesions, confirming the validity of the computational method in these specific settings [12, 27].

Among morphofunctional methods, OFR tended to show better diagnostic performance than QFR (AUC 0.95 vs. 0.91, p = 0.115), in line with the retrospective studies [16]. The lack of statistical significance can be explained by the difference in sample size between both studies, as AUC values are consistently similar. This prospective study was powered to estimate the AUC in OFR rather than for a comparison vs. QFR, that was only an exploratory secondary objective. Both morphofunctional methods rely on an accurate reconstruction of the coronary anatomy to enable a precise computation of physiology. Nonetheless, angiography-based methods like QFR share all the intrinsic limitations of angiography itself, namely foreshortening, vessel overlap or calcium interfering with adequate edge detection. Conversely, OFR can overcome all these limitations and render high-resolution luminograms, thus offering a clear advantage for an optimal computation of physiology that can be instrumental in some particular cases.

Pullback speed during the OCT acquisition had negligible effect on computation of OFR. The diagnostic accuracy remained excellent irrespective of the pullback speed, provided the same coronary segment was imaged. High pullback speed (36 mm/s) is however preferred because it allows longer pullbacks and less contrast, so the computation takes into account the true luminogram in a longer coronary segment that is otherwise assumed as physiologically inert in the lower speed (shorter pullback).

The possibility to integrate physiology within an ordinary OCT catheter opens new perspectives in interventional cardiology. It will be reassuring for QFR in case of challenging borderline lesions. Moreover, OFR permits the operator to conform to the highest standards currently recommended by guidelines, while complying with most of reimbursement policies in developed countries, where a single adjuvant tool for PCI can be invoiced. A single catheter can be used to assess the functional severity of all pertinent lesions, other morphological features (ruptured plaque, dissection, etc.) and finally to guide and optimise PCI. This is particularly interesting for the assessment of lesions with a high priori likelihood of PCI. Finally, OFR does not require hyperemia, like other computational methods [18], sparing the patient discomfort and circumventing the contraindications of vasodilator drugs.

Limitations of the study

This is a pivotal general study of agreement performed on an unselected real-world population of patients with an indication for FFR. The impact of microvascular resistance, plaque composition, collaterals and other relevant variables on the accuracy of OFR needs to be understood in future dedicated studies. The feasibility reported for OFR refers to patients with a coronary anatomy considered a priori suitable for OCT imaging by the operator.

All the OFR computations in this study were performed offline in a central corelab. This approach optimises the performance of the new method and guarantees methodological homogeneity. The diagnostic performance of OFR calculated on-site by trained local staff of the cathlab is hitherto unknown and will require specific evaluation in further dedicated studies.

Conclusions

The prospective computation of OFR is feasible and reproducible in a real-world series, resulting in excellent agreement with FFR and better diagnostic performance than angiography-based morphofunctional methods or than a MLA cut-off, irrespective of the pullback speed used in the OCT acquisition.

Impact on daily practice

Optical flow ratio appears as the most accurate morphofunctional method hitherto to estimate FFR. This enables the integration of accurate physiology and high-resolution imaging within a single catheter. This information is instrumental for modern PCI guidance, in order to comply with current evidence-supported and guidelines-recommended standards, as with the principles of personalised medicine. Morphofunctional methods allow the reconcilement between precision PCI and the reimbursement policy of many countries, where a single adjuvant tool for PCI can be invoiced.

Acknowledgements

Shengxian Tu would like to acknowledge the support by the National Key Research and Development Program of China (Grant No. 2016YFC0100500), the Natural Science Foundation of China (Grant No. 81871460), and by the Program of Shanghai Technology Research Leader.

Conflict of interest: The authors have declared no conflict of interest in relation to this study, with the exception that Shengxian Tu received research support from Pulse medical imaging technology. Other authors report no conflicts of interest regarding this manuscript.

References

1. De Bruyne B, Pijls NHJ, Kalesan B, et al. Fractional flow reserve-guided PCI versus medical therapy in stable coronary disease. N Engl J Med. 2012; 367(11): 991–1001, doi: 10.1056/NEJMoa1205361, indexed in Pubmed: 22924638.
2. Tonino PAL, De Bruyne B, Pijls NHJ, et al. FAME Study Investigators. Fractional flow reserve versus angiography for guiding percutaneous coronary intervention. N Engl J Med. 2009; 360(3): 213–224, doi: 10.1056/NEJMoa0807611, indexed in Pubmed: 19144937.
3. Bech GJ, De Bruyne B, Pijls NH, et al. Fractional flow reserve to determine the appropriateness of angioplasty in moderate coronary stenosis: a randomized trial. Circulation. 2001; 103(24): 2928–2934, doi: 10.1161/01.cir.103.24.2928, indexed in Pubmed: 11413082.
4. Toth GG, Toth B, Johnson NP, et al. Revascularization decisions in patients with stable angina and intermediate lesions: results of the international survey on interventional strategy. Circ Cardiovasc Interv. 2014; 7(6): 751–759, doi: 10.1161/CIRCINTERVENTIONS.114.001608, indexed in Pubmed: 25336468.
5. Härle T, Zeymer U, Hochadel M, et al. Real-world use of fractional flow reserve in Germany: results of the prospective ALKK coronary angiography and PCI registry. Clin Res Cardiol. 2017; 106(2): 140–150, doi: 10.1007/s00392-016-1034-5, indexed in Pubmed: 27599974.
6. Lee HS, Lee JM, Nam CW, et al. Consensus document for invasive coronary physiologic assessment in Asia-Pacific countries. Cardiol J. 2019; 26(3): 215–225, doi: 10.5603/CJ.a2019.0054, indexed in Pubmed: 31225632.
7. Gutiérrez-Chico JL, Regar E, Nüesch E, et al. Delayed coverage in malapposed and side-branch struts with respect to well-apposed struts in drug-eluting stents: in vivo assessment with optical coherence tomography. Circulation. 2011; 124(5): 612–623, doi: 10.1161/CIRCULATIONAHA.110.014514, indexed in Pubmed: 21768536.
8. Gutiérrez-Chico JL, Wykrzykowska J, Nüesch E, et al. Vascular tissue reaction to acute malapposition in human coronary arteries: sequential assessment with optical coherence tomography. Circ Cardiovasc Interv. 2012; 5(1): 20–29, S1, doi: 10.1161/CIRCINTERVENTIONS.111.965301, indexed in Pubmed: 22319063.
9. Gutiérrez-Chico JL, Alegría-Barrero E, Teijeiro-Mestre R, et al. Optical coherence tomography: from research to practice. Eur Heart J Cardiovasc Imaging. 2012; 13(5): 370–384, doi: 10.1093/ehjci/jes025, indexed in Pubmed: 22330231.
10. Ali ZA, Maehara A, Généreux P, et al. ILUMIEN III: OPTIMIZE PCI Investigators. Optical coherence tomography compared with intravascular ultrasound and with angiography to guide coronary stent implantation (ILUMIEN III: OPTIMIZE PCI): a randomised controlled trial. Lancet. 2016; 388(10060): 2618–2628, doi: 10.1016/S0140-6736(16)31922-5, indexed in Pubmed: 27806900.
11. Gonzalo N, Escaned J, Alfonso F, et al. Morphometric assessment of coronary stenosis relevance with optical coherence tomography: a comparison with fractional flow reserve and intravascular ultrasound. J Am Coll Cardiol. 2012; 59(12): 1080–1089, doi: 10.1016/j.jacc.2011.09.078, indexed in Pubmed: 22421301.
12. Li Y, Gutiérrez-Chico JL, Holm NR, et al. Impact of side branch modeling on computation of endothelial shear stress in coronary artery disease: coronary tree reconstruction by fusion of 3D angiography and OCT. J Am Coll Cardiol. 2015; 66(2): 125–135, doi: 10.1016/j.jacc.2015.05.008, indexed in Pubmed: 26160628.
13. Neumann FJ, Sousa-Uva M, Ahlsson A, et al. 2018 ESC/EACTS Guidelines on myocardial revascularization. Eur Heart J. 2018; 40(2): 87–165, doi: 10.1093/eurheartj/ehy394.
14. Tian F, Yu W, Huang J, et al. First presentation of integration of intravascular optical coherence tomography and computational fractional flow reserve. Int J Cardiovasc Imaging. 2019; 35(4): 601–602, doi: 10.1007/s10554-018-1491-1, indexed in Pubmed: 30390169.
15. Yu W, Huang J, Jia D, et al. Diagnostic accuracy of intracoronary optical coherence tomography-derived fractional flow reserve for assessment of coronary stenosis severity. EuroIntervention. 2019; 15(2): 189–197, doi: 10.4244/EIJ-D-19-00182, indexed in Pubmed: 31147309.
16. Huang J, Emori H, Ding D, et al. Comparison of diagnostic performance of intracoronary optical coherence tomography-based and angiography-based fractional flow reserve for evaluation of coronary stenosis. EuroIntervention. 2020 [Epub ahead of print], doi: 10.4244/EIJ-D-19-01034, indexed in Pubmed: 31951207.
17. Tu S, Barbato E, Köszegi Z, et al. Fractional flow reserve calculation from 3-dimensional quantitative coronary angiography and TIMI frame count: a fast computer model to quantify the functional significance of moderately obstructed coronary arteries. JACC Cardiovasc Interv. 2014; 7(7): 768–777, doi: 10.1016/j.jcin.2014.03.004, indexed in Pubmed: 25060020.
18. Tu S, Westra J, Yang J, et al. Diagnostic accuracy of fast computational approaches to derive fractional flow reserve from diagnostic coronary angiography: the international multicenter FAVOR pilot study. JACC Cardiovasc Interv. 2016; 9(19): 2024–2035, doi: 10.1016/j.jcin.2016.07.013, indexed in Pubmed: 27712739.
19. Prati F, Cera M, Ramazzotti V, et al. Safety and feasibility of a new non-occlusive technique for facilitated intracoronary optical coherence tomography (OCT) acquisition in various clinical and anatomical scenarios. EuroIntervention. 2007; 3(3): 365–370, doi: 10.4244/eijv3i3a66, indexed in Pubmed: 19737719.
20. Gutiérrez-Chico JL, Cortés C, Schincariol M, et al. A formula to calculate the contrast volume required for optimal imaging quality in optical coherence tomography with non-occlusive technique. Cardiol J. 2018; 25(5): 574–581, doi: 10.5603/CJ.a2018.0112, indexed in Pubmed: 30246237.
21. Xu B, Tu S, Qiao S, et al. Diagnostic accuracy of angiography-based quantitative flow ratio measurements for online assessment of

coronary stenosis. J Am Coll Cardiol. 2017; 70(25): 3077–3087, doi: 10.1016/j.jacc.2017.10.035, indexed in Pubmed: 29101020.

22. Westra J, Andersen BK, Campo G, et al. Diagnostic performance of in-procedure angiography-derived quantitative flow reserve compared to pressure-derived fractional flow reserve: the FAVOR II Europe-Japan study. J Am Heart Assoc. 2018; 7(14), doi: 10.1161/JAHA.118.009603, indexed in Pubmed: 29980523.
23. Karanasos A, Tu S, van Ditzhuijzen NS, et al. A novel method to assess coronary artery bifurcations by OCT: cut-plane analysis for side-branch ostial assessment from a main-vessel pullback. Eur Heart J Cardiovasc Imaging. 2015; 16(2): 177–189, doi: 10.1093/ehjci/jeu176, indexed in Pubmed: 25227268.
24. Finet G, Gilard M, Perrenot B, et al. Fractal geometry of arterial coronary bifurcations: a quantitative coronary angiography and intravascular ultrasound analysis. EuroIntervention. 2008; 3(4): 490–498, doi: 10.4244/eijv3i4a87, indexed in Pubmed: 19736093.
25. Liao JJZ. Sample size calculation for an agreement study. Pharm Stat. 2010; 9(2): 125–132, doi: 10.1002/pst.382, indexed in Pubmed: 19507134.
26. Gutiérrez-Chico JL, Zhao S, Chatzizisis YS. Vorticity: At the crossroads of coronary biomechanics and physiology. Atherosclerosis. 2018; 273: 115–116, doi: 10.1016/j.atherosclerosis.2018.04.001, indexed in Pubmed: 29665968.
27. Gutierrez-Chico JL, Cortes C, Jaguszewski M, et al. A simplified formula to calculate fractional flow reserve in sequential lesions circumventing the measurement of coronary wedge pressure: The APIS-S pilot study. Cardiol J. 2019; 26(4): 310–321, doi: 10.5603/CJ.a2019.0067, indexed in Pubmed: 31257567.

VIA MEDICA

ORIGINAL ARTICLE

Cardiology Journal
2020, Vol. 27, No. 4, 362–367
DOI: 10.5603/CJ.a2019.0020

ISSN 1897–5593

Anisocytosis predicts postoperative renal replacement therapy in patients undergoing heart valve surgery

Piotr Duchnowski[1], Tomasz Hryniewiecki[1], Mariusz Kuśmierczyk[2], Piotr Szymański[1]

[1]Department of Acquired Cardiac Defects, Institute of Cardiology, Warsaw, Poland
[2]Department of Cardiosurgery and Transplantology, Institute of Cardiology, Warsaw, Poland

Abstract

Background: *Acute kidney injury (AKI) is one of the serious postoperative complications in patients undergoing heart valve surgery. The aim of the present study was to identify selected biomarkers to predict AKI requiring renal replacement.*

Methods: *A prospective study was conducted on a group of 751 patients undergoing heart valve surgery. The data on risk factors, preoperative complete blood count, course of operations and postoperative period was assessed. The primary endpoint at the 30-day follow-up was postoperative AKI requiring renal replacement therapy. The secondary end-point was death from all causes in patients with postoperative AKI requiring renal replacement.*

Results: *The primary endpoint occurred in 46 patients. At multivariate analysis: age, red cell distribution width (RDW) and C-reactive protein remained independent predictors of the primary endpoint. Hemoglobin and RDW were associated with an increased risk of death.*

Conclusions: *Elevated RDW is associated with a higher risk of postoperative AKI and death in patients with AKI.* (Cardiol J 2020; 27, 4: 362–367)

Key words: anisocytosis, red cell distribution width, valve surgery, acute kidney injury

Introduction

Acute kidney injury (AKI) in patients undergoing heart valve surgery is one of the serious postoperative complications associated with prolonged hospitalization, increased mortality as well as the occurrence of chronic kidney disease [1–3]. The diagnosis of AKI is based on two functional markers, an increase of serum creatinine and a reduction of urinary excretion. Predictors of perioperative AKI in patients undergoing heart surgery include preoperative creatinine level, end-stage renal disease, 2-2 phenotype of haptoglobin, advanced age, diabetes mellitus, congestive heart failure, generalized atherosclerosis, cardiovascular collapse, nitric oxide, cyanotic heart disease, duration of surgery and elevated postoperative lactate level [4–9]. In patients with severe AKI, oliguria and fluid accumulation, renal replacement therapy is the basic method of treatment [10]. Hemodiafiltration seems to represent the gold standard in the field of replacement of renal function in patients undergoing heart valve surgery [11–13].

Red cell distribution width (RDW) is a parameter that reflects the variability of the size of red blood cells (anisocytosis). Elevated RDW is a result of erythrocytes production dysfunction related to a deficiency of folic acid, iron, vitamin B12 or ongoing inflammation as well as increased destruction of erythrocytes e.g. in the course of hemolysis. Previous studies have indicated the predictive ability of RDW in various cardiovascular disorders [14–24]. Identifying risk factors for developing AKI and aggressive early intervention is extremely important to optimize outcomes in patients with heart valve disease. Therefore, the aim of the present study

Address for correspondence: Piotr Duchnowski, MD, PhD, Department of Acquired Cardiac Defects, Institute of Cardiology, ul. Alpejska 42, 04–628 Warszawa, Poland, tel: +48 22 343 41 91, e-mail: duchnowski@vp.pl

Received: 9.11.2018 Accepted: 7.02.2019

was to identify and evaluate selected biomarkers to predict AKI requiring renal replacement therapy in patients undergoing heart valve surgery.

Methods

A prospective study was conducted on a group of consecutive patients with hemodynamically significant valvular heart disease (aortic stenosis, aortic regurgitation, mitral stenosis and/or mitral regurgitation) that qualified for cardiac surgery and subsequently underwent elective replacement or repair of a valve/valves. The exclusion criteria were: patients under 18 years of age, a lack of consent to participate in the study, hemolytic disease, blood transfusion before surgery in the last 3 months, active neoplastic diseases, autoimmune diseases, chronic inflammatory bowel and active endocarditis. One day prior to surgery a blood sample for biomarkers was collected from each patient. Full blood counts were measured from K_2EDTA samples using a Sysmex K-4500 electronic counter. The glomerular filtration rate (GFR) was estimated based on a simplified MDRD pattern: GFR (mL/min/1.73 m^2) = 186.3 × [creatinine concentration (mg/dL)] – 1.154 × [age (years)] – 0.203 × C, where C stood: for men — 1, for women — 0.742. Chronic renal failure was defined as chronic (lasting at least 3 months) impaired renal function, understood as a reduction in GFR < 60 mL/min/1.73 m^2 and included the following stages of chronic kidney disease (CKD), stage 3 CKD (GFR 45–59 mL/min/1.73 m^2), stage 3b CKD (GFR 30–44 mL/min/1.73 m^2), stage 4 CKD (GFR 15–29 mL/min/1.73 m^2) and stage 5 CKD (GFR < 15 mL/min/1.73 m^2). AKI was diagnosed as an increase in serum creatinine (SCr) by at least 0.3 mg/dL (26.5 μmol/L) within 48 h or a urine volume of less than 0.5 mL/kg/h for 6 h. The decision to start hemodiafiltration was made by the team of anesthesiologists responsible for the patient with the diagnosis of AKI and persisting high parameters of the kidneys (creatinine and/or urea) and anuria despite intensive conservative treatment. Continuous veno-venous hemodiafiltration was performed in all of the patients qualifying for renal replacement therapy. The primary end-point was perioperative AKI requiring renal replacement therapy. The secondary end-point was death from all causes in patients with perioperative renal replacement therapy. Patient follow-up was for 30 days or until death. The follow-up of discharged patients was conducted through direct observation during hospitalization and clinic visits for 30 days subsequent to surgery. The study was conducted at the Institute of Cardiology, Warsaw, Poland between January 1 2014 and September 30 2018. The protocol was approved by The Institutional Ethics Committee.

Statistical analysis

Statistical analysis was performed using the SAS version 9.2. Data are presented as the mean ± standard deviation and frequency (percentage). The Shapiro-Wilk test of normality was used to test sample distribution. Intergroup comparisons were made using the Mann–Whitney U test, the Pearson's χ^2 test or Student t-test. Delta 1 RDW value (Δ1RDW) defined as RDW measured 48 h after surgery minus preoperative RDW. Delta 2 RDW value (Δ2RDW) defined as RDW measured 94 h after surgery minus preoperative RDW. Logistic regression was used to assess relationships between variables. The following covariates: age, aortic cross-clamp time, cardiopulmonary bypass time, preoperative atrial fibrillation, body mass index (BMI), GFR, chronic obstructive airways disease, coronary artery disease, current smoker, dyslipidemia, EuroSCORE II, hypertension, insulin dependent diabetes mellitus, left ventricular ejection fraction, New York Heart Association (NYHA) classes, peripheral atherosclerosis, previous myocardial infarction, pulmonary blood pressure, stroke history, total cholesterol, creatinine, high sensitivity troponin T, C-reactive protein (CRP), hematocrit, hemoglobin, mean corpuscular hemoglobin, mean corpuscular volume, platelets, preoperative RDW, RDW measured 48 h after surgery (RDW1), RDW measured 96 h after surgery (RDW2), Δ1RDW, Δ2RDW and white blood cell count were investigated for association with endpoints in univariate analysis. Significant determinants ($p < 0.05$) identified from univariate analysis were subsequently entered into multivariate models. Predictive value of RDW was assessed by a comparison of the areas under the receiver operator characteristics of the respective curve. On the basis of the Youden index, a cut-off point was determined that met with the criterion of maximum sensitivity and specificity for perioperative renal replacement therapy.

Results

The study group included 751 consecutive patients who underwent replacement or repair of a valve/valves. The mean age was 63.5 ± 13 (Table 1). Two hundred twenty (29%) patients had preoperative chronic renal failure (stage 3a

Table 1. Baseline characteristics of the study population.

Characteristics of patients (n = 751)	Values	Values with RRT	Values without RRT	P
Age [years]	63.5 ± 13	69 ± 10	61 ± 13	0.002
Male: men	426 (57%)	22 (47%)	404 (57%)	NS
Body mass index [kg/m^2]	27 ± 9	26 ± 7	27 ± 10	NS
NYHA (classes)	2.6 ± 0.5	2.8 ± 0.8	2.4 ± 0.5	0.004
LV ejection fraction [%]	56 ± 12	54 ± 13	58 ± 10	NS
Pulmonary blood pressure [mmHg]	43 ± 17	55 ± 19	40 ± 9	0.005
EuroSCORE II [%]	3.55 ± 3.4	7 ± 5	3 ± 2	0.006
Atrial fibrillation	318 (42%)	33 (71%)	285 (40%)	0.004
Chronic renal failure (GFR < 60 mL/min/1.73 m^2)	220 (29%)	25 (54%)	195 (27%)	0.03
Chronic obstructive airways disease	42 (6%)	4 (8%)	38 (5%)	NS
Coronary artery disease	185 (24%)	9 (19%)	176 (25%)	NS
Peripheral atherosclerosis	55 (7%)	5 (7%)	38 (6%)	NS
Previous myocardial infarction	79 (10%)	6 (13%)	73 (10%)	NS
Stroke history	50 (7%)	1 (2%)	49 (7%)	NS
Hypertension	468 (62%)	26 (56%)	442 (62%)	NS
Insulin dependent diabetes mellitus	26 (3%)	1 (2%)	25 (3%)	NS
Current smoker	145 (19%)	8 (15%)	137 (29%)	NS
Cholesterol (total) [mmol/L]	4.7 ± 0.9	4.4 ± 1.2	4.8 ± 0.9	0.03
Hematocrit [%]	46 ± 10	37 ± 13	47 ± 9	0.001
Hemoglobin [g/dL]	13.7 ± 1.5	12.2 ± 1.8	14 ± 1.4	0.003
RDW [%]	13.8 ± 1.1	15.5 ± 2	13.5 ± 1.0	< 0.001
RDW1 [%]	14.2 ± 1.3	15.8 ± 2.1	14 ± 1.4	0.01
RDW2 [%]	14.4 ± 1.4	15.9 ± 2.2	14.1 ± 1.3	0.04
Δ1RDW	0.4 ± 0.2	0.3 ± 0.1	0.5 ± 0.4	NS
Δ2RDW	0.6 ± 0.3	0.4 ± 0.2	0.6 ± 0.3	NS
C-reactive protein [mmol/L]	93 ± 32	136 ± 48	90 ± 28	0.002
CRP [mg/dL]	0.44 ± 0.35	0.89 ± 0.6	0.34 ± 0.3	0.002
Hs-TnT [ng/L]	36 ± 28	73 ± 52	22 ± 17	0.003
Platelets [1000/uL]	192 ± 60	188 ± 58	195 ± 62	NS
Aortic cross-clamp time [min]	91 ± 39	94 ± 41	89 ± 30	NS
Cardiopulmonary bypass time [min]	115 ± 45	121 ± 46	112 ± 42	0.04
Hemodiafiltration time [days]	3 ± 2			
Main procedures				
AVR	219 (29%)	15 (32%)	204 (28%)	NS
AVR + supracoronary ascending aortic replacement	82 (11%)	3 (7%)	79 (11%)	NS
AVP	4 (0.5%)			
Bentall procedure	55 (7%)			
David procedure	5 (0.6%)			
AVR + MVR	68 (9%)	9 (19%)	79 (11%)	0.4
AVR + MVP	17 (2%)			
AVP + MVP	7 (1%)			
MVP	149 (20%)	9 (20%)	140 (19%)	ns
MVR	145 (19%)	10 (21%)	135 (19%)	ns
Concomitant procedures				
Coronary artery bypass grafting	104 (14%)	14 (30%)	90 (12%)	0.4

The values are represented by the mean and a measure of the variation of the internal standard deviation. AVR — aortic valve replacement; AVP — aortic valve plasty; GFR — glomerular filtration rate; Hs-TnT — high sensitivity troponin T; LV — left ventricle; MVR — mitral valve replacement; MVP — mitral valve plasty; NYHA — New York Heart Association; RDW — red cell distribution width (preoperative); RDW1 — red cell distribution width measured 48 hours after surgery; RDW2 — red cell distribution width measured 96 h after surgery; Δ1RDW — defined as RDW measured 48 h after surgery — preoperative RDW; Δ2RDW — defined as RDW measured 96 h after surgery — preoperative RDW; RRT — renal replacement therapy

Table 2. Analysis of predictive factors for the occurrence of postoperative renal replacement therapy.

Variable	Univariate analysis			Multivariate analysis		
	Odds ratio	95% CI	P	Odds ratio	95% CI	P
Age [years]	1.066	1.031–1.103	0.002	1.082	1.019–1.162	0.02
CBT [min]	1.202	1.101–1.303	0.04			
CRP [mg/dL]	2.442	1.546–3.556	0.002	2.386	1.416–3.268	0.04
Creatinine [mmol/L]	1.160	1.094–1.242	0.001			
GFR [mL/min/1.73 m^2]	0.944	0.927–0.962	0.004			
Hemoglobin [g/dL]	0.595	0.491–0.721	0.001			
LVEF [%]	0.966	0.944–0.988	0.003			
RDW [%]	1.697	1.290–2.233	0.0002	1.578	1.208–2.544	0.003
RDW1 [%]	1.798	1.135–2.448	0.009			

CBT — cardiopulmonary bypass time; CRP — C-reactive protein; GFR — glomerular filtration rate; LVEF — left ventricular ejection fraction; RDW — red cell distribution width (preoperative); RDW1 — red cell distribution width measured 48 h after surgery

CKD — 151 patients, stage 3b CKD — 52 patients, stage 4 CKD — 17 patients and stage 5 CKD — 0 patients). All procedures were performed through a midline sternotomy incision under general anesthesia in normothermia. The mean preoperative RDW level was 13.8% ± 1.1. Table 1 shows characteristics of patients studied. Forty-six patients required renal replacement therapy (25 patients with preoperative chronic renal failure). The statistically significant predictors of postoperative renal replacement therapy at univariate and multivariate analysis are presented in Table 2. At multivariate analysis: age (odds ratio [OR] 1.082; 95% confidence interval [CI] 1.019–1.162; p = 0.02), RDW (OR 1.578; 95% CI 1.208–2.544; p = 0.003) and CRP (OR 2.386; 95% CI 1.416–3.268; p = 0.04) remained independent predictors of the primary endpoint. The optimal cut-off point for postoperative renal replacement therapy was calculated at > 14.3% RDW (sensitivity 80%, specificity 76%). The area under receiver operator characteristic curve for postoperative AKI requiring renal replacement therapy for RDW is 0.804 (95% CI 0.772–0.832) (Fig. 1). Twenty-eight patients with AKI requiring renal replacement therapy died in 30-day follow-up (15 patients with preoperative chronic renal failure). Cause of death in all patients was the increasing multi-organ failure. Statistically significant predictors of death from all causes in patients with postoperative renal replacement therapy at univariate and multivariate analysis are presented in Table 3. At multivariate analysis, hemoglobin (OR 1.015; 95% CI 1.004–1.026; p = 0.01) and RDW (OR 1.288; 95% CI 1.152–1.422; p = 0.04) remained predictors of mortality.

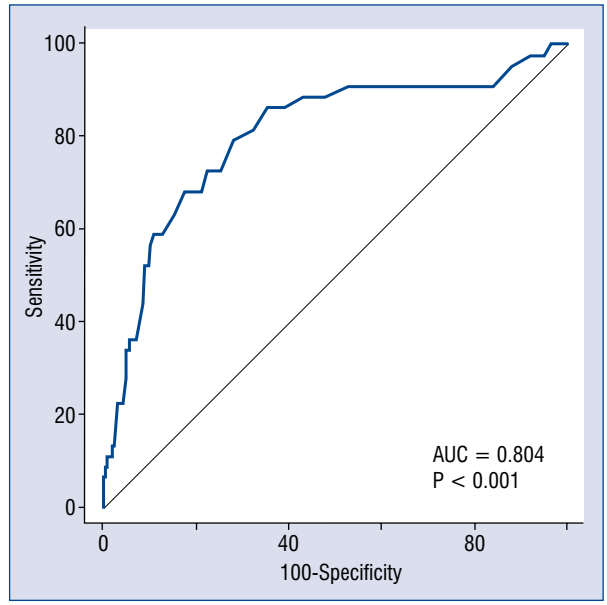

Figure 1. Area under receiver operating characteristic curve (AUC) of red cell distribution width for a renal replacement therapy following valve replacement/repair surgery.

Discussion

Acute kidney injury requiring renal replacement therapy is a common and significant complication after heart valve surgery. The present study revealed that this complication was seen in 6% of patients following heart valve surgery. The aim of this study was the evaluation and identification of predictors perioperative AKI requiring renal replacement therapy in the early postoperative

Table 3. Analysis of predictive factors for the occurrence of death in patients with renal replacement therapy.

Variable	Univariate analysis			Multivariate analysis		
	Odds ratio	95% CI	P	Odds ratio	95% CI	P
Age [years]	1.069	1.003–1.145	0.04			
Hemoglobin [g/dL]	0.614	0.410–0.907	0.01	1.015	1.004–1.026	0.01
RDW [%]	1.433	1.185–1.781	0.02	1.288	1.152–1.422	0.04

CI — confidence interval; RDW — red cell distribution width

period in patients undergoing heart valve surgery. In the present work RDW remained an independent predictor of AKI requiring renal replacement therapy and death from all causes in patients with primary endpoint. RDW is an inexpensive, simple and widely accessible parameter designated for each patient during a standard blood test. Predictive ability of the RDW in various cardiovascular disorders have been reported in numerous publications. However, information regarding the usefulness of RDW in patients undergoing heart valve surgery is very limited [14, 17–27]. The predictive power of the RDW for perioperative stroke and multiple organ dysfunction syndrome was previously demonstrated [17, 24]. According to available research, there are no reports describing the usefulness of RDW in anticipation of the renal replacement therapy in an early postoperative period in patients undergoing valve surgery. Zou et al. [28] described that an elevated RDW might be an independent prognostic factor for the severity and poor prognosis of AKI in patients undergoing cardiac surgery. Moreover, available literature has shown that higher values of RDW are associated with worse prognosis in patients with AKI treated with continuous renal replacement therapy [29]. The pathophysiological mechanisms that explain the relationship between increased RDW values and a worse prognosis are not clear. According to current knowledge, elevated RDW is the cause of impaired microcirculation. The older erythrocytes gradually lose the ability to deform the cell membrane. This feature is very important during the squeezing of anucleate cells through the vessels of small diameter in organs such as the kidneys. The rigid and large erythrocytes observed in patients with elevated values, RDW cannot squeeze through the capillaries and thus impair blood flow through microcirculation leading to renal tissue ischemia [30]. On the other hand, some authors connect RDW with a patient's physiologic reserve — the ability of cells to defend against the strong stress of hypoxia [31]. The reserve is very important in such stressful situations such as heart valve surgery. Elevated RDW, meant to reflect a reduced physiological reserve, may explain the fact of a higher incidence of serious complications in the postoperative period, such as postoperative AKI.

Conclusions

Red cell distribution width is a parameter that reflects the variability of the size of red blood cells (anisocytosis). Elevated RDW is a result of erythrocytes production dysfunction related to a deficiency of folic acid, iron, vitamin B12 or ongoing inflammation as well as increased destruction of erythrocytes e.g. in the course of hemolysis. The results of this study indicate that the RDW is a useful parameter for estimating the risk of postoperative renal replacement therapy and renal replacement therapy-related mortality in patients undergoing heart valve surgery. This was a single-center study that included a limited number of participating patients. In future studies, enlarging the group may allow confirmation of the results obtained. Further studies are needed to clarify the pathomechanisms linking an increased risk of perioperative renal replacement therapy in patients with a higher RDW.

Funding: Statutory work at the Institute of Cardiology, no 1705.

Conflict of interest: None declared

References

1. Knight JB, Lebovitz EE, Gelzinis TA, et al. Preoperative risk factors for unexpected postoperative intensive care unit admission: A retrospective case analysis. Anaesth Crit Care Pain Med. 2018; 37(6): 571–575, doi: 10.1016/j.accpm.2018.02.002, indexed in Pubmed: 29455034.

2. Tőth R, Breuer T, Cserép Z, et al. Acute kidney injury is associated with higher morbidity and resource utilization in pediatric patients undergoing heart surgery. Ann Thorac Surg. 2012; 93(6): 1984–1990, doi: 10.1016/j.athoracsur.2011.10.046, indexed in Pubmed: 22226235.
3. Lopez-Delgado JC, Esteve F, Torrado H, et al. Influence of acute kidney injury on short- and long-term outcomes in patients undergoing cardiac surgery: risk factors and prognostic value of a modified RIFLE classification. Crit Care. 2013; 17(6): R293, doi: 10.1186/cc13159, indexed in Pubmed: 24330769.
4. Liu Y, Zhang H, Liu Y, et al. Risk factors and short-term prognosis of preoperative renal insufficiency in infective endocarditis. J Thorac Dis. 2018; 10(6): 3679–3688, doi: 10.21037/jtd.2018.06.11, indexed in Pubmed: 30069366.
5. Dhoble A, Zhao Y, Vejpongsa P, et al. National 10-year trends and outcomes of isolated and concomitant tricuspid valve surgery. J Cardiovasc Surg (Torino). 2019; 60(1): 119–127, doi: 10.23736/S0021-9509.18.10468-X, indexed in Pubmed: 29969002.
6. Lei C, Berra L, Rezoagli E, et al. Nitric oxide decreases acute kidney injury and stage 3 chronic kidney disease after cardiac surgery. Am J Respir Crit Care Med. 2018; 198(10): 1279–1287, doi: 10.1164/rccm.201710-2150OC, indexed in Pubmed: 29932345.
7. Amini S, Abbaspour H, Morovatdar N, et al. Risk factors and outcome of acute kidney injury after congenital heart surgery: a prospective observational study. Indian J Crit Care Med. 2017; 21(12): 847–851, doi: 10.4103/ijccm.IJCCM_459_16, indexed in Pubmed: 29307966.
8. Feng C, Naik BI, Xin W, et al. Haptoglobin 2-2 phenotype is associated with increased acute kidney injury after elective cardiac surgery in patients with diabetes mellitus. J Am Heart Assoc. 2017; 6(10), doi: 10.1161/JAHA.117.006565, indexed in Pubmed: 28982674.
9. Olivero JJ, Olivero JJ, Nguyen PT, et al. Acute kidney injury after cardiovascular surgery: an overview. Methodist Debakey Cardiovasc J. 2012; 8(3): 31–36, indexed in Pubmed: 23227284.
10. Romagnoli S, Ricci Z, Ronco C. Perioperative acute kidney injury: prevention, early recognition, and supportive measures. Nephron. 2018; 140(2): 105–110, doi: 10.1159/000490500, indexed in Pubmed: 29945154.
11. Ronco C. Hemodiafiltration: technical and clinical issues. Blood Purification. 2015; 40(1): 2–11, doi: 10.1159/000437403.
12. den Hoedt CH, Bots ML, Grooteman MPC, et al. CONTRAST Investigators. Online hemodiafiltration reduces systemic inflammation compared to low-flux hemodialysis. Kidney Int. 2014; 86(2): 423–432, doi: 10.1038/ki.2014.9, indexed in Pubmed: 24552852.
13. Eremenko AA, Pavlov MV, Kolpakov PE, et al. [The influence of continuous veno-venous haemodiafiltration start time on multiple organ dysfunction syndrome treatment results in cardiac surgery patients]. Anesteziol Reanimatol. 2013(2): 63–66, indexed in Pubmed: 24000655.
14. Duchnowski P, Hryniewiecki T, Stokłosa P, et al. Number of erythrocytes as a prognostic marker in patients undergoing heart valve surgery. Kardiol Pol. 2018; 76(4): 791–793, doi: 10.5603/KP.2018.0076, indexed in Pubmed: 29652422.
15. Aslan D, Gümrük F, Gürgey A, et al. Importance of RDW value in differential diagnosis of hypochrome anemias. Am J Hematol. 2002; 69(1): 31–33, indexed in Pubmed: 11835328.
16. Montagnana M, Cervellin G, Meschi T, et al. The role of red blood cell distribution width in cardiovascular and thrombotic disorders. Clin Chem Lab Med. 2011; 50: 635–41.
17. Duchnowski P, Hryniewiecki T, Kusmierczyk M, et al. Red cell distribution width is a prognostic marker of perioperative stroke in patients undergoing cardiac valve surgery. Interact Cardiovasc Thorac Surg. 2017; 25(6): 925–929, doi: 10.1093/icvts/ivx216, indexed in Pubmed: 29049563.
18. Montagnana M, Cervellin G, Meschi T, et al. The role of red blood cell distribution width in cardiovascular and thrombotic disorders. Clin Chem Lab Med. 2011; 50: 635–641.
19. Salvagno GL, Sanchis-Gomar F, Picanza A, et al. Red blood cell distribution width: A simple parameter with multiple clinical applications. Crit Rev Clin Lab Sci. 2015; 52(2): 86–105, doi: 10.3109/10408363.2014.992064, indexed in Pubmed: 25535770.
20. Duchnowski P, Hryniewiecki T, Stokłosa P, et al. Red Cell Distribution Width as a Prognostic Marker in Patients Undergoing Valve Surgery. J Heart Valve Dis. 2017; 26: 714–720.
21. Tonelli M, Sacks F, Arnold M, et al. Relation between red blood cell distribution width and cardiovascular event rate in people with coronary disease. Circulation. 2008; 117: 163–168.
22. Duchnowski P, Hryniewiecki T, Kuśmierczyk M, et al. The usefulness of selected biomarkers in aortic regurgitation. Cardiol J. 2019; 26(5): 477–482, doi: 10.5603/CJ.a2018.0108, indexed in Pubmed: 30234893.
23. Balta S, Demirkol S, Aydogan M, et al. Red cell distribution width is a predictor of mortality in patients undergoing coronary artery bypass surgery. Eur J Cardiothorac Surg. 2013; 44(2): 396–397, doi: 10.1093/ejcts/ezt073, indexed in Pubmed: 23428577.
24. Duchnowski P, Hryniewiecki T, Kuśmierczyk M, et al. Red cell distribution width as a predictor of multiple organ dysfunction syndrome in patients undergoing heart valve surgery. Biol Open. 2018; 7(10), doi: 10.1242/bio.036251, indexed in Pubmed: 30127093.
25. Magri CJ, Chieffo A, Latib A, et al. Red blood cell distribution width predicts one-year mortality following transcatheter aortic valve implantation. Int J Cardiol. 2014; 172(2): 456–457, doi: 10.1016/j.ijcard.2013.12.216, indexed in Pubmed: 24529824.
26. Aung N, Dworakowski R, Byrne J, et al. Progressive rise in red cell distribution width is associated with poor outcome after transcatheter aortic valve implantation. Heart. 2013; 99: 1261––1266.
27. Duchnowski P, Hryniewiecki T, Koźma M, et al. High-sensitivity troponin T is a prognostic marker of hemodynamic instability in patients undergoing valve surgery. Biomark Med. 2018; 12(12): 1303–1309, doi: 10.2217/bmm-2018-0186, indexed in Pubmed: 30520660.
28. Zou Z, Zhuang Y, Liu L, et al. Role of elevated red cell distribution width on acute kidney injury patients after cardiac surgery. BMC Cardiovasc Disord. 2018; 18: 166.
29. Vashistha T, Streja E, Molnar MZ, et al. Red cell distribution width and mortality in hemodialysis patients. Am J Kidney Dis. 2016; 68(1): 110–121, doi: 10.1053/j.ajkd.2015.11.020, indexed in Pubmed: 26786297.
30. Patel KV, Mohanty JG, Kanapuru B, et al. Association of the red cell distribution width with red blood cell deformability. Adv Exp Med Biol. 2013; 765: 211–216.
31. Friedman JS, Lopez MF, Fleming MD, et al. SOD2-deficiency anemia: protein oxidation and altered protein expression reveal targets of damage, stress response, and antioxidant responsiveness. Blood. 2004; 104(8): 2565–2573, doi: 10.1182/blood-2003-11-3858, indexed in Pubmed: 15205258.

VIA MEDICA

ORIGINAL ARTICLE

Cardiology Journal
2020, Vol. 27, No. 4, 368–375
DOI: 10.5603/CJ.a2020.0060

ISSN 1897–5593

Catheter directed thrombolytic therapy and aspiration thrombectomy in intermediate pulmonary embolism with long term results

Zoltan Ruzsa[1, 2], Zoltan Vámosi[2], Balázs Berta[3], Balázs Nemes[1], Károly Tóth[2], Nándor Kovács[2], Endre Zima[1], Dávid Becker[1], Béla Merkely[1]

[1]Semmelweis University of Budapest, Heart and Vascular Center, Budapest, Hungary
[2]Bács-Kiskun County Hospital, Cardiology Division, Invasive Cardiology, Kecskemét, Hungary
[3]Department of Cardiology, Isala Hospital, Zwolle, The Netherlands

Abstract

Background: *Catheter directed thrombolysis (CDT) and thrombectomy represent well established techniques for the treatment of intermediate pulmonary embolism (IPE). The long-term effect of catheter directed thrombolysis of IPE is unknown.*

Methods: *Clinical, interventional and echocardiographic data from 80 consecutive patients with IPE who were treated with CDT were evaluated. Primary end-points were technical success and major adverse events. Secondary end-points were cardiovascular mortality, all-cause mortality, clinical success, rate of bleeding complications, improvement in pulmonary pressure and echocardiography parameters. CDT completed with alteplase (10 mg bolus and 1 mg/h maintenance dose) through a pig-tail catheter for 24 h. After 24 h, control pulmonary angiography was performed.*

Results: *In total, 80 patients with a mean age of 59.0 ± 16.8 years were treated. CDT was successful after the first post-operative day in 72 (90%) patients, but thrombus aspiration and fragmentation was performed due to failed thrombolysis in 8 (10%) patients. Final technical and clinical success was reached in 79 (98.8%) and 77 (96.3%) patients, respectively. The mean CDT time in IPE was 27.8 ± ± 9.6 h. Invasive pulmonary pressure dropped from 57.5 ± 16.7 to 38.9 ± 13.5 ($p < 0.001$). A caval filter was implanted in 4 (5%) patients. The 1-year major adverse events and cardiovascular mortality rate was 4.0% and 1.4%, respectively. Access site complications (6 major and 6 minor) were encountered in 12 (16.2%) patients.*

Conclusions: *Catheter directed thrombolysis in submassive pulmonary embolism had excellent results. However, additional mechanical thrombectomy was necessary in some patients to achieve good clinical outcomes.* (Cardiol J 2020; 27, 4: 368–375)

Key words: pulmonary embolism, local thrombolysis

Introduction

Venous thromboembolic disease is an underdiagnosed disease spectrum with a high mortality and morbidity rate. Recent advances in interventional cardiology, pharmacotherapeutics and modern surgical management in tertiary cardiac care centers have tremendously improved the present treatment of pulmonary embolism (PE). PE is commonly classified as high-risk, intermediate-risk, and low-risk to help determine the required treatment [1]. Despite recent advances in mechanical thrombectomy (MT) and catheter directed thrombolysis (CDT), the primary treatment is systemic thrombolysis (ST) in intermediate- and high-risk PE [1]. ST is associated with a high rate of

Address for correspondence: Zoltán Ruzsa, MD, PhD, Associate Professor, Semmelweis University, Heart and Vascular Center, Budapest, 1122, Városmajor Street 68, Hungary, tel: 0036203338490, e-mail: zruzsa25@gmail.com

Received: 2.12.2019 Accepted: 2.02.2020

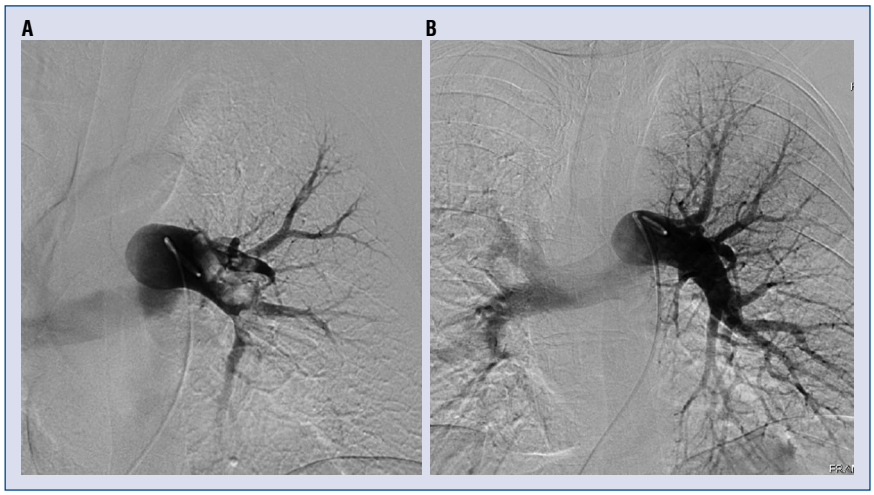

Figure 1. Angiography and catheter directed thrombolysis of a 63-year-old woman presenting with acute dyspnea and referred for pulmonary angiography; **A.** Selective angiography from right femoral vein access shows nearly complete left main pulmonary artery occlusion and elevated pulmonary pressures. Selective thrombolysis with 10 mg tissue plasminogen activator, followed by 1 mg/h-maintained infusion was initiated; **B.** Control angiography shows complete resolution of the thrombi and decreased pulmonary pressure.

recanalization in intermediate PE (IPE), but bleeding complications are very frequent and hazardous [2]. Despite recent advances in IPE, MT and CDT have a IIb indication in the recent European and American College of Cardiology guidelines [1, 2]. When thrombolysis is contraindicated or has failed, urgent surgical embolectomy or catheter embolectomy may be lifesaving procedures in high-risk PE. The aim of the study was to investigate the safety and efficacy of CDT and MT in IPE and to investigate the long-term effects on functional status and pulmonary pressure.

Methods

Clinical, interventional and echocardiographic data from 80 consecutive patients with IPE who were treated with CDT were evaluated. Diagnosis was made by computed tomography or pulmonary angiography and transthoracic ultrasound.

Inclusion criteria were: intermediate pulmonary embolism (defined as normotensive patients with PE and evidence of right ventricular dysfunction) and patients who underwrote the patient form.

Exclusion criteria were: contraindications for the local administration of thrombolytic therapy (stroke or transient ischemic attack, head trauma, or other active intracranial or intraspinal disease within 12 months; major surgery within 7 days; recent active bleeding from a major organ); and massive PE (defined as syncope, systemic arterial hypotension, cardiogenic shock, or resuscitated cardiac arrest).

Primary end-points were: technical success and major adverse events.

Secondary end-points were: all-cause mortality, cardiovascular mortality, clinical success, rate of bleeding complications, improvement in pulmonary pressure, blood gas analysis, and echocardiography parameters.

Procedure description

The access site for CDT was the contralateral femoral vein. The common femoral vein was punctured in a regular fashion, but in vascular cases, vascular ultrasound guidance was used when the puncture was difficult. Pulmonary angiography and invasive pulmonary pressure measurement were performed before CDT (Fig. 1A). CDT was done with alteplase (10 mg bolus and 1 mg/h maintenance dose) through a pig-tail catheter for 24 h. After 24 h, control pulmonary angiography and invasive pressure measurement was done (Fig. 1B). During the procedure, intravenous unfractionated heparin was continued at intermediate intensity with a goal activated partial thromboplastin time of 40–60 s. MT was performed when the thrombus burden was flow limiting or the systolic pulmonary pressure had not decreased by 25% or to the normal level (Fig. 2A). Thrombus fragmentation with the pigtail catheter was done in cases of extreme flow limiting thrombus. Thrombus aspiration was done with a 7 F guiding catheter and long 7 F sheath using a 50-mL syringe for manual aspiration (Fig. 2B). After removal of the catheters, the access site was manually compressed for a minimum of

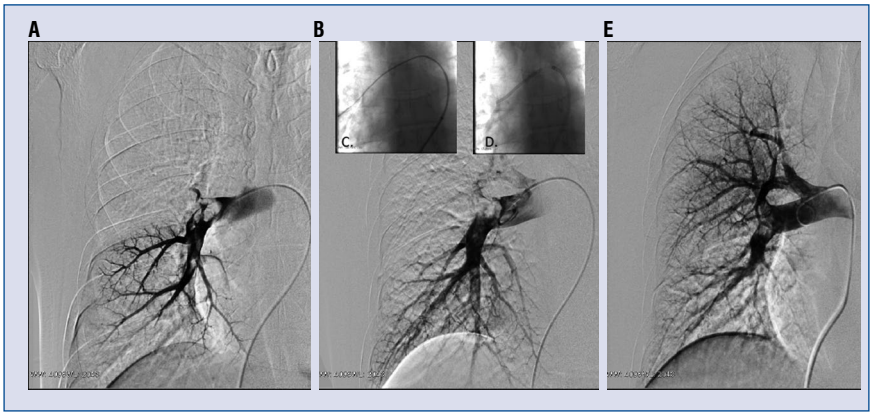

Figure 2. Catheter directed thrombolysis and mechanical thrombectomy of a 68-year-old man presenting with acute dyspnea; **A.** Selective angiography from right femoral vein access shows nearly complete right main pulmonary artery occlusion and elevated systolic pulmonary pressure (70 mmHg). Selective thrombolysis with 10 mg tissue plasminogen activator, followed by 1 mg/h-maintained infusion was initiated; **B.** Control angiography shows incomplete thrombus resolution and hemodynamic result (systolic pulmonary pressure: 70 mmHg), therefore a 7 F 90 cm sheath was advanced in the right main pulmonary artery over a long 360 J tip guidewire (**C**) and mechanical thrombectomy was done with a 100 cm Judkins right guiding catheter (**D**); **E.** Control angiography shows complete resolution of the thrombi and decreased systolic pulmonary pressure (40 mmHg).

5 min. Insertion of inferior vena cava filters was discouraged unless the patient developed a contraindication to therapeutic-dose systemic anticoagulation or if the patient suffered recurrent PE despite therapeutic levels of anticoagulation. Postoperatively, patients were treated with systemic anticoagulation and compression hose, and follow-up was completed at specified intervals.

Pulmonary angiography with digital subtraction was done on the next postoperative day in all patients. Thrombus burden was categorized as: occlusive or large (75–100% of the lumen) (Grade 3), medium (50–75% of the lumen) (Grade 2), small (0–50% of the lumen) (Grade 1) or no visible thrombus (Grade 0).

Twelve-lead electrocardiography was done in all patients at admission and before discharge.

Transthoracic ultrasound was performed before and after thrombolytic therapy. Routine right heart measurements were performed to investigate right ventricular function.

Post procedural follow-up

Access arteries were investigated physically after the procedure. All patients underwent detailed clinical follow-up examinations at two and 12 months after the procedure.

Definitions

Pulmonary hypertension was quantified by systolic pulmonary artery pressure as normal (< 40 mmHg), mild hypertension ("40–60" > > 90 mmHg), moderate hypertension ("60––90" > 90 mmHg) and severe hypertension (> 90 mmHg) [3].

Major adverse events were assessed as the composite of cardiovascular death, myocardial infarction, stroke, and repeated revascularization of the target vessel by surgical thrombectomy at 2 months and 12 months.

Bleeding events were classified by the Global Utilization of Streptokinase and Tissue Plasminogen Activator for Occluded Coronary Arteries (GUSTO) bleeding criteria [3]; major bleeding was defined as either GUSTO moderate or GUSTO severe/life-threatening bleeding events.

A major vascular access complication was defined as a diminished or lost arterial pulse or the presence of any pseudoaneurysm or arteriovenous fistula during clinical follow-up. A minor complication was defined as a hematoma requiring no further treatment that measures at least "≤ 5" cm in diameter at the femoral puncture site. Major bleeding was defined as a fall in hemoglobin of more than 3 gm/dL or any bleeding requiring a blood transfusion.

A technical success was when the invasive pulmonary pressure decreased by 25% and there was no clot in the main pulmonary branch.

Primary technical success was defined as the moment when CDT reached the end points, and secondary technical success was defined as the moment when CDT was followed by MT.

Clinical success was an improvement in at least one clinical category of the New York Heart Association classification.

Statistical analysis

Statistical analysis was performed using commercially available Graph Pad Prism 8.0 software (USA). Each continuous variable was expressed as the mean ± standard deviation or as the median (interquartile range), as appropriate. Each categorical variable was expressed as a percentage. The various patient cohorts were compared using either the Mann-Whitney test or the Kruskal-Wallis test. Probability values not exceeding 0.05 were considered significant.

Results

In total, 80 patients with submassive and massive pulmonary embolism were treated with CDT and MT. Demographic and clinical data and etiology of the pulmonary emboli are summarized in Table 1.

Angiographic and procedural results are summarized in Table 2.

In total, 80 patients with a mean age of 59 ± ± 16.8 years were treated. CDT was successful after the first post-operative day in 72 (90%) patients, but thrombus aspiration and fragmentation was performed due to failed thrombolysis in 8 (10%) patients. Final technical and clinical success was reached in 79 (98.8%) and 77 (96.3%) patients, respectively. The mean CDT time in IPE was 27.8 ± 9.6 h. The pulse rate and systolic blood pressure at presentation was 104.4 ± 17.62 bpm and 128.9 ± 18.7 mmHg, respectively. Invasive pulmonary pressure dropped from 57.5 ± 16.7 to 39.9 ± 13.3 and finally to 38.9 ± 13.5 ($p < 0.001$). Pre- and post-procedural pulmonary pressure is summarized in Figure 3. A caval filter was implanted in 4 (5%) patients. Two patients received it in the acute phase (2.5%): one due to large iliac vein thrombosis and the other one due to recurrent PE with decreased pulmonary reserve. During follow up caval filter was implanted also in 2 (2.5%) patients. The indication was in both patient's contraindication of oral anticoagulation due to major bleeding under post-procedural oral anticoagulation therapy (one gynecological and one cerebral focus).

Echocardiographic parameters are summarized in Table 3.

All patients had pre-procedural elevated right ventricular systolic pressure (55 [46–66] mmHg), but due to left ventricular enlargement the typical D sign was not present in 4 (5.0%) patients.

Table 1. Demographic data.

Age [years]	59.0 ± 16.8
Female	38 (47.5%)
Hypertension	50 (62.5%)
Hyperlipidemia	39 (48.8%)
Diabetes mellitus	7 (8.8%)
Obesity	16 (20.0%)
Active smokers	4 (5.1%)
Coronary artery disease	3 (3.8%)
Peripheral artery disease	4 (5.0%)
Renal failure	18 (22.5%)
Positive family history (PE)	2 (2.5%)
Causes of the deep venous thrombosis and PE	
Idiopathic	49 (59.8%)
Tumor	13 (16.3%)
Oral anticonceptions	2 (2.5%)
Trauma or Immobility	8 (10.0%)
Hypercoagulability	9 (11.3%)

PE — pulmonary embolism

Table 2. Angiographic and procedural data.

Angiographic data	
Thrombi location:	
Proximal main branch and central	40 (50.0%)
Distal main branch	36 (45.0%)
Distal segment	4 (5.0%)
Thrombi side:	
Right	14 (17.5%)
Left	15 (18.8%)
Both	51 (63.8%)
Procedural data	
Contrast consumption [mL]	64.2 ± 26.3
Fluoroscopy time [min]	4.77 ± 1.9
X-ray dose [dyn]	358.1 ± 170.1
Dose area product [dyn/cm^2]	2.7 ± 1.6
Average lysis time [h]	27.8 ± 9.6
Technical success	79 (98.8%)
Procedural technique:	
Catheter directed thrombolysis	80 (100.0%)
Additional thrombectomy	12 (15.0%)
Prolonged thrombolysis (> 24 h)	16 (20.0%)
Balloon dilatation	2 (2.5%)
Invasive pulmonary pressure [mmHg]:	
Before thrombolysis	57.5 ± 16.7
First postoperative day	39.9 ± 39.9*
Second postoperative day or FINAL pressure	38.9 ± 13.5*

*$p < 0.01$

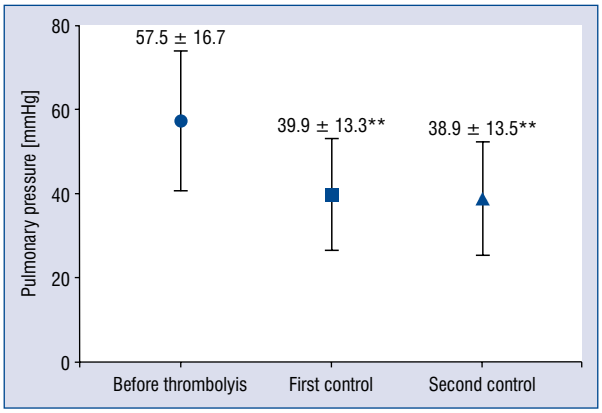

Figure 3. Invasive systolic pulmonary pressures before and after thrombolysis; **p < 0.01.

D sign was post-procedural not present in 93.8% and during follow-up in 95.0% of the patients. Tricuspid annular plane systolic excursion and pulmonary pressure has been improved after CDT and MT from 18 [16–20] to 22 [20–24] mm (p = = 0.005) and from 55 [46–66] to 40 [40–48] mmHg (p < 0.001), respectively.

Procedural complications are summarized in Table 4.

As indicated in Table 3, intraprocedural complications were not observed. Worsening heart failure or renal failure was not detected in the investigated population. The rates of major and minor vascular access complications were 7.5% (4 major subcutaneous hematomas and 2 retroperitoneal hematomas) and 7.5% (6 subcutaneous hematomas), respectively.

One-year follow-up

Clinical success at discharge was reached in 77 (96.2%) patients. The 1-year major adverse events and cardiovascular mortality rates were 4% and 1.4%, respectively. The overall 1-year mortality rate was 6.7% (1 cardiovascular and 5 tumor-associated).

Discussion

According to available research, this study is the first to show long-term clinical benefit in patients who underwent CDT and MT in IPE through long-term analysis.

Systemic full dose thrombolysis in a recent meta-analysis reduced the risk for death and cardiovascular collapse but increased the risk for major bleeding and hemorrhagic stroke [4]. The PEITHO study was a randomized, double blind study of 1,005 submassive PE patients comparing the thrombolytic agent tenecteplase with heparin to a placebo with heparin [5]. Death or hemodynamic decompensation occurred within 7 days from randomization in 2.6% of the patients in the tenecteplase group compared to 5.6% in the placebo group. However, stroke occurred in 2.4% in the tenecteplase group compared to 0.2% in the placebo group. The long-term follow-up in the PEITHO study showed no survival (98.3% vs. 98%) or functional (36% vs. 20.1%) or echocardiographic benefit in the thrombolysis arm compared with the anticoagulation arm [6].

Catheter interventions using thrombolytic drugs include CDT and pharmacomechanical thrombolysis. Their application was introduced due to a high rate of bleeding events during sys-

Table 3. Echocardiographic parameters.

ECHO	Preinterventional (n = 80)	Post interventional (n = 80)	One-year follow-up (n = 74)	P
LVEF [%]	57 [53–60]	58 [54–60]	60 [56–60]	< 0.001
PP	55 [46–66]	40 [40–48]	35 [30–40]	< 0.001
D sign:				< 0.001
0	4 (5.0%)	75 (93.8%)	76 (95.0%)	
1	76 (95.0%)	5 (6.2%)	4 (5.0%)	
RV/LV:				< 0.001
< 1	4 (5.0%)	51 (63.8%)	71 (95.9%)	
≅1	21 (26.3%)	24 (30.0%)	0 (0.0%)	
> 1	55 (68.8%)	5 (6.3%)	3 (4.1%)	
TAPSE	18 [16–20]	22 [20–24]	24 [22–27]	0.005

LV — left ventricle; LVEF — left ventricular ejection fraction; RV — right ventricle; PP — pulmonary pressure; TAPSE — tricuspid annular plane systolic excursion

Table 4. Procedural complications and major adverse events (MAE).

	One-month follow-up	One-year follow-up
Summary of MAE		
Cardiovascular death	0 (0%)	1 (1.4%)
Intracranial bleeding	1 (1.2%)	2 (2.7%)
Myocardial infarction	0 (0%)	0 (0%)
Repeat revascularization	0 (0.0%)	1 (1.3%)
All MAE's	1 (1.2%)	3 (4.0%)
Death (all)	1 (1.2%)	5 (6.7%)
Periprocedural complication		
Respiratory failure	0 (0%)	–
Cardiogenic shock	0 (0%)	–
Stroke/Cerebral bleeding	1 (1.2%)	–
Pulmonary vascular complications		
Perforation	0 (0%)	–
Major distal embolization	0 (0%)	–
Bleeding complications		
Intracranial bleeding	1 (1.2%)	2 (2.7%)
Access site complications:		
Major	6 (7.5%)	6 (7.5%)
Minor	6 (7.5%)	6 (7.5%)
All bleeding complications	13 (16.2%)	13 (16.2%)

temic thrombolysis. The principal mechanism of transcatheter therapy is to either dissolve and/or directly remove the clot with direct thrombus aspiration, fragmentation, administration of local thrombolytic drug or combination of these mechanisms. Thrombus removal is applied to immediately restore blood flow to pulmonary circulation, with subsequent improvement in the right ventricular strain, hemodynamic status, and oxygenation. Today, the choice lies between streptokinase, recombinant tissue plasminogen activator and urokinase. The choice of procedure and tools differs based on the severity of the PE and estimated bleeding risk [7]. There are only a few prospective clinical trials examining CDT alone [8–10], ultrasound facilitated CDT [11, 12] or CBT with thrombus fragmentation and/or mechanical thrombectomy [12, 13] in the setting of intermediate-risk PE, but a head to head comparison of different techniques remains non-existant.

The main advantages of CDT are simplicity, high effectiveness and relatively low bleeding risk. The goal for CDT is to achieve similar efficacy to systemic thrombolysis and potentially decrease the rate of major and intracranial bleeding by delivering a significantly lower dose of thrombolytic drug directly into the thrombus over an extended period of time (12–24 h) through a pig-tail or dedicated thrombolytic catheter. The MAPPET-3 trial was the first CDT controlled trial in submassive PE using 100 mg alteplase plus heparin or heparin only. The incidence of in-hospital mortality was significantly higher in the heparin-plus-placebo group than in the heparin plus alteplase group ($p = 0.006$), and the probability of 30-day event-free survival was higher in the heparin-plus-alteplase group ($p = 0.005$) [8]. The MOPETT study was a randomized controlled trial of 121 patients comparing 'safe dose' thrombolytic (half of the full dose) with anticoagulation and an anticoagulation only group. Pulmonary artery pressures were significantly lower after 48 h in the thrombolytic group than in the anticoagulation group (16 vs. 10 mmHg reduction, $p < 0.001$) [9]. In a recent publication by Carrmona et al. [10], local low-dose urokinase thrombolysis was done in submassive PE and an initially high pulmonary artery pressure after CTD (systolic 52.4 vs. 35.2 [17.2, 95% CI 14.5–19.9]), and follow-up ultrasound showed improvement in right ventricular dysfunction. No life-threatening hemorrhagic complications were reported. The 6-month survival was 96.5% [10].

The present study shows similar results, but the primary end-point was reached only in 90% of patients with CDT, and additional thombectomy was done in 9.6% of the patients to achieve the primary end-point, which was reached finally in 100% of the patients.

The main disadvantages of CDT are still the high bleeding risk [7] and the limited effectiveness of the thrombolytic drug in old thrombi. Bleeding can be puncture related or due to the systemic effect of the thrombolytic drug. Puncture related complications can be reduced by ultrasound assisted femoral vein puncture [14]; however, in the current study population, traditional femoral vein puncture was used, and the rate of access site bleeding was relatively high. Periprocedural major bleeding (intracerebral or gastrointestinal) was not observed; however, 2 patients had major cerebral bleeding at the 1-year follow-up after initiation of novel anticoagulants. The results of a recent meta-analysis of 35 interventional and observational ("real world") studies on CDT calculated a pooled rate of 6.6% for major bleeding, with a 3.9% major bleeding and 2.6% in hospital mortality rate in the "stable hemodynamic status" group [15].

Ultrasound accelerated thrombolysis can be more effective than simple local thrombolysis and can reduce the bleeding complications, but a head to head comparison has not been done comparing the two techniques. The phase 2 ULTIMA (Ultrasound Accelerated Thrombolysis of Pulmonary Embolism) trial randomized 59 patients with acute main- or lower-lobe PE and an echocardiographic right-to-left ventricular dimension ratio of 1.0 to receive unfractionated heparin plus a catheter-directed, ultrasound-assisted thrombolytic regimen of 10 to 20 mg recombinant tissue plasminogen activator over 15 h, as opposed to heparin alone. Reduced-dose local thrombolysis significantly reduced the subannular right-to-left ventricular dimension ratio between the baseline and a 24-h follow-up without an increase in bleeding complications [11]. The PERFECT registry, which also lacked a control arm, included 101 patients with high-risk and intermediate-risk PE. There were no major or intracranial bleeding events with CDT [16].

Aspiration thrombectomy is a new treatment method and is the rational choice to aspirate thrombi from the vascular bed without using a thrombolytic. The potential complication is the distal embolization and pulmonary artery trauma, and the effectiveness is not well known. MT can be done with dedicated devices or with a simple guiding catheter [12]. In the present study group, aspiration thrombectomy was applied in 12 patients with a 100% technical and 90% clinical success without escalation of major bleeding events.

Limitations of the study

The main limitation of the study is the lack of a randomized control arm. Another limitation is that right heart catheterization was not performed in the patient after the 1-year follow-up.

Conclusions

Catheter directed thrombolysis in submassive PE had excellent results. However, additional mechanical thrombectomy and angioplasty was necessary in several patients to achieve a good clinical outcome.

Conflict of interest: None declared

References

1. Konstantinides SV, Torbicki A, Agnelli G, et al. Task Force for the Diagnosis and Management of Acute Pulmonary Embolism of the European Society of Cardiology (ESC). 2014 ESC guidelines on the diagnosis and management of acute pulmonary embolism. Eur Heart J. 2014; 35(43): 3033–69, 3069a, doi: 10.1093/eurheartj/ehu283, indexed in Pubmed: 25173341.
2. Jaff MR, McMurtry MS, Archer SL, et al. American Heart Association Council on Cardiopulmonary, Critical Care, Perioperative and Resuscitation, American Heart Association Council on Peripheral Vascular Disease, American Heart Association Council on Arteriosclerosis, Thrombosis and Vascular Biology. Management of massive and submassive pulmonary embolism, iliofemoral deep vein thrombosis, and chronic thromboembolic pulmonary hypertension: a scientific statement from the American Heart Association. Circulation. 2011; 123(16): 1788–1830, doi: 10.1161/CIR.0b013e318214914f, indexed in Pubmed: 21422387.
3. Hoeper MM, Bogaard HJ, Condliffe R, et al. Definitions and diagnosis of pulmonary hypertension. J Am Coll Cardiol. 2013; 62(25 Suppl): D42–D50.
4. Marti C, John G, Konstantinides S, et al. Systemic thrombolytic therapy for acute pulmonary embolism: a systematic review and meta-analysis. Eur Heart J. 2015; 36(10): 605–614, doi: 10.1093/eurheartj/ehu218, indexed in Pubmed: 24917641.
5. Meyer G, Vicaut E, Danays T, et al. Fibrinolysis for Patients with Intermediate-Risk Pulmonary Embolism. N Engl J Med. 2014; 370(15): 1402–1411, doi: 10.1056/nejmoa1302097.
6. Konstantinides SV, Vicaut E, Danays T, et al. Impact of thrombolytic therapy on the Long-Term outcome of intermediate-risk pulmonary embolism. J Am Coll Cardiol. 2017; 69(12): 1536–1544, doi: 10.1016/j.jacc.2016.12.039, indexed in Pubmed: 28335835.
7. Abraham P, Arroyo DA, Giraud R, et al. Understanding haemorrhagic risk following thrombolytic therapy in patients with intermediate-risk and high-risk pulmonary embolism: a hy-

pothesis paper. Open Heart. 2018; 5(1): e000735, doi: 10.1136/openhrt-2017-000735, indexed in Pubmed: 29531763.

8. Konstantinides S, Geibel A, Heusel G, et al. Heparin plus alteplase compared with heparin alone in patients with submassive pulmonary embolism. N Engl J Med. 2002; 347(15): 1143–1150, doi: 10.1056/NEJMoa021274, indexed in Pubmed: 12374874.
9. Sharifi M, Bay C, Skrocki L, et al. Moderate pulmonary embolism treated with thrombolysis (from the "MOPETT" Trial). Am J Cardiol. 2013; 111(2): 273–277, doi: 10.1016/j.amjcard.2012.09.027, indexed in Pubmed: 23102885.
10. Carmona SA, Redondo MP, Franco LN, et al. Local low-dose urokinase thrombolysis for the management of haemodynamically stable pulmonary embolism with right ventricular dysfunction. EuroIntervention. 2018; 14(2): 238–246, doi: 10.4244/eij-d-17-00544.
11. Kucher N, Boekstegers P, Müller OJ, et al. Randomized, controlled trial of ultrasound-assisted catheter-directed thrombolysis for acute intermediate-risk pulmonary embolism. Circulation. 2014; 129(4): 479–486, doi: 10.1161/CIRCULATIONAHA.113.005544, indexed in Pubmed: 24226805.
12. Piazza G, Hohlfelder B, Jaff MR, et al. A prospective, single-arm, multicenter trial of ultrasound-facilitated, catheter-directed, low-dose fibrinolysis for acute massive and submassive pulmonary embolism: the SEATTLE II study. JACC Cardiovasc Interv. 2015; 8(10): 1382–1392, doi: 10.1016/j.jcin.2015.04.020, indexed in Pubmed: 26315743.
13. Ciampi-Dopazo JJ, Romeu-Prieto JM, Sánchez-Casado M, et al. Aspiration thrombectomy for treatment of acute massive and submassive pulmonary embolism: initial single-center prospective experience. J Vasc Int Radiol. 2018; 29(1): 101–106.
14. Yamagata K, Wichterle D, Roubícek T, et al. Ultrasound-guided versus conventional femoral venipuncture for catheter ablation of atrial fibrillation: a multicentre randomized efficacy and safety trial (ULTRA-FAST trial). Europace. 2018; 20(7): 1107–1114, doi: 10.1093/europace/eux175, indexed in Pubmed: 28575490.
15. Bajaj NS, Kalra R, Arora P, et al. Catheter-directed treatment for acute pulmonary embolism: Systematic review and single-arm meta-analyses. Int J Cardiol. 2016; 225: 128–139, doi: 10.1016/j.ijcard.2016.09.036, indexed in Pubmed: 27718446.
16. Kuo WT, Banerjee A, Kim PS, et al. Pulmonary embolism response to fragmentation, embolectomy, and catheter thrombolysis (PERFECT): initial results from a prospective multicenter registry. Chest. 2015; 148(3): 667–673, doi: 10.1378/chest.15-0119, indexed in Pubmed: 25856269.

VIA MEDICA

ORIGINAL ARTICLE

Cardiology Journal
2020, Vol. 27, No. 4, 376–383
DOI: 10.5603/CJ.a2018.0118

ISSN 1897–5593

High-sensitive troponin T increase after hemodialysis is associated with left ventricular global longitudinal strain and ultrafiltration rate

Serkan Ünlü[1, 2, 3], Asife Şahinarslan[1], Burak Sezenöz[1], Orhan Mecit Uludağ[3], Gökhan Gökalp[1], Özden Seçkin[1], Selim Turgay Arınsoy[4], Özlem Gülbahar[5], Nuri Bülent Boyacı[1]

[1]Department of Cardiology, Faculty of Medicine, Gazi University, Ankara, Turkey
[2]Department of Cardiology, Atatürk Chest Diseases and Chest Surgery Education and Research Hospital, Ankara, Turkey
[3]Department of Pharmacology, Faculty of Pharmacy, Gazi University, Ankara, Turkey
[4]Department of Nephrology, Faculty of Medicine, Gazi University, Ankara, Turkey
[5]Department of Medical Biochemistry, Faculty of Medicine, Gazi University, Ankara, Turkey

Abstract

Background: *Circulating troponin levels are both stable and higher in patients with end-stage renal disease, even in the absence of acute coronary syndrome. These patients commonly have underlying cardiac problems that frequently cause troponin elevation. The effect of hemodialysis (HD) on troponin levels has not been well elucidated. Thus, investigated herein is the relationship between the changes in troponin levels along with left ventricular deformation and volume depletion in patients with end-stage renal disease.*

Methods: *Patients included were between 18 and 85 years of age and were receiving hemodialysis for at least 6 months. High sensitive cardiac troponin T (hs-cTnT) levels were studied in blood samples taken at the beginning and end of HD. Two-dimensional speckle tracking strain imaging was used to evaluate myocardial contractility.*

Results: *Seventy patients (50.7 ± 16.9 years of age, 27 women) were included in study. The mean volume of ultrafiltration was 3260 ± 990 mL. A significant increase in circulating hs-cTnT levels was observed, as well as a prominent decrease in left ventricular global longitudinal strain (GLS) after HD (52.4 ± 40.2 ng/L vs. 66.8 ± 48.5 ng/L, $p < 0.001$ and 20.1 ± 3.6% vs. 16.8 ± 3.8% $p < 0.001$, respectively). Moreover, ultrafiltration rate and GLS were found as the strongest independent variables in relation to the relative increase in hs-cTnT.*

Conclusions: *Hemodialysis can cause a significant increase in hsTnT. This can jeopardize the accuracy of clinical diagnoses based on hs-TnT measurements. GLS may be used as a determinant of this hs-TnT increase. The influence of HD on the cardiovascular system should be kept in mind to prevent unnecessary interventions.* (Cardiol J 2020; 27, 4: 376–383)

Key words: dialysis, high-sensitive, load, speckle, troponin

Introduction

Troponins (Tn) are structural proteins involved in the regulation of skeletal and cardiac muscle contractility and cardiac troponins (cTn) are being used as sensitive and specific markers of cardiac injury [1]. Recently developed, new generation, high-sensitive cardiac troponin (hs-cTn)

Address for correspondence: Serkan Ünlü, MD, MSc., Atatürk Chest Diseases and Chest Surgery Education and Research Hospital, Keçiören – Sanatoryum, Ankara, Turkey, tel: +905452472750, e-mail: unlu.serkan@gmail.com

Received: 2.08.2018 Accepted: 24.09.2018

assays [2, 3] made it possible to detect cTn levels in lower concentrations and provided faster diagnostic information, which resulted in a reduced duration of patient hospitalization [4]. However, a variety of conditions can cause an increase in hs-cTn in the absence of ischemic heart disease [1], one of these conditions being, patients with end-stage kidney disease who were shown to have higher circulating Tn levels compared to the normal population [5–12]. In these patients, underlying cardiac problems that frequently lead to cTn elevation are also common. However, the relationship between renal function disorders and the cTn increment is still not fully understood. The effect of dialysis on cTn levels has also not been robustly elucidated. Long-term cTn measurements in patients receiving dialysis therapy were shown to be higher than reference values without acute exacerbations [7, 8, 12, 13]. There are, however, few studies examining the acute effect of dialysis on cTn levels. Moreover, end-stage renal disease increases the likelihood of having concomitant heart disease and structural abnormalities such as left ventricular (LV) hypertrophy which also causes electrocardiographic findings that mimic ischemia. Thus, clinicians are obliged to depend on Tn measurements to diagnose acute coronary syndromes. In addition, higher ultrafiltration volumes may result in myocardial stunning [14–16] and show an impact on cTn levels. LV global longitudinal strain (GLS) — a marker of LV systolic function — is associated with poor prognosis and has been suggested to be a better prognostic indicator than conventional LV ejection fraction (EF) in patients with chronic kidney disease [17, 18]. Therefore, the present study was to investigate (i) the change in circulating hs-cTnT levels with hemodialysis (HD); (ii) the relationship between changes in hs-cTnT levels and volume depletion and (iii) changes in LV deformation as assessed by two-dimensional (2D) strain echocardiography with HD.

Methods

Study population

This study had a cohort of 70 patients, who were followed up in the Hemodialysis Unit of Gazi University Medical School Nephrology Department. Patients between 18 and 85 years of age, who were receiving systemic bicarbonate HD 3 times a week for at least 6 months were included. Patients with LV systolic dysfunction (< 53%) [19], evident coronary artery disease and moderate to severe valvular heart disease, atrial fibrillation, acute coronary syndrome, infectious and inflammatory conditions and pulmonary embolism were excluded from the study. This study was approved by the local ethical committee.

Study protocol

Blood samples and echocardiographic acquisitions were obtained by providing 72 h between HD sessions in order to achieve higher volume changes. Dry weight is targeted for each patient during HD sessions. Blood pressure, weight and heart rate were measured before and after HD. The ultrafiltration volume and rate were recorded.

Blood samples

Blood samples were collected immediately before and after HD. HsTnT levels were measured with a high sensitive troponin assay (Elecsys® Troponin T hs, Roche Diagnostics) with lower detection and upper reference (99th percentile) limits of 3 ng/L and 14 ng/L, respectively.

Echocardiography

All images were acquired and measurements were performed by an experienced sonographer (SÜ) with a GE Vivid 7 Dimension ultrasonography machine (GE Vingmed Ultrasound, Horten, Norway) equipped with a 3.5 MHz transducer, immediately before and after HD. Electrocardiogram and respiration of patients were monitored. Echocardiographic images with at least three cardiac cycles were recorded at the end of expiration. The images were then transferred to a vendor-specific workstation and analysed with EchoPAC, BT 13 (GE Vingmed Ultrasound, Horten, Norway) software. All echocardiographic measurements were performed according to recent guidelines [19].

LV strain and strain rate analysis

Apical 4-, 3-, 2-chamber views were acquired with high frame rate (> 60 fps) for 2D speckle tracking strain analysis. To define the region of interest, the endocardial surface was identified by manually placing at least 15 markings in all apical views. End-diastole was indicated by the peak of the R-wave on the electrocardiogram. Average GLS were measured as the mean of GLS from 4-, 3-, 2-chamber apical views. All strain and echocardiographic measurements were performed by SÜ, who has a long experience with deformation imaging.

Statistical analysis

Continuous variables are presented as mean ± standard deviation and categorical data are presented as percentages or frequencies. Kolmogorov-Smirnov was used to check for normality of distribution for continuous variables. The paired t-test and Wilcoxon test were used to compare parametric and nonparametric continuous variables, respectively, before and after HD. Categorical variables were compared by the χ^2 test. The Pearson correlation test was used to evaluate the relationship among changes in hs-cTnT levels, GLS and fluid volume withdrawal. Univariate linear regression analysis with conventional clinical variables (age, gender etc.) and contributors with a significant correlation were entered in a multiple linear regression model. Possible collinearity was checked by using a tolerance and variance inflation factor. Variables with a tolerance of less than 0.10 and a variance inflation factor of 10 and above were withdrawn from the multivariate linear regression model. A two-tailed p-value of < 0.05 was considered as statistically significant. All data were analysed with SPSS v.23.0.

Results

Among 80 patients screened, 70 of them were included in this study. Seven patients were excluded because of newly diagnosed LV systolic dysfunction, it was not possible to collect blood samples after HD in 3 patients. The baseline characteristics of participants are presented in Table 1. A decrease in both systolic and diastolic blood pressures and an increase in heart rate after HD was observed. However, no significant tachycardia (> 100 bpm) was detected after HD, except in 3 patients. The mean volume of ultrafiltration was 3260 ± 990 mL. Comparison of clinical vital signs before and after HD is shown in Table 2.

A significant increase in serum hs-cTnT levels after HD was observed (52.4 ± 40.2 ng/L vs. 66.8 ± ± 48.5 ng/L, $p < 0.001$; Fig. 1). A relative change in hs-cTnT and ultrafiltration rate showed a significant correlation (Fig. 2).

The size of LV and left atrium decreased after HD, whereas LV EF remained unchanged. LV GLS also notably decreased after HD. Data of echocardiographic parameters are listed in Table 3. The relative change in GLS showed strong correlations with relative change in hs-cTnT (Fig. 3) and ultrafiltrated volume (Fig. 4).

In a linear regression analyses, relative change in GLS, ultrafiltration rate ultrafiltrated volume, and relative change in heart rate were significantly correlated with the relative change in hs-cTnT. Ultrafiltrated volume was removed from multivariate analysis since a high collinearity was found with ultrafiltration rate. Multivariate linear regression analysis revealed that the ultrafiltration rate and the relative change of LV GLS were the strongest independent variables associated with an increase in hs-cTnT levels (Table 4).

Discussion

In this study, the acute impact of HD on hs-cTnT levels were investigated. The main findings can be summarized as follows: (i) hs-cTnT levels

Table 1. Baseline characteristics of the participants.

Parameters	Mean/Frequency (n = 81)
Age [year]	50.7 ± 16.9
Gender (male)	43 (61.4%)
BMI [kg/m^2]	23.5 ± 4.4
Duration of HD [month]	78.2 ± 58.7
Ultra-filtrated volume [mL]	3260 ± 990
Ultrafiltration rate [mL/kg/h]	11.6 ± 3.0
Hypertension	27 (33.3%)
Hyperlipidemia	24 (29.6%)
Diabetes mellitus	14 (17.2%)
Glomerulonephritis	10 (12.3%)
Other	13 (16.1%)
Primary unknown renal failure	7 (8.6%)

BMI — body mass index; HD — hemodialysis; Other — polycystic kidney disease, amyloidosis, nephrolithiasis, vesicoureteral reflux, pyelonephritis, autoimmune diseases, toxic nephropathy

Table 2. Vital clinical parameters before and after hemodialysis (HD).

Parameters	Before HD	After HD	P
Systolic blood pressure [mmHg]	123.3 ± 21.7	104.2 ± 21.6	< 0.001
Diastolic blood pressure [mmHg]	74.4 ± 12.9	62.6 ± 13.1	< 0.001
Heart rate [bpm]	78 ± 15	86 ± 16	< 0.001
Weight [kg]	70.4 ± 17.6	66.6 ± 15.2	< 0.001

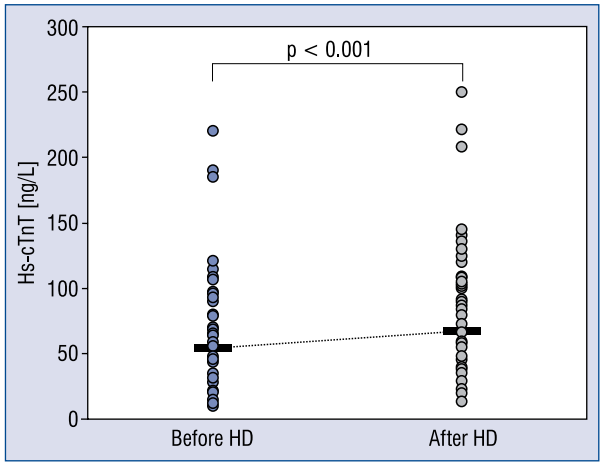

Figure 1. High-sensitive cardiac troponin T (hs-cTnT) levels before and after hemodialysis (HD). Comparison between mean values before and after HD is presented. Significance is indicated on the graph.

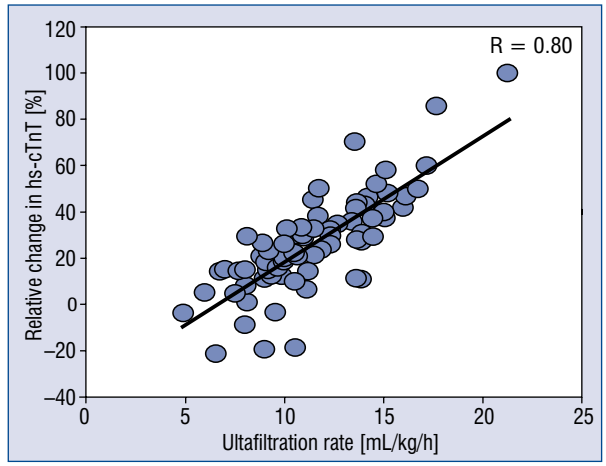

Figure 2. Comparison between relative change of high-sensitive cardiac troponin T (hs-cTnT) (y-axis) and the ultrafiltration rate (x-axis). The correlation coefficient (R) is indicated. P value is < 0.001.

Table 3. Echocardiographic measurements before and after hemodialysis (HD).

Parameters	Before HD	After HD	P
Dimensions. areas and volumes of left heart			
LV end-diastolic diameter (cm)	4.4 ± 0.7	4.0 ± 0.8	< 0.001
LV end-diastolic volume (ml)	75.3 ± 22.7	68.5 ± 29.7	< 0.001
LV end-systolic volume [mL]	26 ± 11.2	23.8 ± 17.8	0.401
LV ejection fraction [%]	66.0 ± 11.5	64.2± 10.6	0.071
LA diameter [cm]	5.1 ± 1.4	4.7± 1.4	< 0.001
LA area [cm^2]	29.9± 10.6	19.9 ± 10.3	< 0.001
LA volume index [mL/m^2]	48.7 ± 16.3	33.4 ± 16.1	< 0.001
Doppler measurements of left ventricle			
E [cm/s]	99 ± 24.8	65.5 ± 23.1	< 0.001
A [cm/s]	94 ± 92.1	76.7 ± 26.9	< 0.001
E/A	1.18 ± 0.6	0.92 ± 0.34	< 0.001
Tissue Doppler measurements of left ventricle			
$E'_{lateral}$ [cm/s]	11.1 ± 2.8	10.1 ± 2.8	0.001
$A'_{lateral}$ [cm/s]	12.5 ± 4.1	10.2 ± 3.4	< 0.001
$S'_{lateral}$ [cm/s]	11.1 ± 10.2	9.6 ± 2.9	< 0.001
$E/E'_{lateral}$	8.8 ± 3.8	6.3 ± 2.9	< 0.001
E'_{septal} [cm/s]	10.9 ± 2.5	10.1 ± 2.8	0.001
A'_{septal} [cm/s]	8.8 ± 2	7.9 ± 2.4	< 0.001
S'_{septal} [cm/s]	10 ± 3.6	8 ± 2.6	< 0.001
E/E'_{septal}	9.6 ± 3.7	8.0 ± 2.4	< 0.001
Speckle tracking echocardiography			
LV GLS [%]	–20.1 ± 3.6	–16.8 ± 3.8	< 0.001

GLS — global longitudinal strain; LA — left atrium; LV — left ventricle

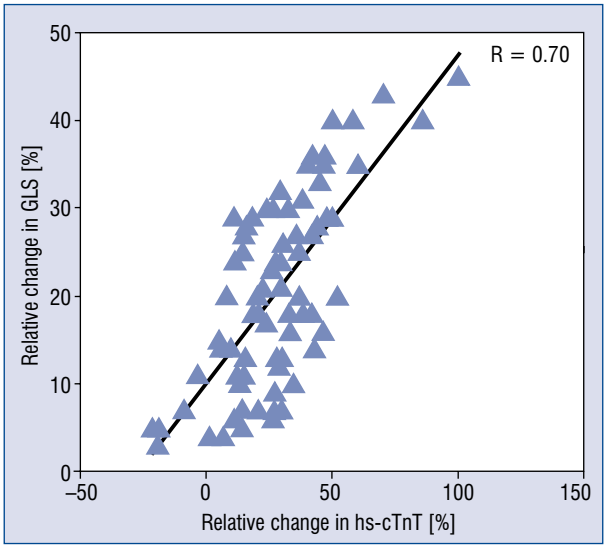

Figure 3. Comparison between relative change of global longitudinal strain (GLS) measurements (y-axis) and relative change in high-sensitive cardiac troponin T (hs-cTnT) (x-axis). The correlation coefficient (R) is indicated. P value is < 0.001.

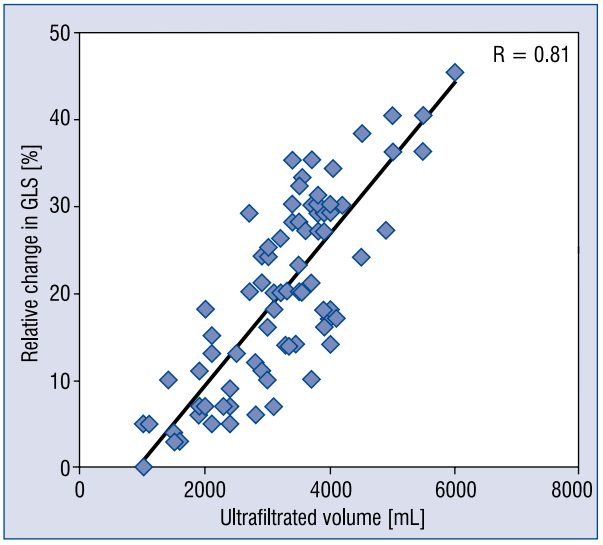

Figure 4. Comparison between relative change of global longitudinal strain (GLS) measurements (y-axis) and the ultrafiltrated volume (x-axis). The correlation coefficient (R) is indicated. P value is < 0.001.

Table 4. Determinants of relative increase in high sensitive troponin T levels after hemodialysis.

Parameters	Univariate		Multivariate	
	r	p	R^2	p
Age [year]	–0.200	0.159		
Gender	–0.187	0.282		
Change in systolic BP	0.386	0.10		
Change in diastolic BP	0.248	0.147	0.826	
Change in heart rate	0.49	0.045		
Change in LV GLS	0.70	< 0.0001		0.001
Change in LV EDV	0.350	0.106		
Ultrafiltration rate [mL/kg/h]	0.80	< 0.0001		< 0.0001

BP — blood pressure; EDV — end-systolic volume; GLS — global longitudinal strain; LV — left ventricle

show a statistically significant increase after HD, (ii) relative change in hs-cTnT levels shows strong correlation with ultrafiltration rate, (iii) LV systolic function evaluated by 2D speckle tracking analysis deteriorates with high rapid volume depletion, (iv) the relative change in GLS and ultrafiltration rate are independently associated with a relative hs-cTnT increase after HD.

Selection of study population

There have been several studies which aimed to investigate the impact of HD on cTn levels [7, 8, 10–13, 20–23]. According to available research, none of the studies evaluated the relation of ultrafiltration rate, deformation indices and changes in circulating cTn levels. Therefore, it was decided to investigate patients with end-stage kidney disease at a time when the highest volume change can be achieved. By having 3200 mL of average ultrafiltration volume, it was believed that this would obtain the highest possible volume changes in the literature. In addition, patients without significant cardiac diseases, except LV hypertrophy, were enrolled to avoid possible effects of cardiac pathologies on changes in cTn levels.

Changes in vital signs and cardiac function with HD

In the present study, both systolic and diastolic blood pressures decreased after HD, which is

a physiologic and expected response to a loss of fluid and modest decrease in afterload. The heart rate of subjects studied increased after HD as a physiologic response to reduced circulating volume.

Impact of HD on circulating hs-cTn levels

In present study, an almost 30% relative increase in hs-cTn levels was found. In available literature, conflicting results have been presented about cTn change with HD [7, 8, 10–13, 20–22]. The current perception is to expect a modest relative decrease in circulating cTn levels after HD [13]. However, the rate of ultrafiltrated volume could also have an impact on cTn change. The current study showed that ultrafiltrated volume showed a strong correlation with the relative change in hs-cTn levels.

Elevated cTn concentrations after HD may reflect increased concentration due to reduced clearance with limited residual renal function [24]. Recurrent myocardial damage could be a potent reason for cTn elevation [15]. Since the present population had a mean of almost 7 years for receiving HD, chronicity of renal replacement therapy could have caused cardiac and renal structural damage which could lead to a cTn increase in each session of HD. Moreover, it has been claimed that HD can lead to myocardial stunning especially in high ultrafiltration rates which can also lead to acute elevation of hs-cTn T levels [14, 25]. Since these patients are at greater risk of coronary artery disease development, high volume depletion may cause reflex tachycardia and ischemia as a result of supply-demand mismatch during HD sessions, which may contribute to cTn elevation as well as LV hypertrophy.

Impact of HD on echocardiographic parameters

Although LV and left atrial dimensions, areas and volumes were significantly reduced, no significant change in LV EF was observed. Since EF is a relative measurement, volume change is not expected to affect EF measurements in individuals with normal systolic function. Nonetheless, there are conflicting findings about LV EF change with volume depletion evidenced in research literature, which could be due to differing sample sizes and methodologies of the studies.

Two-dimensional speckle tracking is a method developed for functional assessment of LV. 2D speckle tracking derived GLS has now emerged as a new index of LV function [19, 26]. GLS appears to be robust and more sensitive for detection of subtle functional changes, providing complementary and superior information over conventional LV EF measurements [27, 28]. In the present study, a significant reduction in LV GLS by being highly affected from volume change was found. Myocardial stunning could also lead to a decrease in LV GLS by having an impact on myocardial contractility. LV systolic function evaluated with GLS during and after HD may present cardiac systolic dysfunction. Thus patients should be closely monitored and clinicians should be aware of possible transient, cardiac decompensation, considering concomitant hs-cTn elevation.

Clinical perspective of hs-cTnT increase after HD

Chest pain is the most common cause of visits to emergency department and almost one-quarter of these patients are diagnosed with acute coronary syndrome [1, 4]. To exclude acute myocardial infarction in patients with acute onset of chest pain, 6–12 h of follow-up was needed with older generations of cTn assays [4, 29]. It was therefore raising a significant burden on the health care system and the possibility of developing faster diagnostic algorithms would be a great advantage [4]. Patients with end stage kidney disease have increased circulating cTn levels. In the present population cTn levels were shown to be high but stable compared to reference values. However, conflicting findings are present on the acute effect of HD on cTn levels [8, 13, 24, 30]. Nevertheless, clinicians must mainly rely on cTn measurements since patients with chronic kidney disease also have the most cardiovascular risk factors and ischemic findings on electrocardiography which could be present due to LV hypertrophy. High blood pressure, hyperdynamic circulation due to arteriovenous shunt, volume overload and increased pulse pressure can cause myocardial strain and result in elevated cTn in this population [14, 15, 25]. Moreover, recurrent myocardial damage due to decreased myocardial blood flow caused by HD plays an important role in cardiac remodeling [14, 16]. Thus, high ultrafiltration rates and volumes are especially shown to be associated with myocardial stunning [25]. Herein an almost 30% relative increase in hs-cTnT levels with HD and it was demonstrated that this increase is highly correlated with the ultrafiltration rate. It was also shown that high ultrafiltration volumes have a substantial impact on systolic function of LV. Relative change in LV GLS also showed a very strong correlation with the ultrafiltrated rate. Moreover, LV GLS was found to be one of the strongest independent variables in relation to a relative hs-cTnT increase.

Therefore, it can be claimed that the rate of ultrafiltration has a substantial impact on hs-cTnT change and myocardial contractility which can be also related to an hs-cTnT increase. As suggested in the recent guidelines [25], ultrafiltration rates and volumes should be minimized to suit what is best for patients to achieve hemodynamic stability and tolerability. Additional HD sessions should be considered for patients instead of extensive ultrafiltration rates [25]. Patients on HD therapy presenting with chest pain must still be managed by measuring serial cTn levels, the change in cTn may help in clinical decision making as to whether it is acute coronary syndrome or not.

Limitations of the study

In this present study it was endeavoured to enrol an adequate number of patients to represent a population with end-stage kidney disease. There was no possibility of telemetric monitoring or obtaining electrocardiogram records which may have played an additional role on possible causes of cTn elevation before and after HD, however it was not needed clinically since none of subjects had related symptoms. Since patients with coronary artery disease were excluded and the present population included patients without previous coronary angiogram, an inability to evaluate the possible role of significant coronary stenosis causing ischemia in these patients might have interfered with the results. The aim of this study was to investigate the acute effects of HD on hs-cTnT levels and its relation with ultrafiltration rate and therefore, hs-cTnT measurements on 12th or 24th h after HD could not be presented. Moreover, HD has various effects on cardiovascular dynamics, although we found ultrafiltration rate and LV GLS as independent variables related to a relative increase of hs-cTnT, exact mechanisms of this increase in hs-cTnT level require further investigation and cannot be quintessentially elucidated with the present findings. To avoid possible variability in measurements of echocardiographic parameters, a single observer (SÜ), who has substantial experience in echocardiography and deformation imaging, performed all echocardiographic analyses of the image datasets.

Conclusions

In the present study, it was shown that hs-cTnT levels show a significant increase after HD which can jeopardize the accuracy of clinical diagnoses based on hs-cTnT measurements. A strong correlation was present among relative changes in hs-cTnT levels, LV GLS, and ultrafiltration rate. LV GLS was found to be one of the strongest independent variables associated with the relative hs-cTnT increase. Rapid volume depletion substantially effected myocardial contractility and resulted in possible myocardial damage. The rate of ultrafiltration should be minimized to avoid possible negative consequences. Considering the effect of HD with high ultrafiltration rate on circulating hs-cTnT levels, it could be of use to prevent misdiagnosis.

Conflict of interest: None declared

References

1. Thygesen K, Alpert J, Jaffe A, et al. Third universal definition of myocardial infarction. Nat Rev Cardiol. 2012; 9(11): 620–633, doi:10.1038/nrcardio.2012.122.
2. Westermann D, Neumann JT, Sörensen NA, et al. High-sensitivity assays for troponin in patients with cardiac disease. Nat Rev Cardiol. 2017; 14(8): 472–483, doi: 10.1038/nrcardio.2017.48, indexed in Pubmed: 28383022.
3. Apple FS, Collinson PO. Analytical characteristics of high-sensitivity cardiac troponin assays. Clin Chem. 2012; 58(1): 54–61, doi: 10.1373/clinchem.2011.165795, indexed in Pubmed: 21965555.
4. Roffi M, Patrono C, Collet JP, et al. 2015 ESC Guidelines for the management of acute coronary syndromes in patients presenting without persistent ST-segment elevation: Task Force for the Management of Acute Coronary Syndromes in Patients Presenting without Persistent ST-Segment Elevation of the European Society of Cardiology (ESC). Eur Heart J. 2016; 37(3): 267–315, doi: 10.1093/eurheartj/ehv320, indexed in Pubmed: 26320110.
5. Hassan HC, Howlin K, Jefferys A, et al. High-sensitivity troponin as a predictor of cardiac events and mortality in the stable dialysis population. Clin Chem. 2014; 60(2): 389–398, doi: 10.1373/clinchem.2013.207142, indexed in Pubmed: 24185551.
6. Mishra RK, Li Y, DeFilippi C, et al. CRIC Study Investigators. Association of cardiac troponin T with left ventricular structure and function in CKD. Am J Kidney Dis. 2013; 61(5): 701–709, doi: 10.1053/j.ajkd.2012.11.034, indexed in Pubmed: 23291148.
7. Pianta TJ, Horvath AR, Ellis VM, et al. Cardiac high-sensitivity troponin T measurement: a layer of complexity in managing haemodialysis patients. Nephrology (Carlton). 2012; 17(7): 636–641, doi: 10.1111/j.1440-1797.2012.01625.x, indexed in Pubmed: 22694299.
8. Kumar N, Michelis MF, DeVita MV, et al. Troponin I levels in asymptomatic patients on haemodialysis using a high-sensitivity assay. Nephrol Dial Transplant. 2011; 26(2): 665–670, doi: 10.1093/ndt/gfq442, indexed in Pubmed: 20656755.
9. deFilippi C, Wasserman S, Rosanio S, et al. Cardiac troponin T and C-reactive protein for predicting prognosis, coronary atherosclerosis, and cardiomyopathy in patients undergoing long-term hemodialysis. JAMA. 2003; 290(3): 353–359, doi: 10.1001/jama.290.3.353, indexed in Pubmed: 12865376.
10. Yakupoglu U, Ozdemir FN, Arat Z, et al. Can troponin-I predict cardiovascular mortality due to myocardial injury in hemodialysis patients? Transplant Proc. 2002; 34(6): 2033–2034, indexed in Pubmed: 12270303.

11. Apple FS, Murakami MM, Pearce LA, et al. Predictive value of cardiac troponin I and T for subsequent death in end-stage renal disease. Circulation. 2002; 106(23): 2941–2945, indexed in Pubmed: 12460876.
12. Fredericks S, Chang R, Gregson H, et al. Circulating cardiac troponin-T in patients before and after renal transplantation. Clin Chim Acta. 2001; 310(2): 199–203, indexed in Pubmed: 11498086.
13. Chen M, Gerson H, Eintracht S, et al. Effect of Hemodialysis on Levels of High-Sensitivity Cardiac Troponin T. Am J Cardiol. 2017; 120(11): 2061–2064, doi: 10.1016/j.amjcard.2017.08.026, indexed in Pubmed: 29033047.
14. Dasselaar JJ, Slart RH, Knip M, et al. Haemodialysis is associated with a pronounced fall in myocardial perfusion. Nephrol Dial Transplant. 2009; 24(2): 604–610, doi: 10.1093/ndt/gfn501, indexed in Pubmed: 18775808.
15. Burton JO, Jefferies HJ, Selby NM, et al. Hemodialysis-induced cardiac injury: determinants and associated outcomes. Clin J Am Soc Nephrol. 2009; 4(5): 914–920, doi: 10.2215/CJN.03900808, indexed in Pubmed: 19357245.
16. Bemelmans RHH, Boerma EC, Barendregt J, et al. Changes in the volume status of haemodialysis patients are reflected in sublingual microvascular perfusion. Nephrol Dial Transplant. 2009; 24(11): 3487–3492, doi: 10.1093/ndt/gfp267, indexed in Pubmed: 19515801.
17. Hensen LCR, Goossens K, Delgado V, et al. Prognostic implications of left ventricular global longitudinal strain in predialysis and dialysis patients. Am J Cardiol. 2017; 120(3): 500–504, doi: 10.1016/j.amjcard.2017.04.054, indexed in Pubmed: 28579125.
18. Krishnasamy R, Isbel NM, Hawley CM, et al. Left ventricular global longitudinal strain (GLS) is a superior predictor of all-cause and cardiovascular mortality when compared to ejection fraction in advanced chronic kidney disease. PLoS One. 2015; 10(5): e0127044, doi: 10.1371/journal.pone.0127044, indexed in Pubmed: 25978372.
19. Lang R, Badano L, Mor-Avi V, et al. Recommendations for cardiac chamber quantification by echocardiography in adults: an update from the American Society of Echocardiography and the European Association of Cardiovascular Imaging. Eur Heart J Cardiovasc Imaging. 2015; 16(3): 233–271, doi: 10.1093/ehjci/jev014.
20. Peetz D, Schütt S, Sucké B, et al. Prognostic value of troponin T, troponin I, and CK-MBmass in patients with chronic renal failure. Med Klin (Munich). 2003; 98(4): 188–192, doi: 10.1007/s00063-003-1243-3, indexed in Pubmed: 12715142.
21. Schmidt A, Stefenelli T, Schuster E, et al. Informational contribution of noninvasive screening tests for coronary artery disease in patients on chronic renal replacement therapy. Am J Kidney Dis. 2001; 37(1): 56–63, indexed in Pubmed: 11136168.
22. Conway B, McLaughlin M, Sharpe P, et al. Use of cardiac troponin T in diagnosis and prognosis of cardiac events in patients on chronic haemodialysis. Nephrol Dial Transplant. 2005; 20(12): 2759–2764, doi: 10.1093/ndt/gfi125, indexed in Pubmed: 16188899.
23. Mavrakanas TA, Sniderman AD, Barré PE, et al. High ultrafiltration rates increase troponin levels in stable hemodialysis patients. Am J Nephrol. 2016; 43(3): 173–178, doi: 10.1159/000445360, indexed in Pubmed: 27064739.
24. Ellis K, Dreisbach AW, Lertora JL. Plasma elimination of cardiac troponin I in end-stage renal disease. South Med J. 2001; 94(10): 993–996, indexed in Pubmed: 11702827.
25. Daugirdas J, Depner T, Inrig J, et al. KDOQI Clinical Practice Guideline for Hemodialysis Adequacy: 2015 Update. Am J Kidney Dis. 2015; 66(5): 884–930, doi: 10.1053/j.ajkd.2015.07.015.
26. Voigt JU, Pedrizzetti G, Lysyansky P, et al. Definitions for a Common Standard for 2D Speckle Tracking Echocardiography: Consensus Document of the EACVI/ASE/Industry Task Force to Standardize Deformation Imaging. J Am Soc Echocardiogr. 2015; 28(2): 183–193, doi: 10.1016/j.echo.2014.11.003.
27. Galderisi M, Cosyns B, Edvardsen T, et al. Standardization of adult transthoracic echocardiography reporting in agreement with recent chamber quantification, diastolic function, and heart valve disease recommendations: an expert consensus document of the European Association of Cardiovascular Imaging. Eur Heart J Cardiovasc Imaging. 2017; 18(12): 1301–1310, doi: 10.1093/ehjci/jex244, indexed in Pubmed: 29045589.
28. Farsalinos KE, Daraban AM, Ünlü S, et al. Head-to-Head Comparison of Global Longitudinal Strain Measurements among Nine Different Vendors: The EACVI/ASE Inter-Vendor Comparison Study. J Am Soc Echocardiogr. 2015; 28(10): 1171–1181, e2, doi: 10.1016/j.echo.2015.06.011, indexed in Pubmed: 26209911.
29. Saenger AK, Beyrau R, Braun S, et al. Multicenter analytical evaluation of a high-sensitivity troponin T assay. Clin Chim Acta. 2011; 412(9-10): 748–754, doi: 10.1016/j.cca.2010.12.034, indexed in Pubmed: 21219893.
30. Fahim MA, Hayen AD, Horvath AR, et al. Biological variation of high sensitivity cardiac troponin-T in stable dialysis patients: implications for clinical practice. Clin Chem Lab Med. 2015; 53(5): 715–722, doi: 10.1515/cclm-2014-0838, indexed in Pubmed: 25527812.

VIA MEDICA

ORIGINAL ARTICLE

Cardiology Journal
2020, Vol. 27, No. 4, 384–393
DOI: 10.5603/CJ.a2018.0101

ISSN 1897–5593

Coexistence and management of abdominal aortic aneurysm and coronary artery disease

Mateusz K. Hołda[1, 2], Paweł Iwaszczuk[1], Karolina Wszołek[1], Jakub Chmiel[1], Andrzej Brzychczy[3], Mariusz Trystuła[3], Marcin Misztal[3]

[1]Department of Cardiac and Vascular Diseases, Jagiellonian University Medical College, Krakow, Poland
[3]HEART — Heart Embryology and Anatomy Research Team, Department of Anatomy, Jagiellonian University Medical College, Krakow, Poland
[3]Department of Vascular Surgery and Endovascular Procedures, John Paul II Hospital, Krakow, Poland

Abstract

Background: *Abdominal aortic aneurysm (AAA) and coronary atherosclerosis share common risk factors. In this study, a single-center management experience of patients with a coexistence of AAA and coronary artery disease (CAD) is presented.*

Methods: *271 consecutive patients who underwent elective AAA repair were reviewed. Coronary imaging in 118 patients was considered suitable for exploration of AAA coexistence with CAD.*

Results: *Significant coronary stenosis (> 70%) were found in 65.3% of patients. History of cardiac revascularization was present in 26.3% of patients, myocardial infarction (MI) in 31.4%, and 39.8% had both. In a subgroup analysis, prior history of percutaneous coronary intervention (PCI) (OR = 6.9, 95% CI 2.6–18.2, p < 0.001) and patients' age (OR = 1.1, 95% CI 1.0–1.2, p = 0.007) were independent predictors of significant coronary stenosis. Only 52.0% (40/77) of patients with significant coronary stenosis underwent immediate coronary revascularization prior to aneurysm repair: PCI in 32 cases (4 drug-eluting stents and 27 bare metal stents), coronary artery bypass graft in 8 cases. Patients undergoing revascularization prior to surgery had longer mean time from coronary imaging to AAA repair (123.6 vs. 58.1 days, p < 0.001). Patients undergoing coronary artery evaluation prior to AAA repair had shorter median hospitalization (7 [2–70] vs. 7 [3–181] days, p = 0.007) and intensive care unit stay (1 [0–9] vs. 1 [0–70] days, p = 0.014) and also had a lower rate of major adverse cardiovascular events or multiple organ failure (0% vs. 3.9%, p = 0.035). A total of 11.0% of patients had coronary artery aneurysms.*

Conclusions: *Patients with AAA might benefit from an early coronary artery evaluation strategy.* (Cardiol J 2020; 27, 4: 384–393)

Key words: abdominal aortic aneurysm, coronary artery aneurysm, coronary arteriography, coronary artery disease

Introduction

Abdominal aortic aneurysm (AAA) is the local pathologic dilation of the abdominal aorta and is defined as an aorta size greater than 30 mm or a local dilation of abdominal aorta of more than 50%, as compared to aortic diameter measured distally to dilatation [1]. The prevalence of AAA in the general population ranges from 1.0% to 1.3% among females and 3.9–7.2% in males, with an upward trend observed in older populations [2, 3]. Age, male gender, personal history of coronary artery disease (CAD), smoking, and hypertension are associated with the presence of AAA [4, 5]. The open surgical or endovascular aneurysm repair (EVAR) methods are the treatments of choice, and

Address for correspondence: Mateusz K. Hołda, MD, PhD, HEART — Heart Embryology and Anatomy Research Team, Department of Anatomy, Jagiellonian University Medical College, ul. Kopernika 12, 31–034 Kraków, Poland, tel/fax: +48 12 422 95 11, e-mail: mkh@onet.eu

Received: 25.06.2018 Accepted: 23.07.2018

no pharmacological management is available to effectively limit the disease progression [1, 2, 6, 7]. AAA and coronary atherosclerosis share common risk factors [8]. Both the prevalence of CAD in patients with AAA and the AAA prevalence in CAD patients are significantly higher relative to the general population [9]. The frequency of CAD in patients with AAA was estimated to be as high as 65% [10]. Comorbid CAD increases the perioperative risk of death and myocardial ischemia during AAA repair, as well as long-term clinical outcomes [11, 12]. Intuitively, the preoperative evaluation of coronary atherosclerosis, subsequent percutaneous coronary intervention (PCI) or coronary artery bypass graft (CABG) and myocardial revascularization should enhance postoperative prognosis [13, 14]. The preoperative evaluation of the existence of concomitant coronary stenosis appears to be reasonable [15, 16]. However, the optimal treatment of patients with both AAA and CAD remains controversial. Some studies show no benefits of prophylactic coronary interventions before major vascular surgery [15, 17], while others recommended this approach for the prevention of perioperative complications [18–20]. Current European Society of Cardiology and European Society of Anesthesiology Joint Task Force Guidelines advocate similar indications for coronary artery angiography (CAG) as in non-surgical settings and recommend CAG prior to non-urgent noncardiac surgery in patients with proven myocardial ischemia or unstable chest pain (Canadian Cardiovascular Society class III or IV) despite pharmacological treatment (recommendation class I C). These recommendations also suggest that preoperative CAG might be considered in stable patients scheduled for carotid endarterectomy (class IIb B), which is an intermediate-risk intervention, while disregarding the high-risk AAA patients [21].

In this study, experience in the management of patients with concomitant AAA and CAD is presented. The specific aim of current study was to re-analyze the coexistence of AAA and CAD in a contemporary sample, and finally to evaluate the complication rates associated with different approaches. One of the leading hypotheses is that patients with AAA might benefit from an early coronary artery evaluation strategy and receiving optimal CAD management/therapy prior to AAA repair.

Methods

Two hundred and seventy-one consecutive patients were retrospectively reviewed (247 males, 24 females) who underwent an elective AAA open surgery or EVAR from January 2008 through December 2015 at John Paul II Hospital in Krakow, Poland. CAG or multiple-slice coronary computed tomography (CT) angiography was available in 144 patients, out of whom 115 patients had undergone coronary imaging within 1 year prior to AAA repair, 1 patient underwent CAG simultaneously with EVAR procedure, and 2 patients were subjected to CAG within 2 months postoperatively. Coronary imaging in these 118 patients (106 males, 12 females) were deemed suitable for exploration of AAA coexistence with coronary pathology. Among those patients, classical CAG was performed in 89.8% (106/118), in the remaining 10.2% of patients (12/118), Electrocardiogram (ECG)-gated multi-row contrast-enhanced CT was performed using 64- to 256-row scanners.

To analyze factors associated with the presence of significant coronary stenosis, patients with prior CABG were additionally excluded, who inherently all had significant stenosis (n = 17). Clinical data and postoperative complications were recorded for all 271 patients.

To sum up, three subsets of analyses were performed: logistic regression of predictors of coronary stenosis (n = 101), coexistence and management of significant stenosis (n = 118), and finally an analysis of complication rates in all patients (n = 271) dichotomized by the facts of then, current preoperative coronary evaluation.

The AAA repair was performed either using open surgery or EVAR technique. Each patient was qualified for EVAR or classic repair by a vascular team comprising vascular surgeons, angiologists, interventional cardiologists, and anesthesiologists. The treatment decisions were based on the procedural guidelines, depending on the anatomy of the lesion, required scope of the procedure, perioperative risk, and comorbid conditions, including contraindications to general anesthesia, as well as the overall state of health and prognosis. The conducting physician and vascular team also decided whether preoperative coronary artery evaluation was necessary. Demographics, past medical history, information on treatments, and results of laboratory and imaging tests of all patients from the study group were collected from the patient medical records. The study complied with local bioethics committee regulations according to the Declaration of Helsinki.

Statistical analysis

Data are presented as percentages, mean values with corresponding standard deviations or

medians and ranges as appropriate. The Shapiro-Wilk was used test to determine if quantitative data were normally distributed. The Levene test was relied upon to verify variance homogeneity. The Student t-test and Mann-Whitney U test were used to statistically compare the two groups, as appropriate. Analysis of variance (ANOVA) was performed if a discriminating factor categorized quantitative variables into more than two groups and variance homogeneity assumption was fulfilled. In post-hoc analyses, we relied on the Tukey test of multiple comparisons. A multiple logistic regression model was built by the inclusion of all univariately significant predictors along all available established risk factors and subsequent backward elimination (α for inclusion and elimination was set at 0.05). Additionally, graphs were generated to illustrate these analyses. Statistical analyses were conducted using STATISTICA v12 (StatSoft Inc., 2014). A p-value of less than 0.05 was considered significant.

Results

Patients characteristics

Clinical characteristics of all enrolled patients are summarized in Table 1. No death during the AAA repair procedure was observed, and only one in-hospital death was observed due to massive bleeding and cardiac arrest in an urgent patient without coronary artery evaluation prior to AAA open repair. History of cardiac revascularization (PCI or CABG) was present in 26.3% of cases and history of MI in 31.4%, while 39.8% of patients had both.

Coronary artery stenosis in AAA patients

In patients who underwent coronary artery imaging, significant coronary stenosis (> 70%) were found in 65.3% (77/118). The distribution of significant stenosis between major coronary branches is shown in Figure 1. Overall, the single-vessel disease was found in 34.7% of patients, two-vessel in 11.9%, and three-vessel in 11.0%. In 7.6% of all cases, there was significant stenosis of the left main coronary artery. Almost all patients had visible atherosclerotic coronary lesions and in only 2.5% (3) of patients had no atherosclerotic evidence found in standard CAG.

Predictors of coronary stenoses in AAA patients

The presence of significant coronary lesions in multiple logistic regression analysis was assessed in a subgroup of patients with coronary artery imaging but without a prior history of CABG (n = 101), who inherently all presented with significant lesions (n = 17). Factors univariately associated with the presence of significant atherosclerosis included prior history of PCI (odds ratio [OR] = 6.1, 95% confidence interval [CI] 2.5–15.2, p < 0.001), MI (OR = 2.8, 95% CI 1.1–7.4, p = 0.036), and age (OR = 1.1, 95% CI 1.0–1.2, p = 0.017). The model (area under the curve [AUC] = 0.78, 95% CI 0.7–0.8; R2 Nagelkerka = 0.30) was built by additionally adjusting for sex and sum of modifiable cardiovascular risk factors (which were univariately insignificant). Independent predictors of significant stenosis comprised the only history of prior PCI (OR = 6.9, 95% CI 2.6–18.2, p < 0.001) and age (OR = 1.1, 95% CI 1.0–1.2, p = 0.007). The proportion of patients with significant coronary artery stenosis reached 80.9% (38/47), if there was a PCI in anamnesis, however, as much as 40.7% (22/54) of patients with AAA and no history of PCI or the CABG had significant coronary lesions.

Management of significant stenosis in AAA patients

Only 52.0% (40/77) of patients with significant coronary stenosis underwent immediate coronary revascularization prior to aneurysm repair: ad hoc PCI in 32 cases and urgent CABG in 8 cases. Patients undergoing revascularization prior to surgery had longer mean time from coronary artery imaging to AAA repair, compared with the remaining patients with significant coronary stenosis (123.6 vs. 58.1 days, p < 0.001; Fig. 2), although there was no difference in mean AAA diameter (60.3 vs. 60.3 mm, p = 0.996). ANOVA and the Tukey post hoc analyses revealed that PCI with drug-eluting stent or drug-eluting balloon (DES or DEB), as well as CABG, were interventions that significantly postponed AAA repair, as shown in Figure 3 [194.0 days; p = 0.02, and 158.3 days, p = 0.04, respectively vs. 63.0 days for conservative therapy; p < 0.001 for the model). Interestingly, out of 32 patients qualified to ad hoc PCI revascularization, only four were implanted with DES, and one restenosis was treated with DEB, while 27 patients (84.4% of PCI patients) were implanted with bare metal stents (BMS) due to imminent surgery. Nevertheless, complete anatomical revascularization (defined as the absence of significant lesions or chronic occlusion that are not secured by a bypass) prior to AAA repair was achieved in only 52.5% of patients (62/118).

Table 1. Clinical characteristics of enrolled patients.

	Patients who underwent AAA repair (n = 271)	Patients who underwent AAA repair and coronary artery imaging (n = 118)	Patients who underwent AAA repair and coronary artery imaging without prior CABG (n = 101)
Clinical features			
Age [years]	68.9 ± 7.7	68.9 ± 6.6	69.3 ± 6.5
Male sex	91.1%	89.8%	89.1%
Hypertension	87.8%	92.4%	92.1%
Dyslipidemia	74.3%	79.7%	81.2%
Diabetes or prediabetes*	24.0%	31.4%	29.7%
Smoking	33.2%	33.9%	34.7%
COPD	10.0%	8.5%	7.9%
Atrial fibrillation	11.4%	11.9%	10.9%
Peripheral atherosclerosis**	48.0%	55.1%	57.4%
History of MI	31.7%	32.2%	28.7%
History of PCI	27.7%	41.5%	46.5%
History of CABG	18.5%	14.4%	0%
Heart failure	21.0%	23.7%	17.8%
EVAR	42.8%	32.2%	31.7%
Symptomatic AAA	26.2%	23.7%	23.8%
AAA diameter, median (range) [mm]	59.0 (32–91)	58.0 (38–90)	58.0 (38–90)
Complications			
Perioperative MI	0.7%	0.8%	1.0%
Cardiac arrest	0.4%	0%	0%
Perioperative stroke	0.4%	0%	0%
Perioperative TIA	0.7%	0%	0%
MACE	1.8%	0.8%	1.0%
MOF	1.5%	0%	0%
MACE or MOF	2.2%	0.8%	1.0%
Reoperation need	3.7%	2.5%	3.0%
Red blood cell transfusion	17.0%	19.5%	18.8%
Plasma transfusion	8.9%	11.0%	10.9%
ICU stay median (range) [days]	1 (0–70)	1 (0–9)	1 (0–9)
In-hospital stay, median (range) [days]	7 (2–181)	7 (2–70)	7 (2–22)

*Prediabetes includes impaired fasting glucose and impaired glucose tolerance; **Peripheral atherosclerosis encompasses significant lesions in carotid and lower extremity arteries; AAA — abdominal aortic aneurysm; CABG — coronary artery bypass grafting; COPD — chronic obstructive pulmonary disease; EVAR — endovascular aneurysm repair; ICU — intensive care unit; MACE — major adverse cardiovascular event (MI or cardiac arrest or stroke or TIA); MI — myocardial infarction; MOF — multiple organ failure; PCI — percutaneous coronary intervention; TIA — transient ischemic attack

Coronary artery evaluation prior to AAA and postoperative outcomes

Patients who had undergone coronary artery evaluation (and treatment if indicated) prior to aneurysm repair had shorter median stay in the intensive care unit and hospitalization time (Table 2). They also tended to have lower major adverse cardiovascular event (MACE) rate, which reached statistical significance after grouping together with multiple organ failure (MOF) (Table 2). These better outcomes were observed despite the higher incidence of cardiovascular risk factors in this group, such as impaired lipid or glucose metabolism, history of prior PCI or presence of peripheral

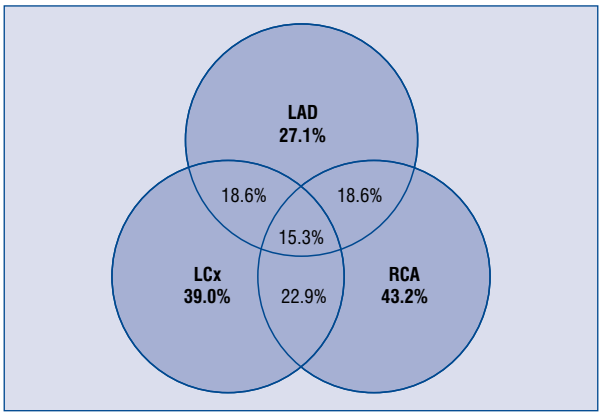

Figure 1. The distribution of significant stenosis (> 70%) between major coronary branches (n = 118). LCx — left circumflex artery; LAD — left anterior descending artery; RCA — right coronary artery.

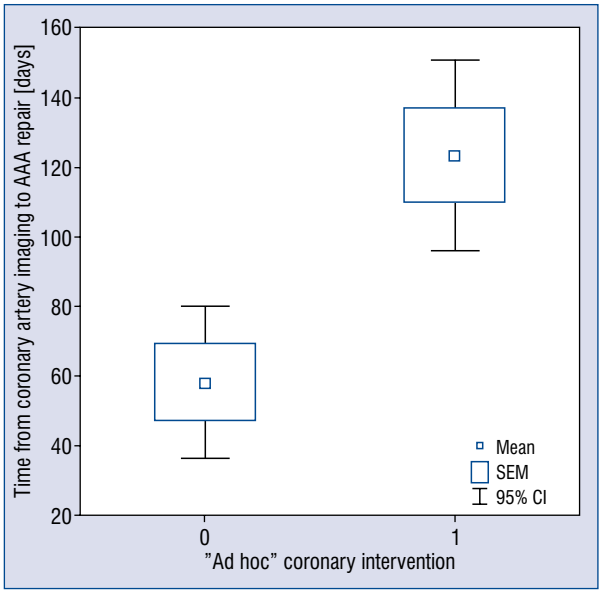

Figure 2. Mean time from coronary artery imaging to abdominal aortic aneurysm (AAA) repair for patients with significant coronary stenosis who did not have coronary intervention (Group 0) and who underwent ad hoc revascularization prior to surgery (Group 1) ($p < 0.001$); CI — onfidence interval; SEM — standard error of the mean.

atherosclerosis (Table 2). Also, these patients were less frequently undergoing EVAR, and yet the need for transfusion of red blood cell concentrates and plasma were similar (Table 2). Based on the present retrospective data, the approximate number needed to treat in avoiding one major complication through preoperative coronary evaluation is 26.

Coexistence of AAA and other vascular pathologies

Abdominal aortic aneurysm were accompanied by common iliac artery aneurysms in 25.4% (30/118), and in another 27.1% of patients (32/118), non-aneurysmatic iliac ectasia was present. A significant proportion of patients (11.0%, 13/118) also presented with aneurysmatic lesions in coronary arteries, which were equally distributed between

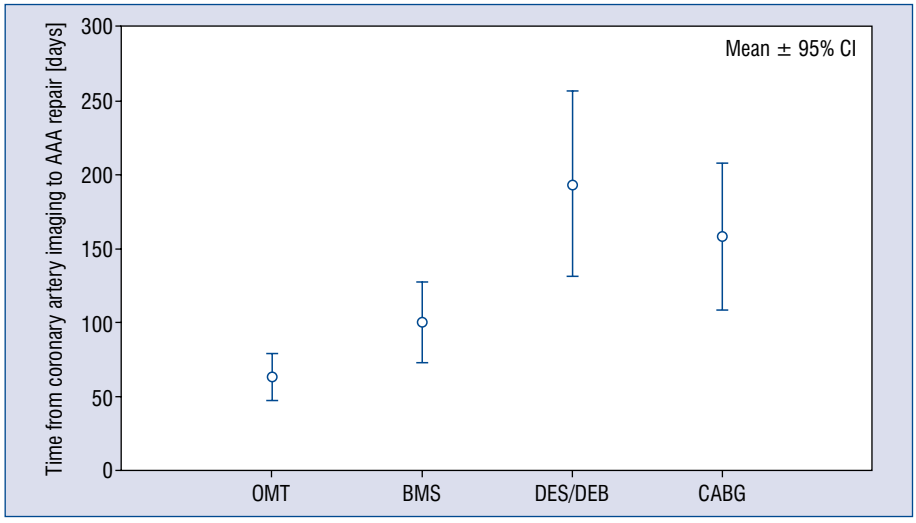

Figure 3. Comparison of mean time from coronary artery imaging to abdominal aortic aneurysm (AAA) repair for patients with optimal medical therapy (OMT) of coronary artery disease and patients with different types of interventions; BMS — bare metal stent; CABG — coronary artery bypass graft; DEB — drug-eluting balloons; DES — drug-eluting stents; CI — confidence interval.

Table 2. Clinical features and comparisons of patients who had undergone coronary artery imaging within 12 months prior to abdominal aortic aneurysm (AAA) repair and remaining subjects undergoing elective AAA repair.

	Patients who had undergone coronary artery imaging within 12 months prior to AAA repair (n = 115)	Remaining subjects undergoing elective AAA repair (n = 156)	P
Clinical features			
Age [years]	69.0 ± 6.7	68.9 ± 8.4	0.907
Male sex	90.4%	91.7%	0.724
Hypertension	92.2%	84.6%	0.060
Dyslipidemia	**80.7%**	**69.5%**	**0.038**
Diabetes or prediabetes*	**31.3%**	**18.6%**	**0.015**
Smoking	34.6%	36.9%	0.702
COPD	8.7%	11.0%	0.538
Atrial fibrillation	12.3%	11.0%	0.739
Peripheral atherosclerosis**	**56.1%**	**42.9%**	**0.031**
History of MI	31.3%	32.1%	0.896
History of PCI	**41.7%**	**17.4%**	**0.000**
History of CABG	14.8%	21.3%	0.173
Heart failure	24.8%	18.8%	0.241
EVAR	**32.2%**	**51.3%**	**0.002**
Symptomatic AAA	23.6%	33.1%	0.104
AAA diameter, median (range) [mm]	58.5 (38–90)	59.0 (32–91)	0.562
Complications			
Perioperative MI	0%	1.3%	0.330
Cardiac arrest	0%	0.6%	0.576
Perioperative stroke	0%	0.6%	0.576
Perioperative TIA	0%	1.3%	0.330
MACE	0%	3.2%	0.061
MOF	0%	2.6%	0.108
MACE or MOF	**0%**	**3.9%**	**0.035**
Reoperation need	2.6%	4.5%	0.628
Red blood cell transfusion	20.0%	14.7%	0.254
Plasma transfusion	11.3%	7.1%	0.223
In-hospital death	0%	0.6%	0.576
ICU stay, median (range) [days]	**1 (0–9)**	**1 (0–70)**	**0.014**
In-hospital stay, median (range) [days]	**7 (2–70)**	**7 (3–181)**	**0.007**

*Prediabetes includes impaired fasting glucose and impaired glucose tolerance; **Peripheral atherosclerosis encompasses significant lesions in carotid and lower extremity arteries; AAA — abdominal aortic aneurysm; CABG — coronary artery bypass grafting; COPD — chronic obstructive pulmonary disease; EVAR — endovascular aneurysm repair; ICU — intensive care unit; MACE — major adverse cardiovascular event (MI or cardiac arrest or stroke or TIA); MI — myocardial infarction; MOF — multiple organ failure; PCI — percutaneous coronary intervention; TIA — transient ischemic attack

right and left coronary artery trees. According to the classification of Markis et al. [22], 1 patient was identified with type I aneurysm (0.9%) and 2 patients with type II aneurysms (1.7%), of whom 1 had already undergone surgical removal of the proximal right coronary artery aneurysm followed by its chronic occlusion. Additionally, 5 patients with type III and 5 with type IV aneurysms were detected (4.2% each).

Discussion

Among patients undergoing noncardiac surgery, major vascular surgery is associated with

a high risk of perioperative MI. The highest incidence of periprocedural MI is observed in patients undergoing open AAA repair (3.7%). Moreover, patients with MI had higher overall complication rates and mortality, emphasizing the necessity of preventing this morbid complication [23]. The current study confirms that the prevalence of CAD in a contemporary sample of patients with AAA is considerably high — two-thirds of patients undergoing AAA repair had significant coronary stenosis. This is similar to previous reports reaching 65%, despite better risk factor management and modern pharmacotherapy available [10, 15, 24, 25]. Even patients without any prior history of cardiac revascularization had significant lesions (found in 2 of every 5 subjects), and those already after PCI had significant lesions in as much as 4 in every 5 patients. It is still unclear whether this high association between the presence of AAA and atherosclerosis is causal or simply due to shared risk factors, as well as which risk factors contribute most to this phenomenon [8, 26, 27].

Coronary revascularization is an established method of reducing cardiovascular events, but interestingly, a randomized trial carried out in patients undergoing major vascular surgery failed to demonstrate the benefits of prophylactic CAD treatment for the clinical outcomes in patients with angiographically determined coronary artery stenosis [17, 28]. Current guidelines indicate that there is no known benefit for elective coronary revascularization of asymptomatic lesions prior to AAA repair [17]. Also, Hosokawa et al. [15] show that in patients undergoing AAA open repair and coronary artery intervention, the cardiac event-free rate was comparable with that of other groups, although mortality was higher. On the other hand, Kordowicz et al. [29] conclude that simultaneous open repair of AAA and cardiac surgery is a feasible option for patients with CAD. Similar conclusions were reached by Sumin et al. [20], where CAG and preventive revascularization before AAA surgery were associated with less perioperative complications, MIs, and lower mortality. Moreover, Sun et al. [18], after retrospective analysis of 368 Chinese patients with AAA, concluded that myocardial evaluation and subsequent revascularization before AAA surgery could improve the clinical outcome in patients with severe CAD.

Because elective open surgical aneurysm repair is considered high-risk surgery, when AAA and symptomatic CAD are detected, coronary artery revascularization (PCI or CABG) should be performed before AAA open repair [30]. However, the prevalence of asymptomatic, significant CAD in patients with AAA was found to be as high as 61% and, moreover, 31% of these patients fulfilled indications for coronary revascularization [31]. There is, therefore, a significant group of patients with asymptomatic but severe CAD that do not undergo coronary artery evaluation and necessary revascularization before high-risk AAA surgery. In the current study, 65.3% of all patients with AAA who underwent coronary evaluation have significant coronary stenosis (≥ 70% diameter), with 40.7% of those were without prior history of PCI or CABG. Only 52% of those patients underwent immediate coronary revascularization prior to AAA repair, and the intervention was associated with postponement of surgery or EVAR. Furthermore, revascularization was performed using optimal techniques (CABG or PCI with DES/DEB) only in 32.5% of cases, and BMS was implanted in the remaining 67.5% of patients (because of a need for an immediate AAA repair). We also found that patients who underwent coronary artery evaluation (and treatment if indicated) prior to AAA repair had shorter median intensive care unit stay and whole hospitalization time, as well as lower MACE or MOF rate (Table 2). Interestingly, better outcomes in patients with coronary imaging were observed despite a higher prevalence of cardiovascular risk factors in this group, which could be explained by the fact that they were probably more carefully diagnosed, and pharmacotherapy was better optimized, subject to the individual approach of the conducting physicians. Furthermore, patients with prior coronary imaging were less frequently undergoing EVAR, and there was no statistically significant difference in the need for red blood cell concentrates and plasma transfusion, despite probably more frequent current or recent dual antiplatelet therapy (exact pharmacotherapy was not recorded in the current study). These observations lead us to conclude that coronary artery evaluation should be performed in all patients with diagnosed AAA at the earliest possible stage.

The overall incidence of coronary artery aneurysm is estimated to be from 0.3% to 5.3% [32]. The present study brought significantly increased prevalence of the coronary artery aneurysms, that was found in 11.0% of all patients. Other authors also noted that there is a high incidence (of up to 17%) of coronary aneurysms in patients with aortic aneurysms in both thoracic and abdominal segments [33]. However, pathophysiological mechanisms behind coronary artery aneurysms remain debatable; the phenomenon of their co-occurrence

with the AAAs could have several reasonable explanations. First, the most common cause of coronary artery aneurysms is CAD, which is also the main risk factor for AAA development [34]. Second, hereditary connective tissue disorders and mutations in matrix metalloproteinases genes can result in both aortic and coronary aneurysms [32, 35]. Moreover, the coronary artery aneurysms might have an iatrogenic origin and occur as a complication after balloon angioplasty or stent implantation, interventions that were frequent in the present study population [32]. Finally, chronic inflammation might be associated with the coexistence of the AAAs, CAD, and coronary artery aneurysms [36]. Patients with aneurysmal coronary disease are usually asymptomatic and, even in the absence of obstructive CAD, have an increased risk of MI and mortality rate similar to patients suffering from three-vessel obstructive CAD [37, 38]. In this light, patients with AAA might additionally benefit from early coronary artery evaluation [39].

Limitations of the study

The current study is not without limitations. This study was a retrospective, cross-sectional, single-center study, which might contribute to selection bias. However, results were comparable to other reports. A relatively large sample size was presented for the field, but were too small to reliably assess any rare observations [15, 24, 25]. The qualification criteria for coronary artery evaluation were subject to the individual practice of the conducting physician and not a randomization process. Hence, it was only possible to retrospectively approximate, rather than directly compare, the differences in outcomes between patients undergoing preoperative coronary evaluation and those entering the procedure without such preprocedural assessment. The identified factors influencing the decision to evaluate coronary arteries before surgery included: history of hypercholesterolemia, diabetes, prior PCI, and qualification for classical AAA open repair, as indicated in Table 2. Moreover, due to the retrospective nature of the study, complications were derived from medical records and not proactively assessed throughout hospitalization, for instance, by routine monitoring of cardiac biomarkers [40]. Due to the structure of the database, it was not possible to identify patients that were scheduled for aneurysm repair and died before hospital admission. This is a major limitation. However, the probability of such a scenario is low, because all patients were scheduled and managed based on an individualized risk-benefit approach, and patients with a high risk of rupture were treated urgently. Moreover, coronary imaging performed outside of the center might have been missed and was not indicated in the medical history. However, this seems unlikely. Patients that had undergone coronary imaging more than 1 year prior to AAA repair (n = 26) from the analysis of coexistence were also arbitrary excluded. On the other hand, only relevant, current CAG were analyzed, which is a major advantage of this study, and allowed a demonstration of the importance of preoperative evaluation of CAD.

Conclusions

In conclusion, major findings from the current study are: (1) despite advancements in risk factor management, still 2 of every 3 patients undergoing coronary artery evaluation prior to AAA repair have significant coronary lesions; (2) prior history of PCI and patient age are independent predictors of significant coronary stenoses; (3) patients undergoing "last-minute" coronary imaging receive suboptimal, conservative therapy or PCI with BMS; (4) nevertheless, patients subjected to preoperative coronary evaluation and treatment had a lower incidence of composite end-point comprising MACE and MOF; and (5) patients with AAA have a higher probability of the presence of coronary artery aneurysms. It can be concluded that patients with AAA might benefit from an early coronary artery evaluation strategy.

Conflict of interest: None declared

References

1. Erbel R, Aboyans V, Boileau C, et al. 2014 ESC Guidelines on the diagnosis and treatment of aortic diseases: Document covering acute and chronic aortic diseases of the thoracic and abdominal aorta of the adult. The Task Force for the Diagnosis and Treatment of Aortic Diseases of the European Society of Cardiology (ESC). Eur Heart J. 2014; 35(41): 2873–2926, doi: 10.1093/eurheartj/ehu281, indexed in Pubmed: 25173340.
2. Moll FL, Powell JT, Fraedrich G, et al. Management of abdominal aortic aneurysms clinical practice guidelines of the European society for vascular surgery. Eur J Vasc Endovasc Surg. 2011; 41 Suppl 1: S1–S58, doi: 10.1016/j.ejvs.2010.09.011, indexed in Pubmed: 21215940.
3. Dereziński T, Fórmankiewicz B, Migdalski A, et al. Występowanie tętniaków aorty brzusznej w populacji miejsko-wiejskiej w centralnej Polsce — Gniewkowo Aortic Study. Kardiol Pol. 2017; 75(7): 705–710, doi: 10.5603/kp.a2017.0071.
4. Golledge J, Muller J, Daugherty A, et al. Abdominal aortic aneurysm: pathogenesis and implications for management.

Arterioscler Thromb Vasc Biol. 2006; 26(12): 2605–2613, doi: 10.1161/01.ATV.0000245819.32762.cb, indexed in Pubmed: 16973970.
5. Ye Zi, Bailey KR, Austin E, et al. Family history of atherosclerotic vascular disease is associated with the presence of abdominal aortic aneurysm. Vasc Med. 2016; 21(1): 41–46, doi: 10.1177/1358863X15611758, indexed in Pubmed: 26566659.
6. Antiochos P, Monney P, Fournier S, et al. Endovascular management of heavily calcified abdominal aorta dissection during transcatheter aortic valve implantation. Cardiol J. 2016; 23(6): 655––656, doi: 10.5603/CJ.2016.0107, indexed in Pubmed: 27976796.
7. Treptau J, Ebnet J, Akin M, et al. Angiographic detection of fatal acute aortic dissection Stanford type A under resuscitation. Cardiol J. 2016; 23(6): 620–622, doi: 10.5603/CJ.2016.0103, indexed in Pubmed: 27976792.
8. Van Kuijk JP, Flu WJ, Dunckelgrun M, et al. Coronary artery disease in patients with abdominal aortic aneurysm: a review article. J Cardiovasc Surg (Torino). 2009; 50(1): 93–107, indexed in Pubmed: 19179995.
9. Elkalioubie A, Haulon S, Duhamel A, et al. Meta-Analysis of abdominal aortic aneurysm in patients with coronary artery disease. Am J Cardiol. 2015; 116(9): 1451–1456, doi: 10.1016/j.amjcard.2015.07.074, indexed in Pubmed: 26347003.
10. Hertzer NR, Beven EG, Young JR, et al. Coronary artery disease in peripheral vascular patients. A classification of 1000 coronary angiograms and results of surgical management. Ann Surg. 1984; 199(2): 223–233, indexed in Pubmed: 6696538.
11. Mukai S, Yao H, Miyamoto T, et al. The long-term follow-up results of elective surgical treatment for abdominal aortic aneurysms. Ann Thorac Cardiovasc Surg. 2002; 8(1): 38–41, indexed in Pubmed: 11916441.
12. Roger VL, Ballard DJ, Hallett JW, et al. Influence of coronary artery disease on morbidity and mortality after abdominal aortic aneurysmectomy: a population-based study, 1971-1987. J Am Coll Cardiol. 1989; 14(5): 1245–1252, indexed in Pubmed: 2808978.
13. Rinckenbach S, Hassani O, Thaveau F, et al. Current outcome of elective open repair for infrarenal abdominal aortic aneurysm. Ann Vasc Surg. 2004; 18(6): 704–709, doi: 10.1007/s10016-004-0114-6, indexed in Pubmed: 15599628.
14. Sasaki Y, Isobe F, Kinugasa S, et al. Influence of coronary artery disease on operative mortality and long-term survival after abdominal aortic aneurysm repair. Surg Today. 2004; 34(4): 313–317, doi: 10.1007/s00595-003-2708-y, indexed in Pubmed: 15052444.
15. Hosokawa Y, Takano H, Aoki A, et al. Management of coronary artery disease in patients undergoing elective abdominal aortic aneurysm open repair. Clin Cardiol. 2008; 31(12): 580–585, doi: 10.1002/clc.20335, indexed in Pubmed: 19072880.
16. Borioni R, Tomai F, Pederzoli A, et al. Coronary risk in candidates for abdominal aortic aneurysm repair: a word of caution. J Cardiovasc Med (Hagerstown). 2014; 15(11): 817–821, doi: 10.2459/JCM.0000000000000150, indexed in Pubmed: 25251942.
17. McFalls EO, Ward HB, Moritz TE, et al. Coronary-artery revascularization before elective major vascular surgery. N Engl J Med. 2004; 351(27): 2795–2804, doi: 10.1056/NEJMoa041905, indexed in Pubmed: 15625331.
18. Sun T, Cheng Yt, Zhang Hj, et al. Severe coronary artery disease in Chinese patients with abdominal aortic aneurysm: prevalence and impact on operative mortality. Chin Med J (Engl). 2012; 125(6): 1030–1034, indexed in Pubmed: 22613526.
19. Wolff T, Baykut D, Zerkowski HR, et al. Combined abdominal aortic aneurysm repair and coronary artery bypass: presentation of 13 cases and review of the literature. Ann Vasc Surg. 2006; 20(1): 23–29, doi: 10.1007/s10016-005-9324-9, indexed in Pubmed: 16378145.
20. Sumin AN, Korok EV, Panfilov SD, et al. [Myocardial revascularization before abdominal aortic surgery in patients with ischemic heart disease]. Kardiologiia. 2013; 53(4): 62–68, indexed in Pubmed: 23952955.
21. Kristensen SD, Knuuti J, Saraste A, et al. 2014 ESC/ESA Guidelines on non-cardiac surgery: cardiovascular assessment and management: The Joint Task Force on non-cardiac surgery: cardiovascular assessment and management of the European Society of Cardiology (ESC) and the European Society of Anaesthesiology (ESA). Eur Heart J. 2014; 35(35): 2383–2431, doi: 10.1093/eurheartj/ehu282, indexed in Pubmed: 25086026.
22. Markis JE, Joffe CD, Cohn PF, et al. Clinical significance of coronary arterial ectasia. Am J Cardiol. 1976; 37(2): 217–222, indexed in Pubmed: 1108631.
23. Sutzko DC, Andraska EA, Obi AT, et al. Risk factors associated with perioperative myocardial infarction in major open vascular surgery. Ann Vasc Surg. 2018; 47: 24–30, doi: 10.1016/j.avsg.2017.08.030, indexed in Pubmed: 28893702.
24. Kioka Y, Tanabe A, Kotani Y, et al. Review of coronary artery disease in patients with infrarenal abdominal aortic aneurysm. Circ J. 2002; 66(12): 1110–1112, indexed in Pubmed: 12499615.
25. Kishi K, Ito S, Hiasa Y. Risk factors and incidence of coronary artery lesions in patients with abdominal aortic aneurysms. Intern Med. 1997; 36(6): 384–388, indexed in Pubmed: 9213182.
26. Hernesniemi JA, Vänni V, Hakala T. The prevalence of abdominal aortic aneurysm is consistently high among patients with coronary artery disease. J Vasc Surg. 2015; 62(1): 232–240.e3, doi: 10.1016/j.jvs.2015.02.037, indexed in Pubmed: 26115925.
27. Takagi H, Umemoto T. ALICE (All-Literature Investigation of Cardiovascular Evidence) Group. Coronary artery disease and abdominal aortic aneurysm growth. Vasc Med. 2016; 21(3): 199–208, doi: 10.1177/1358863X15624026, indexed in Pubmed: 26842623.
28. Poldermans D, Schouten O, Vidakovic R, et al. A clinical randomized trial to evaluate the safety of a noninvasive approach in high-risk patients undergoing major vascular surgery: the DECREASE-V Pilot Study. J Am Coll Cardiol. 2007; 49(17): 1763–1769, doi: 10.1016/j.jacc.2006.11.052, indexed in Pubmed: 17466225.
29. Kordowicz A, Ghosh J, Baguneid M. A single centre experience of simultaneous open abdominal aortic aneurysm and cardiac surgery. Interact Cardiovasc Thorac Surg. 2010; 10(1): 63–66, doi: 10.1510/icvts.2009.219105, indexed in Pubmed: 19854792.
30. Jaffery Z, Grant A. Multisystem revascularization. Ochsner J. 2009; 9(4): 211–219, indexed in Pubmed: 21603446.
31. Marsico F, Giugliano G, Ruggiero D, et al. Prevalence and severity of asymptomatic coronary and carotid artery disease in patients with abdominal aortic aneurysm. Angiology. 2015; 66(4): 360–364, doi: 10.1177/0003319714540319, indexed in Pubmed: 24965380.
32. Abou Sherif S, Ozden Tok O, Taşköylü Ö, et al. Coronary artery aneurysms: a review of the epidemiology, pathophysiology, diagnosis, and treatment. Front Cardiovasc Med. 2017; 4: 24, doi: 10.3389/fcvm.2017.00024, indexed in Pubmed: 28529940.

33. Balderston JR, Giri J, Kolansky DM, et al. Coronary artery aneurysms associated with ascending aortic aneurysms and abdominal aortic aneurysms: pathophysiologic implications. Catheter Cardiovasc Interv. 2015; 85(6): 961–967, doi: 10.1002/ccd.25726, indexed in Pubmed: 25379626.
34. Cohen P, O'Gara PT. Coronary artery aneurysms: a review of the natural history, pathophysiology, and management. Cardiol Rev. 2008; 16(6): 301–304, doi: 10.1097/CRD.0b013e3181852659, indexed in Pubmed: 18923233.
35. Lamblin N, Bauters C, Hermant X, et al. Polymorphisms in the promoter regions of MMP-2, MMP-3, MMP-9 and MMP-12 genes as determinants of aneurysmal coronary artery disease. J Am Coll Cardiol. 2002; 40(1): 43–48, indexed in Pubmed: 12103254.
36. Kuivaniemi H, Platsoucas CD, Tilson MD. Aortic aneurysms: an immune disease with a strong genetic component. Circulation. 2008; 117(2): 242–252, doi: 10.1161/CIRCULATIONAHA.107.690982, indexed in Pubmed: 18195185.
37. al-Harthi SS, Nouh MS, Arafa M, et al. Aneurysmal dilatation of the coronary arteries: diagnostic patterns and clinical significance. Int J Cardiol. 1991; 30(2): 191–194, indexed in Pubmed: 2010241.
38. Baman TS, Cole JH, Devireddy CM, et al. Risk factors and outcomes in patients with coronary artery aneurysms. Am J Cardiol. 2004; 93(12): 1549–1551, doi: 10.1016/j.amjcard.2004.03.011, indexed in Pubmed: 15194034.
39. Mariscalco G, Mantovani V, Ferrarese S, et al. Coronary artery aneurysm: management and association with abdominal aortic aneurysm. Cardiovasc Pathol. 2006; 15(2): 100–104, doi: 10.1016/j.carpath.2005.11.005, indexed in Pubmed: 16533698.
40. Botto F, Alonso-Coello P, Chan MTV, et al. Myocardial injury after noncardiac surgery: a large, international, prospective cohort study establishing diagnostic criteria, characteristics, predictors, and 30-day outcomes. Anesthesiology. 2014; 120(3): 564–578, doi: 10.1097/ALN.0000000000000113, indexed in Pubmed: 24534856.

VIA MEDICA

ORIGINAL ARTICLE

Cardiology Journal
2020, Vol. 24, No. 4, 394–403
DOI: 10.5603/CJ.a2018.0103

ISSN 1897–5593

Prognostic significance of red cell distribution width and its relation to increased pulmonary pressure and inflammation in acute heart failure

Ryszard Targoński[1], Janusz Sadowski[1], Magdalena Starek-Stelmaszczyk[1], Radosław Targoński[2], Andrzej Rynkiewicz[1]

[1]Department of Cardiology, University of Warmia and Mazury in Olsztyn, Poland
[2]Pomeranian Cardiology Centers, Gdansk, Poland

Abstract

Background: *Red cell distribution width (RDW) in acute heart failure (AHF) is accepted as a prognostic indicator with unclear pathophysiological ties. The aim of this study was to evaluate the prognostic value of RDW in AHF patients in relation to clinical and echocardiographic data.*

Methods: *170 patients with AHF were retrospectively studied. All patients had laboratory testing and an echocardiogram performed within 24 h of admission to the Cardiology Department.*

Results: *During the mean 193 ± 111 days of follow-up, 33 patients died. More advanced age, high RDW and low peak early diastolic velocity of the lateral mitral annulus (MVe') were independent predictors of all-cause mortality with hazard ratios of: 1.05 (95% CI 1.02–1.09), $p < 0.005$, 1.40 (95% CI 1.22–1.60), $p < 0.001$, and 0.77 (95% CI 0.63–0.93), $p < 0.007$, respectively. In a stepwise multiple linear regression model, RDW was correlated with hemoglobin concentration (standardized $\beta = –0.233$, $p < 0.001$), mean corpuscular volum (standardized $\beta = –0.230$, $p < 0.001$), mean corpuscular hemoglobin concentration (standardized $\beta = –0.207$, $p < 0.007$), the natural logarithm of C-reactive protein (CRP) (standardized $\beta = 0.184$, $p < 0.004$) and tricuspid regurgitation peak gradient (TRPG) values (standardized $\beta = 0.179$, $p < 0.006$), whereas MVe' was correlated with atrial fibrillation (standardized $\beta = 0.269$, $p < 0.001$).*

Conclusions: *The present data demonstrates a novel relation between higher levels of RDW and elevated TRPG and high sensitivity CRP values in patients with AHF. These findings suggest that RDW, the most important mortality predictor, is independently associated with elevated pulmonary pressure and systemic inflammation in patients with AHF. Moreover, in AHF patients, more advanced age and decreased MVe' are also independently associated with total mortality risk.* (Cardiol J 2020; 27, 4: 394–403)

Key words: acute heart failure, red cell distribution width, anemia, MVe', tricuspid regurgitation peak gradient, high sensitivity C-reactive protein

Introduction

Heart failure (HF) is becoming one of the most important cardiovascular syndromes due to its increasing prevalence, high mortality and increasing cost of care. Despite progress in therapeutic methods for acute heart failure (AHF), it still carries a grim prognosis and that is why searching for reliable predictors of mortality is of utmost importance [1]. Among them, red cell distribution width (RDW) was found to be the cheapest and most widely available indicator. The RDW was established to be a strong predictor of mortality in the general population above 45 years of age [2], as well as during sepsis, trauma and in critically ill patients [3–5]. Several studies confirmed that RDW predicts mortality in acute and chronic heart failure (CHF) [5–9]. It was reported that an increasing

Address for correspondence: Dr. Ryszard Targoński, Department of Cardiology, University of Warmia and Mazury in Olsztyn, ul. Niepodległości 44, 10–045 Olsztyn, Poland, tel/fax: +48 895326202, e-mail: rtarg@op.pl

Received: 13.02.2018 Accepted: 10.06.2018

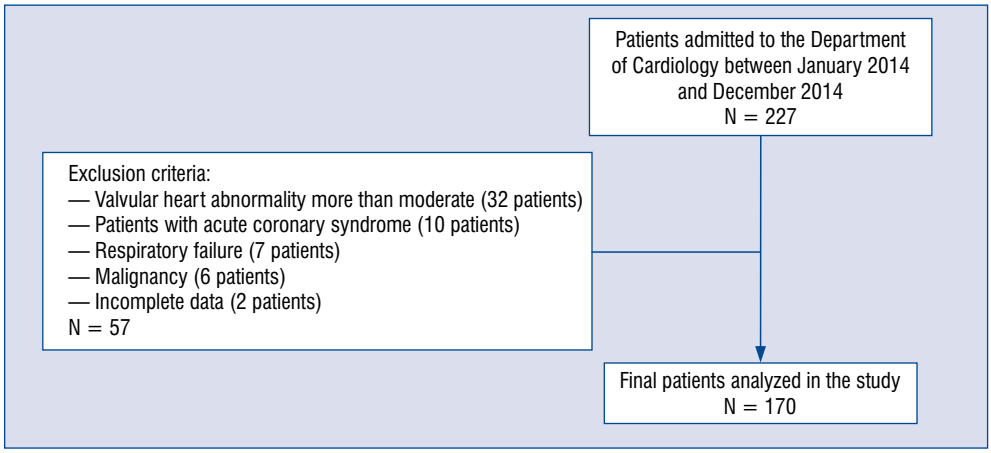

Figure 1. The flow chart of case enrolment of our study according to the inclusive and exclusive criteria.

RDW value is associated with cytokine activation, impaired iron mobilization and decreased hemoglobin (Hb) levels [10–12]. Furthermore, impaired deformability of erythrocytes (RBC) caused by proinflammatory cytokines can also be manifested as increased RDW [4]. The exact mechanism of how elevated RDW is associated with an adverse prognosis has not been entirely elucidated and its relation to clinical findings has not been fully explained. Recently, it was documented that high RDW values were independently associated with increased left ventricular (LV) end diastolic pressure [13]. Data concerning the association of RDW with echocardiographic findings in AHF are scarce and ambiguous [5, 6, 14]. The aim of the present study was to evaluate the mid-term prognostic value of RDW in AHF with regards to clinical and echocardiographic data.

Methods

The retrospective study included 170 patients chosen from 237 consecutive patients admitted to the hospital due to recent resting dyspnea caused by decompensation of CHF. All patients had N-terminal pro-B-type natriuretic peptide (NT-proBNP) plasma levels that were above 300 units and signs of systolic and/or diastolic LV dysfunction in resting transthoracic echocardiography (ECHO) performed within 24 h of admission. The following exclusion criteria were applied: age younger than 18 years, valvular heart abnormality higher than moderate, acute coronary syndrome, dyspnea due to concomitant respiratory failure, malignancy and incomplete data (Fig. 1). All patients were treated according to the current guidelines for congestive heart failure (HF). Pharmacotherapy on admission was presented in Tables 1 and 2. Each patient underwent a standard echocardiogram (Vivid 5, GE Vingmed) using an adaptive 1.3–4.0 MHz transducer. Left atrial diameter (LAd), LV end-diastolic diameter (LVEDD) and right ventricular end-diastolic diameter (RVEDD) were assessed. The tricuspid regurgitation peak gradient (TRPG) was calculated according to the simplified Bernoulli formula, and was measured using a continuous wave Doppler in the modified apical 4-chamber view. The transmitral early diastolic velocity (E) was assessed from the mitral inflow velocity. The LV ejection fraction (LVEF) was measured using the Simpson biplane method. Tissue Doppler myocardial imaging (TDI) was used to assess the peak early diastolic velocity of the lateral mitral annulus (MVe') by placing the Doppler sample volume over the lateral side of the mitral annulus at the posterior leaflet. Venous blood samples were taken for determination of serum creatinine, sodium level, high sensitivity C-reactive protein (hsCRP), D-dimer, NT-proBNP and a complete blood count. Laboratory analysis was performed using a COBAS C-6000 Analyzer (Roche Diagnostic GmGH, Mannheim, Germany). Baseline hematologic analyses were performed using SYSMEX XT 1800i. The reference range for RDW was 11.5–14.5%. The glomerular filtration rate (GFR) was calculated according to the Modification of Diet in Renal Disease (MDRD) formula. Follow-up began on of the day of admission to the Cardiology Department due to AHF. The endpoint of this study was all-cause mortality, including in-hospital and post-discharge deaths. The study protocol was approved by the Warmia

Table 1. Baseline characteristics and treatments in patients who died or survived.

Variable	Survivors (n = 137)	Non-survivors (n = 33)	P
Age [years]	73.9 ± 12.5	78.3 ± 9.4	0.1
Sex, male	75 (54.7%)	14 (42.42%)	0.2
Diabetes mellitus	44 (32.12%)	16 (48.48%)	0.08
Hypertension	92 (67.15%)	21 (63.64%)	0.7
CAD	20 (14.60%)	9 (27.27%)	0.08
COPD	23 (16.79%)	7 (21.21%)	0.6
History of DVT	9 (6.57%)	6 (18.18%)	0.04
Acute infection	50 (36.5%)	9 (27.27%)	0.3
Heart rate [bpm]	78.42 ± 17.03	85.6 ± 15.89	0.03
BP systolic [mmHg]	136.8 ± 26.5	133.3 ± 21.7	0.5
BP diastolic [mmHg]	80.8 ± 15.2	82.0 ± 14.4	0.7
Weight [kg]	83.1 ± 19.5	77.6 ± 11.8	0.1
BMI [kg/m^2]	30.9 ± 6.5	28.3 ± 4.2	0.03
NT-proBNP [pg/mL]	2539 [1431–5496]	4240 [2028–9090]	0.03
Hb [g/dL]	12.8 ± 2.3	11.8 ± 2.7	0.04
RDW [%]	15.0 ± 1.8	16.9 ± 2.9	0.00003
Ht [%]	39.07 ± 6.27	37.03 ± 7.84	0.1
MCV [fL]	90.78 ± 6.88	90.66 ± 9.44	0.9
MCHC [g/dL]	32.87 ± 1.69	32.44 ± 1.46	0.2
Leukocytes [G/mL]	8.3 ± 3.3	7.7 ± 3.2	0.3
PLT [G/mL]	217.8 ± 126.9	186.1 ± 92.3	0.2
Na [mmol/L]	139.2 ± 4.3	137.9 ± 5.1	0.1
Creatinine [mg/dL]	1.2 ± 0.4	1.3 ± 0.6	0.3
eGFR [mL/min/1.73 m^2]	62.5 ± 26.5	58.5 ± 23.6	0.4
CRP [mg/L]	3.7 [1.5-12.7]	14.0 [5.0-34.8]	0.0005
D-dimer [μg/mL]	0.9 [0.5-1.5]	1.7 [0.7-3.1]	0.02
LBBB	12 (8.76%)	3 (9.09%)	1.0
RBBB	6 (4.38%)	3 (9.09%)	0.3
AF	68 (49.64%)	16 (48.49%)	0.91
LAd [cm]	4.9 ± 0.8	4.9 ± 0.6	0.8
LVEDD [cm]	5.6 ± 0.9	5.5 ± 1.0	0.9
RVEDD [cm]	3.3 ± 0.7	3.3 ± 0.7	0.9
EF [%]	43.1 ± 15.2	41.6 ± 17.2	0.6
TRPG [mmHg]	35.9 ± 13.6	42.2 ± 14.4	0.02
E [cm/s]	94.9 ± 29.4	84.7 ± 26.6	0.07
MVe' [cm/s]	8.5 ± 2.6	7.3 ± 1.7	0.01
E/MVe'	12.4 ± 4.7	12.5 ± 2.7	0.8
Mitral regurgitation	24 (17.52%)	5 (15.15%)	0.8
ACEI/ARB	129 (94.16%)	27 (81.82%)	0.02
Spironolactone	74 (54.01%)	23 (69.70%)	0.1
Furosemide	103 (75.18%)	26 (78.79%)	0.7
Chlortalidone	44 (32.12%)	6 (18.18%)	0.1
Hydrochlorothiazide	24 (17.52%)	5 (15.15%)	0.8
Oral anticoagulant	89 (64.96%)	18 (54.55%)	0.3
Statins	76 (55.47%)	13 (39.39%)	0.1
Beta-blockers	118 (86.13%)	25 (75.76%)	0.1

Data are shown as mean ± standard deviation/median [IQR]/patients' number (%); IQR — range from 1st to 3rd quartile; CAD — coronary artery disease; COPD — chronic obstructive pulmonary disease; DVT — deep vein thrombosis; BP — blood pressure; BMI — body mass index; NT-proBNP — N-terminal pro-B-type natriuretic peptide; Hb — hemoglobin; RDW — red blood cell distribution width; Ht — hematocrit; MCV — mean corspuscular volume; MCHC — mean corpuscular hemoglobin concentration; PLT — platelet count; eGFR — estimated glomerular filtration rate; CRP — C-reactive protein; LBBB — left bundle branch block; RBBB — right bundle branch block; AF — atrial fibrillation; LAd — left atrium diameter; LVEDD — left ventricular end-diastolic diameter; RVEDD — right ventricular end-diastolic diameter; EF — ejection faction; TRPG — tricuspid regurgitation peak gradient; E — early diastolic mitral inflow velocity; MVe' — peak early diastolic velocity of the mitral annulus lateral portion; ACEI — angiotensin converting enzyme inhibitor; ARB — angiotensin receptor blocker

Table 2. Total mortality in relation to clinical measures.

Variable	Univariate Cox proportional survival analysis (n = 170)				Multivariate Cox proportional survival analysis (n = 170)			
	HR	95% CI		P	HR	95% CI		P
Age [years]	1.034	1.000	1.070	0.05	1.050	1.015	1.087	0.005
Sex, male	0.658	0.330	1.313	0.2				
Diabetes mellitus	1.698	0.858	3.361	0.1				
Hypertension	0.834	0.410	1.696	0.6				
CAD	2.169	0.895	5.257	0.09				
COPD	1.328	0.576	3.062	0.5				
History of DVT	2.169	0.895	5.257	0.09				
Acute infection	1.420	0.660	3.055	0.4				
Heart rate [bmp]	1.022	1.006	1.038	0.007				
Systolic BP [mmHg]	0.978	1.007	0.317	1.0				
Diastolic BP [mmHg]	1.003	0.980	1.026	0.8				
Weight [kg]	0.983	0.964	1.003	0.1				
BMI [kg/m^2]	0.934	0.882	0.989	0.02				
NT-proBNP [pg/mL]	1.629	1.161	2.285	0.005				
Hb [g/dL]	0.880	0.771	1.005	0.06				
RDW [%]	1.348	1.194	1.522	< 0.001	1.396	1.221	1.596	< 0.001
Ht [%]	0.966	0.919	1.016	0.2				
MCV [fL]	0.991	0.947	1.036	0.7				
MCHC [g/dL]	0.855	0.700	1.043	0.1				
Leukocytes [G/mL]	1.030	0.895	1.185	0.7				
PLT [G/mL]	0.997	0.992	1.001	0.2				
Na [mmol/L]	0.962	0.894	1.034	0.3				
Creatinine [mg/dL]	1.544	0.810	2.945	0.2				
eGFR [mL/min/1.73 m^2]	0.994	0.980	1.009	0.4				
CRP [mg/L]	1.476	1.184	1.841	0.001				
D-dimer [μg/mL]	1.195	1.076	1.326	0.001				
LBBB	1.074	0.328	3.520	0.9				
RBBB	2.346	0.715	7.694	0.2				
AF	0.996	0.503	1.971	1.0				
LAd [cm]	0.965	0.647	1.439	0.9				
LVEDD [cm]	0.987	0.681	1.431	0.9				
RVEDD [cm]	0.881	0.532	1.459	0.6				
EF [%]	0.993	0.972	1.015	0.5				
TRPG [mmHg]	1.023	1.001	1.046	0.04				
E [cm/s]	0.985	0.971	0.999	0.03				
MVe' [cm/s]	0.846	0.746	0.958	0.009	0.767	0.632	0.931	0.007
E/MVe'	1.016	0.941	1.097	0.7				
Mitral regurgitation	0.996	0.503	1.971	1.0				
ACEI/ARB	0.339	0.140	0.822	0.02				
Spironolactone	1.614	0.768	3.395	0.2				
Furosemide	1.156	0.502	2.664	0.7				
Chlortalidone	0.459	0.189	1.112	0.09				
Hydrochlorothiazide	1.013	0.390	2.633	1.0				
Oral anticoagulant	0.670	0.338	1.330	0.3				
Statins	0.537	0.267	1.079	0.08				
Beta-blockers	0.468	0.211	1.040	0.06				

HR — hazard ratio; CI — confidential interval. The meaning of other abbreviations are the same as in Table 1.

and Masuria Medical Chamber Ethics Committee (no. 435/06).

Statistical analysis

Normally distributed variables were reported as mean and standard deviation. Variables that did not have a normal distribution were reported as median and interquartile range. Depending on the type of distribution of the variables, the groups were compared using the Student t test or the Mann-Whitney test. The χ^2 test was used to compare qualitative variables between groups. A value of $p < 0.05$ was considered statistically significant.

Variables selected to be tested in multivariate analysis were those with $p < 0.1$ in the univariate model. Multivariate survival analysis was performed using the Cox proportion hazard model to determine which factors were significantly associated with death after adjustment for the other variables. A stepwise selection was done using a p to remove and a p to enter into the model ≤ 0.05 with both prior backward selection after inclusion of all selected variables and then forward selection.

For the receiver operator characteristic (ROC) Youden Index was used to find the optimal cut-off points for the best discrimination of death risk. Kaplan-Meier survival curves analysis for the optimal cut-off point of RDW was created and statistical comparison between survival curves was done using the log-rank test.

Linear regression analysis was used to evaluate association between clinical variables and the most important independent death predictors. Identified variables ($p < 0.1$) were considered to enter in a stepwise manner to the multivariate linear regression model. The variable retention criterion was set at ≤ 0.05.

All statistical analysis was performed using STATSTICA 12 software.

Results

The study included 170 patients (males 47.7%). The mean observation time was 193 ± ± 111 days. Within the follow-up period, 33 (19.4%) patients died.

The baseline characteristics of the survivor and non-survivor groups are presented in Table 1. For survivors, the mean age was 73.9 ± 12.5 and for non-survivors the mean age was 78.3 ± 9.4 years ($p = 0.1$). A history of deep vein thrombosis was more frequent in the non-survivors group (18.2% vs. 6.6%, $p < 0.04$). There was a similar prevalence of reported comorbidities and acute infections in both studied groups. The number of subjects with anemia in survivors and non-survivors in the study group was 56 (40.88%) and 19 (57.58%), respectively ($p = 0.08$). After exclusion of anemic subjects, the median value of RDW in survivors and non-survivors was 14.4 (13.8–15.5) and 15.7 (14.6–17.30), respectively ($p = 0.03$). Treatment with angiotensin-converting enzyme inhibitor/angiotensin receptor blocker (ACEI/ARB) was significantly more frequent in the survivors group. Biochemical and clinical analyses revealed significantly higher concentration of NT-proBNP, CRP, D-dimer, and higher RDW and TRPG values in non-survivors (Table 1). In the non-survivors group, significantly lower Hb concentration and diminished MVe' values were found.

The univariate relative risk of mortality in relation to clinical variables is listed in Table 2. The presence of advanced age, higher values of NT-proBNP, CRP, D-dimer, RDW, TRPG, and lower values of mitral E and MVe' were related to total mortality.

The multivariate relative risk of mortality in relation to clinical variables is presented in Table 2. Advanced age, increased RDW value and decreased lateral MVe' velocity were retained as independent predictors for all-cause mortality with hazard ratios of 1.05 (95% CI 1.02–1.09), $p < 0.005$, 1.40 (95% CI 1.22–1.60), $p < 0.001$, and 0.77 (95% CI 0.63–0.93), $p < 0.007$, respectively.

In the univariate linear regression analysis, RDW was positively correlated with the natural logarithm of CRP (LnCRP), TRPG, NT-proBNP and RVEDD. Negative RDW correlation was found with Hb, hematocrit, mean corpuscular volume (MCV) and mean corpuscular hemoglobin concentration (MCHC) values. In the stepwise multiple linear regression model, RDW was correlated with Hb, MCV, MCHC, LnCRP and TRPG values (Table 3).

In the stepwise multiple linear regression model, MVe' was correlated with the presence of atrial fibrillation (AF) (standardized $\beta = 0.269$, $p < 0.001$).

In the whole study group the ROC curve analysis for RDW revealed that area under curve (AUC) was 0.72 (95% CI 0.62–0.82; $p < 0.0001$). The ROC curve analysis in the subgroup without anemia revealed AUC of 0.69 (95% CI 0.53–0.84; $p < 0.02$). RDW value ≥ 14.6 was found to be the optimal cut-off point for the discrimination of death risk. The same value of optimal cut-off point was found for non-anemic patients. RDW value ≥ 14.6 in the whole study group was found to have sensitivity and specificity of 86% and 51% and for non-anemic patients 78.6% and 56.0%, respectively.

Table 3. Univariate and multivariate analysis of association of patient characteristics with RDW.

Variable	Univariate linear regression analysis			Multivariate linear regression analysis		
	β unstandarised ± SD	β standarised	P	β unstandarised ± SD	β standarised	P
Age [years]	–0.014 ± 0.014	–0.078	0.3			
Sex, male	0.175 ± 0.168	0.080	0.3			
Diabetes mellitus	0.140 ± 0.175	0.062	0.4			
Hypertension	–0.289 ± 0.175	–0.126	0.1			
CAD	0.275 ± 0.224	0.095	0.2			
COPD	–0.348 ± 0.217	–0.123	0.1			
DVT history	0.001 ± 0.265	0	1.0			
Acute infection	–0.064 ± 0.177	–0.028	0.7			
Heart rate [bpm]	0.018 ± 0.010	0.143	0.06			
Systolic BP [mmHg]	–0.0003 ± 0.007	–0.003	1.0			
Diastolic BP [mmHg]	–0.006 ± 0.011	–0.038	0.6			
Weight [kg]	–0.002 ± 0.009	–0.016	0.8			
BMI [kg/m^2]	–0.028 ± 0.027	–0.079	0.3			
NT-proBNP [pg/mL]	0.000 ± 0.000	0.181	0.02			
Hb [g/dL]	–0.356 ± 0.065	–0.392	< 0.001	–0.212 ± 0.065	–0.233	0.001
Ht [%]	–0.108 ± 0.024	–0.331	< 0.001			
MCV [fL]	–0.108 ± 0.021	–0.369	< 0.001	–0.067 ± 0.02	–0.23	0.001
MCHC [g/dL]	–0.557 ± 0.092	–0.425	< 0.001	–0.271 ± 0.099	–0.207	0.007
Leukocytes [G/mL]	–0.042 ± 0.051	–0.064	0.4			
PLT [G/mL]	0.002 ± 0.001	0.094	0.2			
Na [mmol/L]	–0.053 ± 0.037	–0.109	0.2			
Creatinine [mg/dL]	0.572 ± 0.347	0.127	0.1			
eGFR [mL/min/1.73 m^2]	0.004 ± 0.006	0.051	0.5			
LnCRP [mg/L]	0.330 ± 0.109	0.229	0.003	0.266 ± 0.092	0.184	0.004
D-dimer [μg/mL]	0.160 ± 0.085	0.143	0.06			
LBBB	–0.267 ± 0.297	–0.069	0.4			
RBBB	0.603 ± 0.374	0.123	0.1			
AF	0.142 ± 0.169	0.065	0.4			
LAd [cm]	0.335 ± 0.209	0.123	0.1			
LVEDD [cm]	0.167 ± 0.179	0.072	0.4			
RVEDD [cm]	0.523 ± 0.238	0.168	0.03			
EF [%]	–0.010 ± 0.011	–0.073	0.3			
TRPG [mmHg]	0.035 ± 0.012	0.227	0.003	0.028 ± 0.01	0.179	0.006
E [cm/s]	0.004 ± 0.006	0.057	0.5			
MVe' [cm/s]	0.003 ± 0.003	0.078	0.3			
E/MVe'	0.051 ± 0.039	0.101	0.2			
Mitral regurgitation	0.286 ± 0.223	0.098	0.2			

SD — standard deviation; the meaning of all abbreviations are the same as in Table 1 and Table 2.

When Kaplan-Meier survival curves for 1-year mortality were constructed, patients with RDW ≥ 14.6 had a 1-year cumulative survival probability of 65% compared with 92% for those with RDW < 14.6 ($p < 0.001$ in log-rank test) (Fig. 2). Number of patients at risk in the group assessed with RDW ≥ 14.6 was 97 and in the group with RDW < 14.6 was 73 subjects.

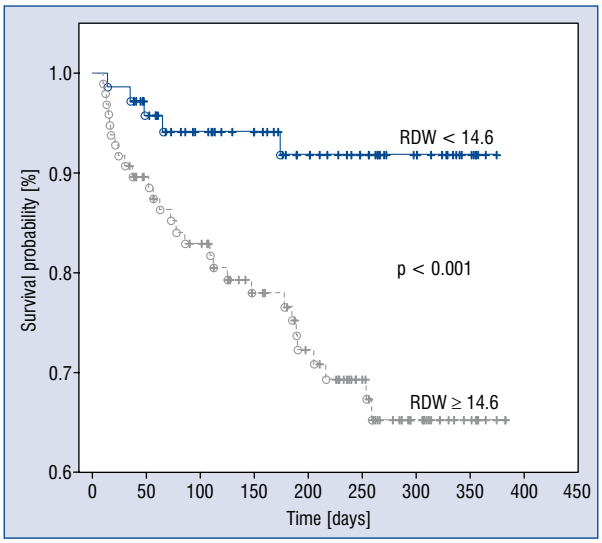

Figure 2. Kaplan-Meier survival curves for total mortality in 170 patients with acute heart failure with red cell distribution width (RDW) ≥ 14.6 (n = 97) and RDW < 14.6 (n = 73).

Discussion

Elevated RDW on admission is the most powerful independent predictor of all-cause mortality in AHF patients. A 1% RDW increase predicted an almost 40% increase in total mortality risk, which is consistent with previously reported data in AHF [6, 7, 15–17].

There are numerous reasons for RDW elevation under different clinical conditions. Traditionally, an isolated rise in RDW is the first abnormality seen in early iron deficiency and coupled with a low MCV is regarded as being diagnostic of absolute iron deficiency [16, 17]. Hemoglobin concentration and automatically measured red cell indices are considered sensitive indicators of systemic iron status [18]. It was found that iron deficiency is an ominous finding in CHF [17]. As the deficit worsens, the MCHC falls with a further reduction in MCV. In the present study, increased RDW was independently correlated with a low Hb level, as well as decreased MCV and MCHC values. Similar correlations have been described by other authors [8, 19] in AHF patients. In a recent study by Senthong et al. [13] this correlation was observed in patients who underwent elective coronary angiography. Moreover, van Kimmenade et al. [8] found no correlation between increased RDW and serum iron, TIBC, serum transferin saturation and ferritin level. Allen et al. [10] demonstrated similar findings in CHF patients. They additionally found a correlation between elevated RDW and high eyrthropoetin levels, normal iron binding capacity and ferritin levels. All results are consistent with a state of impaired iron mobilization and the inhibition of erythropoietin-induced erythrocyte maturation, the hallmark of anemia in chronic diseases [20]. There is an increasing recognition that in the AHF population, the ability to mobilize and use existing iron stores may be impaired even in the setting of adequate overall total body iron [21]. This is sometimes referred to as "reticuloendothelial block", and it is mediated in part by the overexpression of hepcidin; a peptide hormone secreted by the liver which is upregulated by inflammation and acts as a regulator of human iron metabolism [10, 22].

In the entire study group, an association between lower MCV, MCHC and Hb concentration with higher RDW may indicate an underlying iron deficiency, but it cannot be excluded that the RDW value is also modified by erythrocyte destruction and ineffective iron utilization for red cell production [23]. In rodent models of sepsis, decreases in Hb content and erythrocyte deformability resulting in RDW elevation was shown to be most profound in the second-oldest subpopulation of cells accounting for 20% of total circulating erythrocytes [24]. On the other hand, it was demonstrated that RDW elevation is caused by a rise of immature erythrocyte forms [11].

In the present study group, increased RDW was independently positively correlated with hs-CRP level. Lippi et al. [23] demonstrated a similar correlation in an unselected population between high RDW and elevated CRP concentration. It was reported that inflammation alters erythropoiesis by direct myelosuppression of erythroid precursors, promotion of red cell apoptosis, reduction of erythropoietin production, reduced iron bioavailability, and erythropoietin resistance in erythroid precursor cell lines. CRP contributes to stimulating the secretion of cytokines and tissue factor, it also induces the expression of adhesion molecules from endothelial cells [25]. Inflammatory cytokines also suppress erythrocyte maturation, allowing newer, larger reticulocytes to enter the circulation and skew the RDW distribution [4]. An inverse correlation between RDW and MCV, MCHC and Hb values indicate that proliferation and new erythrocytes entering into circulation are less important than erythrocyte destruction in the study group. The median hsCRP value in the non-survivors group was 14.0 (5.0–34.8) mg/L. The elevation of hsCRP above 10 mg/L should be evaluated for noncardiovascular etiologies, most likely resulting from an infection [26]. The prevalence of acute

infection was similar for both the survivors and non-survivors group. Therefore, it seems that in AHF patients studied, destruction of erythrocytes is associated not only with HF related vascular inflammation but probably also with severity of the superimposed infection.

The inflammatory process, particularly accompanying HF, is an important pro-thrombotic factor. In the present study, D-dimer concentration was significantly higher in the non-survivors group in univariate regression analysis and a significant positive correlation between D-dimer and RDW was observed. No patients had clinical symptoms of recent deep vein thrombosis or acute coronary syndrome, so activated fibrinolysis is rather connected with other vascular territories. Itani et al. [7] found that a higher DIC score was independently associated with risk of death in AHF patients. Interestingly, it was reported that in patients with hypoxemia and pulmonary hypertension due to HF, endothelial dysfunction and ongoing intravascular coagulation was associated with the occurrence of ischaemic and thrombotic pulmonary events [27]. In a mixed etiology pulmonary hypertension population, it was demonstrated that elevated RDW levels were inversely correlated with Hb and MCV values which is in line with the present results [12]. Tandon et al. [28] described extensive thrombotic pulmonary vascular changes at various stages of organization with pulmonary iron deposits seen in 70% of cases in patients with severe pulmonary hypertension due to isolated mitral stenosis. Similar abnormalities were described in HF and pulmonary hypertension [29].

According to available research, the current study provides the first data evaluating the relationship between the RDW and TRPG values in AHF. An independent direct positive correlation between RDW with TRPG values in the present study group may indicate the role of elevated pulmonary artery pressure on the modification of RDW values. It has been proven that blood stasis, due to low cardiac output, passive vascular distension, and systemic inflammation leads to endothelial dysfunction by means of neurohormonal activation [30]. Costello et al. [31] have described disruption of some or all layers of the alveolar-capillary unit by elevated capillary hydrostatic pressures, a phenomenon they referred to as pulmonary capillary stress failure. When all of the layers are disrupted, RBCs may be seen traversing the alveolarcapillary membrane. It was found that RBC destruction releases free Hb, and these react with nitric oxide to form inactive nitrate and methemoglobin, thus leading to endothelial dysfunction [32]. Recently in a murine model of hemolysis, a significant reduction in nitric oxide bioavailability due to free Hb was shown to be accompanied by platelet activation and the activation of a coagulation pathway resulting in thrombosis, pulmonary hypertension, right ventricular failure and eventually death [32]. The impact of increased pulmonary pressure on vascular endothelial cells in AHF may lead to erythrocyte damage and serve as an important modifier of the RDW. Free Hb leads to further microcirculation damage and creation of a self-perpetuating vicious circle. It has been demonstrated that unfractionated heparin treatment in cardio-renal syndrome and peripheral vein thrombosis without pulmonary embolism resulted in lowering pulmonary arterial hypertension and increased plasma anticoagulants indicating the thrombotic nature of the underlying pathology which plays an important role in pulmonary circulation of AHF patients [33].

Results herein demonstrate that decreased MVe', unlike LVEF and other echocardiographic data including the E/MVe' ratio in AHF patients, independently predicts risk of death. Gandhi et al. [34] first described that the impairment of diastolic dysfunction in patients with sinus rhythm is associated with the development of acute pulmonary edema with normal and unchanged LVEF. The MVe' value is a key indicator of diastolic function because it reflects both relaxation and restoration forces [35]. It is commonly assumed that in the failing heart, MVe' is modified by diastolic pressure but is less load dependent than transmitral flow velocities [35]. However, AF changes the ventricular diastolic filling profile from double to single phase, leading to a significant increase of maximal MVe' velocity, falsely denotes a better LV diastolic function. The prevalence of AF in the survival and nonsurvival groups was similar; therefore, AF is not likely to be a factor affecting MVe' predictability of death in the present study group. It was demonstrated that early diastolic mitral annulus velocity in patients with LV systolic dysfunction and sinus rhythm was found to be a powerful predictor of cardiac mortality. Moreover, MVe' emerged as the best prognosticator for long-term follow-up and was even more accurate than the E/e' ratio, incremental to other clinical or echocardiographic variables in patients with impaired LV systolic function [36]. It was also reported that the presence of diastolic dysfunction provides important prognostic insights in patients with HF, especially preserved ejection fraction and sinus rhythm [36, 37]. According to available research, there is no published data concerning the prog-

nostic impact of MVe' in AHF groups consisting of patients with preserved as well as reduced ejection fraction. However, further analysis of a larger mixed HF population with and without AF are needed to establish absolute predictive values separately for patients with AF and those with sinus rhythm.

Limitations of the study

The present study has several limitations.

Firstly, the study was performed at a single center with a small, retrospective sample size, which raises a concern of whether the sample is representative. However, demographic, clinical, and biological characteristics of the present study collectively correspond with the respective characteristics reported from other studies of AHF [6, 19].

Secondly, analysis of precise indices of iron metabolism, transfusion status or nutritional deficiency was not carried out.

Thirdly, analysis of TRPG was performed instead of a direct invasive pulmonary pressure estimation.

Conclusions

The present data demonstrates a novel relation between higher levels of RDW, elevated TRPG and elevated hsCRP values in patients with AHF. These findings suggest that RDW, the most important mortality predictor, is independently associated with elevated pulmonary pressure and systemic inflammation in patients with AHF. Moreover, more advanced age and a decreased MVe' are also independently associated with total mortality risk in AHF patients.

Conflict of interest: None declared

References

1. Roger VL. Epidemiology of heart failure. Circ Res. 2013; 113(6): 646–659, doi: 10.1161/CIRCRESAHA.113.300268, indexed in Pubmed: 23989710.
2. Patel K, Ferrucci L, Ershler W, et al. Red blood cell distribution width and the risk of death in middle-aged and older adults. Arch Intern Med. 2009; 169(5): 515, doi: 10.1001/archinternmed.2009.11.
3. Jo YH, Kim K, Lee JH, et al. Red cell distribution width is a prognostic factor in severe sepsis and septic shock. Am J Emerg Med. 2013; 31(3): 545–548, doi: 10.1016/j.ajem.2012.10.017, indexed in Pubmed: 23380094.
4. Scharte M, Fink MP. Red blood cell physiology in critical illness. Crit Care Med. 2003; 31(12 Suppl): S651–S657, doi:10.1097/01.CCM.0000098036.90796.ED, indexed in Pubmed: 14724462.
5. Dai Y, Konishi H, Takagi A, et al. Red cell distribution width predicts short- and long-term outcomes of acute congestive heart failure more effectively than hemoglobin. Exp Ther Med. 2014; 8(2): 600–606, doi: 10.3892/etm.2014.1755, indexed in Pubmed: 25009627.
6. Sotiropoulos K, Yerly P, Monney P, et al. Red cell distribution width and mortality in acute heart failure patients with preserved and reduced ejection fraction. ESC Heart Fail. 2016; 3(3): 198–204, doi: 10.1002/ehf2.12091, indexed in Pubmed: 27818784.
7. Itani R, Minami Y, Haruki S, et al. Prognostic impact of disseminated intravascular coagulation score in acute heart failure patients referred to a cardiac intensive care unit: a retrospective cohort study. Heart Vessels. 2017; 32(7): 872–879, doi: 10.1007/s00380-017-0946-y, indexed in Pubmed: 28120034.
8. van Kimmenade RRJ, Mohammed AA, Uthamalingam S, et al. Red blood cell distribution width and 1-year mortality in acute heart failure. Eur J Heart Fail. 2010; 12(2): 129–136, doi: 10.1093/eurjhf/hfp179, indexed in Pubmed: 20026456.
9. Felker GM, Allen LA, Pocock SJ, et al. Red cell distribution width as a novel prognostic marker in heart failure: data from the CHARM Program and the Duke Databank. J Am Coll Cardiol. 2007; 50(1): 40–47, doi: 10.1016/j.jacc.2007.02.067, indexed in Pubmed: 17601544.
10. Allen LA, Felker GM, Mehra MR, et al. Validation and potential mechanisms of red cell distribution width as a prognostic marker in heart failure. J Card Fail. 2010; 16: 230–238.
11. Bazick HS, Chang D, Mahadevappa K, et al. Red cell distribution width and all-cause mortality in critically ill patients. Crit Care Med. 2011; 39(8): 1913–1921, doi: 10.1097/CCM.0b013e31821b85c6, indexed in Pubmed: 21532476.
12. Hampole CV, Mehrotra AK, Thenappan T, et al. Usefulness of red cell distribution width as a prognostic marker in pulmonary hypertension. Am J Cardiol. 2009; 104: 868–872.
13. Senthong V, Hudec T, Neale S, et al. Relation of red cell distribution width to left ventricular end-diastolic pressure and mortality in patients with and without heart failure. Am J Cardiol. 2017; 119(9): 1421–1427, doi: 10.1016/j.amjcard.2017.01.036, indexed in Pubmed: 28285713.
14. Oh J, Kang SM, Hong N, et al. Relation between red cell distribution width with echocardiographic parameters in patients with acute heart failure. J Card Fail. 2009; 15: 517–522.
15. Pascual-Figal DA, Bonaque JC, Redondo B, et al. Red blood cell distribution width predicts long-term outcome regardless of anaemia status in acute heart failure patients. Eur J Heart Fail. 2009; 11(9): 840–846, doi: 10.1093/eurjhf/hfp109, indexed in Pubmed: 19696056.
16. Aslan D, Gümrük F, Gürgey A, et al. Importance of RDW value in differential diagnosis of hypochrome anemias. Am J Hematol. 2002; 69(1): 31–33, indexed in Pubmed: 11835328.
17. Okonko DO, Mandal AKJ, Missouris CG, et al. Disordered iron homeostasis in chronic heart failure: prevalence, predictors, and relation to anemia, exercise capacity, and survival. J Am Coll Cardiol. 2011; 58(12): 1241–1251, doi: 10.1016/j.jacc.2011.04.040, indexed in Pubmed: 21903058.
18. Tkaczyszyn M, Comín-Colet J, Voors AA, et al. Iron deficiency and red cell indices in patients with heart failure. Eur J Heart Fail. 2018; 20(1): 114–122.
19. Makhoul BF, Khourieh A, Kaplan M, et al. Relation between changes in red cell distribution width and clinical outcomes in acute decompensated heart failure. Int J Cardiol. 2013; 167: 1412–1416.

20. Weiss G, Goodnough LT. Anemia of chronic disease. N Engl J Med. 2005; 352(10): 1011–1023, doi: 10.1056/NEJMra041809, indexed in Pubmed:15758012.
21. Opasich C, Cazzola M, Scelsi L, et al. Blunted erythropoietin production and defective iron supply for erythropoiesis as major causes of anaemia in patients with chronic heart failure. Eur Heart J. 2005; 26(21): 2232–2237, doi: 10.1093/eurheartj/ehi388, indexed in Pubmed: 15987710.
22. Ganz T. Hepcidin, a key regulator of iron metabolism and mediator of anemia of inflammation. Blood. 2003; 102(3): 783–788, doi: 10.1182/blood-2003-03-0672.
23. Lippi G, Targher G, Montagnana M, et al. Relation between red blood cell distribution width and inflammatory biomarkers in a large cohort of unselected outpatients. Arch Pathol Lab Med. 2009; 133: 628–632.
24. Condon MR, Kim JE, Deitch EA, et al. Appearance of an erythrocyte population with decreased deformability and hemoglobin content following sepsis. Am J Physiol Heart Circ Physiol. 2003; 284(6): H2177–H2184, doi: 10.1152/ajpheart.01069.2002, indexed in Pubmed: 12742829.
25. Papageorgiou N, Tousoulis D, Androulakis E, et al. Inflammation and right ventricle: the hunting of the missing link. Int J Cardiol. 2013; 168(4): 3152–3154, doi: 10.1016/j.ijcard.2013.07.082, indexed in Pubmed: 23910446.
26. Pearson TA, Mensah GA, Alexander RW, et al. Markers of inflammation and cardiovascular disease: application to clinical and public health practice: A statement for healthcare professionals from the Centers for Disease Control and Prevention and the American Heart Association. Circulation. 2003; 107(3): 499–511, indexed in Pubmed: 12551878.
27. Lopes AA, Caramurú LH, Maeda NY. Endothelial dysfunction associated with chronic intravascular coagulation in secondary pulmonary hypertension. Clin Appl Thromb Hemost. 2002; 8(4): 353–358, indexed in Pubmed: 12516685.
28. Tandon HD, Kasturi J. Pulmonary vascular changes associated with isolated mitral stenosis in India. Br Heart J. 1975; 37(1): 26–36, indexed in Pubmed: 1111557.
29. Guazzi M, Naeije R. Pulmonary Hypertension in Heart Failure: Pathophysiology, Pathobiology, and Emerging Clinical Perspectives. J Am Coll Cardiol. 2017; 69(13): 1718–1734, doi: 10.1016/j.jacc.2017.01.051, indexed in Pubmed: 28359519.
30. Chen D, Assad-Kottner C, Orrego C, et al. Cytokines and acute heart failure. Crit Care Med. 2008; 36(1 Suppl): S9––S16, doi:10.1097/01.CCM.0000297160.48694.90, indexed in Pubmed: 18158483.
31. Costello ML, Mathieu-Costello O, West JB. Stress failure of alveolar epithelial cells studied by scanning electron microscopy. Am Rev Respir Dis. 1992; 145(6): 1446–1455, doi: 10.1164/ajrccm/145.6.1446, indexed in Pubmed: 1596017.
32. Hu W, Jin R, Zhang J, et al. The critical roles of platelet activation and reduced NO bioavailability in fatal pulmonary arterial hypertension in a murine hemolysis model. Blood. 2010; 116(9): 1613–1622, doi: 10.1182/blood-2010-01-267112, indexed in Pubmed: 20511540.
33. Targonski R, Sadowski J, Cyganski PA. Impact of anticoagulation on the effectiveness of loop diuretics in heart failure with cardiorenal syndrome and venous thromboembolism. Blood Coagul Fibrinolysis. 2014; 25(2): 180–182, doi: 10.1097/MBC.0000000000000012, indexed in Pubmed: 24284867.
34. Gandhi SK, Powers JC, Nomeir AM, et al. The pathogenesis of acute pulmonary edema associated with hypertension. N Engl J Med. 2001; 344(1): 17–22, doi: 10.1056/NEJM200101043440103, indexed in Pubmed: 11136955.
35. Flachskampf FA, Biering-Sørensen T, Solomon SD, et al. Cardiac Imaging to Evaluate Left Ventricular Diastolic Function. JACC Cardiovasc Imaging. 2015; 8(9): 1071–1093, doi: 10.1016/j.jcmg.2015.07.004, indexed in Pubmed: 26381769.
36. Wang M, Yip G, Yu CM, et al. Independent and incremental prognostic value of early mitral annulus velocity in patients with impaired left ventricular systolic function. J Am Coll Cardiol. 2005; 45(2): 272–277, doi: 10.1016/j.jacc.2004.09.059, indexed in Pubmed: 15653027.
37. Zile MR, Gottdiener JS, Hetzel SJ, et al. Prevalence and significance of alterations in cardiac structure and function in patients with heart failure and a preserved ejection fraction. Circulation. 2011; 124(23): 2491–2501, doi: 10.1161/CIRCULATIONAHA.110.011031, indexed in Pubmed: 22064591.

VIA MEDICA

REVIEW ARTICLE

Cardiology Journal
2020, Vol. 27, No. 4, 404–420
DOI: 10.5603/CJ.a2020.0087

ISSN 1897–5593

Artificial intelligence and automation in valvular heart diseases

Qiang Long[1, 2], Xiaofeng Ye[1], Qiang Zhao[1]

[1]Department of Cardiac Surgery, Ruijin Hospital, Shanghai, China
[2]Shanghai Jiao Tong University School of Medicine, Shanghai, China

Abstract

Artificial intelligence (AI) is gradually changing every aspect of social life, and healthcare is no exception. The clinical procedures that were supposed to, and could previously only be handled by human experts can now be carried out by machines in a more accurate and efficient way. The coming era of big data and the advent of supercomputers provides great opportunities to the development of AI technology for the enhancement of diagnosis and clinical decision-making. This review provides an introduction to AI and highlights its applications in the clinical flow of diagnosing and treating valvular heart diseases (VHDs). More specifically, this review first introduces some key concepts and subareas in AI. Secondly, it discusses the application of AI in heart sound auscultation and medical image analysis for assistance in diagnosing VHDs. Thirdly, it introduces using AI algorithms to identify risk factors and predict mortality of cardiac surgery. This review also describes the state-of-the-art autonomous surgical robots and their roles in cardiac surgery and intervention. (Cardiol J 2020; 27, 4: 404–420)

Key words: artificial intelligence, machine learning, valvular heart diseases, medical image analysis, transcathether aortic valve implantation

Introduction

Artificial intelligence (AI), which is a branch of computer science that attempts to create machines that perform tasks as though they possessed human brainpower, and this is gradually changing the landscape of the healthcare industry [1]. Clinical procedures that were supposed to, and could only be performed by human experts previously can now been carried out by machines in a more accurate and efficient way. Recently, cardiologists and radiologists have cooperated with computer scientists and have developed a fully automated echocardiography interpretation system for clinical practice [2]. Cardiovascular diseases affect 48% of the population (≥ 20 years old) and is the leading cause of death [3]. Echocardiography is an effective method to monitor the state of the heart and allows early diagnosis before the onset of symptoms. However, in primary care clinics and poorer regions, there are inadequately experienced radiologists for echocardiography interpretation, let alone patient follow-up. There is group of researchers who trained AI systems using over 14,000 echocardiograms for multiple tasks including view classification and quantification of chamber volume, ejection fraction and longitudinal strain. The AI system validated its accuracy in diagnosing several cardiac diseases after testing on over 8000 cardiograms obtained from routine clinical flow [2]. Such an AI system holds great potential for the transformation of current clinical practice models as well as the popularization of quality healthcare.

The above example is only the tip of the iceberg in the application of AI in medicine for over half a century. Since "AI" was first proposed by John MacCarthy at the Dartmouth College Conference in 1956, great efforts have been made for applying AI to almost all phases of clinical practice. In 1960s, the concept of "computer-assisted diagno-

Address for correspondence: Xiaofeng Ye; Qiang Zhao, Department of Cardiac Surgery, Ruijin Hospital, No. 197 Ruijin Er Road, Shanghai, 200025, China, tel: +8613817382575, +8615777167216, e-mail: xiaofengye@hotmail.com; zq11607@rjh.com.cn

Received: 2.03.2020 Accepted: 5.06.2020

sis" emerged with attempts to use mathematical formalism to interpret clinical problems, although they have little practical value, it has paved the way for subsequent expert systems [4]. In 1970s, researchers began to shift attention to studying the reasoning process of clinicians and simulate it on computer systems, which gave birth to the first generation of medical AI products, i.e. MYCIN. It attempts to diagnose infectious diseases and provide appropriate medication therapies based on over 200 rules that in the form of "if (precondition), then (conclusion or action)". Although MYCIN showed reliability in 63% of the cases of bacteremia [5], it is more like an advanced version of a textbook which has the function of automatic retrievals with little "intelligence". Moreover, the interactions between each rule should be defined by human experts which is extremely arduous with increasingly new knowledge added to the system. However, automatic interpretation of electrocardiograms has gained great benefits from the rule-based AI system. During the same period, a new model, i.e. the probabilistic reasoning was used to simulate the process of expert decision making [6]. Unlike the categorical mode of reasoning utilized by MYCIN, the probabilistic model assign weight to every symptom and clinical finding to indicate its possibility of occurrence for a certain disease. Based on this, new systems including the present illness program, INTERNIST, CASNET were developed [4]. With the introduction of "artificial neural network" in 1980s, machine learning began to flourish. Machine learning endows computers with the ability to learn patterns from data and perform tasks without explicit programming [7]. It has showed great power in developing robust risk prediction models, redefining patient classes and other tasks with the popularization of electronic health records and digital imaging systems [8]. In 2006, the introduction of deep learning by LeCun et al. [9] achieved unprecedented progress in image recognition and other domains, which brought a new renaissance to the development of AI and made automated medical imaging interpretation one of the hottest topics in AI. AI can generally be classified as either weak AI or strong AI. Strong AI is an intelligence construct that has the ability to understand and think as a human being. Weak AI is limited to a specific or narrow area, which is often designed to perform time-consuming tasks and analyze data in ways that humans sometimes cannot. In this review, a brief introduction to AI is provided and highlights its application in the clinical flow of diagnosing and treating valvular heart diseases, including heart sound auscultation, medical image analysis (echocardiography, cardiac computed tomography [CT] and cardiac magnetic resonance [CMR]), risk factor identification, mortality prediction and robotic surgery.

Key concepts in AI

Machine learning

In essence, machine learning is an extension to traditional statistical methods for dealing with large data sets and variables. It enables computers to learn rules and even uncover new patterns from data through a series of algorithms. Most importantly, machine learning can gradually optimize the "reasoning process" between inputs and outputs. Machine learning can be broadly classified into three classes: supervised learning, unsupervised learning and reinforcement learning.

In supervised learning, machines learn the mapping relations between input variables and labeled outcomes and are able to predict outcomes according to inputs. For example, after training with echocardiograms that are labeled with given disease categories, machines are able to assign these disease labels to new echocardiograms. Common computational approaches in supervised learning include artificial neural network (ANN), support vector machine, k-nearest neighbor, naive Bayesian model and decision tree model, among others. Unsupervised learning aims to uncover hidden structures in unlabeled data and classify it into separate categories, which means machines are only trained with input variables and automatically find potential classification rules. For example, with unsupervised learning, machines uncovered three cardiac phenotypes in patients diagnosed with type 2 diabetes mellitus according to their echocardiograms [10]. Common computational approaches include hierarchical clustering, k-means clustering and principle component analysis. Reinforcement learning signifies that machines learn strategies which can obtain the maximum reward through interaction with the environment or outcomes. Unlike the static mode of supervised or unsupervised learning, it is a dynamic learning process. Q-learning, an example of reinforcement learning, has been utilized in clinical trials of lung cancer to find the optimal individualized therapies [11].

Artificial neural network and deep learning

Artificial neural network is composed of multiple interconnected artificial neurons which mimic the biological brain. As mentioned above, ANN is

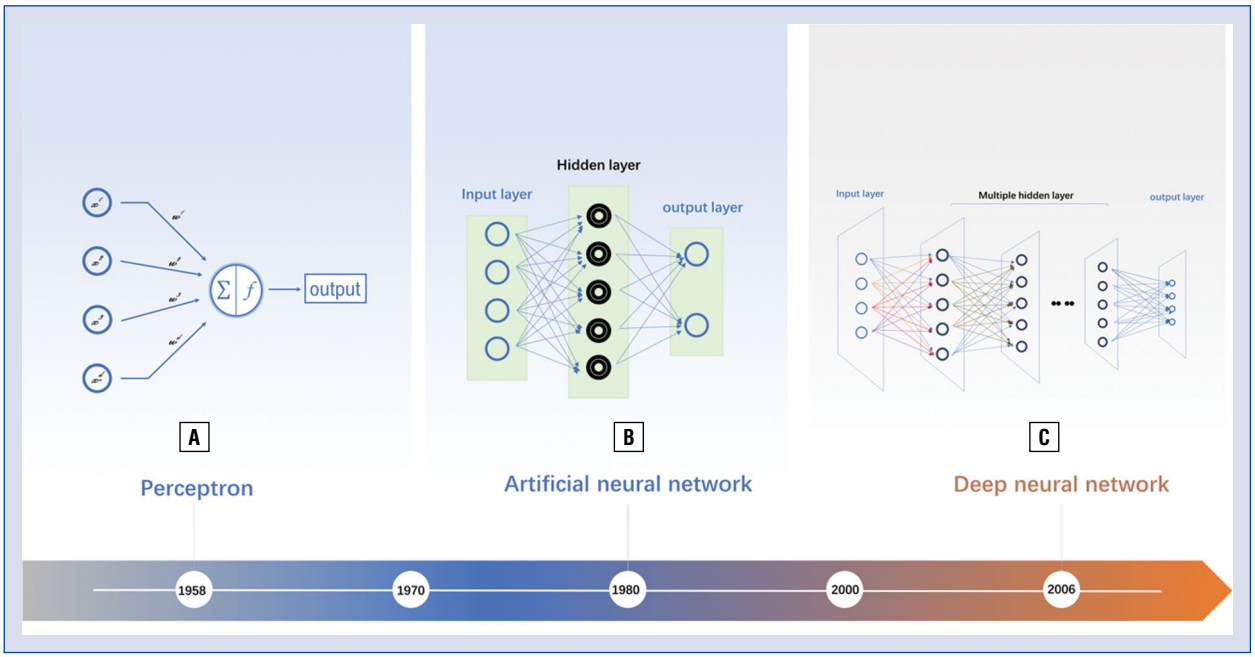

Figure 1. Schematic diagram of the evolvement of artificial neural network. Perceptron, also called single layer neural network, was proposed by Rosenblatt in 1958 (**A**), classic artificial neural network, also known as double layer neural network or multilayer perceptron (**B**), deep neural network (**C**).

actually a computational model. ANN learns from large amounts of data and continuously optimizes the weight of each connection between neurons. Figure 1B shows a typical ANN, which is also called multilayer perceptron, is composed of three layers: input layer, hidden layer and output layer. Each layer contains multiple neurons that are responsible for different functions. The input layer receives numerical variables from data, each value in first layer neurons combines with the weight of the connection, which is then propagated to a hidden layer where the values are integrated, while an output layer generates the final value which represents an outcome. Each neuron in the hidden layer can also set up a threshold to determine whether the information should propagate to the next layer. Now suppose that a database that includes patient data (such as age, body mass index, laboratory results and images results) prior to cardiac surgery and operation results (alive or dead), a mortality prediction model can be built with ANN. Patient variables are input into the neurons in the first layer, the outputs are set as 1 for alive and 0 for dead. The weight of each connection and the excitation threshold of each neuron in the hidden layer are gradually optimized by learning from the data. In this way, after trained with sufficient cases, the ANN model can be accurate enough to predict surgical outcome in new patients.

It can be imagined that, with more hidden layers, the computational results will be more accurate, but this meanwhile requires greater computational power using more training data. Thanks to the rapid development of computer processors and arrival of the era of big data, and also the introduction of "pre-training process", "fine-tuning technique" by Hinton et al. [12] which decreases the training time substantially, multilayer ANN which is also known as "deep learning" becomes a reality. It now represents the most advanced AI technology. The biggest advantage of deep neural network is that it allows the computing model to automatically extract the features of the data by abstracting the data layer by layer and learning the representative and discriminant features.

Computer vision

Computer vision is a main research field in AI, which simulates the human vision with imaging systems and computers. The main tasks involved in computer vision can be divided into three levels [13]. The basic level includes image acquiring and processing techniques such as noise filtering, image enhancement, image segmentation, pattern

recognition. For middle level computer vision, computers should be able to draw conclusions and make decisions based on the information obtained from the basic level. For the top level, computers have the capability to "think" and can understand images like humans do. For now, the first two levels of computer vision are mostly applied to the analysis of medical images and assist in diagnosis. As described below, many algorithms and commercial software have been developed for automating the analysis of medical images, which are more accurate and efficient compared to human endeavour.

Expert system

Expert systems are in their earliest application of AI in medicine, and will keep playing an important role in healthcare. In brief, expert systems are a computer program that simulates human experts in solving problems [14]. It is also called a knowledge-based system because it contains a large amount of knowledge and experience from experts. A typical medical expert system is composed of two modules: knowledge base and control system, the latter can be further divided into a human-computer interactive component, an explanation component, a knowledge acquisition component and an inference engine. The knowledge base is composed of medical knowledge from experts, case-specific knowledge from patients and intermediate results from the reasoning process [14].

Application of AI and automation in diagnosis of valvular heart diseases

AI-assisted "cardiac auscultation"

In spite of the diverse alternatives of imaging tools being the major diagnostic approach to valvular heart diseases (VHDs), physical examination, is the cornerstone of clinical diagnosis and should be the primary screening method for VHDs [15]. Common physical examinations for VHDs include general inspection, pulse palpation, percussion of heart boarder and heart sound auscultation, etc. [16]. Among these, auscultation plays a key role of diagnosing VHDs.

Valvular heart diseases manifest as heart murmurs or/and extra heart sound before the stress of hemodynamic changes causing other signs and symptoms including dyspnea, fatigue, angina, cough and hemoptysis. While cardiac auscultation provides significant diagnostic and prognostic information for cardiac disease, it is not an easy skill to master, especially when innocent murmurs are confronted. Although experienced clinicians have reached an accuracy over 90% in identifying innocent murmurs from pathologic murmurs, less-experienced residents and primary care physicians perform less than satisfactorily [17]. In addition, auscultation is a highly subjective process which may cause bias when evaluating the intensity, location and shape of murmurs. For over a century, tools for cardiac auscultation is a mechanical stethoscope, however, it can neither store nor play back sounds [15]. Thanks to the invention of electronic (digital) stethoscope, the forgoing problems have been well solved, more than that, it provides clinicians with a handy way of "seeing" the heart sound through phonocardiogram. AI-assisted cardiac auscultation in practice refers to the auto-interpretation of phonocardiogram, which belongs to the domain of signal processing. Key steps involved in heart sound analysis could be summarized as segmentation, feature extraction and classification as shown in Figure 2 [18]. Each step is fulfilled through a multitude of algorithms with the ultimate goal of precisely identifying the pathological events underlying heart sounds.

Heart sounds segmentation. Segmentation aims to locate the fundamental elements including the first heart sound (S1), systolic period, the second heart sound (S2) and diastolic period in each cardiac cycle. Training machines to think like human so as to solve problems is to mimic the thinking process of human brain to a certain extent. When interpreting heart sounds, A human expert would firstly locate the two fundamental heart sounds then discriminate S1 from S2 by its pitch, intensity and duration, finally the systolic and diastolic regions are determined, as is the process with computational analysis, but in a more logical and mathematical way.

In the early exploration of heart sound segmentation, electrocardiograph or/and carotid pulse was/were obtained concurrently with phonocardiogram [19, 20]. Transformation equation $g(n)$ was used to compute the smooth energy curve of electrocardiograph signal, then the peaks in $g(n)$ was determined as the beginning of S1 and the systolic period, the dicrotic notch of carotid pulse curve was recognized as the beginning of S2 [19]. This approach apparently is impractical in routine clinical work. Envelop-based (or amplitude threshold-based) segmentation algorithm was first introduced by Liang et al. [21] to locate S1 and S2. Envelop of a signal signifies the smooth curves outlining its upper or lower extremes [22]. The envelop of the original heart sound waveform was first extracted using specific transformation equa-

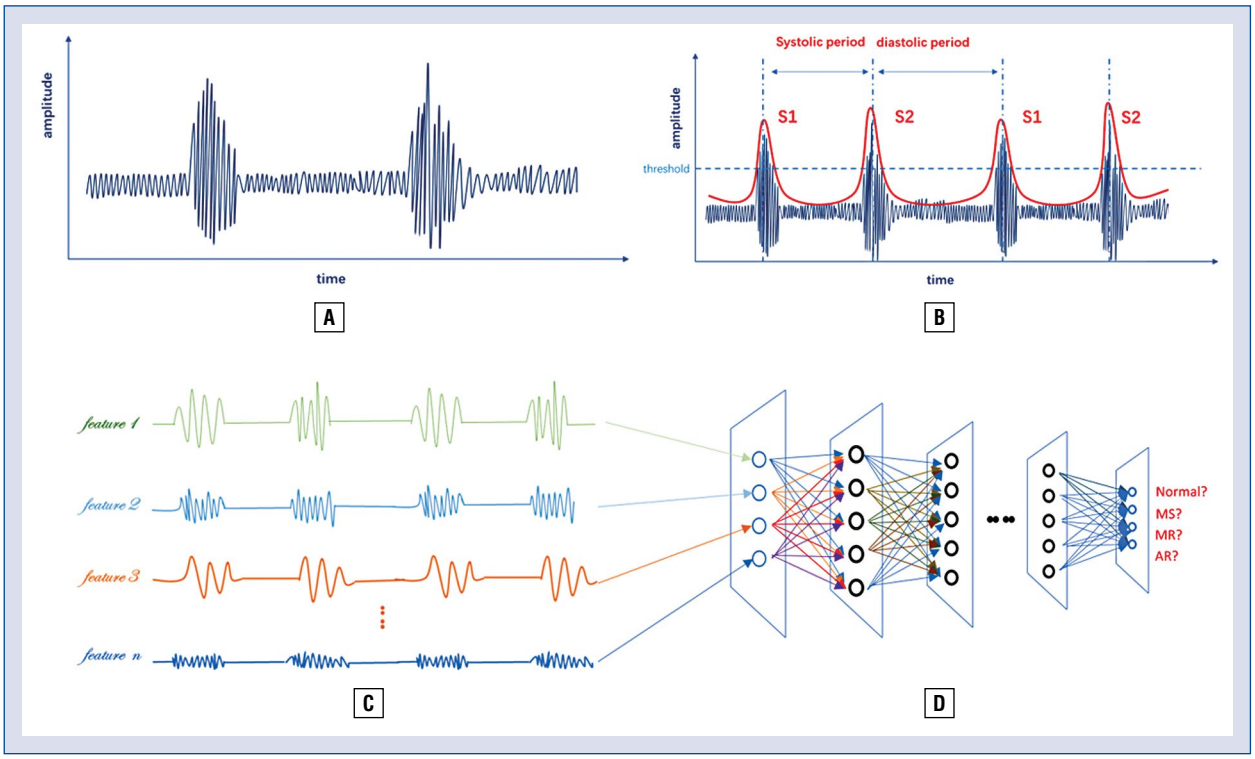

Figure 2. Process of artificial intelligence-assisted auscultation. A normal phonocardiogram (**A**), heart sound segmentation (**B**), feature extraction (**C**), heart sound classification by deep neural network (**D**).

tions, then a threshold value was selected to filter noise and low intensity signals, the peaks exceed the threshold value were recognized as the S1 and S2, S1 was differentiated form S2 based on an assumption that the systolic period was shorter than the diastolic period [21]. A well-fitted extraction equation would allow only two peaks to exceed the threshold when interpreting the normal heart sound, therefore identification accuracy depends largely on an envelope extraction equation. Diverse methods are used to calculate the envelope were created including normalized average Shannon energy [21], single-DOF analytical model [23], wavelet decomposition method [24], Viola integral approach [25], and others. However, the envelope-based segmentation method often leads to problems like weak peaks or extra peaks which reduce accuracy of the results.

The application of machine learning algorithms to heart sound segmentation based on features substantially improves the segmentation results (see feature extraction below). Hidden Markov Model (HMM) is the most widely used in the task [26–28]. To train the HMM, adequate samples prelabeled with the accurate location of S1, S2, systolic and diastolic period are required at the output end; sequences of feature vectors extracted from original phonocardiogram or transformed envelope are used as the observation end of HMM. Recently, utilization of deep learning achieves even higher precision compared to other classification methods in heart sound segmentation [29, 30].

Feature extraction and feature selection. This step aims to select and extract discriminative features either for more precise segmentation of heart sound or for following the disease classification step. Feature means the characteristic of an object by which the human brain recognizes and distinguishes it automatically. The concept of feature is similar to "variable" in regression analysis. Features that can be recognized by machines tend to be presented in the form of numbers or symbols. A human expert draws physiological or pathological information from heart sound through features including heart rate, heart rhythm, timing and shape of the murmur, pitch of the heart sound, and extra heart sound among others. As for phonocardiogram, the features are based on time-domain, frequency-domain, and time-frequency complex domain [31]. Time-domain features include intervals (interval of S1 and S2, systolic intervals, diastolic intervals, the ratio of each component to the cardiac

cycle etc.) and amplitude (mean absolute amplitude of S1 and S2 interval). Frequency-domain features refer to the power spectrum of each heart sound component across frequency bands [29]. Theoretically the more input of features into machine training, the better the classification performance it will achieve. In practice, with the number of training samples being set, the classification performance will drop off when the number of feature inputs exceeds a certain value. In order to exclude the redundant features and improve the classification efficiency, feature selection is often required [32].

Classification and detection of VHDs. This step aims to classify the phonocardiograms into cardiac disease categories using suitable classifiers. Classifier in machine learning refers to the algorithm that learns to assign labels to testing data from training data. This learning process can be supervised or unsupervised. Briefly speaking, supervised learning assigns given labels to data while unsupervised learning seeks labels that could be assigned to data. In the present case, labels are given disease categories like mitral stenosis, mitral regurgitation, aortic stenosis, etc. therefore, supervised learning algorithms/classifiers are utilized. The common classifiers used in heart sound classification include a support vector machine [24, 33–36], neural networks [37, 38], HMM [39], etc. After a careful combination of algorithms used in segmentation, feature extraction and classification, previous studies showed promising and inspiring results in detecting VHDs from phonocardiograms (Table 1). For instance, an intelligent diagnostic system developed by Sun [24] could discriminate aortic regurgitation, mitral regurgitation, pulmonary stenosis with accuracy of 98.9%, 98.4% and 98.7%, respectively. Thompson et al. [17] utilized a murmur detection algorithm developed by CSD labs to distinguish no murmurs and innocent murmurs from pathologic murmurs. 3180 phonocardiograms recorded at five different chest location from 603 cases were tested, the algorithm had good sensitivity, specificity and accuracy in detecting a pathologic murmur, which are 93%, 81% and 88%, respectively. The algorithm showed the highest accuracy (90%) using recordings from the left upper and lower sternal boarder. However, it was unable to analyze the recordings with precision which had a high heart rate and low signal quality [17].

AI-assisted interpretation of echocardiography

Although heart sounds auscultation is convenient, cost-effective and a quick way to diagnose VHDs, it only provides qualitative diagnostic information. To further confirm the diagnosis of VHDs as well as to assess the etiology, severity, ventricular responses and prognosis, imaging tools including echocardiography, CMR, multi-slice CT (MSCT) or even cardiac catheterization are indispensable [40].

Echocardiography is the "heart" of cardiology. It is the preferred method of diagnosing and guiding the treatment of VHDs as well as other cardiac diseases. However, echocardiographic examination is a time-consuming process which usually takes hours from inspection, analysis to formal report which make it impractical in emergency settings. Moreover, typical echocardiographic examination produces large amounts of data including images from multiple views and up to 70 videos which would cause cognitive overload and be prone to error. In addition, due to the characteristic of multiple views in examination, the problems of intra-observer and inter-observer variability inevitably arise. The application of AI and automation in echocardiography would a allow consistent, quick and accurate measurement which promises a more accurate diagnosis and improved patient care.

Image segmentation-valve leaflet detection and tracking. Segmentation and recognition of anatomical structures from original medical images are preprocessing steps for subsequent quantitative analysis and diagnosis. Morphological characteristics and motion pattern of the heart valves are key information to diagnose VHDs and to assist surgical valve repair or percutaneous intervention. While many studies have sought the approaches to segment heart chambers and detect endocardial boarder which were reviewed by Noble and Boukerroui [41], relatively few studies of the segmentation of heart valves and annulus have been published. The reasons for difficulty in segmenting and tracking the heart valves in echocardiographic sequences can be summarized as follows: (1) poor image quality due to low frame rate, speckle noise and artifact which may result in missing boundaries; (2) lack of features to discriminate heart valve from adjacent myocardium for those structures have similar intensity and texture; (3) fast and irregular valve motion making it hard to establish correspondence between frames. Reported approaches for valve segmentation including active contour models [42, 43], thin tissue detector combined with graph cut [44], outlier detection method [45, 46], J-spline method [47], multi-atlas joint label fusion [48], trajectory spectrum learning algorithm [49] and neural network [50].

Table 1. Sensitivity/specificity or accuracy of artificial intelligence-assisted auscultation system in detecting valvular heart diseases.

Reference	Year	Algorithm	Testing samples	Normal (%)	AS (%)	AR (%)	AS+AR (%)	MS (%)	MR (%)	MS+MR (%)	PS (%)	PR (%)
Fahad et al. [39]	2018	HMM	80 abnormal HSs and 150 normal HSs	100/99.33		92/100		96/98.54	93.33/99.50			
Sun [24]	2015	SVM	588 abnormal HSs from 49 patients, 325 normal HSs from healthy individuals	99.8		98.8			98.4		98.7	
Zhang et al. [33]	2014	SVM	40 abnormal HSs and 75 normal HSs	98.67	85			95				
Safara et al. [34]	2013	SVM	43 abnormal HSs and 16 normal HSs	98/100	97.44/98.40	100/100			95.65/98.31			
Kwak et al. [35]	2012	HMM	53 abnormal HSs, 80 normal HSs	99	67	67	67	83	67	80		
Uğuz [37]	2012	ANN	40 abnormal HSs, 20 normal HSs	95				95			95	
Kumar et al. [36]	2010	SVM	81 abnormal HSs from 51 patients		93.02/91.29	94.78/93.98			95.20/96.33		100/100	93.21/95.80
Olmez et al. [38]	2003	ANN	240 abnormal HSs from 20 patients, 48 normal HSs from 4 healthy individuals	100	97.9	100		100	100		97.9	

If more than one testing methods were utilized in the study, only the method with highest sensitivity/specificity or accuracy is presented; ANN — artificial neural network; AR — aortic regurgitation; AS — aortic stenosis; HMM — hidden Markov model; HS — heart sound; MR — mitral regurgitation; MS — mitral stenosis; PR — pulmonary regurgitation; PS — pulmonary stenosis; SVM — support vector machine

Active contour models (ACM) is the first and most widely used segmentation algorithm for the heart valve [51, 52]. The segmentation process is based on ACM and is initiated by manual placement of contour close to the target, which means it is not fully automated. Zhou et al. [45] formulated the problems of valve detection and tracking as outliner detection in the low-rank representation based on different motion patterns between leaflets and the heart wall, which is fully automated requiring no user interaction [46]. Recently, there is a growing trend of applying machine learning to valve segmentation. This approach shifts the manual input to a training phase which makes segmentation fully automated [50]. Ionasec et al. [49] utilized spectrum learning algorithm and boundary detectors to locate and refine mitral leaflets based on anatomical landmarks in four-dimensional (4D) transesophageal echocardiograms and CT which allows precise morphological and functional quantification, and a large amount of data as well as high computational power were required to train the model. Recently, a novel UNet architecture based on a convolutional neural network was utilized by Costa et al. [50] to segment mitral valves in PLAX and A4C views. The biggest strength of UNet architecture is that it does not require a large training dataset to produce accurate results.

Automated quantitative analysis. Precise and reliable quantitative analysis of stenosis and regurgitation is crucial to severity assessment, prognosis prediction and to evaluate whether surgery or intervention is needed. Proximal isovelocity surface area (PISA) method is widely used in measuring mitral valve orifice area and calculating the regurgitant volume [53]. Conventional PISA method of two-dimensional echocardiography is based on the assumption that the shape of the proximal flow convergence region is hemispheric, which is not quite true [54]. The development of three-dimensional (3D) color Doppler echocardiography enables direct measurement of PISA without assumptions, thereby reducing errors [54]. However, it is not indicated for routine clinical use because it is a time-consuming procedure, thus in desperate need of an automated algorithm. Grady et al. [55] proposed the first automated PISA measurement system based on a random walker algorithm. The system was initiated by the manual input of two points (one at the valve annulus and one at the coaptation site), followed by automated segmentation of valve annulus and the isovelocity region. The segmentation results were then used to generate 3D meshes for computing PISA. *In vitro* experiments validated its accuracy in measuring PISA, effective regurgitant surface area (EROA) and regurgitant volume. Further *in vivo* experiments showed that measurement of EROA on patients with magnetic resonance (MR) by automated algorithm was significantly correlated with manual measurement of vena contracta [55]. Cobey et al. [56] proposed another novel automated method based on Halcon HDevelop Machine Vision. 3D images of PISA were first sliced into 2 mm-thick sequential cuts, the algorithm traced the boundary of each slice and the arc lengths between each slice from which the 3D surface area was generated and computed. Another method of quantitatively assessing MR is to use regurgitant fraction which is calculated from mitral inflow and stroke volume [53]. Wang et al. [57] proposed a novel automated system for estimating mitral inflow and aortic outflow. The system first detected the left ventricular wall, mitral annulus and left ventricular outflow tract using marginal space learning and placed the measurement plane. The 3D motions of these structures were tracked through a whole cardiac circle to construct and adjust the measurement plane, then the volume of mitral inflow and left ventricular outflow was computed by aggregating color flow values in the 3D space [57].

In addition to these pioneering studies, several commercial software have been developed including Mitral Valve Quantification (Philips Medical Imaging, Andover, MA) [58], eSie Valve (Siemens Healthcare, Mountain View, CA, USA) [59], Mitral Valve Navigator (Philips Medical Systems) [60], Auto Valve Analysis (Siemens; California, USA) [61], eSie PISA Volume Analysis (Siemens Medical Solutions USA, Inc., Mountain View, CA) [62] which aim to automate the quantitative analysis of 3D echocardiography. These approaches can reduce the measurement time substantially and provide more accurate and reproducible results. The aforementioned automated algorithms and commercial software have validated their reliability in quantitatively measuring aortic and mitral valve apparatus parameters and regurgitation volume [54, 63, 64] as shown in Table 2.

AI-assisted interpretation of cardiac CT images

Computed tomography is not employed as the preferred diagnostic method of VHD. It generally serves as a complementary role when echocardiography is insufficient or inclusive. Nevertheless, cardiac CT has prominent advantages in the evaluation of valve calcification and annulus geometry.

Table 2. Automated software and algorithms in quantification analysis of three-dimensional echocardiography.

Reference	Year	Software/ /algorithm	Function	Reference method	Samples	ICC/intergroup difference between software/algorithm and reference method)	Intra-observer variability (ICC)	Inter-observer variability (ICC)
Mediratta et al. [58]	2017	Mitral Valve Quantification (QLAB version 9.0.1; Philips Medical Imaging, Andover, MA; USA)	For measurement of aortic annulus area, perimeter and diameter	Computed tomography	52 patients	ICC of annulus area, perimeter, area-derived diameter, perimeter--derived diameter: 0.91, 0.90, 0.91, 0.89	0.83, 0.85, 0.81, 0.85, respectively	0.70, 0.72, 0.72, 0.71, respectively
Aquila et al. [59]	2016	eSie Valve Software (Siemens Healthcare, Mountain View, CA, USA)	For measurement of mitral valve parameters	Manual measurement	61 patients	ICC of inter-commissure diameter, mitral annular area, anterior leaflet length, posterior leaflet length: 0.84, 0.94, 0.83, 0.67	0.999, 0.992, 0.984, 0.937, respectively	0.997, 0.957, 0. 963, 0.936, respectively
Kagiyama et al. [60]	2015	Mitral Valve Navigator (Philips Medical Systems)	For measurement of mitral valve parameters	Mitral Valve Quantification (Philips Medical Systems)	74 patients	Cronbach's alpha of commissural width, anteroposterior diameter, annulus area: 0.902, 0.934, 0.938	Not available	0.945, 0.959, 0.961, respectively
Calleja et al. [61]	2013	Auto Valve Analysis (Siemens; California, USA)	For measurement of aortic annulus diameter, leaflet anatomy and coronary ostium height	Computed tomography	40 patients	Intergroup difference (p value) of left, non--coronary, right leaflet: 0.76, 0.06, 0.29; left and right coronary height: 0.003, 0.001	Annulus diameters at sagittal and coronal view: 0.97, 0.92	Annulus diameters at sagittal and coronal view: 0.91, 0.93
Agustin et al. [62]	2013	eSie PISA Volume Analysis (Siemens Medical Solutions USA, Inc., Mountain View, CA)	For measurement of EROA and RVol	Manual measurement by 3D planimetry	90 patients	ICC of EROA, RVol: 0.97, 0.97	Not available	Not available
Choi et al. [63]	2015	Based on Wang [71]	For measurement of aortic RVol	CMR	32 patients	ICC of aortic RVol: 0.93, AR severity: k = 0.94	0.98	0.96
Thavendiranathan et al. [64]	2013	Based on Grady [69]	For measurement of mitral RVol	CMR	35 patients	ICC of Integrated PISA-derived RVol, flow volume-derived RVol: 0.92, 0.91	0.99, 0.93, respectively	0.95, 0.96, respectively

Not all results are listed in the table; 3D — three-dimensional; AR — aortic regurgitation; CMR — cardiac magnetic resonance; EROA — effective regurgitant orifice area; ICC — interclass correlation coefficient; PISA — proximal isovelocity surface area; RVol — regurgitant volume

It is the golden standard for annulus sizing and an indispensable tool in preoperative planning of transcatheter aortic valve replacement (TAVR). Reliable measurement of aortic valve annulus size, aortic root dimension and the height of coronary ostia are crucial for appropriate transcatheter valve prosthesis selection and intraprocedural valve positioning which may improve success rate and reduce postoperative complications. In recent years, advances in 3D image techniques have enabled reconstruction of patient-specific models of aortic valve apparatus. Several automated algorithms and commercial software for aortic valve segmentation and quantification have been developed for preoperative planning of transcathether aortic valve implantation (TAVI).

Patient-specific 3D modeling of aortic valve. Ionasec et al. [49, 65] proposed the first dynamic patient-specific aortic valve model from 4D CT images. A generic physiological model which can represent aortic valve and its pathological variations was constructed first, patient-specific parameters of the model were estimated from volumetric sequences by trajectory spectrum learning, marginal space learning and discriminative learning. Their study was further improved with shape forest to constrain the classical statistical shape model [66]. Waechter et al. [67] extracted the aortic valve geometry from CT images using model-based segmentation and applies pattern search method to detect the coronary ostia. The whole heart geometry (including heart chambers and great vessels) was first roughly modeled, a generic aortic mesh model was established and boundary detector were trained by annotated images aiming to build more detailed models of the aortic valve and root, the coronary ostia was then detected on the surface of the aortic root. Segmentation results allowed a series of clinical measurements including the diameters of annulus and the distance between ostia and aortic valve, etc. Considering that VHDs often involve multivalvular lesion which require joint assessment, Grbic et al. [68] proposed an integrated model for quantification of all heart valves from 4D CT images based on marginal space learning and multi-linear shape models. Another study of Grbic et al. [69] extracted both the volumetric model of the aortic valve and calcification, which is closely correlated with postoperative regurgitation [70].

Landmarks detection and quantitative measurement. A number of parameters should be measured with precision for surgical planning before TAVI. These include annulus diameter, annulus area, angulation of annulus plane and the distance from annulus to coronary ostia to name a few. The annulus diameter is crucial for selection of the appropriate valve prosthesis. Size mismatching may either cause post-operative perivalvular regurgitation or annulus rupture. A short distance between aortic annulus and coronary ostia indicates elevated risk of coronary obstruction after valve deployment. Annulus plane angulation determines the position of an X-ray tube C-arm during operations to achieve an optimal view of valve delivery [71].

Accurate segmentation of the aorta, aortic valve apparatus and detection of anatomic landmarks (coronary ostium, aortic commissures and aortic hinges) is the prerequisite for reliable measurement of the above parameters. Zheng et al. [72] proposed a robust hierarchical approach by first segmenting the global aorta using marginal space learning from which the position of the anatomical landmarks can be roughly inferred, followed by using specific landmark detectors to refine each landmark. Elattar et al. [73, 74] used thresholding and connected component analysis to detect the region of interest, from which aortic root was extracted using 3D normalized cut. Two coronary ostia and three valve hinge points were then detected on the surface of aortic root by intensity projection map and Gaussian curvature map. Lalys et al. [75] used a hybrid approach which integrated thresholding, model-based method, statistical-based method and a 3D contour model in the procedure, however, a user-specific point is needed to define the volume of interest. Recently, colonial walk algorithm, which is a machine learning method, was utilized by Al et al. [76] to automatically localize the landmarks. Several commercial software including three mensio valves (3mensio Medical Imaging BV, the Netherlands) [77, 78, 81], Syngo (Siemens Healthcare, Erlangen, Germany) [79], IntelliSpace Portal (Philips Medical Systems, Cleveland, OH) [80], have been available for routine clinical use. Together with the aforementioned algorithms, these pioneering techniques showed reliable aortic annulus measurements as shown in Table 3.

A comparative study between 3mensio, IntelliSpace Portal (version 7.0), IntelliSpace Portal (version 9.0) and manual measurement concerning annulus parameters, time-cost and reproducibility was performed [81]. Results showed that IntelliSpace Portal (version 9.0) allowed the fastest and most reproducible measurements, parameters derived from either method can be used interchangeably in prosthesis sizing. Moreover, Samim et al. [71] performed a prospective cohort study to

Table 3. Automated software and algorithms in quantification analysis of aortic valve apparatus.

Reference	Year	Software/ /algorithm	Reference method	Samples	Correlation/bias	Inter- -observer variability	Intra- -observer variability
Dankerl et al. [79]	2017	Syngo, CT TAVI Planning (version VB10A, Siemens Healthcare, Erlangen, Germany)	Manual measurement (software: NA)	30 patients	Distance from annular plane to coronary ostia: r = 0.97 (right); r = 0.93 (left) Annulus area: r = 0.89 Annulus diameter: r = 0.89 (maximum diameter); r = 0.82 (minimum diameter)	NA	NA
Guez et al. [80]	2017	Intellispace Portal (Philips Medical Systems, Cleveland, OH)	Manual measurement using 3D Brilliance workstation (Philips Healthcare)	74 patients	Annular diameter in systole: r = 0.85 (minimum), r = 0.87 (maximum diameter) Annular diameter in diastole: r = 0.89 (for both minimum and maximum diameter) Annular area: r = 0.93 (systole), r = 0.94 (systole)	NA	NA
Watanabe et al. [77]	2013	3mensio Valves (version 5.1, 3mensio Medical Imaging BV, the Netherlands)	Manual measurement using dedicated workstation (EBW, Philips Healthcare)	105 patients	Average bias: mean annulus diameter: 1.15 mm, left coronary ostium height: 1.61 mm, right coronary ostium height: 3.45 mm	ICC: 0.93 to 0.98	ICC: 0.94 to 0.98
Delgado et al. [78]	2011	3mensio Valves (version 4.1.sp1, Medical Imaging BV, Bilthoven, The Netherlands)	Manual measurement using Vitrea2 software (Vital Images, Minneapolis, MN)	90 patients	ICC of annulus diameter, LVOT diameter, sinus of Valsalva height, coronary ostium height: 0.97 to 0.99	ICC: 0.90 to 0.99	ICC: 0.95 to 0.99
Lalys et al. [75]	2019	Hybrid approach: model- -based method, active contour model, atlas-based registration, learning-based detection	Manual measurement (software: NA)	50 patients	Detection bias of aortic leaflets 1.96 ± 0.84 mm, 2.34 ± 0.78 mm and 1.23 ± 1.12 mm (right, left and non-coronary ostia) Measurement bias: annulus diameter: 1.31 ± 0.75 mm, coronary ostia heights 1.96 ± 0.87 mm (right), 1.80 ± 0.74 mm (left)	NA	NA
Al et al. [76]	2018	Colonial walk	Manual measurement (software: NA)	71 patients	Mean detection bias of hinge points, commissure points and coronary ostia: 2.09 ± 1.20 mm Measurement bias: aortic annulus diameter: 0.94 ± 0.83 mm, annulus to ostia distance: 0.98 ± 0.90 mm	NA	NA
Elattar et al. [73]	2016	3D normalized cut and intensity map	Manual measurement (software: NA)	40 CTA images	landmark segmentation bias: 2.38 ± 1.56 mm Measurement: ICC of annulus radius: 0.84, annulus to ostia distance: 0.73	NA	NA
Elattar et al. [74]	2014	3D normalized cut method	Manual delineation	20 patients	Dice coefficient of aortic root segmentation: 0.95 ± 0.03	Dice coefficient: 0.951 ± 0.03	NA
Zheng et al. [72]	2012	Marginal space learning and optimization-cased method	Manual measurement (software: NA)	319 C-arm CT volume images	Segmentation bias: aortic hinges 2.09 ± ± 1.18 mm, coronary ostia 2.07 ± 1.53 mm, aortic commissure: 2.17 ± 1.88 mm Measurement bias: distance from annulus plane to coronary ostia 2.10 ± 1.86 mm (left), 2.51 ± 2.03 mm (right)	NA	NA

Not all results are listed in the table; 3D — three-dimensional; CTA — cardiac magnetic resonance; CT — computed tomography; ICC — interclass correlation coefficient; LVOT — left ventricular outflow tract; NA — not available

compare angiography and MSCT (using 3mensio) in predicting the annulus plane and choosing the C-arm position [71]. The study included 35 patients in an angiography cohort and 36 patients in an MDCT cohort. The utilization of MDCT was associated with a significant reduction of prosthesis implanting time, radiation exposure and contrast delivery. A reduction of postoperative complications and 30-day mortality was observed in patients in the MDCT cohort.

AI-assisted interpretation of CMR

Cardiac magnetic resonance is the second-line technique in the assessment of VHDs. A standard CMR scan takes about an hour followed by tedious image processing which is both time and labor consuming. However, it is the golden standard in the assessment of cardiac morphology, volume and function due to its high spatial resolution [82]. MR cine imaging and phase-contrast velocity imaging are gaining increasing importance in studying valvular function. Particularly, CMR have advantages over other imaging tools in the quantification of regurgitation when the regurgitant jet is highly eccentric.

Automated cardiac chamber segmentation and cardiac volume measurement have been widely studied in MR images as reviewed by Bernard et al. [83] and Petitjean et al. [84]. Several large CMR image datasets (Sunnybrook, STACOM, MICCAI RV and kaggle), which are free to access, have been released in the last decade in conjunction with international challenges to automatically segment left ventricle, right ventricle, end-diastolic volume and end-systolic volume [83]. Commercial software such as SuiteHEART® (Neosoft, Pewaukee, Wisconsin, USA) which allows automated quantification of biventricular volumes and function is now available [85]. The regurgitant volume and fraction in isolated aortic or mitral regurgitation can be calculated from left ventricle and right ventricle stroke volume [82], however, to date, the aforementioned automated methods have not applied in quantification of valve regurgitation. AI-assisted CMR which allows automated diagnosis of VHDs is underexplored. However, several pioneering studies have achieved many valuable results. Fries et al. [86] developed a novel supervised deep learning model for aortic valve malformation classification using unlabeled MR images. 570 patients were classified as bicuspid aortic valve from a cohort of 9230 patients from the UK biobank. These individuals showed a significant lower major adverse cardiac event-free survival rate compared to individuals with a normal aortic valve.

Risk factor identification and in-hospital mortality prediction of cardiac surgery

Preoperative assessment of surgical risk is an important procedure in cardiac surgery which guides the selection of surgery, intervention or nonsurgical treatment. Great progress has been made in risk factor identification and mortality prediction. Risk score models including EuroSCORE, STS score and ACEF scores have been widely used [87]. The linear regression model is the most widely used in analyzing a correlation between risk variables and cardiac adverse events. However, there is a growing trend of utilizing machine learning methods in developing prediction models which outperform traditional scoring systems.

Nilsson et al. [88] were among the first to use an ANN model to identify risk factors and predict mortality in cardiac surgery. 72 risk factors were evaluated from 18,362 patients, 34 of the factors were identified as relevant to mortality. Receiver operating characteristic (ROC) area of the ANN model for mortality prediction was significantly larger than logistic EuroSCORE model (0.81 vs. 0.79). For isolated valve surgery (with or without coronary artery bypass grafting), the ROC area of the ANN model was 0.76 vs. 0.72 of the logistic models. Celi et al. [89] achieved an even larger ROC area using ANN, Bayesian network and logistic regression (0.941, 0.931, 0.854) compared to EuroSCORE (0.648). Allyn et al. [90] utilized a novel ensemble machine learning method which integrates the results from four isolated machine learning algorithms to predict cardiac surgery mortality. 6250 patients were enrolled in the study, Chi-square filtering was utilized to extract relevant variables. Results showed that the ensemble machine learning model had a significantly stronger discriminatory power for operative mortality than EuroSCORE II (ROC area: 0.795 vs. 0.737). Recently, Hernandez-Suarez firstly applied four machine learning algorithms in mortality prediction after TAVI [91]. 10,883 patients were enrolled in the study. Logistic regression, ANN, Naïve bayes and random forest which are the four top supervised learning algorithms all showed good discriminative performance. The best prediction model obtained by logistic algorithm (ROC area: 0.92) have close discriminative power with state-of-the-art National Inpatient Sample TAVR score model.

Moreover, ANN and machine learning algorithm have been applied in other fields such as prediction of length of stay in intensive care unit after cardiac surgery [92], post-operative complications [93], both short-term and long-term mortality after heart transplantation [94]. However, the downside of current studies is that few studies have been dedicated to isolated cardiac surgery procedures which is partially due to a lack of sufficient samples to feed machine training.

Intelligent cardiac operating room: Towards autonomous robotic surgery

The introduction of minimally invasive strategies and a surgical robot in cardiac surgery promises quicker recovery and less postoperative complications and mortality. While having many superiorities over human hands such as tremor resistance and scalable motion, current robotic systems are merely teleoperated devices under human control which entirely possess no autonomy. Since automation has gained great success in other robotic fields which have increased safety, accuracy and efficiency, it is reasonable to assume that the same benefit will be gained by developing autonomous surgical robots. To achieve the level of fully "autonomous", the surgical robot should possess the ability to "see", "think" and "act". "see" refers to perception of the surgical field and itself through sensors. "think" is the process of receiving information and calculating the future status that it needs to achieve in the following "act" [95]. Recently, European research council launch the Autonomous Robotic Surgery (ARS) project aiming to developing a unified framework for the autonomous execution of robotic tasks [96]. Main research objectives include establishment of global action model by analyzing current robotic surgical data, patient specific intervention models, design of controllers, perception of overall surgical situations, and assessment of the surgical robot capability.

Though at an experimental stage, the feasibility of autonomous robots performing simple surgical tasks like suture and knot typing have been demonstrated. Penesar et al. [97] developed a novel Smart Tissue Autonomous Robot (STAR) which was able to perform linear continuous suture, it successfully completed in-vivo end-to-end anastomosis of porcine small intestine with few suturing mistakes, no complications were observed in 7 day follow-up. Although the STAR system realized autonomous suture, the step of knot typing remained manual. In the context of endoscopic surgery or robot-assisted surgery, the task of knot typing is cumbersome which requires manipulation of many subtle movements in a confined space [98]. Through training a recurrent neural network on 3D loop trajectories generated by human surgeon, the Endoscopic Partial-Autonomous Robot (EndoPAR) was able to accurately perform the winding portion of a knot-tying task [99]. To date however, robots are unable to fully perform autonomous knot tying.

Transcatheter therapy has been accepted as an alternative to traditional cardiac valvular surgery especially in patients with high surgical risk in recent years. Catheters are inserted either from peripheral vessel or the cardiac apex to deploy valve prothesis or occlusion device. In either case, the catheters need to be precisely navigated to the intervention site which is a very challenging task in a beating heart. Inspired by wall following, which is used by thigmotactic animals to locate and navigate themselves in low-visibility environments, Fagogenis et al. [100] developed an autonomous intracardiac catheter navigation system. With hybrid imaging and touch sensor installed on the catheter tip, which can provide clear images of what it has touched and identify it as blood, valve or myocardium. The catheter created continuous low-force contact with the surrounding tissue and followed the cardiac wall to achieve autonomous navigation. With the navigation system, authors designed a robotic catheter, inserted from the cardiac apex, which can autonomously navigate to the aortic valve and deploy an occlusion device into the leak site on a porcine model. The in-vivo animal experiments demonstrate that an autonomous robot catheter was non-inferior to human experts [100].

Conclusions

Artificial intelligence is changing the landscape of healthcare. The inclusion of AI and automated algorithms in medical image analysis are very promising for they require less measurement time and meanwhile provide more accurate and reproducible results, which make them ideal helpers in a busy clinical flow. Machine learning methods can make full use of patient data and build more powerful prediction models of cardiac surgery compared to traditional statistical approaches. Moreover, the autonomous surgical robot, although in its infancy, holds great promise for improved safety and efficiency in cardiac surgery

and intervention. In general, AI has enhanced the ability of diagnosis and clinical decision-making in VHDs and taken another step towards precision in medicine.

Conflict of interest: None declared

References

1. Topol EJ. High-performance medicine: the convergence of human and artificial intelligence. Nat Med. 2019; 25(1): 44–56, doi: 10.1038/s41591-018-0300-7, indexed in Pubmed: 30617339.
2. Zhang J, Gajjala S, Agrawal P, et al. Fully automated echocardiogram interpretation in clinical practice. Circulation. 2018; 138(16): 1623–1635, doi: 10.1161/CIRCULATIONAHA.118.034338, indexed in Pubmed: 30354459.
3. Benjamin EJ, Muntner P, Alonso A, et al. Heart Disease and Stroke Statistics — 2019 Update: A Report From the American Heart Association. Vol. 139, Circulation. 2019.
4. Schwartz WB, Patil RS, Szolovits P. Artificial intelligence in medicine. Where do we stand? N Engl J Med. 1987; 316(11): 685–688, doi: 10.1056/NEJM198703123161109, indexed in Pubmed: 3821801.
5. Shortliffe EHA. rule-based comuter rogram for advising hysicians regarding antimicrobial theray selection. In: Proceedings of the Annual ACM Conference. ACM. 1974; 739.
6. Szolovits P, Pauker SG. Categorical and probabilistic reasoning in medical diagnosis. Artif Intell [Internet]. 1978 Aug 1; 11(1–2):115–44. https://www.sciencedirect.com/science/article/abs/pii/0004370278900140 (cited 2019 Aug 20).
7. Beam AL, Kohane IS. Big data and machine learning in health care. JAMA. 2018; 319(13): 1317–1318, doi: 10.1001/jama.2017.18391, indexed in Pubmed: 29532063.
8. Ton J. Cleophas AHZ. Machine Learning in Medicine. 2013;1920–30. https://link.springer.com/content/pdf/10.1007%2F978-94-007-5824-7.pdf.
9. LeCun Y, Bengio Y, Hinton G. Deep learning. Nature. 2015; 521(7553): 436–444, doi: 10.1038/nature14539, indexed in Pubmed: 26017442.
10. Ernande L, Audureau E, Jellis CL, et al. Clinical implications of echocardiographic phenotypes of patients with diabetes mellitus. J Am Coll Cardiol. 2017; 70(14): 1704–1716, doi: 10.1016/j.jacc.2017.07.792, indexed in Pubmed: 28958326.
11. Zhao Y, Zeng D, Socinski MA, et al. Reinforcement learning strategies for clinical trials in nonsmall cell lung cancer. Biometrics. 2011; 67(4): 1422–1433, doi: 10.1111/j.1541-0420.2011.01572.x, indexed in Pubmed: 21385164.
12. Hinton GE, Osindero S, Teh YW. A fast learning algorithm for deep belief nets. Neural Comput. 2006; 18(7): 1527–1554, doi: 10.1162/neco.2006.18.7.1527, indexed in Pubmed: 16764513.
13. Chen C. Computer vision in medical imaging. Vol. 2. World Scientific. 2014.
14. Puppe F. Systematic introduction to expert systems: Knowledge representations and problem-solving methods. Springer Science & Business Media. 2012.
15. Tavel ME. Cardiac auscultation. A glorious past -- but does it have a future? Circulation. 1996; 93(6): 1250–1253, doi: 10.1161/01.cir.93.6.1250, indexed in Pubmed: 8653848.
16. Wang A, Bashore TM. Valvular Heart Disease. 2009.
17. Thompson WR, Reinisch AJ, Unterberger MJ, et al. Artificial intelligence-assisted auscultation of heart murmurs: validation by virtual clinical trial. Pediatr Cardiol. 2019; 40(3): 623–629, doi: 10.1007/s00246-018-2036-z, indexed in Pubmed: 30542919.
18. Dwivedi AK, Imtiaz SA, Rodriguez-Villegas E. Algorithms for automatic analysis and classification of heart sounds-A systematic review. IEEE Access. 2019; 7(c): 8316–45.
19. Lehner RJ, Rangayyan RM. A three-channel microcomputer system for segmentation and characterization of the phonocardiogram. IEEE Trans Biomed Eng. 1987; 34(6): 485–489, doi: 10.1109/tbme.1987.326060, indexed in Pubmed: 3610198.
20. Iwata A, Ishii N, Suzumura N, et al. Algorithm for detecting the first and the second heart sounds by spectral tracking. Med Biol Eng Comput. 1980; 18(1): 19–26, doi: 10.1007/BF02442475, indexed in Pubmed: 6991835.
21. Liang H, Lukkarinen S, Hartimo I. Heart sound segmentation algorithm based on heart sound envelogram. 1997; 24: 105–108.
22. Johnson CR, Sethares WA, Klein AG. Software Receiver Design: Build Your Own Digital Communication System in Five Easy Steps. 2011.
23. Jiang Z, Choi SA. cardiac sound characteristic waveform method for in-home heart disorder monitoring with electric stethoscope. Expert Syst Appl. 2006; 31(2): 286–98.
24. Sun S. An innovative intelligent system based on automatic diagnostic feature extraction for diagnosing heart diseases. Knowledge-Based Syst. 2015; 75: 224–238, doi: 10.1016/j.knosys.2014.12.001.
25. Sun S, Jiang Z, Wang H, et al. Automatic moment segmentation and peak detection analysis of heart sound pattern via short-time modified Hilbert transform. Comput Methods Programs Biomed. 2014; 114(3): 219–230, doi: 10.1016/j.cmpb.2014.02.004, indexed in Pubmed: 24657095.
26. Gill D, Gavrieli N, Intrator N. Detection and identification of heart sounds using homomorphic envelogram and self-organizing probabilistic model. Comput Cardiol. 2005; 32: 957–60.
27. Springer DB, Tarassenko L, Clifford GD. Logistic Regression-HSMM-Based Heart Sound Segmentation. IEEE Trans Biomed Eng. 2016; 63(4): 822–832, doi: 10.1109/TBME.2015.2475278, indexed in Pubmed: 26340769.
28. Schmidt SE, Holst-Hansen C, Graff C, et al. Segmentation of heart sound recordings by a duration-dependent hidden Markov model. Physiol Meas. 2010; 31(4): 513–529, doi: 10.1088/0967-3334/31/4/004, indexed in Pubmed: 20208091.
29. Potes C, Parvaneh S, Rahman A, et al. Ensemble of feature-based and deep learning-based classifiers for detection of abnormal heart sounds. Comput Cardiol. 2016; 43: 621–624.
30. Chen TE, Yang SI, Ho LT, et al. S1 and S2 Heart Sound Recognition Using Deep Neural Networks. IEEE Trans Biomed Eng. 2017; 64(2): 372–380, doi: 10.1109/TBME.2016.2559800, indexed in Pubmed: 28113191.
31. Zhang W, Han J, Deng S. Heart sound classification based on scaled spectrogram and tensor decomposition. Expert Syst Appl. 2017; 84: 220–231.
32. Khalid S, Khalil T, Nasreen SA. survey of feature selection and feature extraction techniques in machine learning. Proc 2014 Sci Inf Conf SAI. 2014; 2014: 372–378.
33. Zhang W, Guo X, Yuan Z, et al. Heart sound classification and recognition based on eemd and correlation dimension. J Mech Med Biol. 2014; 14(04): 1450046.

34. Safara F, Doraisamy S, Azman A, et al. Multi-level basis selection of wavelet packet decomposition tree for heart sound classification. Comput Biol Med. 2013; 43(10): 1407–1414, doi: 10.1016/j.compbiomed.2013.06.016, indexed in Pubmed: 24034732.
35. Kwak C. Kwon O-W. Cardiac disorder classification by heart sound signals using murmur likelihood and hidden Markov model state likelihood. IET Signal Process. 2012; 6(4): 326.
36. Kumar D, Carvalho P, Antunes M, et al. Heart murmur classification with feature selection. Conf Proc IEEE Eng Med Biol Soc. 2010; 2010: 4566–4569, doi: 10.1109/IEMBS.2010.5625940, indexed in Pubmed: 21095796.
37. Uğuz H. A biomedical system based on artificial neural network and principal component analysis for diagnosis of the heart valve diseases. J Med Syst. 2012; 36(1): 61–72, doi: 10.1007/s10916-010-9446-7, indexed in Pubmed: 20703748.
38. Olmez T, Zumray D. Classification of heart sounds using an artificial neural network. Pattern Recognit Lett. 2003; 24: 617–629.
39. Fahad HM, Ghani Khan MU, Saba T, et al. Microscopic abnormality classification of cardiac murmurs using ANFIS and HMM. Microsc Res Tech. 2018; 81(5): 449–457, doi: 10.1002/jemt.22998, indexed in Pubmed: 29363219.
40. Falk V, Baumgartner H, Bax JJ, et al. ESC/EACTS Guidelines for the management of valvular heart disease. Eur J Cardio-thoracic Surg. 2017; 52: 616–664.
41. Noble JA, Boukerroui D. Ultrasound image segmentation: a survey. IEEE Trans Med Imaging. 2006; 25(8): 987–1010, doi: 10.1109/tmi.2006.877092, indexed in Pubmed: 16894993.
42. Mikić I, Krucinski S, Thomas JD. Segmentation and tracking in echocardiographic sequences: active contours guided by optical flow estimates. IEEE Trans Med Imaging. 1998; 17(2): 274–284, doi: 10.1109/42.700739, indexed in Pubmed: 9688159.
43. Martin S, Daanen V, Troccaz J, et al. Tracking of the mitral valve leaflet in echocardiography images. 3rd IEEE Int Symp Biomed Imaging Nano to Macro. 2006; 2006: 181–184.
44. Schneider RJ, Perrin DP, Vasilyev NV, et al. Mitral annulus segmentation from 3D ultrasound using graph cuts. IEEE Trans Med Imaging. 2010; 29(9): 1676–1687, doi: 10.1109/TMI.2010.2050595, indexed in Pubmed: 20562042.
45. Zhou X, Yang C, Yu W. Automatic mitral leaflet tracking in echocardiography by outlier detection in the low-rank representation. Proc IEEE Comput Soc Conf Comput Vis Pattern Recognit. 2012: 972–979.
46. Liu X, Cheung Y, Ming Y, et al. Automatic mitral valve leaflet tracking in Echocardiography via constrained outlier pursuit and region-scalable active contours. Neurocomputing. 2014; 144: 47–57, doi: 10.1016/j.neucom.2014.02.063.
47. Siefert AW, Icenogle DA, Rabbah JPM, et al. Accuracy of a mitral valve segmentation method using J-splines for real-time 3D echocardiography data. Ann Biomed Eng. 2013; 41(6): 1258––1268, doi: 10.1007/s10439-013-0784-8, indexed in Pubmed: 23460042.
48. Pouch AM, Wang H, Takabe M, et al. Fully automatic segmentation of the mitral leaflets in 3D transesophageal echocardiographic images using multi-atlas joint label fusion and deformable medial modeling. Med Image Anal. 2014; 18(1): 118–129, doi: 10.1016/j.media.2013.10.001, indexed in Pubmed: 24184435.
49. Ionasec RI, Voigt I, Georgescu B, et al. Patient-specific modeling and quantification of the aortic and mitral valves from 4-D cardiac CT and TEE. IEEE Trans Med Imaging. 2010; 29(9): 1636–1651, doi: 10.1109/TMI.2010.2048756, indexed in Pubmed: 20442044.
50. Costa E, Martins N, Sultan MS, et al. Mitral valve leaflets segmentation in echocardiography using convolutional neural networks. 6th IEEE Port Meet Bioeng ENBENG 2019 Proc. 2019: 1–4.
51. Shang Y, Yang X, Zhu L, et al. Region competition based active contour for medical object extraction. Comput Med Imaging Graph. 2008; 32(2): 109–117, doi: 10.1016/j.compmedimag.2007.10.004, indexed in Pubmed: 18083344.
52. Sultan MS, Martins N, Costa E, et al. Virtual M-Mode for Echocardiography: A New Approach for the Segmentation of the Anterior Mitral Leaflet. IEEE J Biomed Health Inform. 2019; 23(1): 305–313, doi: 10.1109/JBHI.2018.2799738, indexed in Pubmed: 29994568.
53. Thavendiranathan P, Phelan D, Thomas JD, et al. Quantitative assessment of mitral regurgitation: validation of new methods. J Am Coll Cardiol. 2012; 60(16): 1470–1483, doi: 10.1016/j.jacc.2012.05.048, indexed in Pubmed: 23058312.
54. de Agustín JA, Marcos-Alberca P, Fernandez-Golfin C, et al. Direct measurement of proximal isovelocity surface area by single-beat three-dimensional color Doppler echocardiography in mitral regurgitation: a validation study. J Am Soc Echocardiogr. 2012; 25(8): 815–823, doi: 10.1016/j.echo.2012.05.021, indexed in Pubmed: 22739217.
55. Grady L, Datta S, Kutter O, et al. Regurgitation Quantification Using 3D PISA in Volume Echocardiograhy. In: Fichtinger G, editors. pMedical Image Comuting and Comuter-AssisteIntervention -- MICCAI 2011. Berlin, Heidelberg: Sringer Berlin Heidelberg. 2011: 512–519.
56. Cobey FC, McInnis JA, Gelfand BJ, et al. A method for automating 3-dimensional proximal isovelocity surface area measurement. J Cardiothorac Vasc Anesth. 2012; 26(3): 507–511, doi: 10.1053/j.jvca.2011.12.018, indexed in Pubmed: 22325633.
57. Wang Y, Georgescu B, Datta S, et al. Automatic cardiac flow quantification on 3D volume color Doppler data. Proc - Int Symp Biomed Imaging. 2011; C(Lv): 1688–1691.
58. Mediratta A, Addetia K, Medvedofsky D, et al. 3D echocardiographic analysis of aortic annulus for transcatheter aortic valve replacement using novel aortic valve quantification software: Comparison with computed tomography. Echocardiography. 2017; 34(5): 690–699, doi: 10.1111/echo.13483, indexed in Pubmed: 28345211.
59. Aquila I, Fernández-Golfín C, Rincon LM, et al. Fully automated software for mitral annulus evaluation in chronic mitral regurgitation by 3-dimensional transesophageal echocardiography. Medicine (Baltimore). 2016; 95(49): e5387, doi: 10.1097/MD.0000000000005387, indexed in Pubmed: 27930514.
60. Kagiyama N, Toki M, Hara M, et al. Efficacy and Accuracy of Novel Automated Mitral Valve Quantification: Three-Dimensional Transesophageal Echocardiographic Study. Echocardiography. 2016; 33(5): 756–763, doi: 10.1111/echo.13135, indexed in Pubmed: 26661528.
61. Calleja A, Thavendiranathan P, Ionasec RI, et al. Automated quantitative 3-dimensional modeling of the aortic valve and root by 3-dimensional transesophageal echocardiography in normals, aortic regurgitation, and aortic stenosis: comparison to computed tomography in normals and clinical implications. Circ Cardiovasc Imaging. 2013; 6(1): 99–108, doi: 10.1161/CIRCIMAGING.112.976993, indexed in Pubmed: 23233743.
62. de Agustin JA, Viliani D, Vieira C, et al. Proximal isovelocity surface area by single-beat three-dimensional color Doppler echo-

cardiography applied for tricuspid regurgitation quantification. J Am Soc Echocardiogr. 2013; 26(9): 1063–1072, doi: 10.1016/j.echo.2013.06.006, indexed in Pubmed: 23860094.

63. Choi J, Hong GR, Kim M, et al. Automatic quantification of aortic regurgitation using 3D full volume color doppler echocardiography: a validation study with cardiac magnetic resonance imaging. Int J Cardiovasc Imaging. 2015; 31(7): 1379–1389, doi: 10.1007/s10554-015-0707-x, indexed in Pubmed: 26164059.
64. Thavendiranathan P, Liu S, Datta S, et al. Quantification of chronic functional mitral regurgitation by automated 3-dimensional peak and integrated proximal isovelocity surface area and stroke volume techniques using real-time 3-dimensional volume color doppler echocardiography: In vitro and clini. Circ Cardiovasc Imaging. 2013; 6(1): 125–133.
65. Ionasec RI, Georgescu B, Gassner E, et al. Dynamic Model-Driven Quantitative and Visual Evaluation of the Aortic Valve from 4D CT. In: Metaxas D, editors. Medical Image Comuting and Comuter-Assisted Intervention. MICCAI 2008. Berlin, Heidelberg: Sringer Berlin Heidelberg. 2008: 686–694.
66. Swee JKY, Grbić S. Advanced transcatheter aortic valve implantation (TAVI) planning from CT with ShapeForest. Lect Notes Comput Sci. (including Subser Lect Notes Artif Intell Lect Notes Bioinformatics). 2014; 8674 LNCS(Part 2): 17–24.
67. Waechter I, Kneser R, Korosoglou G, et al. Patient Secific Models for Planning and Guidance of Minimally Invasive Aortic Valve Imlantation. In: Jiang T, Navab N, Pluim JPW, Viergever MA, editors. Medical Image Comuting and Comuter-Assisted Intervention -- MICCAI 2010. Sringer Berlin Heidelberg. 2010: 526–533.
68. Grbic S, Ionasec R, Vitanovski D, et al. Complete valvular heart apparatus model from 4D cardiac CT. Med Image Anal. 2012; 16(5): 1003–1014.
69. Grbic S, Ionasec R, Mansi T, et al. Advanced intervention planning for Transcatheter Aortic Valve Implantations (TAVI) from CT using volumetric models. Proc Int Symp Biomed Imaging. 2013: 1424–1427.
70. Koos R, Mahnken AH, Dohmen G, et al. Association of aortic valve calcification severity with the degree of aortic regurgitation after transcatheter aortic valve implantation. Int J Cardiol. 2011; 150(2): 142–145.
71. Samim M, Stella PR, Agostoni P, et al. Automated 3D analysis of pre-procedural MDCT to predict annulus plane angulation and C-arm positioning: benefit on procedural outcome in patients referred for TAVR. JACC Cardiovasc Imaging. 2013; 6(2): 238–248, doi: 10.1016/j.jcmg.2012.12.004, indexed in Pubmed: 23489538.
72. Zheng Y, John M, Liao R, et al. Automatic aorta segmentation and valve landmark detection in C-arm CT for transcatheter aortic valve implantation. IEEE Trans Med Imaging. 2012; 31(12): 2307–2321, doi: 10.1109/TMI.2012.2216541, indexed in Pubmed: 22955891.
73. Elattar M, Wiegerinck E, van Kesteren F, et al. Automatic aortic root landmark detection in CTA images for preprocedural planning of transcatheter aortic valve implantation. Int J Cardiovasc Imaging. 2016; 32(3): 501–511, doi: 10.1007/s10554-015-0793-9, indexed in Pubmed: 26498339.
74. Elattar MA, Wiegerinck EM, Planken RN, et al. Automatic segmentation of the aortic root in CT angiography of candidate patients for transcatheter aortic valve implantation. Med Biol Eng Comput. 2014; 52(7): 611–618, doi: 10.1007/s11517-014-1165-7, indexed in Pubmed: 24903606.
75. Lalys F, Esneault S, Castro M, et al. Automatic aortic root segmentation and anatomical landmarks detection for TAVI procedure planning. Minim Invasive Ther Allied Technol. 2019; 28(3): 157–164, doi: 10.1080/13645706.2018.1488734, indexed in Pubmed: 30039720.
76. Al WA, Jung HoY, Yun IlD, et al. Automatic aortic valve landmark localization in coronary CT angiography using colonial walk. PLoS One. 2018; 13(7): e0200317, doi: 10.1371/journal.pone.0200317, indexed in Pubmed: 30044802.
77. Watanabe Y, Morice MC, Bouvier E, et al. Automated 3-dimensional aortic annular assessment by multidetector computed tomography in transcatheter aortic valve implantation. JACC Cardiovasc Interv. 2013; 6(9): 955–964, doi: 10.1016/j.jcin.2013.05.008, indexed in Pubmed: 23954060.
78. Delgado V, Ng ACT, Schuijf JD, et al. Automated assessment of the aortic root dimensions with multidetector row computed tomography. Ann Thorac Surg. 2011; 91(3): 716–723, doi: 10.1016/j.athoracsur.2010.09.060, indexed in Pubmed: 21352985.
79. Dankerl P, Hammon M, Seuss H, et al. Computer-aided evaluation of low-dose and low-contrast agent third-generation dual-source CT angiography prior to transcatheter aortic valve implantation (TAVI). Int J Comput Assist Radiol Surg. 2017; 12(5): 795–802, doi: 10.1007/s11548-016-1470-8, indexed in Pubmed: 27604759.
80. Guez D, Boroumand G, Ruggiero NJ, et al. Automated and Manual Measurements of the Aortic Annulus with ECG-Gated Cardiac CT Angiography Prior to Transcatheter Aortic Valve Replacement: Comparison with 3D-Transesophageal Echocardiography. Acad Radiol. 2017; 24(5): 587–593, doi: 10.1016/j.acra.2016.12.008, indexed in Pubmed: 28130049.
81. Baeßler B, Mauri V, Bunck AC, et al. Software-automated multidetector computed tomography-based prosthesis-sizing in transcatheter aortic valve replacement: Inter-vendor comparison and relation to patient outcome. Int J Cardiol. 2018; 272: 267–272, doi: 10.1016/j.ijcard.2018.07.008, indexed in Pubmed: 30017520.
82. Pennell DJ Cardiovascular magnetic resonance Circulation. 2010; 121(5): 692–705.
83. Bernard O, Cervenansky F, Lalande A, et al. Deep learning techniques for automatic MRI cardiac multi-structures segmentation and diagnosis: is the problem solved? IEEE Trans Med Imaging. 2018; 37(11): 2514–2525, doi: 10.1109/TMI.2018.2837502, indexed in Pubmed: 29994302.
84. Petitjean C, Dacher JN. A review of segmentation methods in short axis cardiac MR images. Med Image Anal. 2011; 15(2): 169–184, doi: 10.1016/j.media.2010.12.004, indexed in Pubmed: 21216179.
85. Backhaus SJ, Staab W, Steinmetz M, et al. Fully automated quantification of biventricular volumes and function in cardiovascular magnetic resonance: applicability to clinical routine settings. J Cardiovasc Magn Reson. 2019; 21(1): 24, doi: 10.1186/s12968-019-0532-9, indexed in Pubmed: 31023305.
86. Fries JA, Varma P, Chen VS, et al. Weakly supervised classification of rare aortic valve malformations using unlabeled cardiac MRI sequences. bioRxiv. 2018; 2019: 1–25, doi: 10.1038/s41467-019-11012-3.
87. Nashef SAM, Roques F, Sharples LD, et al. EuroSCORE II. Eur J Cardiothorac Surg. 2012; 41(4): 734–44; discussion 744, doi: 10.1093/ejcts/ezs043, indexed in Pubmed: 22378855.
88. Nilsson J, Ohlsson M, Thulin L, et al. Risk factor identification and mortality prediction in cardiac surgery using artificial neural networks. J Thorac Cardiovasc Surg. 2006; 132(1): 12–19, doi: 10.1016/j.jtcvs.2005.12.055, indexed in Pubmed: 16798296.

89. Celi LA, Galvin S, Davidzon G, et al. A database-driven decision support system: customized mortality prediction. J Pers Med. 2012; 2(4): 138–148, doi: 10.3390/jpm2040138, indexed in Pubmed: 23766893.
90. Allyn J, Allou N, Augustin P, et al. A Comparison of a Machine Learning Model with EuroSCORE II in Predicting Mortality after Elective Cardiac Surgery: A Decision Curve Analysis. PLoS One. 2017; 12(1): e0169772, doi: 10.1371/journal.pone.0169772, indexed in Pubmed: 28060903.
91. Hernandez-Suarez DF, Kim Y, Villablanca P, et al. Machine Learning Prediction Models for In-Hospital Mortality After Transcatheter Aortic Valve Replacement. JACC Cardiovasc Interv. 2019; 12(14): 1328–1338, doi: 10.1016/j.jcin.2019.06.013, indexed in Pubmed: 31320027.
92. LaFaro RJ, Pothula S, Kubal KP, et al. Neural Network Prediction of ICU Length of Stay Following Cardiac Surgery Based on Pre-Incision Variables. PLoS One. 2015; 10(12): e0145395, doi: 10.1371/journal.pone.0145395, indexed in Pubmed: 26710254.
93. Thottakkara P, Ozrazgat-Baslanti T, Hupf BB, et al. Application of Machine Learning Techniques to High-Dimensional Clinical Data to Forecast Postoperative Complications. PLoS One. 2016; 11(5): e0155705, doi: 10.1371/journal.pone.0155705, indexed in Pubmed: 27232332.
94. Nilsson J, Ohlsson M, Höglund P, et al. The International Heart Transplant Survival Algorithm (IHTSA): a new model to improve organ sharing and survival. PLoS One. 2015; 10(3): e0118644, doi: 10.1371/journal.pone.0118644, indexed in Pubmed: 25760647.
95. Moustris GP, Hiridis SC, Deliparaschos KM, et al. Evolution of autonomous and semi-autonomous robotic surgical systems: a review of the literature. Int J Med Robot. 2011; 7(4): 375–392, doi: 10.1002/rcs.408, indexed in Pubmed: 21815238.
96. Grespan L, Fiorini P, Colucci G. Looking Ahead: The Future of Robotic Surgery. In: The Route to Patient Safety in Robotic Surgery [Internet]. Cham: Springer International Publishing. 2019: 157–162, doi: 10.1007/978-3-030-03020-9_13.
97. Panesar S, Cagle Y, Chander D, et al. Artificial Intelligence and the Future of Surgical Robotics. Ann Surg. 2019; 270(2): 223––226, doi: 10.1097/SLA.0000000000003262, indexed in Pubmed: 30907754.
98. Garcia-Ruiz A, Gagner M, Miller JH, et al. Manual vs robotically assisted laparoscopic surgery in the performance of basic manipulation and suturing tasks. Arch Surg. 1998; 133(9): 957–961, doi: 10.1001/archsurg.133.9.957, indexed in Pubmed: 9749847.
99. Mayer H, Gomez F, Wierstra D, et al. system for robotic heart surgery that learns to tie knots using recurrent neural networks. Adv Robot. 2008; 13(14): 1521–1537.
100. Fagogenis G, Mencattelli M, Machaidze Z, et al. Autonomous Robotic Intracardiac Catheter Navigation Using Haptic Vision. Sci Robot. 2019; 4(29), doi: 10.1126/scirobotics.aaw1977, indexed in Pubmed: 31414071.

VIA MEDICA

STUDY PROTOCOL

Cardiology Journal
2020, Vol. 27, No. 4, 421–424
DOI: 10.5603/CJ.a2020.0090

ISSN 1897–5593

Ion channel inhibition against COVID-19: A novel target for clinical investigation

Eliano P. Navarese[1, 2], Rita L. Musci[3], Lara Frediani[4], Paul A. Gurbel[5], Jacek Kubica[1]

[1]Department of Cardiology, Collegium Medicum, Nicolaus Copernicus University, Bydgoszcz, Poland and SIRIO MEDICINE Research Network
[2]Faculty of Medicine University of Alberta, Edmonton, Canada
[3]Department of Cardiology, Azienda Ospedaliera Bonomo, Andria, Italy
[4]Department of Cardiology, Azienda Usl Toscana Nord-Ovest Cardiologia UTIC-Ospedali Riuniti di Livorno, Italy
[5]Sinai Center for Cardiovascular Research, Sinai Hospital of Baltimore, LifeBridgehealth, Baltimore, MD, USA

Introduction

Infection with severe acute respiratory syndrome coronavirus 2 (SARS-CoV-2), also known as coronavirus disease (COVID-19), has been classified by the World Health Organization (WHO) as an ongoing pandemic. Owing to the global emergency, there is an unmet need to identify effective and scalable therapeutic options to attenuate the early stages of virus infection.

SARS-CoV-2 has different stages of the infection cycle. The first phase is characterized by infection and replication of the virus within the host cells. The last phase occurs with cytokine storm leading to cellular apoptosis [1].

We posit the rationale for ion channel inhibition as a novel therapeutic target to counteract SARS-CoV-2 infection and replication. Within this framework, we discuss the potential clinical role of the ion channel inhibitors amiodarone and verapamil against COVID-19 that deserves clinical investigations.

Mechanisms of SARS-CoV-2 entrance into the host cell

SARS-CoV-2 belongs to the family of *Coronaviridae*, which also includes severe acute respiratory syndrome coronavirus (SARS-CoV) and middle east respiratory syndrome coronavirus (MERS-CoV). SARS-CoV-2 is highly contagious and is transmitted primarily via respiratory droplets.

A critical step in the life cycle of SARS-CoV-2 cell entry is the binding of viral spike protein (S protein) subunit S1 to angiotensin converting enzyme 2 (ACE2) receptors that are expressed mainly in human alveolar cells, and protein S priming by host proteases. This process leads to fragmentation in the S1 and S2 subunit interface and catalyzes a membrane fusion reaction [2]. The S2 subunit in turn promotes the fusion of the viral envelope with the host cell membrane [2]. Transmembrane protease, serine 2 (TMPRSS2) cleaves and activates the viral spike glycoproteins, which in turn facilitates virus-cell membrane fusion.

The conformational modification of viral envelope with S protein exposure and fusion with host cell membrane constitute the initial phase of cell entry.

The spike protein therefore plays a dual role in promoting virus entry by mediating receptor binding and then membrane fusion. This phase can be termed "early-entry" of the virus infection.

In the absence of exogenous or membrane-bound proteases that enable entry within the plasma membrane surface, coronaviruses can be internalized via clathrin- and non-clathrin-mediated endocytosis [3], where the S protein is cleaved by cathepsin L, which promotes fusion of viral mate-

Address for correspondence: Prof. Eliano P. Navarese, MD, PhD, FESC, FACC, Interventional Cardiology and Cardiovascular Medicine Research, Department of Cardiology and Internal Medicine, Nicolaus Copernicus University, ul. Skodowskiej-Curie 9, 85–094 Bydgoszcz, Poland, tel: +48 52 585 4023, fax: +48 52 585 4024, e-mail: elianonavarese@gmail.com

Received: 5.06.2020 Accepted: 5.06.2020

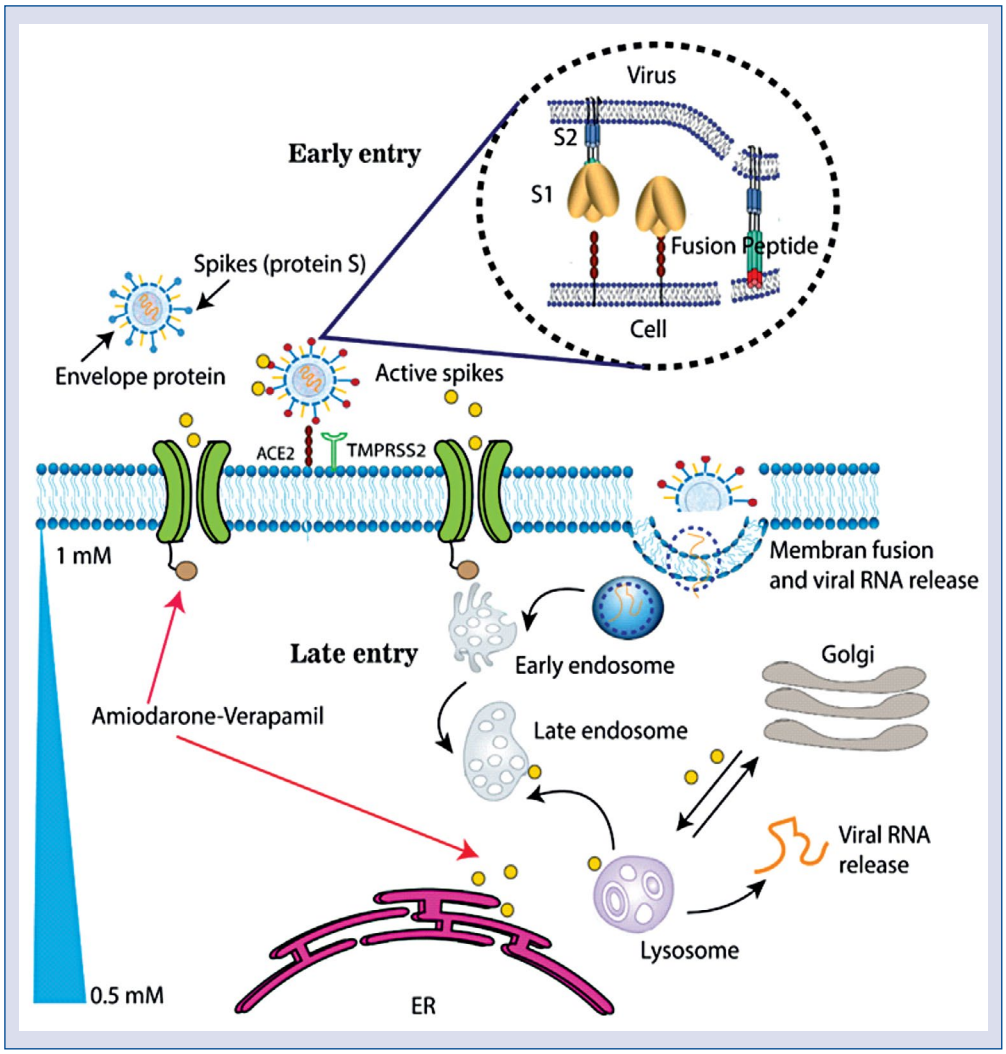

Figure 1. COVID-19 mechanisms of entry. COVID-19 entrance into the host cell takes place in two phases: "early entry" and "late entry". In the "early entry" the viral S protein-subunit S1 binds the angiotensin converting enzyme 2-receptors (ACE2-receptors) on human cells and transmembrane protease-serine 2 (TMPRSS2) facilitates virus-cell membrane fusion. The Ca^{2+} ions promote viral membrane fusion and S protein conformational changes which allow the fusion peptide insertion into the lipid bilayer. In the "late entry" COVID-19 is endocytosed and Ca^{2+} ions have an important role in endocytic vesicles maturation. This process ends with the release of the viral genome into cytoplasm and the subsequent replication of the virus. Amiodarone and verapamil block Ca^{2+} cell membrane and endosomal/ /lysosomal channels interfering with the life-cycle of coronavirus; RNA — ribonucleic acid; S protein — spike protein; S1-S2 — subunit 1 and subunit 2 of S protein; ER — endosplamic reticulum.

rial with endosomal membranes ("late entry"). The final common step is the release of the viral genome into cytoplasm and the subsequent replication of the virus.

These entry mechanisms are shared by the new SARS-CoV-2 with the other members of coronavirus family. Fusion peptides of SARS-CoV and SARS-CoV-2 have been found highly comparable sharing more than 90% homologies in their biological sequences.

Ion channels are multi-subunit, pore-forming membrane proteins that mediate the rapid and selective passage of ions across all cell membranes.

The underlying hypothesis is that SARS--CoV-2 virion entry, host-membrane fusion and the ensuing virus replication in the host cells are governed by ion currents. Within this framework, Ca^{2+} ions are necessary to promote fusion peptide insertion into the lipid bilayer and the endocytosis pathway (Fig. 1). Pharmacological agents that

target ion channels may therefore modulate virus life cycles.

Ion channel regulation of virus life cycle

Early cell entry

A role of Ca^{2+} in viral membrane entry and fusion has been reported. Proteolytic cleavage of the S protein exposes its fusion peptide and initiates membrane fusion. It has been shown that Ca^{2+} plays an active role in stimulating the fusogenic activity of the SARS-CoV fusion peptide via a Ca^{2+} binding pocket [4]. Other experiments have tested the ability of virus pseudo-particles to mediate infection of host cells without and with Ca^{2+} and have shown that intracellular Ca^{2+} enhances MERS-CoV infection by approximately two-fold [5].

Infectivity assays with pseudoparticles expressing SARS-CoV and MERS-CoV S protein demonstrated that SARS-CoV and MERS-CoV entry into host cells was reduced when intracellular Ca^{2+} was chelated [6]. SARS-CoV and MERS-CoV further promote virus entry triggering a process termed membrane ordering that induces a rearrangement of membrane lipid bilayer, enhanced in the presence of Ca^{2+} [7, 8].

Together, these observations lend support to the hypothesis that Ca^{2+} plays an active role in inducing viral membrane fusion. The spike proteins of the SARS-CoV-2 are more robust and resistant than previous members of the coronavirus family.

Ca^{2+} ions interacting with the fusion peptide can induce spatial changes in S protein altering the fusion peptide's structure, and interaction with the cell membrane, promoting infection in MERS-CoV, SARS-CoV and SARS-CoV-2 [7].

Endocytosis (endosome-maturation--late entry)

Endoplasmic reticulum (ER), reticulum-Golgi apparatus and lysosomes are vital components of the host cell machinery used by the SARS-CoV-2 [9]. Spike, envelope and membrane proteins enter the ER, and the nucleocapsid protein is combined with the (+) strand genomic ribonucleic acid (RNA) to become a nucleoprotein complex. They merge into a complete virus particle in the host endoplasmic ER-Golgi apparatus compartment. Ca^{2+} has been found to exert major modulatory roles on ER and lysosomes [10]. While extracellular Ca^{2+} is high, levels drop rapidly in the lumen of newly formed endocytic vesicles, due to the action of efflux pumps [11]. During later stages of endosome maturation, lysosome-late endosome fusion implies the release of Ca^{2+} from the lumen of endocytic organelles, which is used to mediate membrane fusion events at several stages on the endocytic pathway [12]. Such trafficking pathways can therefore lead to the availability of Ca^{2+} during the early entry of the coronavirus and afterwards during the late phase of mature endocytic vesicle formation.

Clinical utility of amiodarone and verapamil in patients with COVID-19

Amiodarone is a benzofuran derivative, an anti-arrhythmic drug commonly used in a variety of settings and is approved for the treatment of ventricular arrhythmias and atrial fibrillation. As a class III antiarrhythmic agent, amiodarone is a non-selective ion channel inhibitor that blocks Ca^{2+}, Na^{+} and K^{+} voltage-gated channels. Amiodarone binds to and then blocks Ca^{2}-channels predominantly during the inactive or resting state associated with the suppression of Ca^{2}-dependant action potentials. Verapamil is a prototypical phenylalkylamine, which exerts antihypertensive, antiarrhythmic and antianginal effects. Verapamil selectively inhibits intracellular transmembrane Ca^{2+} flow through L-type voltage-gated Ca^{2+} channels.

Previous studies have shown the effects of amiodarone on endosomal transport in SARS--CoV-infected cells by blocking Ca^{2+} channels [13]. Other *in vitro* data showed that amiodarone and verapamil, at concentrations routinely reached in human serum can, when employed clinically, act as a host cell-targeting agent that block filovirus entry [14]. These results confirmed that Ca^{2+} channel activity is required during virion entry processes [14].

Another study demonstrated that amiodarone interferes with the fusion of the Ebola viral envelope with the endosomal membrane at concentrations close to those found in patients treated for arrhythmias; an additive inhibitory effect of amiodarone and its pharmacologically active metabolite monodesethyl amiodarone on entry into target cells has been noted [15].

Clinical perspectives

Modulation of host cell ion channel activity by viral proteins is being increasingly identified as an important virus–host interaction. With this background, an ongoing randomized clinical trial (clinicaltrials.gov ID: NCT04351763), will investigate the role of amiodarone and verapamil to inhibit

ion channels in hospitalized patients with proven COVID-19. There is an urgent need to identify stable, effective and scalable therapeutic options against initial stages of virus infection and replication. Ion channel inhibition with the cardiovascular agents amiodarone and verapamil might reduce the severity of disease and the transmission potential of COVID-19.

Conflict of interest: None declared

References

1. Siddiqi HK, Mehra MR. COVID-19 illness in native and immunosuppressed states: A clinical-therapeutic staging proposal. J Heart Lung Transplant. 2020; 39(5): 405–407, doi: 10.1016/j.healun.2020.03.012, indexed in Pubmed: 32362390.
2. Hoffmann M, Kleine-Weber H, Schroeder S, et al. SARS-CoV-2 cell entry depends on ACE2 and TMPRSS2 and is blocked by a clinically proven protease inhibitor. Cell. 2020; 181(2): 271–280.e8, doi: 10.1016/j.cell.2020.02.052.
3. Inoue Y, Tanaka N, Tanaka Y, et al. Clathrin-dependent entry of severe acute respiratory syndrome coronavirus into target cells expressing ACE2 with the cytoplasmic tail deleted. J Virol. 2007; 81(16): 8722–8729, doi: 10.1128/JVI.00253-07, indexed in Pubmed: 17522231.
4. Lai AL, Millet JK, Daniel S, et al. The SARS-CoV fusion peptide forms an extended bipartite fusion platform that perturbs membrane order in a calcium-dependent manner. J Mol Biol. 2017; 429(24): 3875–3892, doi: 10.1016/j.jmb.2017.10.017, indexed in Pubmed: 29056462.
5. Straus MR, Tang T, Lai AL, et al. Ca ions promote fusion of middle east respiratory syndrome coronavirus with host cells and increase infectivity. J Virol. 2020; 94(13), doi: 10.1128/JVI.00426-20, indexed in Pubmed: 32295925.
6. Qian Z, Dominguez SR, Holmes KV. Role of the spike glycoprotein of human Middle East respiratory syndrome coronavirus (MERS-CoV) in virus entry and syncytia formation. PLoS One. 2013; 8(10): e76469, doi: 10.1371/journal.pone.0076469, indexed in Pubmed: 24098509.
7. Tang T, Bidon M, Jaimes JA, et al. Coronavirus membrane fusion mechanism offers a potential target for antiviral development. Antiviral Res. 2020; 178: 104792, doi: 10.1016/j.antiviral.2020.104792, indexed in Pubmed: 32272173.
8. Basso LGM, Vicente EF, Crusca E, et al. SARS-CoV fusion peptides induce membrane surface ordering and curvature. Sci Rep. 2016; 6: 37131, doi: 10.1038/srep37131, indexed in Pubmed: 27892522.
9. de Haan CAM, Rottier PJM. Molecular interactions in the assembly of coronaviruses. Adv Virus Res. 2005; 64: 165–230, doi: 10.1016/S0065-3527(05)64006-7, indexed in Pubmed: 16139595.
10. Raffaello A, Mammucari C, Gherardi G, et al. Calcium at the center of cell signaling: interplay between endoplasmic reticulum, mitochondria, and lysosomes. Trends Biochem Sci. 2016; 41(12): 1035–1049, doi: 10.1016/j.tibs.2016.09.001, indexed in Pubmed: 27692849.
11. Huotari J, Helenius A. Endosome maturation. EMBO J. 2011; 30(17): 3481–3500, doi: 10.1038/emboj.2011.286, indexed in Pubmed: 21878991.
12. Pryor PR, Mullock BM, Bright NA, et al. The role of intraorganellar Ca(2+) in late endosome-lysosome heterotypic fusion and in the reformation of lysosomes from hybrid organelles. J Cell Biol. 2000; 149(5): 1053–1062, doi: 10.1083/jcb.149.5.1053, indexed in Pubmed: 10831609.
13. Stadler K, Ha HR, Ciminale V, et al. Amiodarone alters late endosomes and inhibits SARS coronavirus infection at a post-endosomal level. Am J Respir Cell Mol Biol. 2008; 39(2): 142–149, doi: 10.1165/rcmb.2007-0217OC, indexed in Pubmed: 18314540.
14. Gehring G, Rohrmann K, Atenchong N, et al. The clinically approved drugs amiodarone, dronedarone and verapamil inhibit filovirus cell entry. J Antimicrob Chemother. 2014; 69(8): 2123–2131, doi: 10.1093/jac/dku091, indexed in Pubmed: 24710028.
15. Salata C, Baritussio A, Munegato D, et al. Amiodarone and metabolite MDEA inhibit Ebola virus infection by interfering with the viral entry process. Pathog Dis. 2015; 73(5), doi: 10.1093/femspd/ftv032, indexed in Pubmed: 25933611.

VIA MEDICA

Cardiology Journal
2020, Vol. 27, No. 4, 425–426
DOI: 10.5603/CJ.a2020.0098

ISSN 1897–5593

BRIEF COMMUNICATION

Impact of COVID-19 outbreak and public lockdown on ST-segment elevation myocardial infarction care in Spain

Fernando Rebollal-Leal[1], Guillermo Aldama-López[1], Xacobe Flores-Ríos[1], Pablo Piñón-Esteban[1], Jorge Salgado-Fernández[1], Ramón Calviño-Santos[1], Nicolás Vázquez-González[1], José Manuel Vázquez-Rodríguez[1, 2]

[1]Department of Cardiology, Complejo Hospitalario Universitario de A Coruña, A Coruña, Spain
[2]Instituto de Investigación Biomédica de A Coruña (INIBIC), A Coruña, Spain

Acute ST-segment elevation myocardial infarction (STEMI) is a cardiovascular disease with high morbidity and mortality. Reperfusion therapy using primary percutaneous coronary intervention (pPCI) is the most frequently recommended treatment [1, 2].

"Time is myocardium", therefore, health systems are organized as networks to minimize ischemic time by means of quick diagnosis and prompt myocardial reperfusion. Treatment delays are the simplest indexes of quality of care to monitor the STEMI network: time-to-first-medical-contact (FMC), door-to-device (DTD) time and total ischemic time (TIT) are key parameters for assessing the efficiency of the pPCI pathway [1, 2].

Coronavirus disease 2019 (COVID-19) has submitted to the healthcare systems an enormous strain in the nations where it is widespread [3], with implications for their ability to maintain operational integrity to high acuity patients [4]. To date, little is known about the influence of the disease on STEMI care systems.

Herein, it was sought to describe the impact of the COVID-19 outbreak on STEMI care at a tertiary level hospital with a 700,000-person reference population area in Coruña, a city in the Northwest of Spain. The hospital had offered 24/7 pPCI with a well-established network since 2005 [5], and was maintaining the pPCI system during the pandemic time. Patients with STEMI were included and were admitted via the Emergency Department (ED), the Emergency Medical System (EMS) and non-PCI centers undergoing pPCI during the first 6 weeks of the public lockdown period, i.e. from 15th March to 25th April 2020. These data were compared to those from STEMI patients undergoing pPCI in the same facility for the same time period for the prior 5 years. Exclusion criteria were STEMI inpatients and cardiac arrest patients. Time-to-FMC was defined as the time from patient-reported onset of chest discomfort to the time to establish first medical contact. DTD time was defined as the time between first hospital arrival to wire crossing. TIT was defined as the time from FMC to wire-crossing. Descriptive statistics were summarized as medians with interquartile ranges (IQR). The differences between groups were compared with the Mann-Whitney test. Statistical analysis was performed using STATA version 16. Ethics approval was obtained from the local committee in the study institution.

From 15th March to 25th April 2020, 26 STEMI patients underwent pPCI, while 204 patients underwent pPCI during the same period in the preceding 5 years. During the period of public lockdown, STEMI incidence rate (per 100,000 population-year) significantly decreased (50.51 to 32.19; $p < 0.0001$); time-to-FMC became longer (median, 282 min [IQR 106–465] vs. 86 min [IQR 39–174]; $p < 0.0001$); as well as TIT (median, 341 min [IQR 228–579] vs. 195 min [IQR 140–298]; $p = 0.0005$). No significant differences were found between DTD times (median, 97 min [IQR 33–128] vs. 68 min [IQR 37–106]; $p = 0.57$) (Fig. 1).

Address for correspondence: Fernando Rebollal-Leal, MD, Complejo Hospitalario Universitario A Coruña (CHUAC), Xubias de Arriba nº 84, 2ª planta, tel/fax: +34677138891, 15006 A Coruña, Spain, e-mail: rebollal_nando@yahoo.es

Received: 25.05.2020 Accepted: 26.07.2020

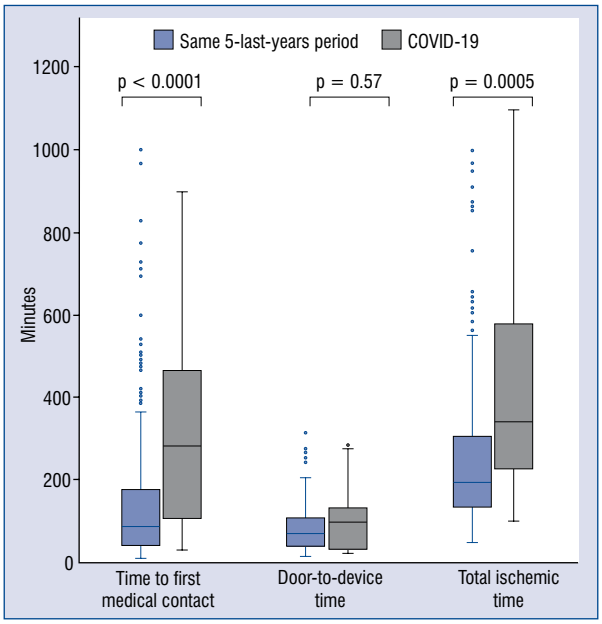

Figure 1. Boxplot comparisons of primary percutaneous coronary intervention (pPCI) pathway times. Boxplot comparisons of pPCI times between ST-segment elevation myocardial infarction (STEMI) patients during COVID-19-time and STEMI patients for the same period of time for the prior 5 years.

Patients with STEMI underwent PPCI during the COVID-19 outbreak are being subjected to longer myocardial reperfusion times. The prolongation of time-to-FMC and TIT can be explained by a patients' hesitation to initiate contact with the healthcare system because they fear a nosocomial infection; and once they decide to seek medical help, it can be delayed due to ED or EMS collapse.

The present study has several limitations. Firstly, this single-center retrospective study was performed over a short period of time, with a low number of patients in the COVID-19 arm. Likewise, it was not possible to completely rule out a temporary trend in lower STEMI incidence.

Both the current COVID-19 outbreak and the public lockdown in most nations of the world demand the development of plans from healthcare systems to mitigate the impact of this communicable pandemic diseases and to protect vulnerable patients with cardiovascular disease from both the nosocomial infection and the self-imposed refrainment from accessing healthcare.

Further investigation is needed to evaluate how COVID-19 affects cardiovascular disease and the healthcare of these patients, as well as clinical outcomes.

Conflict of interest: None declared

References

1. Ibanez B, James S, Agewall S, et al. 2017 ESC Guidelines for the management of acute myocardial infarction in patients presenting with ST-segment elevation: The Task Force for the management of acute myocardial infarction in patients presenting with ST-segment elevation of the European Society of Cardiology (ESC). Eur Heart J. 2018; 39: 119–177.
2. O'Gara P, Kushner F, Ascheim D, et al. 2013 ACCF/AHA Guideline for the Management of ST-Elevation Myocardial Infarction. Circulation. 2013; 127(4): 362–425, doi: 10.1161/cir.0b013e3182742cf6.
3. Li Q, Guan X, Wu P, et al. Early transmission dynamics in Wuhan, China, of novel coronavirus-infected pneumonia. N Engl J Med. 2020; 382(13): 1199–1207, doi: 10.1056/NEJMoa2001316, indexed in Pubmed: 31995857.
4. Dzieciatkowski T, Szarpak L, Filipiak KJ, et al. COVID-19 challenge for modern medicine. Cardiol J. 2020; 27(2): 175–183, doi: 10.5603/CJ.a2020.0055, indexed in Pubmed: 32286679.
5. Aldama G, López M, Santás M, et al. Impact on mortality after implementation of a network for ST-segment elevation myocardial infarction care. The IPHENAMIC study. Rev Esp Cardiol (Engl Ed). 2020; 73(8): 632–642, doi: 10.1016/j.rec.2019.09.031, indexed in Pubmed: 32014432.

VIA MEDICA

IMAGE IN CARDIOVASCULAR MEDICINE

Cardiology Journal
2020, Vol. 27, No. 4, 427–428
DOI: 10.5603/CJ.2020.0112

ISSN 1897–5593

"Shock-Pella": Combined management of an undilatable ostial left circumflex stenosis in a complex high-risk interventional procedure patient

Andrea Buono[1], Alfonso Ielasi[1], Giuseppe De Blasio[2], Maurizio Tespili[1]

[1]Interventional and Clinical Cardiology Unit, S. Ambrogio Cardio-Thoracic Center, Milan, Italy
[2]Cardiology Unit, IRCCS Istituto Ortopedico "Galeazzi", Milan, Italy

A 67-year-old woman with stage 4 chronic kidney disease, implantable cardioverter-defibrillator and a history of multiple coronary interventions, both percutaneous (stenting of anterior descending artery [LAD], ramus and right coronary artery [RCA]) and surgical left internal mammary artery [LIMA] graft on LAD and saphenous vein grafts [SVG] on ramus and RCA), was admitted because of congestive heart failure with evidence of severe left ventricular ejection fraction decrease (25%). Coronary angiography showed occluded LIMA and SVG to ramus, patent SVG to RCA and a critical ostial left circumflex artery (LCx) stenosis (Fig. 1A). Since myocardial perfusion scintigraphy showed no viability on anterior wall and apex (Fig. 1B), a protected LCx lesion revascularization was attempted, positioning a circulatory mechanical support (Impella CP; Abiomed, Danvers, MA). Non-compliant balloons did not fully expand during lesion predilatation, probably due to severe fibrocalcification and protruding ramus stent struts (intravascular ultrasound catheter did not cross the lesion) (Fig. 1C). Intravascular lithotripsy (IVL) was then performed (Shockwave Medical, Fremont, CA), inflating a 3.0 × 12 mm balloon (at 4–6 atm for 8 cycles of 10 pulses each) with angiographic evidence of complete device expansion (Fig. 1D) and subsequent optimal lesion predilation with non-compliant balloon (Fig. 1E). A 3.5 × 15 mm drug-eluting stent was successfully implanted (Fig. 1F). This is a case of complex, high-risk interventional procedure managed with combined strategy "Impella-assisted IVL" to prevent the risk of hemodynamic compromise in a time-demanding procedure where an optimal and aggressive lesion debulking was required.

Conflict of interest: None declared

Address for correspondence: Alfonso Ielasi, MD, FESC, Clinical and Interventional Cardiology Unit, S. Ambrogio Cardio-Thoracic Center, Via Faravelli 16, 20149, Milan, Italy, tel: +39 02-33127714, fax: +39 02-33127717, e-mail: alielasi@hotmail.com; alfonso.ielasi@gmail.com

Received: 31.01.2020 Accepted: 11.04.2020

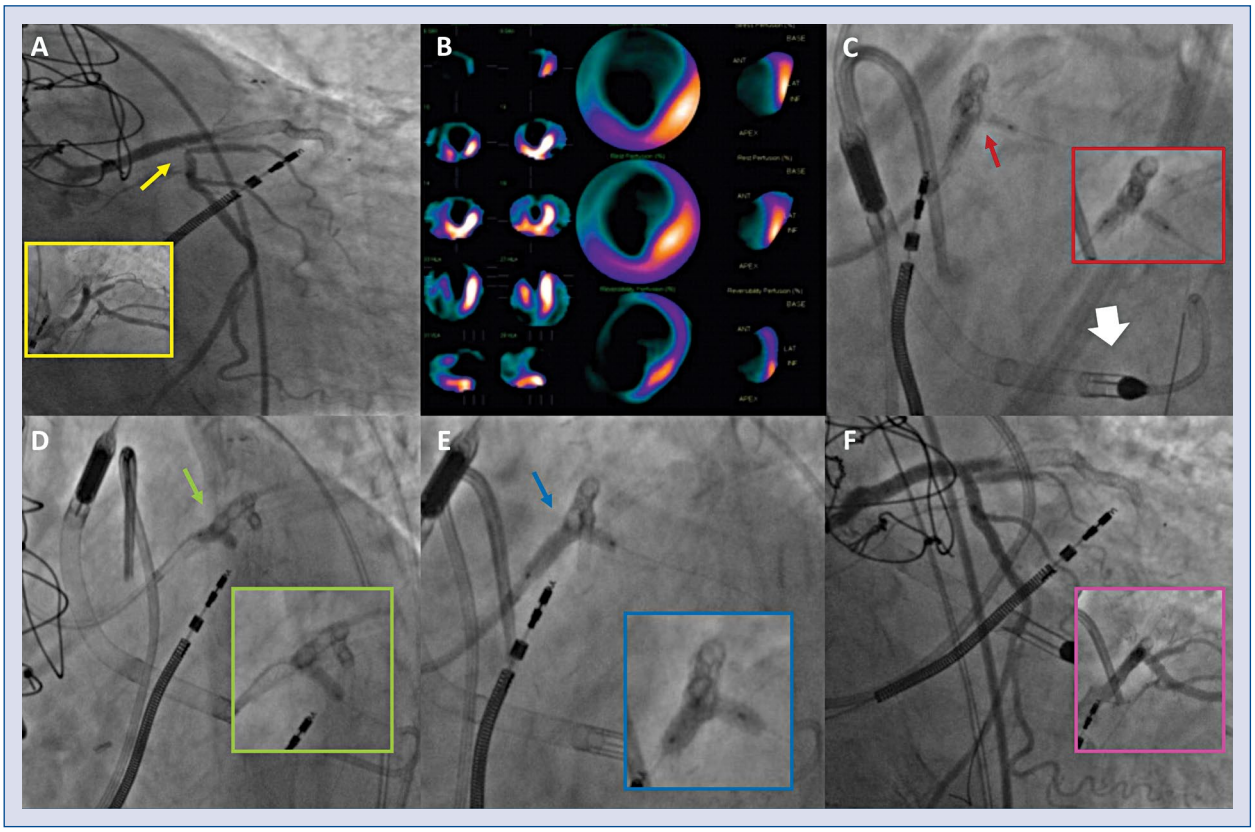

Figure 1. A. Severe ostial left circumflex lesion (yellow arrow); yellow box shows a second angiographic view confirming the critical lesion entity; **B.** Absence of anterior myocardial viability at myocardial perfusion scintigraphy; **C.** Impella CP positioned in the left ventricle across the aortic valve (withe arrow); "dog-bone" sign for an undilatable lesion by multiple non-compliant balloon inflations (red arrow and box); **D.** Optimal Shockwave balloon inflation (green arrow), confirmed in a second angiographic view (green box); **E.** Full 3.5 × 20 mm non-compliant balloon expansion after intravascular lithotripsy (blue arrow and box); **F.** Excellent final angiographic result following ostial left circumflex lesion stenting (pink arrow and box).

VIA MEDICA

IMAGE IN CARDIOVASCULAR MEDICINE

Cardiology Journal
2020, Vol. 27, No. 4, 429–430
DOI: 10.5603/CJ.2020.0113

ISSN 1897–5593

Serial optical coherence tomography findings after drug-coated balloon treatment in de novo coronary bifurcation lesion

Eun Jung Jun[1], Song Lin Yuan[1, 2], Scot Garg[3], Eun-Seok Shin[1]

[1]Department of Cardiology, Ulsan Medical Center, Ulsan, South Korea
[2]Department of Cardiology, Dong-A University Hospital, Busan, South Korea
[3]East Lancashire Hospitals NHS Trust, Blackburn, Lancashire, United Kingdom

A 55-year-old man with a background of current smoking and hypercholesterolemia was admitted with a non-ST-segment elevation myocardial infarction. His cardiac enzymes were raised with a creatine kinase-MB and troponin I of 16.2 ng/mL and 0.55 ng/mL, respectively. Coronary angiography showed a 90% stenosis at the bifurcation of the left anterior descending artery and first septal artery with Thrombolysis in Myocardial Infarction grade 3 flow in both branches (Fig. 1).

The culprit lesion in the left anterior descending artery was dilated with a non-compliant 3.5 × 10 mm balloon at 12 atm, followed by a 3.5 × 20 mm drug-coated balloon (DCB) inflated at 8 atm for 60 s. The ostium of the septal branch was not treated. The final angiographic result was good with no significant dissection. Post-intervention his symptoms resolved. Nine months later, follow-up coronary angiography confirmed adequate patency of the DCB treated segment. Reassuringly the bifurcation looked better on serial optical coherence tomography with a late luminal loss of –0.10 mm (Fig. 1). He remains symptom free 7 years post-intervention.

Although DCBs have shown good safety and efficacy in inhibiting neointimal hyperplasia in coronary artery disease, their role in treating bifurcation lesions remains controversial. This case demonstrates that DCB treatment of the main vessel did not compromise the side branch, but in fact lead to an increase in the luminal area of the side branch ostium at 9-month follow-up optical coherence tomography. These findings suggest that treating the main branch of a bifurcation using a DCB rather than a stent may be an option to avoid compromising the side branch ostium.

Conflict of interest: None declared

Address for correspondence: Eun-Seok Shin, MD, PhD, Department of Cardiology, Ulsan Medical Center, 13, Wolpyeong-ro, 171 beon-gil, Nam-gu, Ulsan, 44686, South Korea, tel: +82-52-259-5425, fax: +82-52-259-5117, e-mail: sesim1989@gmail.com

Received: 13.04.2020 Accepted: 13.04.2020

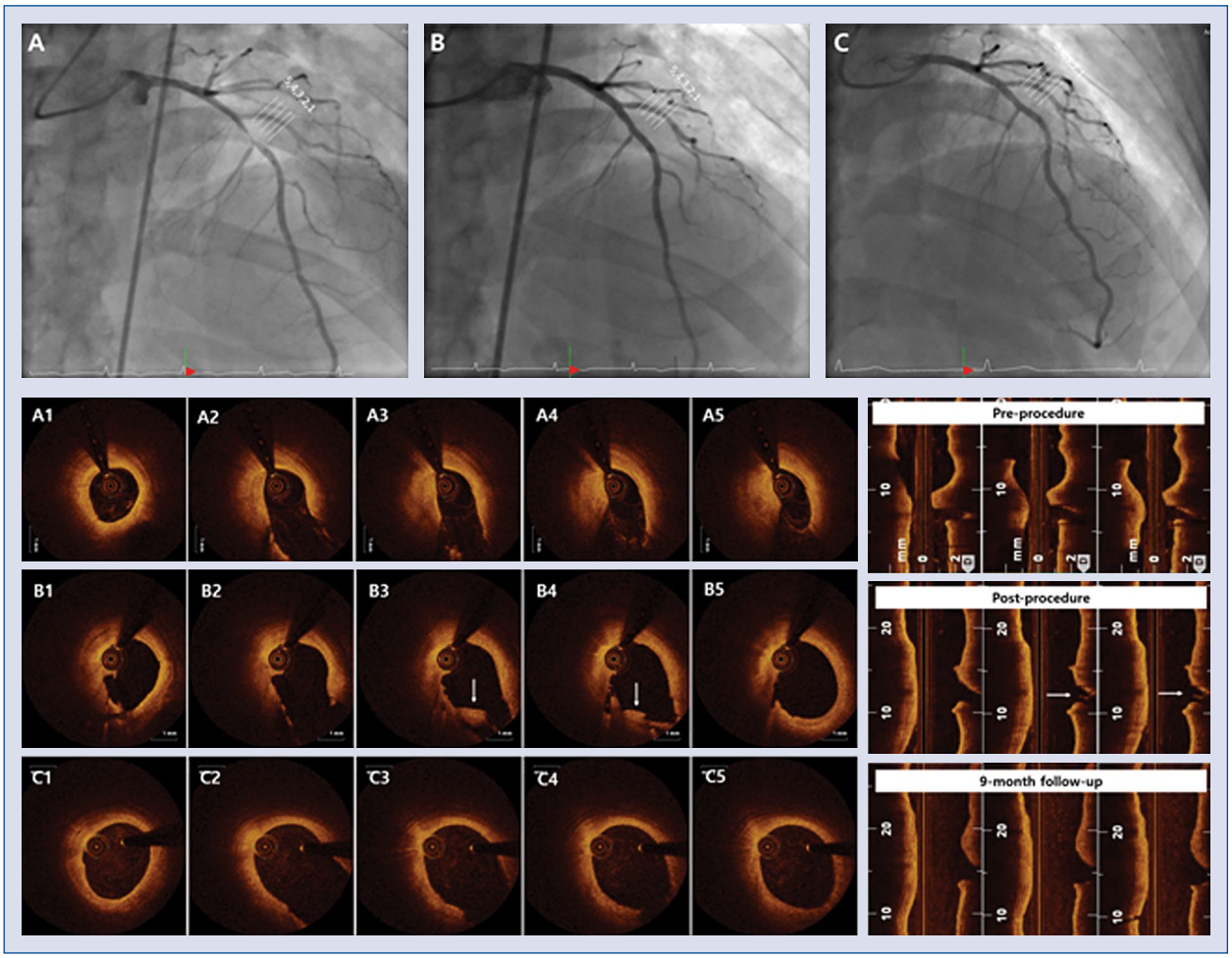

Figure 1. Pre-procedure (**A**), post-procedure (**B**) and 9-month follow-up angiographic images (**C**) coupled to corresponding optical coherence tomography (OCT) images. Pre-procedure angiographic image shows a true bifurcation lesion. After the procedure, the OCT image demonstrates dissection of the main vessel which protruded into the side branch ostium (white arrows). At OCT follow-up, however, the dissection has disappeared, and the lumen area of the main vessel and side branch ostium have increased due to the local drug effect.

VIA MEDICA

IMAGE IN CARDIOVASCULAR MEDICINE

Cardiology Journal
2020, Vol. 27, No. 4, 431–432
DOI: 10.5603/CJ.2020.0114

ISSN 1897–5593

Shockwave intravascular lithotripsy for multiple undilatable in-stent restenosis

Matteo Perfetti[1], Nino Cocco[1], Francesco Radico[2], Irene Pescetelli[3], Nicola Maddestra[1], Marco Zimarino[1, 2]

[1]Interventional Cath Lab, ASL 2 Abruzzo, Chieti, Italy
[2]Institute of Cardiology "G. d'Annunzio University", Chieti, Italy
[3]Cardiovascular Department, ASST Papa Giovanni XXIII, Bergamo, Italy

A 72-year-old patient was admitted for unstable angina; he had undergone previous percutaneous coronary intervention (PCI) with drug-eluting stents (DES) implantation on the right coronary artery (RCA) and left anterior descending artery (LAD) 7 years prior. In-stent restenosis (ISR) was documented on both sites. During PCI of RCA a non-compliant balloon ruptured (**Suppl. Video 1**), causing cardiac arrest. After cardiac resuscitation and adrenaline infusion the procedure was aborted. For the persistence of rest angina, a further attempt was planned with a plaque modification strategy.

Angiography and optical coherence tomography showed diffuse calcifications of the RCA (Fig. 1, upper panel), with a mid-RCA ISR caused by combined DES underexpansion and neo-atherosclerosis and a proximal de novo calcified severe stenosis. Shockwave intravascular lithotripsy (S-IVL; Shockwave Medical, Inc.) was delivered on both sites. A sirolimus eluting balloon (SEB) was then inflated inside the ISR and a DES deployed in the proximal segment, with a good final result (Fig. 1, mid panel).

In-stent restenosis of previous DES at mid-LAD (Fig. 1, lower panel, left side) was similarly due to both neo-atherosclerosis and underexpansion. Four S-IVL cycles followed by inflation of a SEB allowed a good final result (Fig. 1, lower panel, right side).

Shockwave intravascular lithotripsy produces mechanical waves propagating from the balloon (**Suppl. Video 2**) and such waves fracture calcifications without affecting soft tissues; it has been recently proposed for the treatment of both de novo calcified lesion and stent underexpansion. Here S-IVL was used for the treatment of ISR due to both neo-atherosclerosis and DES underexpansion. Further studies are needed to test the safety and efficacy of S-IVL in this subset.

Conflict of interest: None declared

Address for correspondence: Marco Zimarino, MD, PhD, Institute of Cardiology, "G. d'Annunzio" University – Chieti, C/o Ospedale SS. Annunziata, Via dei Vestini, 66013 Chieti, Italy, tel: +39-0871-41512, fax: +39-0871-402817, e-mail: m.zimarino@unich.it

Received: 18.04.2020 Accepted: 21.04.2020

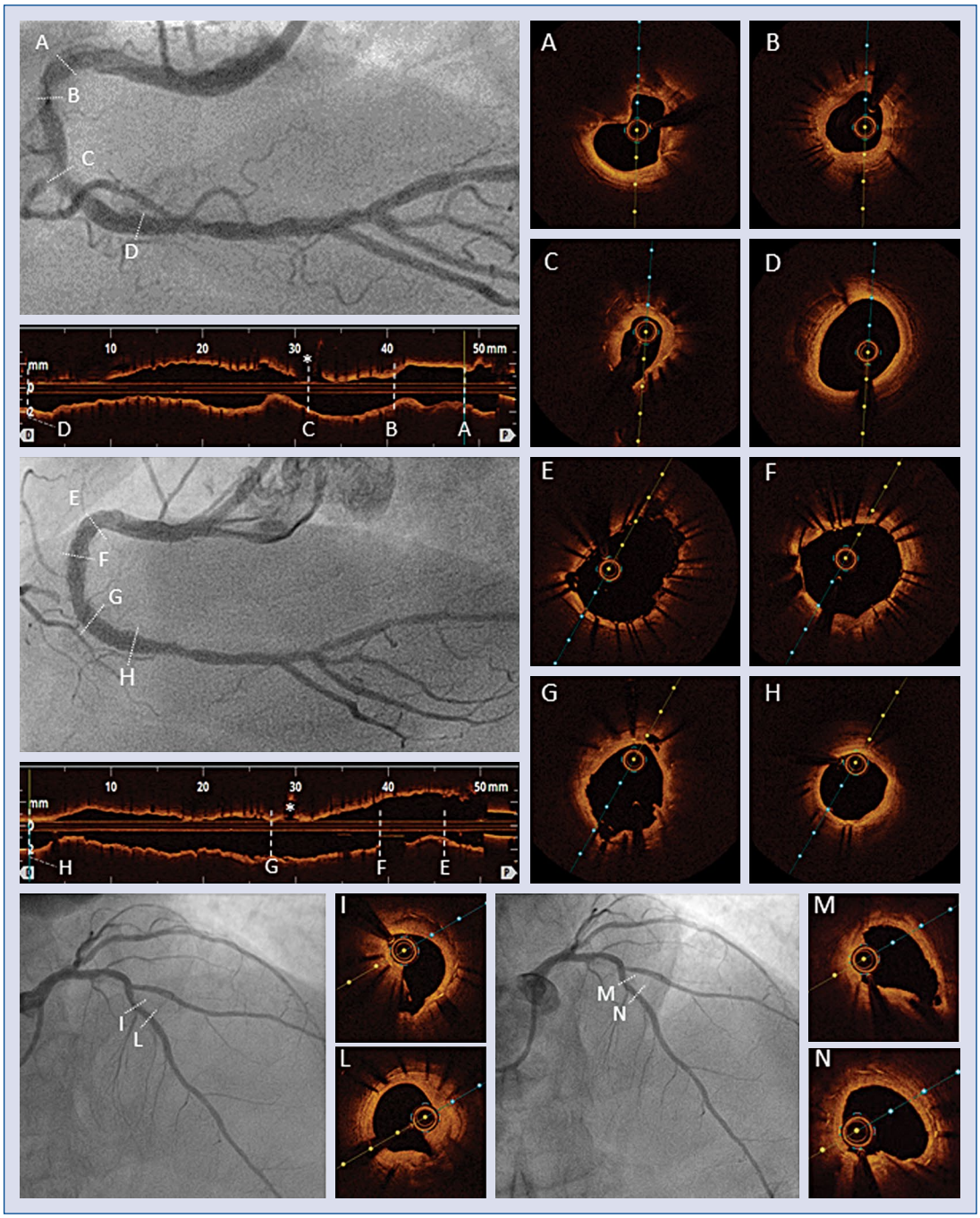

Figure 1. Upper panel: Baseline right coronary artery (RCA): angiography (upper left) of the RCA shows the position of 4 optical coherence tomography (OCT) cross-sections (upper right, **A–D**) reported on the right. **A.** Severely calcified eccentric de novo stenosis of the proximal segment; **B.** Concentric in-stent restenosis (ISR) with neointimal hyperplasia in the early midsegment. Stent underexpansion is detectable; **C.** In-stent restenosis/neo-atherosclerosis of the previously implanted two drug-eluting stents (DES) in overlap with underexpansion of the inner stent; **D.** Non-severe eccentric calcified plaque just below proximal to the DES edge; (*) Acute marginal branch; **Mid panel:** Angiography (left side) and OCT (right side) after 4 cycles of shockwave intravascular lithotripsy (S-IVL) with a 2.5 × 20 mm balloon, subsequent noncompliant 3.0 × 20 mm balloon and 3.5 × 20 mm sirolimus eluting balloon (SEB) inflations inside the ISR and final new 4.0 × 28 mm DES deployment between the proximal edge of the previous DES and de novo proximal RCA lesion; **E, F.** New DES has optimal deployment; **G, H.** Subsequent SEB dilatations achieved satisfactory plaque expansion inside the previously deployed DES; (*) Acute marginal branch; **Lower panel:** Angiography and OCT of baseline left anterior descending artery (left side) show a mid lesion, due to a combined mechanism of stent underexpansion and neo-atherosclerosis (**I, L**); after 4 cycles of S-IVL and inflation of a 3.5 mm SEB an optimal angiographic result is achieved (right side), with good DES expansion and adequate plaque fracture (**M**, **N**).

VIA MEDICA

IMAGE IN CARDIOVASCULAR MEDICINE

Cardiology Journal
2020, Vol. 27, No. 4, 433–434
DOI: 10.5603/CJ.2020.0115

ISSN 1897–5593

Serial optical coherence tomography for characterization of coronary lithotripsy efficacy: How much is enough?

Maksymilian P. Opolski, Jacek Kwiecinski, Rafal Wolny, Artur Debski, Adam Witkowski

Department of Interventional Cardiology and Angiology, National Institute of Cardiology, Warsaw, Poland

Intravascular lithotripsy (IVL) is an emerging treatment for severely calcified lesions. A 74-year-old female with a history of diabetes and chronic kidney disease presented with the Canadian Cardiovascular Society class III angina. Coronary angiography demonstrated a heavily calcified tandem stenosis in the mid right coronary artery (RCA) (Fig. 1A, **Suppl. Video 1**). Following predilatation with 1.25 to 2.5 mm semi-compliant balloons and 3.0 mm non-compliant balloon, the baseline optical coherence tomography (OCT) using saline flush media (as prevention for contrast-induced nephropathy) revealed extensive three-quadrant calcium in the mid RCA (Fig. 1B–C). A 3.5 × 12 mm lithotripsy balloon was subsequently inflated to 4 atm and 20 pulses of sonic pressure (in both lesions in mid RCA) were applied (40 pulses in total), followed by first post-IVL OCT showing deep calcium fracture with significant luminal gain (Fig. 1D, E). After successful delivery of consecutive 20 pulses in each of the two stenoses (80 pulses in total), the second post-IVL OCT demonstrated no further modification of calcification (Fig. 1F). Ultimately, a 3.5 × 38 mm drug-eluting stent was implanted followed by post-dilatation with 4.0 mm non-compliant balloon resulting in good angiographic and OCT result (Fig. 1G–I).

The association between calcium disruption and the specified dosage of mechanical pulses generated by IVL catheter is unknown. The present case demonstrates extensive calcium fractures along with a significant luminal gain following the first 20 pulses of IVL within a balloon-resistant lesion. Interestingly, further applications of IVL (up to 40 pulses per lesion) did not translate into additional calcium modification. This observation provides insights into the efficiency of IVL.

Conflict of interest: None declared

Address for correspondence: Dr. Maksymilian P. Opolski, Department of Interventional Cardiology and Angiology, National Institute of Cardiology, ul. Alpejska 42, 04–628 Warsaw, Poland. tel: +48501444303, fax: +48(22)6133819, e-mail: opolski.mp@gmail.com

Received: 15.04.2020 Accepted: 5.05.2020

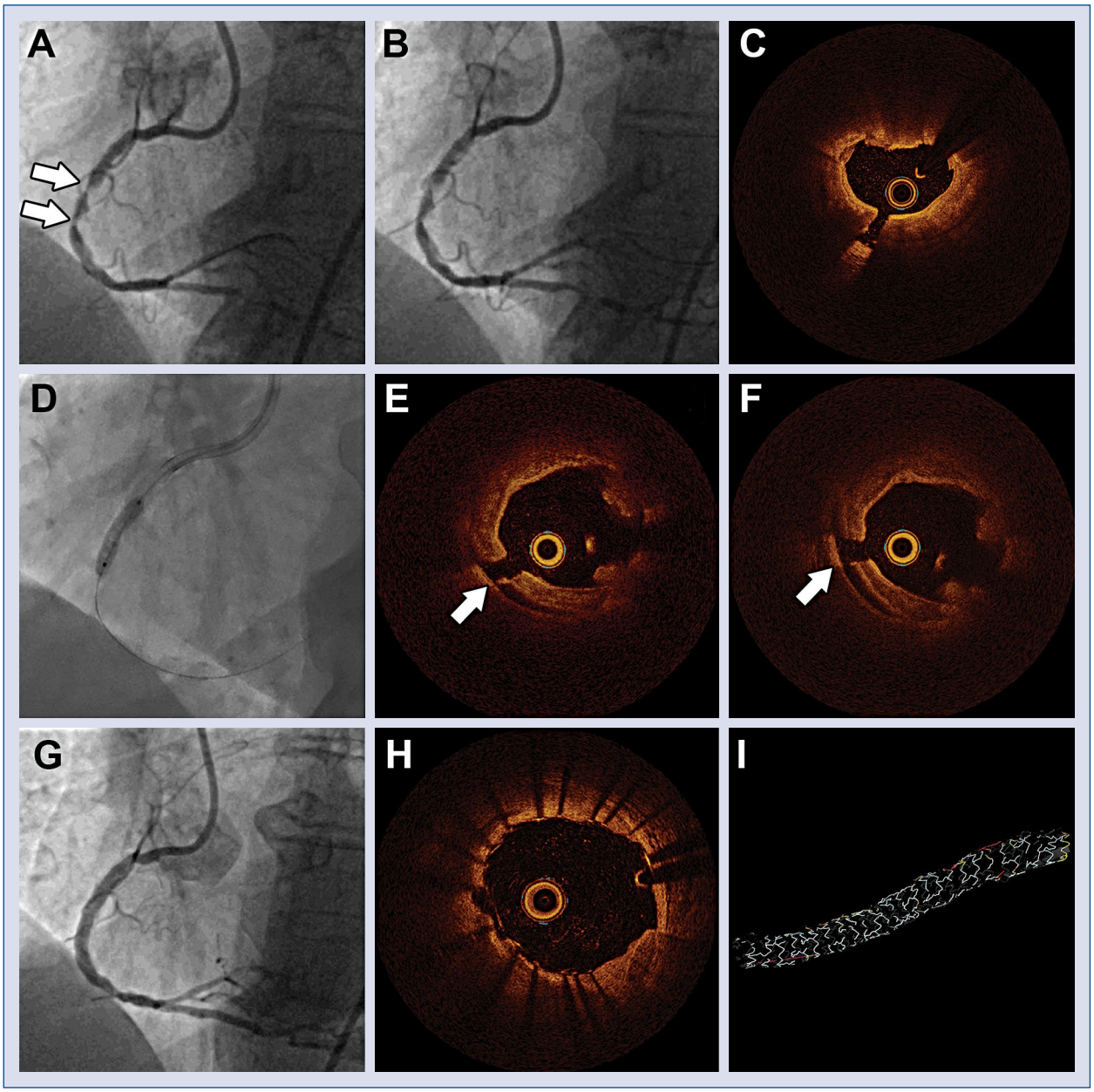

Figure 1. A, B. Invasive angiography showing heavily calcified tandem stenosis (arrows) of the mid-right coronary artery before (**A**) and after (**B**) non-compliant balloon predilatation; **C.** Optical coherence tomography after non-compliant balloon predilatation showing three-quadrant calcification; **D.** Angiographic appearance of the intravascular lithotripsy balloon; **E, F.** Optical coherence tomography after successful delivery of 20 pulses (**E**) and 40 pulses (**F**) of intravascular lithotripsy revealing extensive calcium fracture (arrow); **G–I.** Final angiography (**G**) and optical coherence tomography (**H–I**) showing optimal stent expansion and apposition.

VIA MEDICA

IMAGE IN CARDIOVASCULAR MEDICINE

Cardiology Journal
2020, Vol. 27, No. 4, 435–436
DOI: 10.5603/CJ.2020.0116

ISSN 1897–5593

Left internal mammary spasm mimicking graft dissection in the course of percutaneous coronary intervention of anastomotic in-stent restenosis

Maciej T. Wybraniec[1, 2], Andrzej Kubicius[2, 3], Katarzyna Mizia-Stec[1, 2]

[1]First Department of Cardiology, School of Medicine in Katowice, Medical University of Silesia, Upper Silesia Medical Center, Katowice, Poland
[2]Upper Silesia Medical Center, Katowice, Poland
[3]Department of Cardiology in Cieszyn, Upper Silesia Medical Center, Katowice, Poland

The percutaneous coronary intervention (PCI) of left internal mammary artery (LIMA) bypass to left anterior descending artery (LAD) confers high risk of intractable spasm and graft dissection. This case presents a 67-year-old male, following coronary artery bypass grafting and PCI of LIMA-LAD anastomosis with drug-eluting stent implantation 7 months prior to index hospitalization, who currently presented with inferior wall ST-segment elevation acute myocardial infarction. The coronary angiography performed via right femoral approach showed new significant 90% stenosis within the first diagonal branch and 99% in-stent restenosis in LIMA-LAD anastomosis (Fig. 1A). First, the lesion in LAD/diagonal branch was predilated with a 2.5 mm balloon and a 2.5 × 25 mm sirolimus-eluting stent was implanted. Second, an internal mammary artery guiding catheter was employed and the Whisper LS® guidewire was advanced across the LIMA-LAD restenosis. The lesion was initially predilated with the 2.5 mm balloon and a 2.0 × 23 mm everolimus-eluting stent was implanted (Fig. 1B). Following stent deployment, a severe impairment of LIMA-LAD flow was documented (Fig. 1C, **Suppl. Movie 1**), which was accompanied by aggravation of restrosternal chest pain and reduction of blood pressure (90/60 mmHg). Although LIMA dissection was suspected, double intracoronary bolus of diluted 0.1 mg nitroglycerine led to gradual restoration of Thrombolysis in Myocardial Infarction 3 blood flow (Fig. 1D) and, paradoxically, improvement of hemodynamic status (130/80 mmHg). The patient was discharged home following an uneventful further in-hospital stay. Iatrogenic periprocedural LIMA constriction should always be suspected and vasodilative agents utilized in cases of impaired flow during LIMA PCI.

Conflict of interest: None declared

Address for correspondence: Maciej T. Wybraniec, MD, PhD, First Department of Cardiology, School of Medicine in Katowice, Medical University of Silesia, ul. Ziołowa 47, 40–635 Katowice, Poland, tel: +48 32 359 88 90, fax: +48 32 252 30 32, e-mail: maciejwybraniec@gmail.com

Received: 27.04.2020 Accepted: 15.05.2020

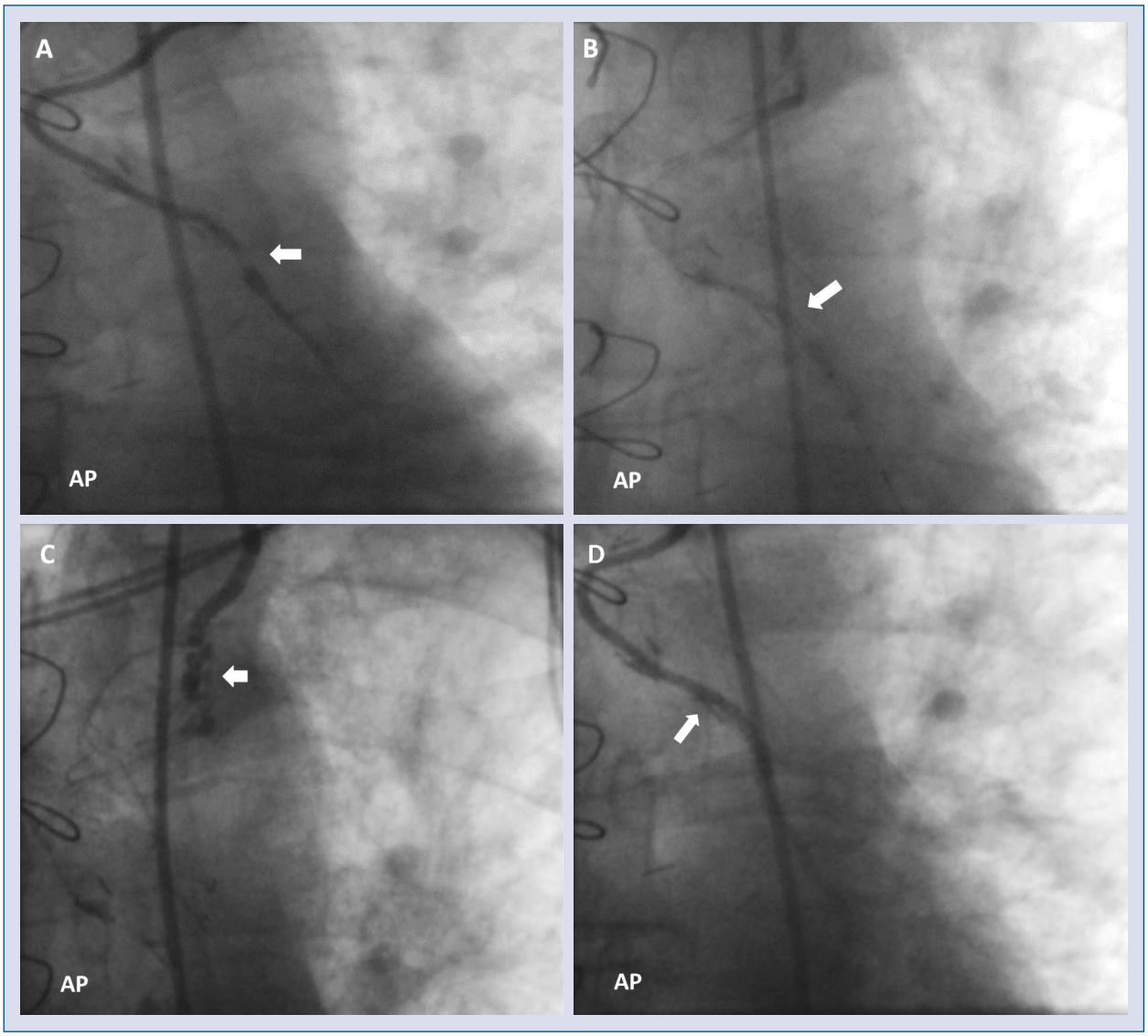

Figure 1. Coronary angiography performed via right femoral approach. **A.** Anterior-posterior (AP) view, arrow — 99% in-stent restenosis in left internal mammary artery (LIMA) to left anterior descending artery anastomosis; **B.** AP view; arrow — implantation of evrolimus-eluting stent within the anastomotic in-stent restenosis; **C.** AP view; arrow — dissection-like impairment of flow within the arterial graft due to severe spasm of LIMA; **D.** AP view; arrow — restoration of Thrombolysis in Myocardial Infarction grade 3 blood flow after intracoronary administration of nitroglycerine.

VIA MEDICA

IMAGE IN CARDIOVASCULAR MEDICINE

Cardiology Journal
2020, Vol. 27, No. 4, 437–438
DOI: 10.5603/CJ.2020.0117

ISSN 1897–5593

Multimodality imaging in the recurrence of left ventricular pseudoaneurysm after surgical correction

Ana Marques[1], Daniel Caldeira[2], Sofia Alegria[1], Ana Rita Pereira[1], Alexandra Briosa[1], Inês Cruz[1], Ana Rita Almeida[1], Isabel João[1], Hélder Pereira[1]

[1]Department of Cardiology, Hospital Garcia de Orta, Almada, Portugal
[2]Centro Cardiovascular da Universidade de Lisboa (CCUL), CAML, Laboratório de Farmacologia Clínica e Terapêutica, Faculdade de Medicina, Universidade de Lisboa, Portugal

A 61-year-old male, former smoker and diabetic patient with a previous medical history noted for an inferior myocardial infarction complicated with left ventricular free wall rupture that had been surgically corrected 6 years prior, presented to the cardiology unit complaining of a new-onset dyspnoea, orthopnoea and fatigue which had started over the month prior to presenting. The transthoracic echocardiography showed left ventricular enlargement with a depressed left ventricular ejection fraction of 35%, and a large cavity communicating with the inferior and inferolateral walls of the left ventricle (aneurysm vs. pseudoaneurysm), without pericardial effusion (Fig. 1A–D). The cardiac magnetic resonance imaging confirmed a free wall rupture at medial and basal segments of the inferior left ventricular wall with a 11 × 9 × 7 cm aneurysmal chamber, with systolic expansion, containing a large and organized thrombus (Fig. 1E–H). These findings confirm the diagnosis of a large pseudoaneurysm. Cardiac surgery was performed without complications.

Conflict of interest: None declared

Address for correspondence: Dr. Ana Isabel Sá Marques Costa, Avenida Torrado da Silva, 2805-267 Almada, Portugal, tel: +351212940294, e-mail: ana.smc.25@gmail.com

Received: 1.03.2020 Accepted: 28.03.2020

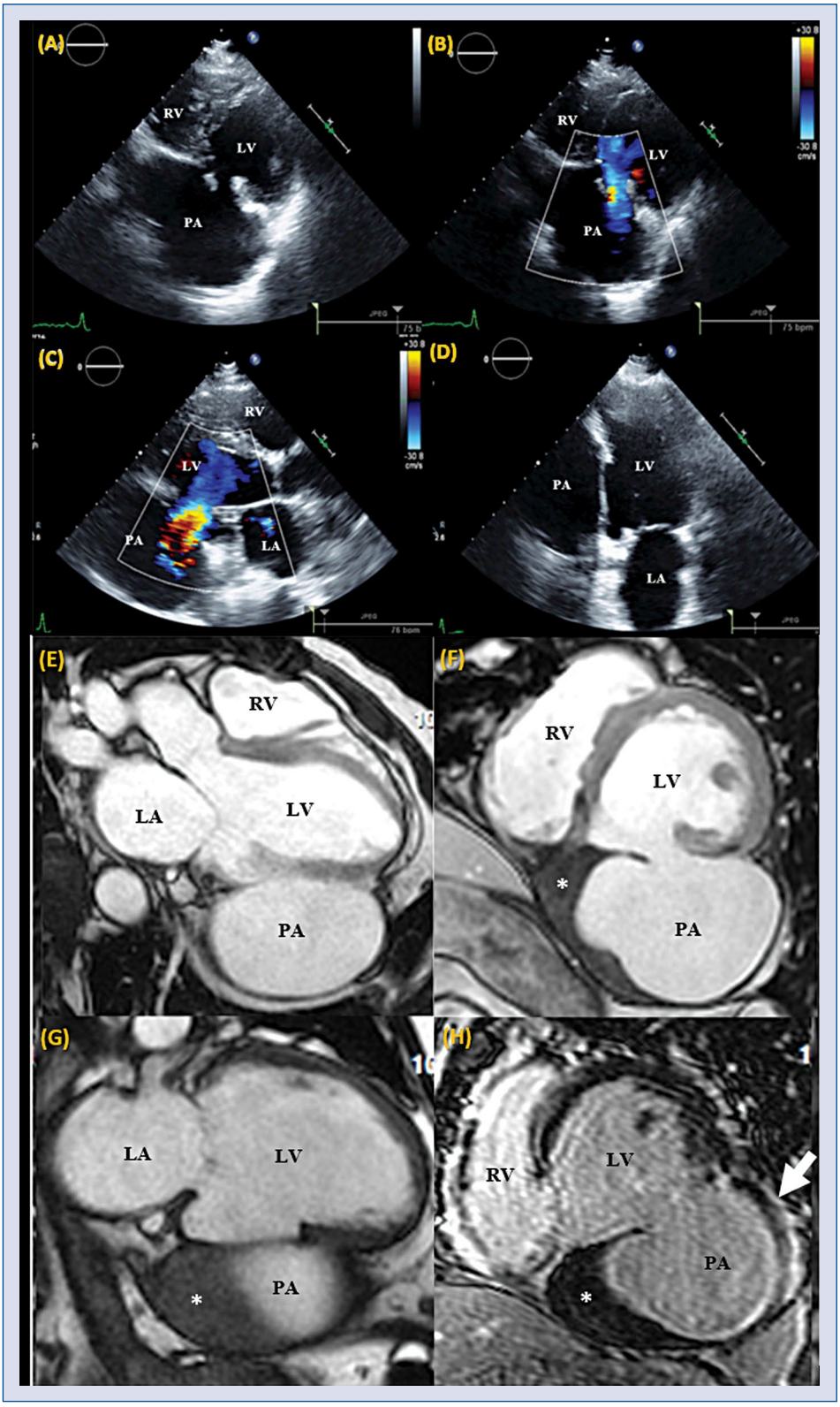

Figure 1. Transthoracic echocardiography parasternal short-axis views (**A**, **B**) and long-axis view (**C**) showing a pseudoaneurysm cavity that communicates with the inferior and inferolateral walls of the left ventricle (LV) through a narrow neck. Transthoracic echocardiography apical two-chamber view showing its relationship with the inferior wall (**D**). Cardiac magnetic resonance imaging — STIR image, oblique left ventricular outflow tract view (**E**), short-axis view (**F**) and two-chamber view (**G**) showing inferior free wall rupture with a large bulging aneurysmal sac containing a thrombus (*) that is adherent to the pericardial space. Delayed gadolinium enhancement of the pericardium adjacent to pseudoaneurysm (arrow) (**H**); LA — left atria; PA — pseudoaneurysm; RV — right ventricle.

VIA MEDICA

IMAGE IN CARDIOVASCULAR MEDICINE

Cardiology Journal
2020, Vol. 27, No. 4, 439–440
DOI: 10.5603/CJ.2020.0118

ISSN 1897–5593

Cerebral embolization from left atrial myxoma causing takotsubo cardiomyopathy complicated with congestive heart failure

Takao Konishi[1], Naohiro Funayama[2], Tadashi Yamamoto[2], Daisuke Hotta[2], Shinya Tanaka[3]

[1]Department of Cardiovascular Medicine, Faculty of Medicine and Graduate School of Medicine, Hokkaido University, Sapporo, Japan
[2]Department of Cardiology, Hokkaido Cardiovascular Hospital, Sapporo, Japan
[3]Department of Cancer Pathology, Faculty of Medicine, Hokkaido University, Sapporo, Japan

An 80-year-old woman who was admitted to a neurosurgery hospital, and was later transferred to cardiology hospital with a diagnosis of cardiac tumor as a possible cause of cerebral infarction. Magnetic resonance imaging and computed tomography (CT) of the brain showed multiple cerebellar infarction (Fig. 1A, B). A 12-lead electrocardiogram showed ST elevations in leads V_3 and V_4 and negative T waves with QT prolongation in leads II, III, aV_F and V_4–V_6 (Fig. 1C). Chest roentgenogram showed cardiomegaly with pulmonary edema (Fig. 1D). The laboratory tests revealed 670 ng/L of troponin T and 1220 pg/mL of B-type natriuretic peptide. Transthoracic echocardiography showed a highly mobile left atrial mass, akinesis in apical wall and hyperkinesis in basal wall of the left ventricle (Fig. 1E, F, arrows; **Suppl. Video S1**). Cardiac CT revealed a cardiac mass in the left atrium (Fig. 1G, arrow), and no significant coronary artery stenosis. Scintigraphic images, using ^{123}I-β-methyl-iodophenyl pentadecanoic acid, showed apical perfusion defect (Fig. 1H, arrowheads). Cardiac tumor resection was performed for the management of impending embolization (Fig. 1I). The histopathological examination confirmed the diagnosis of myxoma. These findings suggested that, takotsubo cardiomyopathy was caused by cerebral infarction from embolization of the left atrial myxoma. Although the combination of these three pathological conditions is rare, it is important to consider the possibility of takotsubo cardiomyopathy when performing surgical treatment for cardiac tumor because hyperhydration during the perioperative period might cause aggravation of heart failure and hypercoagulability during an operation and could result in thromboembolism due to apical thrombi, thus leading to a poor prognosis.

Conflict of interest: None declared

Address for correspondence: Takao Konishi, MD, PhD, Department of Cardiovascular Medicine, Faculty of Medicine and Graduate School of Medicine, Hokkaido University, West 7, North 15, Kita-ku, Sapporo, 060-8638, Japan, tel: +81-11-706-6973, fax: +81-11-706-7874, e-mail: takaokonishi0915@gmail.com

Received: 31.01.2020 Accepted: 21.04.2020

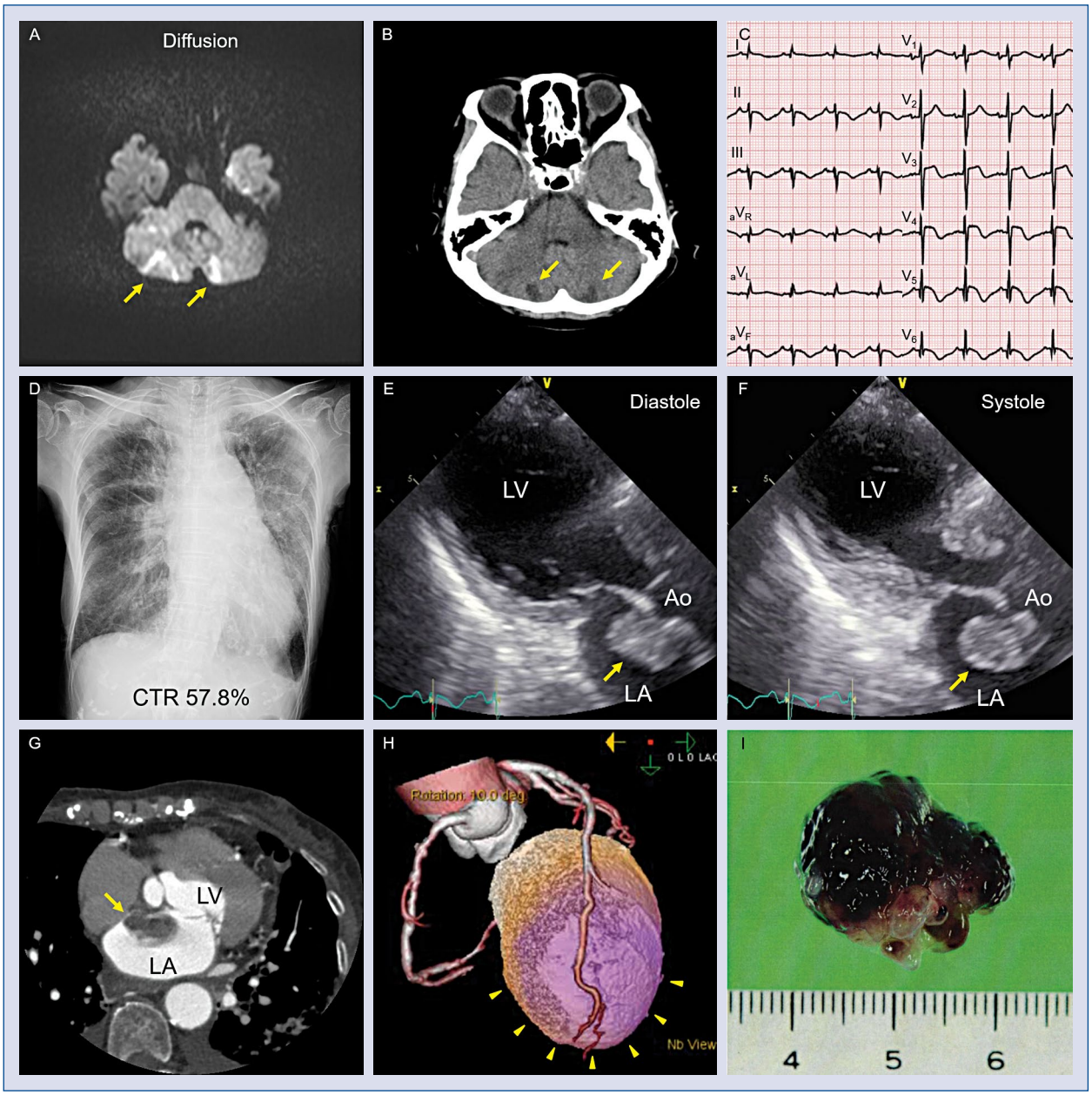

Figure 1. A, B. Magnetic resonance imaging and computed tomography of the brain; **C.** Twelve-lead electrocardiogram; **D.** Chest roentgenogram; **E, F.** Transthoracic echocardiography in diastole (**E**) and systole (**F**); **G.** Cardiac computed tomography; **H.** Cardiac scintigraphy; **I.** Resected tumor; Ao — aorta; LA — left atrium; LV — left ventricle.

VIA MEDICA

IMAGE IN CARDIOVASCULAR MEDICINE

Cardiology Journal
2020, Vol. 27, No. 4, 441–442
DOI: 10.5603/CJ.2020.0119

ISSN 1897–5593

Delayed diagnosis of arterial hypertension in young woman with coarctation of the aorta coexisting with arteria lusoria

Ilona Michałowska[1], Małgorzata Kowalczyk[2], Marcin Demkow[3], Piotr Hoffman[2]

[1]Department of Radiology, Institute of Cardiology, Warsaw, Poland
[2]Department of Congenital Heart Diseases, Institute of Cardiology, Warsaw, Poland
[3]Department of Coronary and Structural Heart Diseases, Institute of Cardiology, Warsaw, Poland

Coarctation of the aorta (CoAo) coexisting with an aberrant right subclavian artery (arteria lusoria) is a rare congenital malformation which can be undiagnosed until adulthood. Presented herein, is the case of a 35-year-old woman in her fifth pregnancy with arterial hypertension diagnosed 2 months earlier. The patient had had 4 natural childbirths. She had suffered from palpitations and a transient episode of aphasia. Blood pressure in the right arm was 102/71 mmHg, in the left arm 166/85 mmHg, and in the lower extremities 95/70 mmHg.

The suspicion of CoAo was confirmed by transthoracic echocardiogram. Continuous wave Doppler discovered a substantial pressure gradient across the descending aorta with a characteristic prolonged diastolic phase (Fig. 1A) with concomitant flattened flow encompassing diastolic phase within the abdominal aorta (Fig. 1B).

Computed tomography angiography (CTA) of the aorta performed after the last childbirth confirmed the diagnosis of CoAo and revealed arteria lusoria (Fig. 1C, arrow) arising distal to the narrowing of the descending aorta. Extensive asymmetrical collateral circulation on the chest wall and on the right side of the neck (Fig. 1D, E, arrows) was demonstrated. The patient underwent successful treatment by balloon angioplasty with stent placement (Fig. 1F, H). Subsequently, CTA of the carotid arteries showed normal blood circulation in the neck (Fig. 1F). Doppler study showed a restored normal flow pattern within the abdominal aorta (Fig. 1G).

The present case emphasizes a pivotal role of CTA in diagnosing CoAo and associated arterial lesions. CoAo should be considered when diagnosing arterial hypertension in younger patients to bring more attention to this condition.

Conflict of interest: None declared

Address for correspondence: Ilona Michałowska, MD, Department of Radiology, Institute of Cardiology, ul. Alpejska 42, 04–628 Warszawa, Poland, tel: +48 22 343 41 68, e-mail: imichalowska@ikard.pl

Received: 21.03.2020 Accepted: 5.05.2020

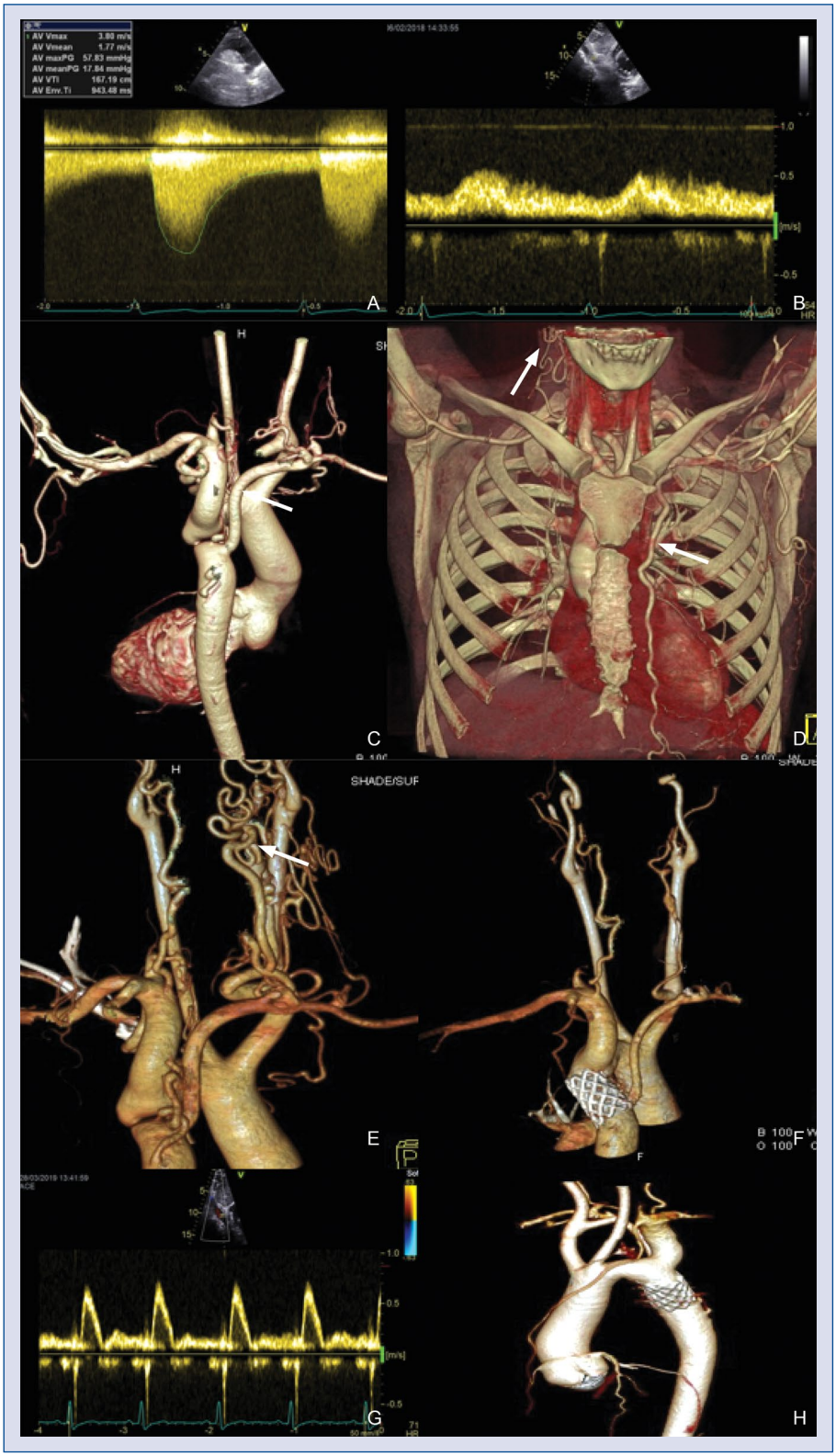

Figure 1. A. Continuous wave (CW) Doppler at coarctation site; **B.** CW Doppler in the abdominal aorta; **C.** Computed tomography angiography (CTA), posterior view — coarctation of the aorta, arteria lusoria (arrow); **D.** CTA — collateral circulation on the chest wall (left side — arrow) and in the neck (right side — arrow); **E.** CTA, posterior view — extensive asymmetrical collateral circulation on the neck (arrow); **F.** CTA after stent implantation (posterior view) — normal blood circulation on the neck; **G.** CW Doppler in abdominal aorta after coarctation treatment; **H.** CTA of thoracic aorta after stent placement.

VIA MEDICA

IMAGE IN CARDIOVASCULAR MEDICINE

Cardiology Journal
2020, Vol. 27, No. 4, 443–444
DOI: 10.5603/CJ.2020.0120

ISSN 1897–5593

Emery-Dreifuss muscular dystrophy as a possible cause of coronary embolism

Atsushi Tada[1], Takao Konishi[1], Takuma Sato[1], Tomoya Sato[1], Takuya Koizumi[1], Sakae Takenaka[1], Yoshifumi Mizuguchi[1], Takahide Kadosaka[1], Ko Motoi[1], Yuta Kobayashi[1], Hirokazu Komoriyama[1], Yoshiya Kato[1], Kazunori Omote[1], Shingo Tsujinaga[1], Rui Kamada[1], Kiwamu Kamiya[1], Hiroyuki Iwano[1], Toshiyuki Nagai[1], Nanase Okazaki[2], Yoshihiro Matsuno[2], Toshihisa Anzai[1]

[1]Department of Cardiovascular Medicine, Faculty of Medicine and Graduate School of Medicine, Hokkaido University, Sapporo, Japan
[2]Department of Surgical Pathology, Hokkaido University Hospital, Sapporo, Japan

A 43-year-old man, who had a history of atrial arrhythmia and anterior myocardial infarction due to coronary embolism presented to the cardiology clinic for further examination. He was previously diagnosed as Emery-Dreifuss muscular dystrophy (EDMD) involving skeletal muscles in the lower limbs. An electrocardiogram showed junctional rhythm at a heart rate of 39 bpm with atrial arrest and poor r progression (Fig. 1A). Echocardiography revealed a left ventricular dilatation and a diffuse hypokinesis of the left ventricle with ejection fraction of 48% (Fig. 1B). Cardiac magnetic resonance imaging demonstrated a subendocardial late gadolinium enhancement at the anterior wall of left ventricle (Fig. 1C), consistent with the old anterior myocardial infarction. Right ventricular endomyocardial biopsy revealed irregular sizes of nuclei with vacuolation and reduced myocardial fibers (Fig. 1D), whereas interstitial fibrosis was not apparent (Fig. 1E). In EDMD, fibrosis or adipose tissue replacement usually starts in the atria, leading to atrial arrhythmias, and then affects the ventricles. This case suggests that EDMD in the early-stage does not necessarily display apparent fibrosis, despite the presence of mild myocardial abnormalities in histopathology. Furthermore, EDMD might be one of the possible causes of early-onset atrial arrhythmias causing coronary artery embolism or embolic cerebral infarction. He underwent cardiac resynchronization therapy defibrillator because he had symptomatic bradycardia and a history of ventricular tachycardia. At the 5-month follow-up, the patient remained well.

Conflict of interest: None declared

Address for correspondence: Takao Konishi, MD, PhD, Department of Cardiovascular Medicine, Faculty of Medicine and Graduate School of Medicine, Hokkaido University, West 7, North 15, Kita-ku, Sapporo, 060-8638, Japan, tel: +81-11-706-6973, fax: +81-11-706-7874, e-mail: takaokonishi0915@gmail.com

Received: 31.01.2020 Accepted: 5.05.2020

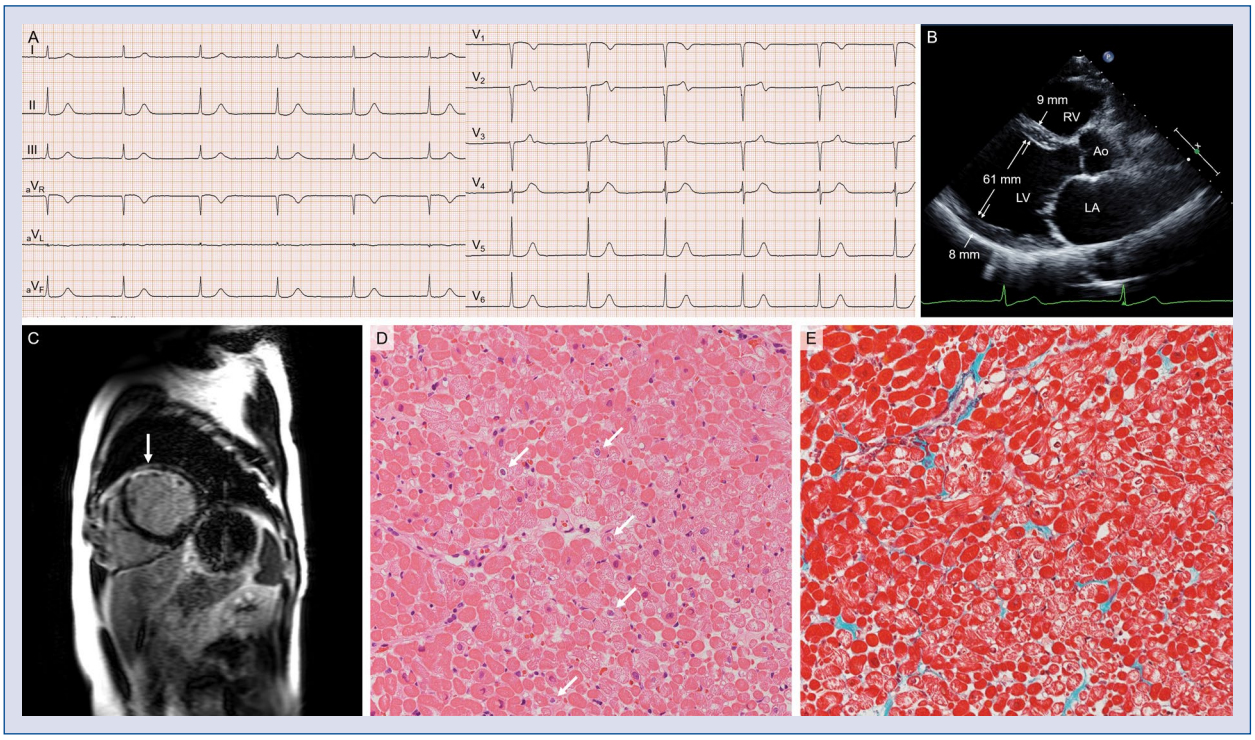

Figure 1. A. A 12-lead electrocardiogram showed atrial arrest with junctional rhythm; **B.** Echocardiogram (parasternal long axis) showing left ventricle (LV) dilatation; LA — left atrium; RV — right ventricle; Ao — aorta; **C.** Cardiac magnetic resonance imaging showing a late gadolinium enhancement (arrow); **D.** Histopathology after hematoxylin and eosin staining showed irregular sizes of nuclei with vacuolation (arrows) and reduced myocardial fibers; **E.** Slight interstitial fibrosis was stained green after elastica-Masson staining.

VIA MEDICA

IMAGE IN CARDIOVASCULAR MEDICINE

Cardiology Journal
2020, Vol. 27, No. 4, 445–446
DOI: 10.5603/CJ.2020.0121

ISSN 1897–5593

A left main disease repeatedly treated with drug-coated balloon in a patient with poor adherence to medications

Song Lin Yuan[1, 2], Eun Jung Jun[1], Moo Hyun Kim[2], Scot Garg[3], Eun-Seok Shin[1]

[1]Department of Cardiology, Ulsan Medical Center, Ulsan, South Korea
[2]Department of Cardiology, Dong-A University Hospital, Busan, South Korea
[3]East Lancashire Hospitals NHS Trust, Blackburn, Lancashire, United Kingdom

A 45-year-old male, heavy smoker, was admitted after a 1-week history of recurrent chest pain at minimal effort. His electrocardiography, cardiac enzyme and echocardiography showed normal. Coronary angiography showed a 95% left main (LM) stenosis with Thrombolysis in Myocardial Infarction (TIMI) grade 2 flow. He declined coronary artery bypass grafting (CABG) or stent implantation, but agreed to treatment with balloon angioplasty using a drug-coated balloon (DCB). He was carefully assessed and gave informed consent.

The lesion was dilated several times with a 3.5 × 10 mm scoring balloon at 12 atm and then a 3.5 × 20 mm DCB was inflated at 14 atm for 60 s. The final angiographic result was good. His angina symptoms were resolved. He remained well until presenting 6 months later with a recurrence of his symptoms. He admitted to discontinuing all his medication, including dual antiplatelet therapy since discharge. Repeat angiography showed a 90% restenosis at the LM with TIMI grade 3 flow. He again declined CABG or stenting. Considering his poor drug compliance, repeat revascularization to the LM with DCB by same technique was performed. Again, the final angiographic result was good and 8 months later, follow-up angiographic and intravascular ultrasound confirmed excellent results (Fig. 1). He has been well without angina for 10 months now.

This case was repeatedly treated with DCB given concerns regarding the patient's poor compliance to medication including antiplatelets. These findings suggest that LM disease may be a potential alternative indication for DCB treatment, especially when patients are unsuitable for long-term antiplatelet therapy or unwilling to undergo CABG or stenting.

Conflict of interest: None declared

Address for correspondence: Eun-Seok Shin, MD, PhD, Department of Cardiology, Ulsan Medical Center, 13, Wolpyeong-ro, 171 beon-gil, Nam-gu, Ulsan, 44686, South Korea, tel: +82-52-259-5425, fax: +82-52-259-5117, e-mail: sesim1989@gmail.com

Received: 21.04.2020 Accepted: 5.05.2020

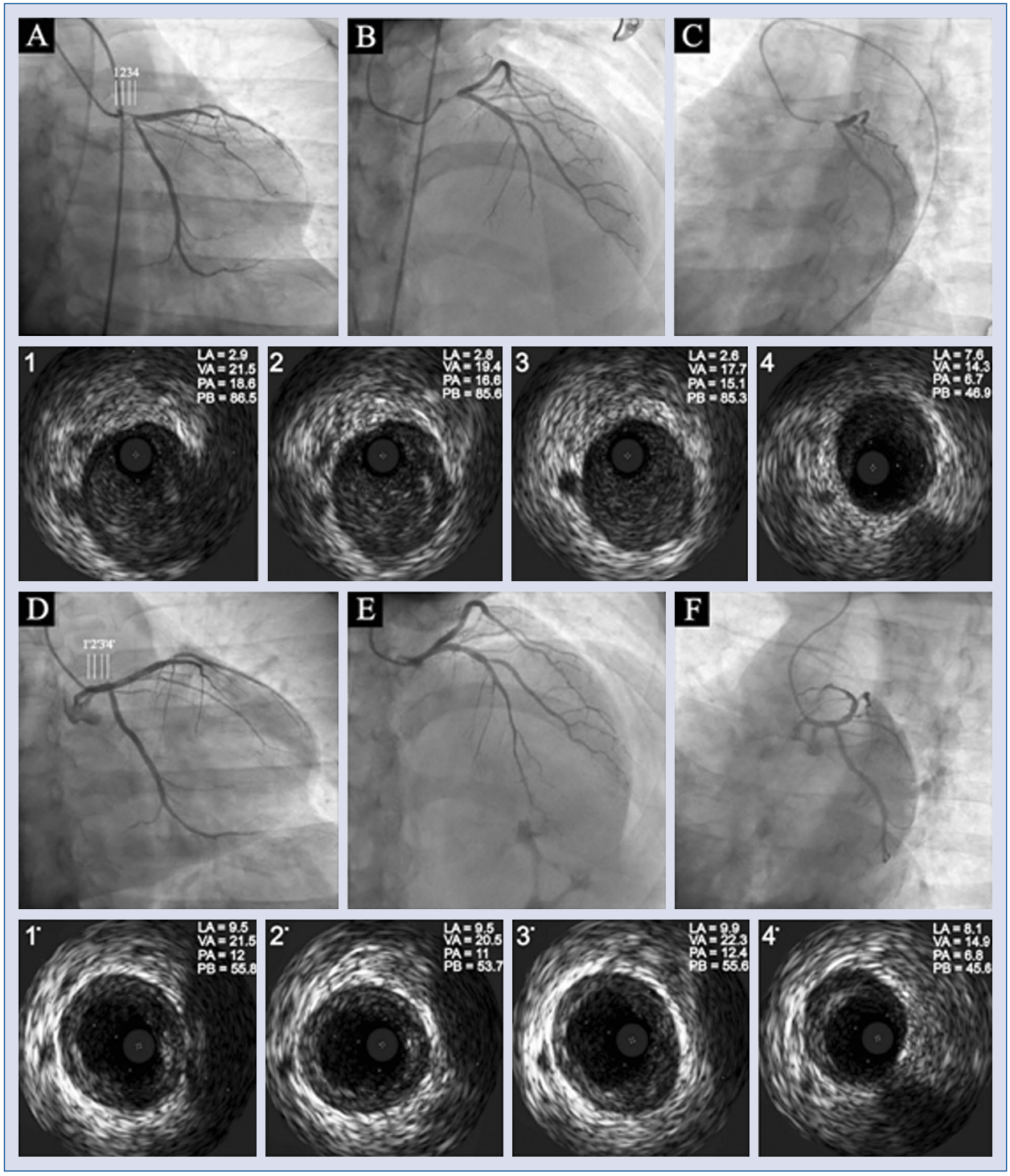

Figure 1. Pre-procedure (**A–C**), follow-up angiographic images (**D–F**) coupled to serial corresponding intravascular ultrasound (IVUS) images. At 8 months follow-up IVUS showed a much greater luminal area and decreased plaque burden in left main compared to baseline IVUS; LA — lumen area, mm^2; VA — vessel area, mm^2; PA — plaque area, mm^2; PB — plague burden, %.

VIA MEDICA

LETTER TO THE EDITOR

Cardiology Journal
2020, Vol. 27, No. 4, 447–448
DOI: 10.5603/CJ.2020.0122

ISSN 1897–5593

Follow-up on results of three-dimensional printed model aided unusual intervention on aneurysm of aortic arch lesser curvature

Robert Sabiniewicz[1], Jarosław Meyer-Szary[1], Lidia Woźniak-Mielczarek[1], Dominika Sabiniewicz[2]

[1]Department of Pediatric Cardiology and Congenital Heart Diseases, Medical University of Gdansk, Poland
[2]2nd Department of Radiology, Medical University of Gdansk, Poland

A recent article "Feasibility of in-house rapid prototyping of cardiovascular three-dimensional models for planning and training non-standard interventional procedures" [1] presented the usefulness of three-dimensional (3D) printed models in planning unusual procedures in atypical structural heart defects. In particular, the model was used to plan the procedure of closing an aneurysm on the lesser curvature of the aortic arch in a patient after previous surgery for aortic coarctation (Fig. 1A). Thanks to the prepared model, the type and size of the closing implant were selected, optimal vascular access path was chosen, and technique of the procedure was practiced. This allowed for shortening the time of procedure, perform it without complications, and with a good direct result. This proves the usefulness of personalized printouts of 3D models described in the literature in planning unusual or complicated interventions [1–3].

Herein, is presented follow-up details and treatment results of a previously presented case. Post 6 months the patient did not present any symptoms or complain of discomfort. A follow-up computed tomography scan showed a good long-term outcome. The aneurysm orifice was closed with an ADO implant remaining in the correct position (Fig. 1B). There was no narrowing or flow disorder in the aortic arch and no inflow to the aneurysm that was completely closed. The procedure of closing the aneurysm prevented its further enlargement or increasing pressure on surrounding structures most importantly the left pulmonary artery. Presented 3D reconstructions compare the baseline situation and the remote outcome of the procedure.

Conflict of interest: None declared

References

1. Meyer-Szary J, Woźniak-Mielczarek L, Sabiniewicz D, et al. Feasibility of in-house rapid prototyping of cardiovascular three-dimensional models for planning and training non-standard interventional procedures. Cardiol J. 2019; 26(6): 790–792, doi: 10.5603/CJ.2019.0115, indexed in Pubmed: 31970736.
2. Luo H, Meyer-Szary J, Wang Z, et al. Three-dimensional printing in cardiology: Current applications and future challenges. Cardiol J. 2017; 24(4): 436–444, doi: 10.5603/CJ.a2017.0056, indexed in Pubmed: 28541602.
3. Sabiniewicz R, Meyer-Szary J, Potaż P, et al. Melody valve implantation pre-procedural planning using custom-made 3D printed model of the region of interest. Adv Intercv Cardiol. 2018; 14(2): 210–211, doi: 10.5114/aic.2018.76419, indexed in Pubmed: 30008780.

Address for correspondence: Jarosław Meyer-Szary, MD, PhD, Assistant teacher, Department of Pediatric Cardiology and Congenital Heart Diseases, Medical University of Gdansk, ul. M. Skłodowskiej-Curie 3a, 80–210 Gdańsk, Poland, tel: +48 58 349 2882, fax: +48 58 349 2890, e-mail: jmeyerszary@gumed.edu.pl

Received: 2.04.2020 Accepted: 5.05.2020

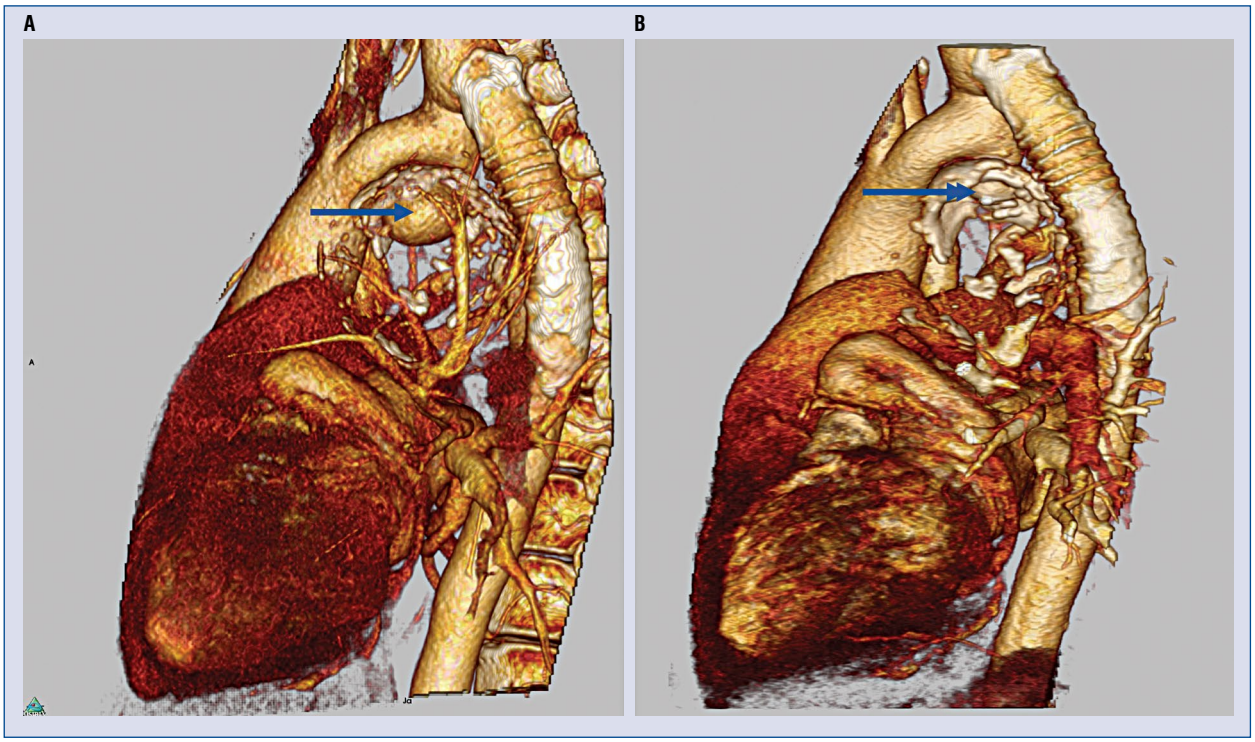

Figure 1. Computed tomography volume rendering reconstruction showing the anatomy before the procedure (**A**) and after (**B**). The arrows show the aneurysm on the lesser curvature of the aortic arch and the ADO implanted to close it. Detrailed description in the text.